BRINGING GPS INTO HARSH ENVIRONMENTS FOR DEFORMATION MONITORING

D. JASON BOND

October 2007

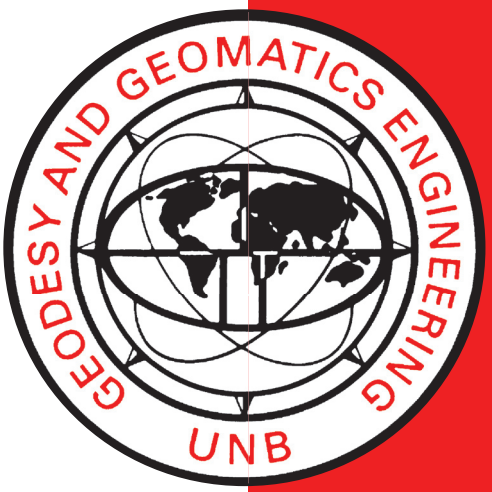

TECHNICAL REPORT
NO. 253

BRINGING GPS INTO HARSH ENVIRONMENTS FOR DEFORMATION MONITORING

D. Jason Bond

Department of Geodesy and Geomatics Engineering
University of New Brunswick
P.O. Box 4400
Fredericton, N.B.
Canada
E3B 5A3

October 2007

PREFACE

This technical report is a reproduction of a dissertation submitted in partial fulfillment of the requirements for the degree of Doctor of Philosophy in the Department of Geodesy and Geomatics Engineering, October 2007. The research was supervised by Dr. Adam Chrzanowski, Dr. Don Kim, and Dr. Anna Szostak-Chrzanowski and funding was provided by the Natural Sciences and Engineering Research Council of Canada.

As with any copyrighted material, permission to reprint or quote extensively from this report must be received from the author. The citation to this work should appear as follows:

Bond, D. J. (2007). *Bringing GPS into Harsh Environments for Deformation Monitoring*. Ph.D. dissertation, Department of Geodesy and Geomatics Engineering, Technical Report No. 253, University of New Brunswick, Fredericton, New Brunswick, Canada, 268 pp.

ABSTRACT

Certain deformation monitoring environments pose severe limitations on the achievable accuracy and precision that can be attained by instrumentation used to monitor deformation behaviour. Large open pit mines are one example. In such environments, it is not uncommon for the degradation in precision of geodetic technologies to be so large that the minimum detectable displacement fails to meet the mine's requirements for displacement detection.

In order to meet these requirements, an innovative approach to deformation monitoring is required. Presented is a technique which capitalizes on the advantages of Global Positioning System (GPS) sensors to provide fully-automated and continuous sub-centimetre displacement detection in real time. Software was developed which utilizes triple-differenced carrier phase observations in a Delayed-State Kalman filter to provide continuous, high precision position updates in a fully automated mode. The software was enhanced to include pseudolite processing capabilities. An interdisciplinary approach was then used to predict deformation behaviour to aid in the design of a geodetic deformation monitoring scheme.

It was shown that the processing strategy employed helps to mitigate the effects of residual tropospheric delay biases. Additionally, it was illustrated that pseudolites can be used to provide more continuous position updates in harsh environment conditions. An

example was also given to demonstrate how deterministic modelling can be used to predict deformation behaviour and how this information can be incorporated into the design of a geodetic deformation monitoring scheme.

ACKNOWLEDGEMENTS

The greatest resource one has is the people that surround them. I have been fortunate to have been surrounded by some of the finest this world has to offer and for that I am extremely grateful. This research and the positive experiences that have come with it are a result of all of those people that I have had the pleasure of cooperating with over the past several years.

In particular, I would like to thank Prof. Adam Chrzanowski as my primary supervisor for his guidance and direction that has led me down a road where opportunities abound. His research initiatives and visions have been monumental to the progression of the discipline of engineering surveys worldwide. I have been privileged to be part of his Canadian Centre for Geodetic Engineering and to witness leading edge research and technologies evolve before me.

I would like to thank my co-supervisor, Prof. Anna Szostak-Chrzanowski, for her innovative ideas as to how our profession can benefit from interdisciplinary research. I have benefitted greatly from our discussions and have been very fortunate to have exposure to the field of geomechanical engineering. I believe that such interdisciplinary research is the way of the future, and through it researchers will find the answers to challenging research problems.

Thanks are given to my co-supervisor Dr. Don Kim for imparting his tremendous theoretical knowledge of GPS and of real-time data handling strategies. Several barriers have been broken through with his advice and this has allowed me to continue to progress in my research. The objectives of this research could not have been achieved without him.

I would also like to thank my colleagues in our department that have helped make this experience a positive one: members of the Canadian Centre for Geodetic Engineering, members of the Geodetic Research Laboratory, professors and fellow students.

Sincere gratitude is given to the various funding bodies that have made this research possible: the Natural Sciences and Engineering Research Council of Canada (NSERC), the Canadian Wireless Telecommunications Association (CWTA), the Public Safety and Emergency Preparedness Canada Research Fellowship in honour of Stuart Nesbitt White, and the Atlantic Canada Opportunities Agency (ACOA).

For their support and understanding of the academic commitments associated with obtaining a doctoral degree, I will forever be indebted to my family and friends. I hope that the successes that I have experienced through this journey serve as motivation to set their goals high and to achieve them.

Last, but not least, I would like to thank my soon to be wife, Danielle. She has heard all of the problems associated with deformation monitoring over the past 3 years and for that she has rightfully earned her own Dr. Phil. I thank her for the sacrifices she has made over the course of this degree with all of my heart.

~

TABLE OF CONTENTS

Page

LIST OF FIGURES

LIST OF TABLES

Page

LIST OF ABBREVIATIONS

DD	Double-Differenced
E,N,U (h)	East, North and Up (or height) solution components
FEM	Finite Element Method
GLONASS	Global Navigation Satellite System (Russian)
GNSS	Global Navigation Satellite System
GPS	Global Positioning System
IAM	Integrated Analysis Method
PL	Pseudolite
PPMS	Precise Position Monitoring System
$PPMS^{+RT}$	Precise Position Monitoring System plus Real-time Capabilities
QD	Quadruple-Differenced
RTK	Real-time Kinematic
RTS	Robotic Total Station
SD	Single-Differenced
TCP	Transmission Control Protocol
TD	Triple-Differenced
UDP	User Datagram Protocol

CHAPTER 1
INTRODUCTION

Presented is the development of a deformation monitoring system based on the Global Positioning System (GPS). The devised system incorporates advanced technology and processing algorithms. The main objective of this research is to devise a methodology to improve the continuity in GPS position updates that can be achieved using existing systems in harsh environments. The position updates should have sub-centimetre precision. The path followed in achieving this objective is traced in the following research papers which comprise this dissertation:

Paper 1 (peer reviewed):

Bond, J., A. Chrzanowski, and F. Wilkins (2005). "Using GPS for Augmenting Deformation Monitoring Systems in Open Pit Mines- Problems and Solutions." *Geomatica*, 59(1):73-82.

Paper 2 (peer reviewed):

Bond, J., A. Chrzanowski, and D. Kim (2007a). "Bringing GPS into Harsh Environments for Deformation Monitoring." *GPS Solutions* (online first status), 11 pp. Available at: http://www.springerlink.com/content/21v2625p46108266/fulltext.pdf, accessed on: 4 October 2007. DOI 10.1007/s10291-007-0059-7

Paper 3:

Bond, J., A. Chrzanowski, D. Kim D (2007b). "Augmenting GPS with Pseudolites for Deformation Monitoring in Harsh Environments." Proceedings of the *Institute of Navigation National Technical Meeting* (ION NTM), 22-24 January, San Diego, CA, USA, CDROM, pp. 486-492. Available at http://www.ion.org/, accessed on: 4 October, 2007.

Paper 4:

Bond, J., A. Szostak-Chrzanowski A and A. Chrzanowski (2007). "Design of Geodetic Monitoring Schemes Using Deterministic Modelling: An Open Pit Mine Example." Proceedings of the *3rd International Symposium on Geo-information for Disaster Management*, Toronto, Ontario, Canada, 22-24 May, Canadian Inst. of Geomatics, 11 pp., CDROM.

Paper 5 (peer reviewed):

Bond, J., D. Kim, A. Chrzanowski, A. Szostak-Chrzanowski (2007). "Development of A Fully Automated, GPS Based Monitoring System for Disaster Prevention and Emergency Preparedness: PPMS^{+RT}" *Sensors* 2007, (7) Special Issue: *Sensors for Disaster and Emergency Management Decision Making*, Eds. J. Levy and Y.Gao, pp. 1028-1046. Available at: http://www.mdpi.org/sensors/list07.htm#new, accessed on: 3 October 2007.

The subsequent subsections will bridge the publications together by using the following approach:

1. The structure of this paper-based dissertation is outlined.
2. Background information describing the challenges associated with meeting the above goal is presented.
3. A statement of the problem is given.

4. The use of GPS for deformation monitoring is discussed.
5. Research and industrial developments related to this investigation are presented.
6. Objectives of this research are listed.
7. Proposed strategies to reach the objectives are presented.
8. A brief overview of the dissertation is provided.

1.1 Dissertation Structure

The structure of the dissertation is depicted in Table 1.1. In each paper, the first author has conducted the primary research and the co-authors have kindly provided advice and suggestions on the paper content.

Table 1.1: Dissertation Structure

Chapter	Content
1	Introduction
2	Paper 1
3	Paper 2
4	Paper 3
5	Paper 4
6	Paper 5
7	Conclusion
Appendices	Additional Results

1.2 Background

Certain deformation monitoring environments pose severe limitations on the achievable precision that can be attained by instrumentation used to monitor deformation behaviour. Large open pit mines are one such example. The steep walls of an open pit limit the effectiveness of satellite positioning technologies by masking some satellite signals and thereby diluting the geometric strength of solutions. Additionally, large height differences between master and rover stations can lead to significant height biases in baseline solutions. In large scale projects where the pit diameter exceeds 1 km, refraction and pointing errors limit the effectiveness of direction measurements made by total station instruments and laser scanners [Bond, et al., 2005]. The steep pit walls also limit the effectiveness of space borne interferometric synthetic aperture radar [Chen et al., 2000]. In such environments, it is not uncommon for the degradation in precision of geodetic technologies to be so large that the minimum detectable displacement exceeds the mine's requirements for displacement detection.

The complex behaviour of an open pit as it responds to changes in its environment (e.g., excavation, increases in water saturation, tectonic movement) also causes tremendous challenges in trying to design an effective deformation monitoring scheme. The zone of deformation must be carefully delineated so that stable regions can be identified for reference points. Local geological characteristics must be analyzed to determine suitable locations for target points as well as their expected displacement rates.

An iterative process of measuring displacements, interpreting deformations and updating the deformation monitoring scheme is required to validate the correctness of the model of the deformation behaviour.

Consequently, addressing the needs for sub-centimetre accuracy and precision of position updates with 95% confidence is not a trivial task in large open pit mines. In order to meet these requirements, an innovative approach to deformation monitoring is required. Presented is a technique which uses GPS sensors to address this need. This technique allows GPS to be used as a stand-alone system or in combination with other sensors. Also presented is an interdisciplinary example to designing geodetic deformation monitoring networks using the principles of rock mechanics and numerical modelling of deformation. This approach does not pre-empt the need to use traditional simulation methods for network design, but rather should be used as a complement to it. The implemented methodology aids in identifying stable regions for reference stations and in providing an indication of the magnitude and direction of expected displacements.

1.3 Problem Statement

The geometric constraints and dynamic conditions encountered in large open pit mines make such an environment one of the most challenging deformation monitoring scenarios. Approaches using total station technology have not been able to provide the

necessary displacement detection accuracy with sufficient update frequency and precision to meet project needs. The purpose of this research is to devise a technique of providing more continuous, high accuracy and high precision position updates in harsh environments than can be currently achieved using existing systems. Although this research focuses on large open pit mines, its application to other steep embankment scenarios such as large dams and volcano slopes can easily be extrapolated. This investigation will focus on GPS sensors for reasons subsequently discussed.

1.4 GPS for Deformation Monitoring

GPS (and in general, GNSS) has certain characteristics that allow for continuous, high precision displacement detection in circumstances where other geodetic technologies cannot. These characteristics include:

a) Line of sight is not required between stations.

b) Updates can be provided at frequencies of 1 Hz and higher.

c) 3 dimensional position information is provided.

d) Millimetre level position information is possible for short baselines (<10 km).

The major disadvantages of using GPS are:

a) The cost of a geodetic grade receiver and antenna, which will ultimately limit the number of units that can be afforded and dictate the spatial resolution of targets that can be monitored using this technology; and
b) Supplying power to GPS units when a large number of targets must be monitored. This can be difficult in inaccessible target areas.
c) Satellite visibility is necessary (at least four satellites are required to obtain a unique solution).

In most cases it will be more practical and economical to use GPS to monitor the stability of other sensors that can provide higher spatial resolution at a lower cost in localized areas (e.g., total stations, laser scanners). It would be impractical to place expensive GPS technology in a zone that is expected to fail, where it may become damaged or lost.

In order to capitalize on the above mentioned benefits of GPS for deformation monitoring in harsh environments, the following major challenges need to be addressed:

a) Residual tropospheric delay biases: (the portion of tropospheric delay that remains after modeling): Due to large height differences between master and rover stations, residual tropospheric delay biases can contaminate the vertical component of GPS baseline solutions. Beutler et al. [1988] have illustrated that

neglecting the differential troposphere causes a 3-5 mm relative height error for every millimetre of difference in zenith delay between stations. In open pit mines meteorological conditions can change rapidly, both spatially and temporally, causing these biases to be highly variable.

b) Limited satellite visibility: The steep pit walls of open pit mines obstruct satellite visibility. This limits the reliability of the solutions as well as the frequency at which updates can be provided. In order to meet sub-centimetre position update requirements with sufficient update frequency, new technologies must be integrated with GPS.

c) Connecting to stable reference points: As precise as the GPS software may be, the overall accuracy of the solution depends upon the validity of the assumption that each reference point is stable. Tremendous care must be taken in choosing suitable reference station locations. Additional sources of information regarding the behaviour of the rock mass must be utilized to make informed decisions.

d) Developing a fully automated GPS processor: A fully automated GPS processor is required to provide continuous updates in real time. Ideally, the results from the processor can be used to provide 'on-time' warnings of impending danger. The processor must be designed to be robust so that false alarms do not occur. Additionally, sub-centimetre position updates should be able to be provided.

Communication links must also be built into the software to allow for data transfer between GPS receivers located on site at target points and a central processing computer.

e) Multipath: In deformation monitoring environments where multipath sources are abundant (e.g., building structures, vehicles) multipath can contaminate the position solutions. Practically every observation site is affected to some degree by multipath. Multipath biases can reach up to $\lambda/4 \approx 4.8$ cm for the original L1 carrier-phase measurement [Leick, 1994].

1.5 Related Research and Industrial Developments

Presented is a brief review of research and industrial developments that have contributed to addressing the challenges associated with using GPS in the harsh environments previously described.

1.5.1 Mitigation of Residual Tropospheric Delay Biases

Much of the research conducted towards high accuracy GPS surveys in regions having large height differences was performed during the late 1980s at the Astronomical

Institute, University of Berne using data collected in the Swiss Alps [Rothacher et al., 1986; Beutler et al., 1988; Gurtner et al., 1989]. Two distinct residual tropospheric delay bias mitigation techniques have emanated from this research.

The first technique involves the estimation of residual tropospheric delay parameters [Gurtner et al., 1989]. In their research, accuracies better than ± 1 cm in height are achieved over baselines having height differences greater than 1000 m. Langley [1995] points out, however, that the strength of the bias estimates depends upon low elevation angle satellites which are generally not visible in an open pit environment.

The second technique uses surface meteorological data and a differential tropospheric model to derive a height dependent profile of the atmosphere in the layer between the reference and rover stations [Rothacher et al., 1986]. Similar accuracies are achieved as in the previous approach [Gurtner et al., 1989]. The major disadvantage of this technique is the cost of supplying meteorological sensors to provide profiles along the observed baselines. This becomes amplified over large scale projects.

In order to provide sub-centimetre precision position updates in large open pit mines using GPS, there is need for the development of a new residual tropospheric delay mitigation technique that does not depend upon the visibility of low elevation satellites and preferably does not add significant hardware costs.

1.5.2 Improved Continuity in Solution Updates

The integration of additional GNSS observations, such as those from the Russian Global Navigation Satellite System (GLONASS) or from the future European Galileo system, offers potentially more continuous and higher precision solution updates than could normally be provided using stand-alone GPS [Martin and Ladd, 1999; Bond, 2004; Van Diggelen, 1997]. Despite offering increased satellite visibility, however, there is no guarantee that satellite geometry will always be of sufficient strength to provide the required level of accuracy and precision in certain environments.

The use of ground-based transmitters of GPS-like signals known as pseudolites (PLs) has been also actively researched as an alternative method of providing continuous position updates in areas of poor satellite visibility [Chen and He, 2006; Rzepecka et al., 2006; Kee et al., 2001; LeMaster and Rock, 2000]. This research has been ongoing since the early 1990s when the first commercial devices became available through *Novariant* (formerly *IntegriNautics*) [Wang, 2002]. *Novariant's* current generation of pseudolites called 'terralites' are deployed as a complete package of transmitters, receivers and software. The package caters to navigation applications and can provide centimetre-level positioning precision [Novariant, 2007].

Research at the University of New South Wales has been devoted to the use of pseudolites for deformation monitoring [Dai et al., 2000; Dai et al., 2001; Wang, 2002].

Test results have demonstrated that the precision (especially the height component), reliability, continuity and integrity of the solutions of a combined GPS and pseudolite system can be improved over stand-alone GPS. These results have served as an impetus for the development of the *Locata* PL deformation monitoring system which offers centimetre-level precision [Barnes et al., 2004].

Despite recent progress, there are still obstacles that remain in achieving a seamless integration of PL technology with GPS. Some of these challenges include tropospheric delay modelling [Dai et al., 2001], accounting for multipath [Michalson and Progri, 2000] and determining accurate PL coordinates [Dai et al., 2002]. The research discussed in this dissertation attempts to address some of these issues that presently prevent sub-centimetre level positioning accuracies from being consistently achieved by combined GPS and PL systems in real world applications.

1.5.3 Incorporation of Deterministic Modelling into Designing a Geodetic Deformation Monitoring Scheme

The connection of measurement sensors to stable reference points is a critical component in the design of geodetic deformation monitoring schemes. Chrzanowski and Szostak-Chrzanowski [1993] have advocated an approach that combines deterministic modelling and geometrical data in an integrated analysis for the design and physical

interpretation of geodetic deformation monitoring schemes. Since the continuous description of a deformation field is a function of the discrete distribution of data, it is beneficial to use physical analysis to identify critical deformation locations (e.g., locations of maximum displacements) [Szostak-Chrzanowski et al., 2006a]. The selection of reference point locations may also be aided by physical analysis by supplying information where discrete points may be assumed as stable. This multidisciplinary approach to geodetic and geotechnical monitoring, deformation analysis and physical interpretation of structural and ground deformations has recently been demonstrated on various monitoring projects as subsequently discussed.

Szostak-Chrzanowski and Massiéra [2006] have demonstrated the importance of the prediction of the magnitude and location of maximum displacements in designing monitoring schemes for large earth dams. Since the responses to loading conditions are different for each dam, the design of monitoring schemes cannot be standardized. Their research illustrates how the results of a monitoring scheme can be compared with the prediction model of deformation to verify design parameters and to determine the causes of unexpected behaviour.

Szostak-Chrzanowski et al. [2003] have illustrated the application of geometrical analysis and physical interpretation to determine the effects of hydrological changes on ground subsidence in a potash mine. Annual monitoring surveys consisting of levelling (designed to meet Canadian 1st order levelling specifications as set by the Surveys and

Mapping Branch of Natural Resources Canada), traversing and GPS have been performed since the mid 1980s to capture geometrical data on the deformation behaviour. Finite element analysis was performed to model the maximum expected subsidence along a selected cross section of the mining operation. The continual process of comparing geometrical results with predicted behaviour has helped identify an aquifer that has caused an inflow of water into the mine. The predicted displacement field has illustrated areas of maximum expected subsidence making it easier to determine where to densify the geodetic network.

Jäger et al. [2006] have incorporated a finite element model (FEM) approach into their GNSS/local positioning sensors/local sensors Online Control and Alarm System (GOCA). The mathematical model of the FEM-based analysis is used to evaluate the optimal sensor configuration. A system analysis adjustment approach is performed by introducing an additional set of unknown parameters that model safety critical parameters that are to be detected by statistical methods by the monitoring system.

Lienhart [2007] has also illustrated this strategy by developing an Integrated Analysis Method (IAM) for spatially distributed and hybrid measurements (various geodetic, geotechnical and fibre optic sensors) taken at different times. The IAM is demonstrated using monitoring data from a monolithic bridge which is characterized by the absence of bridge bearings and expansion joints. The devised approach allows deformations caused

by regular changes (e.g., temperature) to be separated from deformations caused by other sources.

Despite recent progress in this area, more research is still required to demonstrate the benefits of integrated analysis in other applications (e.g., large open pit mines and various types of buildings and bridges).

1.5.4 Development of a Fully Automated, Real-time Monitoring System

Numerous applications of GPS for the purpose of deformation monitoring can be cited since the 1980s. Presented are selected approaches that focus on providing continuous updates for near real-time deformation monitoring:

a) Continuous GPS (CGPS): Regional scale CGPS networks have been used for over a decade in precise determination of crustal deformation in tectonically active regions [Sagiya et al., 2000]. Examples include the Western Canada Deformation Array (WCDA) established by the geological survey of Canada [NRCan, 2007], GPS Earth Observation Network (GEONET) operated by the Geographical Survey Institute in Japan [Sagiya et al., 2000], the Southern California Integrated GPS Network (SCIGN) [Hudnut et al., 2001] and the South Pacific Regional GPS Network (SPRGN) [Geoscience Australia, 2005]. Due to

high accuracy requirements for the displacement rates (which are typically a few mm/year), final solutions are calculated using daily observation files and require the International GNSS Service (IGS) precise satellite orbits, which have about a two week latency. In the case of GEONET, rapid solutions are also achieved within 30 hours using IGS rapid orbits with compromised accuracy [Sagiya et al., 2000]. GEONET also transfers data every 3 hours in highly active regions so that baselines can be calculated using the broadcast ephemeris, in a quasi-real-time mode [Sagiya, 1998]. Unfortunately, the latency of this approach makes it unsuitable for real-time deformation monitoring scenarios requiring a quick response to sudden displacements.

b) *Geodetic*'s Network RTK Positioning Software: Bock [2004] has implemented a wide-area network real-time kinematic (RTK) approach that takes advantage of the surrounding regional CGPS infrastructure. Reference station coordinates evolve with time so as to not degrade the quality and accuracy of RTK positions. This technique has been implemented by the Metropolitan Water District of Southern California [Whitaker and Bock, 2006] to augment their current deformation monitoring system as well as to increase the efficiency of their survey field crews. Centimetre-level accuracy is achieved in real time and daily averaging is used to detect millimetre-level trends of target points [Bock, 2004]. This approach overcomes the latency shortcoming of the previous approach but

does not necessarily provide sub-centimetre level accuracy in real time and its performance in harsh environments has not been demonstrated.

c) *Multibas* at Curtain University of Technology: Forward [2002] has developed *Multibas* GPS software for monitoring steep slopes using RTK processing strategies. To save hardware costs, a multi-antenna approach has been implemented using a co-axial switch (based upon the Hong Kong Polytechnic approach subsequently described). This allows one GPS receiver to monitor several antennas located in the deformation area. Additionally, a stacking approach is used to mitigate the effects of multipath by taking advantage of the day-to-day multipath repeatability. The issues of satellite visibility and residual tropospheric delay are not addressed.

d) *Geodetic Navstar Permanent Object Monitoring* (*GNPOM*): Wübbena et al. [2001] have also developed software that takes advantage of the day-to-day repeatability of multipath. Observations are processed as sideral differences to mitigate the effects of multipath. Millimetre-level accuracy is achieved in real time to track a moving lock. This approach is based on the assumption most of the observation noise will repeat itself. The issues of satellite visibility and residual tropospheric delay are not addressed.

e) *Condor Earth Technologies, Inc*.'s 3D Tracker: Remondi and Brown [2000] have developed software for *Condor Earth Technologies, Inc*. that employs a Delayed-State Kalman filter to process GPS carrier phase measurements as triple differences. The use of triple-differenced observations makes the software less susceptible to false alarms caused by cycle slips. After 24 hour smoothing, precisions of ± 1-3 mm have been achieved for landslide monitoring [Rutledge et al. 2001] and for monitoring subsidence of oil fields [Rutledge et al. 2002]. *Trimble* utilizes Condor's 3D Tracker for structural and ground deformation monitoring [Trimble, 2002]. Results on the performance of this software in harsh environments and its real-time response to displacements have not been published.

f) *Leica*'s *SKI-Pro* Interfaced with *GPS Spider*: Leica's GPS deformation monitoring package utilizes its commercial post-processing software *SKI-Pro* interfaced with its *GPS Spider* data communications package [Van Cranenbroeck and Troyer, 2004]. *SKI-Pro* scripting is used to schedule regular downloads of observations for automatic processing in *SKI-Pro* to produce time series results in near real time [Van Cranenbroeck and Troyer, 2004]. Previous analyses of *SKI-Pro* software have indicated that continuous sub-centimetre displacement accuracies could not be provided in an open pit environment [Bond, 2004].

g) Hong Kong Polytechnic University's Multi-Antenna Approach: Extensive research has been devoted at Hong Kong Polytechnic University towards developing a more cost effective GPS-based monitoring system by implementing a multi-antenna approach [Ding et al. 2000; Ding et al., 2003; Ding et al. 2007]. A dedicated GPS multi-antenna switch (GMAS) has been developed which allows multiple GPS antennas to collect data for target points while using only 1 GPS receiver. The required hardware investments are significantly reduced which makes GPS a more attractive method of deformation monitoring for large scale projects.

h) Hyperbolic Method for Displacement Detection: Ueno et al. [2003] have demonstrated an approach for displacement detection in steep slope environments suffering from poor satellite visibility. Displacements are estimated without differencing the positioning results. Instead, the principles of hyperbolic navigation are used. Knowledge of the expected direction of movement (such as along a slope of maximum inclination) is used to estimate the size of the displacement. The devised technique allows the requirement for good receiver-satellite geometry to be waived, which is necessary when using position estimates to determine displacements.

Despite the wide range of GPS software options and data handling techniques that exist for deformation monitoring, there is no one package that guarantees continuous,

sub-centimetre displacement detection capabilities in harsh environment conditions such as a large open pit mine. Further research is required to develop such a system.

1.5.5 Mitigation of Multipath Biases

Extensive research has been devoted to devising methodologies for mitigating the effects of multipath biases (e.g., [Kim and Langley, 2001; Satirapod and Rizos, 2004; Minami et al., 2000]). This discussion is not comprehensive and is meant to give an overview of some of the more common methods employed, which include [Rizos, 1999a]:

1. Selecting an antenna site that avoids reflective materials that cause multipath,
2. Using a multipath resistant antenna,
3. Using a ground-plane or a choke-ring,
4. Using a receiver that filters out multipath effects,
5. Masking low elevation satellites which are more susceptible to multipath biases than high elevation satellites,
6. Using longer session lengths so that multipath biases will be reduced.

Additionally, research has been devoted to capitalizing on the repeatability of multipath signatures from one sidereal day to the next [Wübbena et al., 2001; Radovanovic, 2000; Ge et al., 2000]. Given the known coordinates of a point, a multipath

signature can be calculated for the GPS carrier phase observations of each satellite. This signature can be removed from GPS data collected on subsequent days since the GPS satellite constellation repeats itself every sidereal day.

Research is ongoing by GPS equipment manufacturer's to introduce new technology that incorporates multipath mitigation techniques. For example, *NovAtel* has developed its proprietary Vision Correlator technology for detecting and removing nearby multipath interference [GPS World, 2005]. This technology measures and processes the synchronization signals of a received pseudorandom noise (PRN) code and precisely measures the received radio frequency characteristics in the time domain of the phase transitions of the modulated satellite signal. Most other GPS antenna manufacturer's also boast multipath mitigating technology, including *Trimble*'s Zephyr antenna [Krantz et al., 2001] and *Leica*'s GPS1200 system [Leica Geosystems, 2007a].

Although biases caused by multipath are always a concern when striving to achieve millimetre level precision using GPS, development of new multipath mitigation techniques will not be focussed on in this research. It will be assumed that the above mentioned techniques and technology can be used to mitigate its effects.

1.6 Objectives

The main objective of this research was to devise a methodology to improve the continuity in GPS position updates in harsh environments that was achievable using existing systems. It was desired that the position updates would have sub-centimetre accuracy and precision. To achieve this overall goal, several supporting goals were identified:

a) Develop a technique to mitigate the effects of residual tropospheric delay biases in differential GPS solutions.

b) Integrate new technology to aid in providing position updates where stand-alone GPS cannot.

c) Demonstrate an interdisciplinary approach to designing a geodetic deformation monitoring scheme by incorporating the principles of rock mechanics and numerical modelling to predict displacements fields.

d) Develop a fully automated GPS processor to provide continuous, high-precision, real time updates.

1.7 Methodology

The proposed methodology for achieving each of the above listed objectives is subsequently described.

1.7.1 Mitigation of Residual Tropospheric Delay Biases

A common technique of eliminating biases is through the differencing of observations. For example, between-receivers differencing (SD: single difference) of GPS observations to the same satellite eliminates satellite clock biases and between-satellite differencing of GPS observations to the same receiver eliminates receiver clock biases. Further differencing between-receivers SDs and between-satellite SDs results in a double-differenced (DD) observable free of both receiver clock and satellite clock biases. The proposed methodology is based upon time differencing of successive DD observations, which yields the triple-differenced (TD) observable [Remondi, 1984].

The appeal of the TD observable to most users is its absence of the integer ambiguity term which cancels out through the time difference if a cycle slip has not occurred. The proposed methodology takes advantage of the nature of the TD observable to significantly reduce the effects of another bias: residual tropospheric delay. It is hypothesized that for observation intervals shorter than a few seconds, the correlation in atmospheric parameters between times t_1 and t_2 would be large and therefore biases originating from them would be significantly reduced.

Although the TD observable used is not new, obtaining high precision results in environments where the DD observable suffers from residual tropospheric delay biases presents another beneficial use. Successfully implemented, this approach would allow the

stability of optical geodetic technology to be monitored in areas having large height differences using GPS. This would help to address the age-old problem of refraction for this application; the stability of optical geodetic technology could be monitored in deformation areas since sight lengths could be reduced to target points.

1.7.2 Improved Continuity in Solution Updates

Assuming that the above described TD approach is successful for reducing the effects of residual tropospheric delay biases, the PL observations will be modeled in the same, TD manner. The attractiveness of the TD, PL observable is that it is a time difference of DD observations and consequently biases common to both observations will cancel. This strategy offers several important benefits for PL data processing:

a) the user no longer needs to solve for the ambiguity term, which allows the system to be less susceptible to biases caused by cycle slips;
b) for observation intervals less than a few seconds, the correlation between PL tropospheric delay parameters at times t_1 and t_2 will be large and biases originating from them were significantly reduced;
c) for observation intervals less than a few seconds, the correlation between low frequency multipath terms at times t_1 and t_2 will be large and biases originating from them will be significantly reduced. The high frequency component will still remain.

Through triple-differencing, most major errors should be significantly reduced from the PL observations.

Additionally, this approach also eliminates the need for accurate PL coordinates which can cause centimetre level biases through DD processing methods [Dai et al., 2000]. Since the PL is stationary between times t_1 to t_2 and it is assumed that the receivers are also stationary, the geometric distance terms involving the PL cancel so that the computed, geometric TD is solely dependent upon the change in the geometry of the reference satellite. Consequently, the accuracy to which the PL coordinates must be known is very forgiving. Approximate coordinates are necessary simply for computing elevation angles to PLs when elevation cut-off constraints are imposed.

The devised methodology allows for smooth integration of PL data into the existing software infrastructure. Successful implementation would result in one of the few software developments capable of incorporating PL technology.

1.7.3 Incorporation of Deterministic Modelling into Designing a Geodetic Monitoring Scheme

Deterministic models of deformation behaviour are derived from mechanical properties of rocks (known *a priori*), relations between the loads (surface and body forces, initial stresses) and internal stresses, and from the physical laws governing the

stress-strain relation [Chrzanowski et al., 1998]. Deterministic modelling requires the solution of complex differential equations. The advent of computers has allowed various numerical methods to be developed and employed to solve such equations. One such method is the finite element method, which is used for this analysis [Zienkiewicz, 1977].

The basis of FEM involves representing the body or structure by a series of smaller units called finite elements. These elements are interconnected at nodal points. Displacement functions are used to approximate the distribution of the actual displacements over each finite element. The unknown magnitudes of the displacement functions are the displacements at the nodal points. Using boundary conditions, the final solution of the equilibrium equations yields values for these displacements [Zienkiewicz, 1977].

Numerical modelling can be an extremely useful tool in the design of geodetic networks for deformation monitoring. This technique has been overlooked by geodetic engineers and its applications to this area have only recently been advocated [Chrzanowski et al., 2007]. The finite element method will be applied in the analysis of a large open pit mine to predict displacement fields at various stages of mining sequence.

Finite element modelling will be performed using SIGMA/W software [GEO-SLOPE, 2007]. It will be demonstrated how the predicted displacement field can be used to:

a) Delineate the deformation zone so that suitable locations for stable reference points could be chosen;
b) Aid in making informed decisions about sensor placement to capture displacements of interest; and
c) Provide information for predicting global deformation behaviour including the expected magnitude and direction of displacements.

Successfully implemented, the results of this research will further the developments of an interdisciplinary approach in the design of deformation monitoring schemes by demonstrating an open pit mine example.

1.7.4 Development of a Fully Automated, Real-time Monitoring System

Post-processing GPS software that handled PL observations will be one of the outcomes of the previous objectives. The software will be developed using Microsoft Visual Studio.NET programming environment [MSDN, 2007a]. In order to move to a fully automated, real-time monitoring system, the following modifications will be required:

a) Development of binary decoding subroutines to read data directly from the GPS receiver of interest;

b) Development of a multi-threaded environment to receive data packets from multiple GPS receivers. This will involve the design of communication links to connect each GPS receiver to the software. Ethernet and serial port options will be offered.
c) Development of subroutines to graphically display position information in real time.

The fully automated version of the software will decode the raw binary data, process the data, output solution, outlier and residual information and display the position updates in real time. The output from the software can then be used to signal unsafe conditions as decided upon by the engineers responsible for safety criteria. Successfully implemented, this research will yield unique, fully automated software that addresses two major challenges frequently encountered in harsh GPS environments: residual tropospheric delay and limited satellite visibility.

1.8 Overview

The paper in Chapter 2 provides important background information by reviewing some of the challenges associated with using GPS for deformation monitoring in large open pit mines that are described in the author's MScE thesis [Bond, 2004]. Further

investigation into the use of meteorological data to model variations in the height component caused by residual tropospheric delay is also presented.

Through these preliminary investigations, commercial software (Leica SKI Pro, Trimble Total Control, Trimble Geomatics Office, Ashtech Prism) and scientific software (DIPOP, Bernese and modified UNB RTK) were tested and it becomes clear that the desired precision cannot be achieved with the desired frequency using conventional processing techniques and technology. Innovative approaches to addressing the problems of residual tropospheric delay and limited satellite visibility are necessary.

The paper in Chapter 3 presents a response to the first objective of this research: develop a technique to mitigate the effects of residual tropospheric delay biases in differential GPS solutions. Entirely new software (Precise Position Monitoring System: PPMS) is created to test whether or not triple-differenced observations over high sample rates will in fact help to reduce the impact of this bias. The same test data from Highland Valley Copper (HVC) Mine, British Columbia (BC), Canada that was processed using commercial and scientific software is reprocessed using PPMS so that the results can be compared. A displacement detection test is also presented to illustrate the capabilities of the software. Additional results of this analysis and of system performance are provided in Appendix I.

The paper in Chapter 4 addresses the second objective of this research: Integrate new technology to aid in providing position updates where stand-alone GPS cannot. Presented is a description of the process of integrating pseudolite technology into PPMS software. Few GNSS processing software packages exist that integrate PL technology. Those that are available do not use the TD approach described. Test results from an experiment conducted at Highland Valley Copper Mine, BC, Canada are illustrated. Results from a displacement detection test conducted at the University of New Brunswick are also provided. Additional information regarding pseudolite noise modelling is provided in Appendix II.

The paper in Chapter 5 addresses the third objective of this research: Demonstrate an interdisciplinary approach to designing a geodetic deformation monitoring scheme by incorporating the principles of rock mechanics and numerical modelling to predict displacements fields. Using FEM in SIGMA/W software, a large open pit mine example is presented. Displacement fields are generated at 5 stages of excavation activity. It is illustrated how this information can be used to delineate the deformation zone, to gain an appreciation of the expected magnitude and direction of displacements and to aid in choosing suitable locations for sensors and targets. Although not explicitly stated in this paper, the findings here support the hypothesis from the second paper that some or all of the GPS receivers in the HVC test are experiencing uplift. Appendix III contains additional information pertaining to this research.

The final publication presented in Chapter 6 responds to the fourth objective of this research: Develop a fully automated GPS processor to provide continuous, high-precision, real-time updates. A description of the modifications required to transform the post processing version of PPMS into a real-time version is presented. Network infrastructure options that will allow the GPS data to be streamed to a central PC are also discussed. A real-time displacement detection test is demonstrated to illustrate the capabilities of the software.

A final summary chapter containing conclusions and recommendations from each of the above papers is then presented. An additional appendix (Appendix IV) is also included to provide a description of the software design and to describe its role in the deformation monitoring process.

CHAPTER 2
USING GPS FOR AUGMENTING DEFORMATION MONITORING SYSTEMS IN OPEN PIT MINES - PROBLEMS AND SOLUTIONS

Jason Bond, Adam Chrzanowski and Rick Wilkins
University of New Brunswick, Fredericton, New Brunswick, Canada

The first author has performed the GPS data processing, compiled the GPS results, performed the GPS data analysis, performed the meteorological data processing and compiled the final manuscript. The second author has offered advice on the compilation of the results and has guided the analysis of the correlation in changes in meteorological parameters with changes in the height component solution. The third author has provided advice on the content of the paper.

The following was originally published as:

Bond, J., A. Chrzanowski, and F. Wilkins (2005). "Using GPS for Augmenting Deformation Monitoring Systems in Open Pit Mines- Problems and Solutions." *Geomatica*, 59(1):73-82.

Abstract

Large open pit mines require continuous monitoring of the stability of the bench walls. In most cases, sub-centimetre accuracy at the 95% confidence level is required in displacement detection of hundreds of targets. Presently, robotic total stations (RTSs) with automatic target recognition provide the most efficient solution for the monitoring problem. In large open pit mines it may be necessary to place the RTS near the bottom of the pit in unstable conditions without visibility to stable reference points. Extensive testing has been performed in a large open pit mine to evaluate the use of GPS in

controlling the stability of the RTSs. The goal was to achieve GPS corrections to the position of RTSs with a standard deviation of ≤ 2.5 mm for each of the three components (N, E, h). Five days of continuous GPS data from different levels of the open pit mine indicated that the main limitations in reaching the accuracy requirements are residual tropospheric delay and limited satellite visibility. To improve the performance of the combined RTS/GPS monitoring system, several alternative solutions have been suggested including the augmentation of GPS with pseudolites and the use of an adaptive filtering technique in processing the GPS data.

2.1 Introduction

The stability of steep walls in open pit mines is a major safety issue. The pit walls may undergo toppling, planar, and wedge displacements [Wilkins et al., 2003a], which may lead to a catastrophic wall failure. In general, there is a slow movement of the rock formation before a failure actually occurs. With continuous monitoring of creep and creep acceleration in a deformation zone, warning can be given to evacuate equipment and personnel in advance of a failure. Due to fracturing of the rock formation and time dependent displacement phenomena, the monitoring system in most of the large open pit mines requires a dense grid of hundreds of targets to be continuously monitored with sub-centimetre accuracy at the 95% confidence level.

Recently, the Canadian Centre for Geodetic Engineering (CCGE) has developed ALERT software suite for fully automated and continuous monitoring of steep embankments and slopes [Duffy et al., 2001; Wilkins et al., 2003b]. The monitoring system supported by ALERT software utilizes robotic total stations (RTSs) with automatic target recognition (e.g., Leica TCA 1800) as the main displacement sensors. The software provides for fully automated data collection, data processing, and displacement calculations with a built-in alarm system that can be configured for different levels of sensitivity, depending on operator set thresholds. The system utilizes algorithms for the automatic detection of unstable reference points by using the weighted similarity transformation of displacements [Chen et al., 1990], a method developed at the CCGE. The ALERT system has already been successfully implemented in several large open pit mines and in monitoring a number of large earth dams.

In order to obtain sub-centimetre accuracies, atmospheric refraction and pointing errors must be contained by restricting the maximum distance between an RTS and a target (retro-reflecting prism) to 1000 m (unless the observations are averaged over prolonged periods of time, e.g., daily averages). Averaging is not acceptable when near real-time monitoring results are required. Therefore, in large open pit mines with diameters exceeding 1000 m, the RTSs must be placed near the bottom of the mine in order to shorten the distance to the monitored wall (Figure 2.1). In turn, this creates problems of sighting stable reference points beyond the rim of the mine and of possible RTS instabilities. In these types of applications, it may be possible to use GPS to

continuously monitor the position of the RTS. Figure 2.1 portrays how a combined GPS and RTS system may function. It is illustrative only, since in practice a more robust network would be implemented.

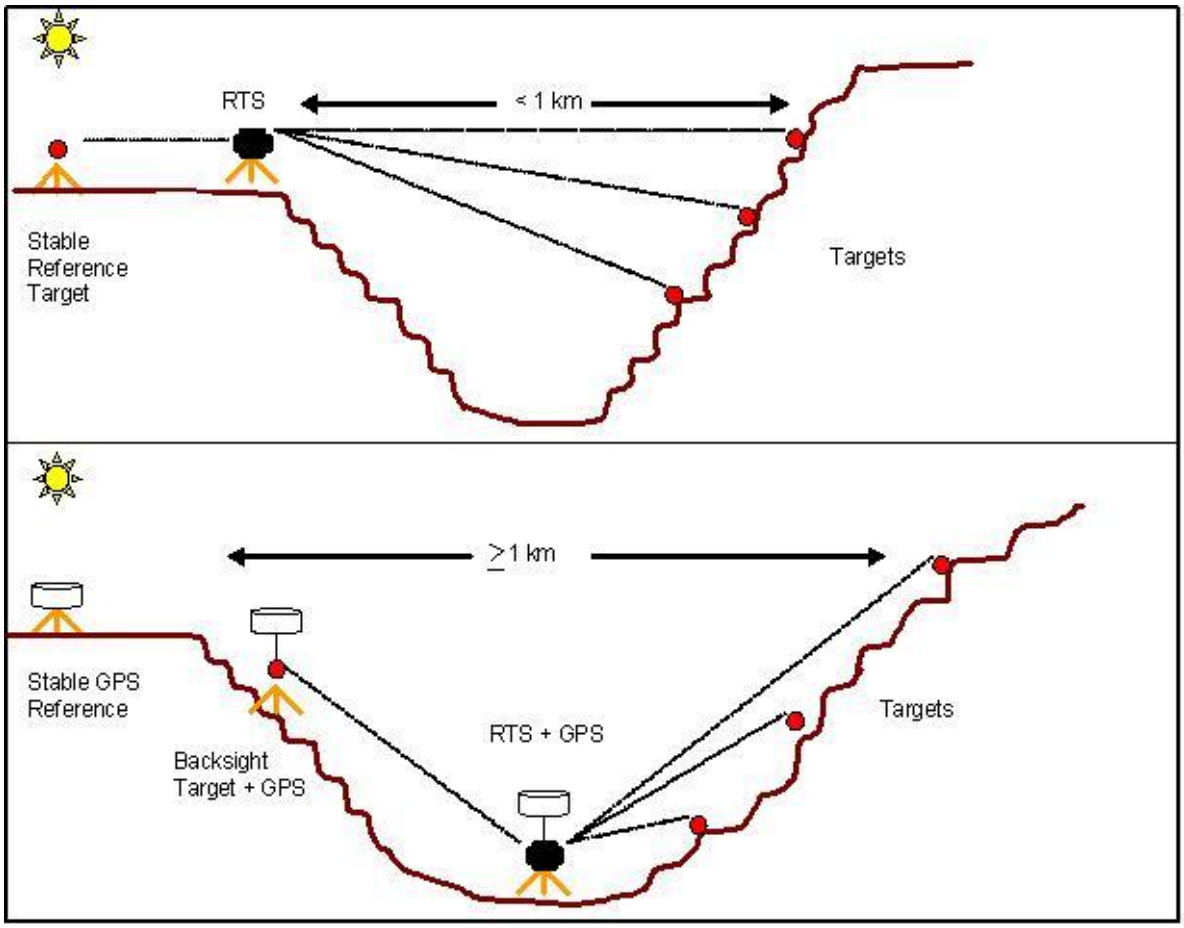

Figure 2.1: ALERT Implementation with Distances a) Less than 1 km and b) Greater than 1 km

Currently, the CCGE is creating a fully automated RTS/GPS hybrid system as part of the ALERT software suite. The goal of the hybrid system is to obtain corrections to the RTS position components (northings, eastings, and heights) with a standard deviation ≤

2.5 mm in a fully automated mode of operation. This accuracy requirement is not easily satisfied in the adverse conditions of open pit mines in which visibility to low elevation angle satellites is obscured by the pit walls. In addition, the height difference between the RTS/GPS at the bottom of the mine and the reference GPS station may be in the order of several hundred metres. As a preliminary step in the development of the hybrid RTS/GPS system, an extensive field test on the achievable accuracy of GPS in large open pit mines was performed during the summer of 2003. This paper summarizes the results of the test.

2.2 Test Site Description

The GPS field test was conducted in a large open pit mine in western Canada at an elevation of about 1500 m above mean sea level. Figure 2.2 gives an aerial view of the mine, which is approximately 2 km in diameter and has a depth of over 600 m. The CCGE's ALERT system is currently used at this mine site using Leica TCA 1800 and TCA2003 RTSs as the primary sensors. The RTSs are protected from the harsh environment by housing them in glass-paneled shelters.

Figure 2.2: Test Site
[Mining Technology, 2003]

Five GPS receivers (NovAtel DL-4 L1/L2) were used in this test with a continuous data acquisition spanning several days. Figure 2.3 shows the location of the receivers, each having different elevations within the mine. Three of the GPS receivers were located with RTSs (i.e. RTS 1, RTS 2, and RTS 3) while the remaining two were used as reference stations 987 and 424. Table 2.1 gives the ellipsoidal height differences and slope distances between stations. In addition, meteorological data was continuously collected at stations 424 and RTS2 with the sensors placed about 3 m above ground.

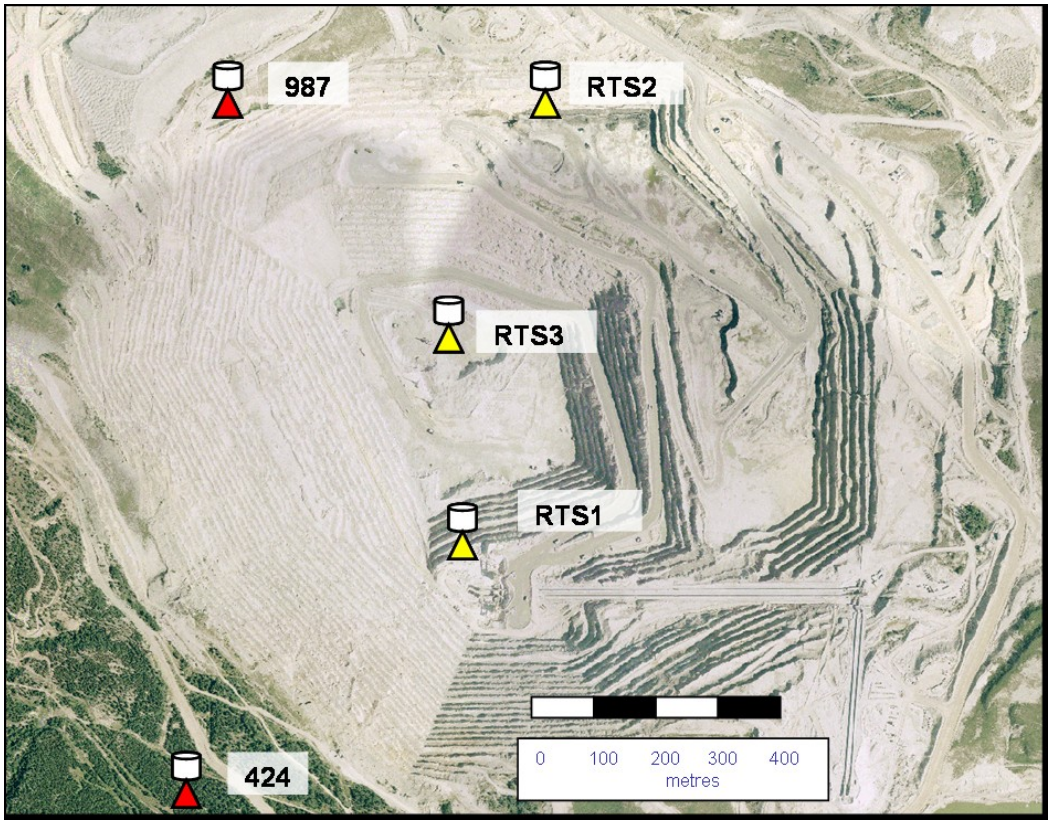

Figure 2.3: Station Locations

Table 2.1: GPS Baseline Lengths

From	To	Ellipsoidal Height Difference [m]	Slope Distance [m]
424	987	316	2534
424	RTS1	512	1426
424	RTS2	360	2538
424	RTS3	677	1876
987	RTS1	197	1291
987	RTS2	45	447
987	RTS3	361	921

The RTS 3 station was located at the bottom of the pit as a temporary set-up of RTS/GPS on a tripod (Figure 2.4). Of all the locations, this was the most inhospitable for collecting GPS data as the south pit wall of the pit created a natural mask angle of 30

degrees. Unfortunately, these lower elevation satellites that are masked are important for obtaining robust GPS solutions and for estimating tropospheric delay parameters [Langley, 1995]. Figure 2.5 and Figure 2.6 illustrate the satellite availability from stations RTS2 and RTS3 respectively. There are several instances during a 24 hour period in which satellite visibility drops to 3 satellites for RTS3, whereas there are typically more than 6 satellites visible from RTS2. Due to the height difference of 677m between RTS3 and reference station 424, one would expect that variations in local tropospheric conditions at antenna sites would cause biases that do not get eliminated through the double differencing process. Better results were expected to be obtained at the RTS2 location as the height difference between RTS2 and the reference station 987 was less than 100 m.

Figure 2.4: RTS+GPS Setup

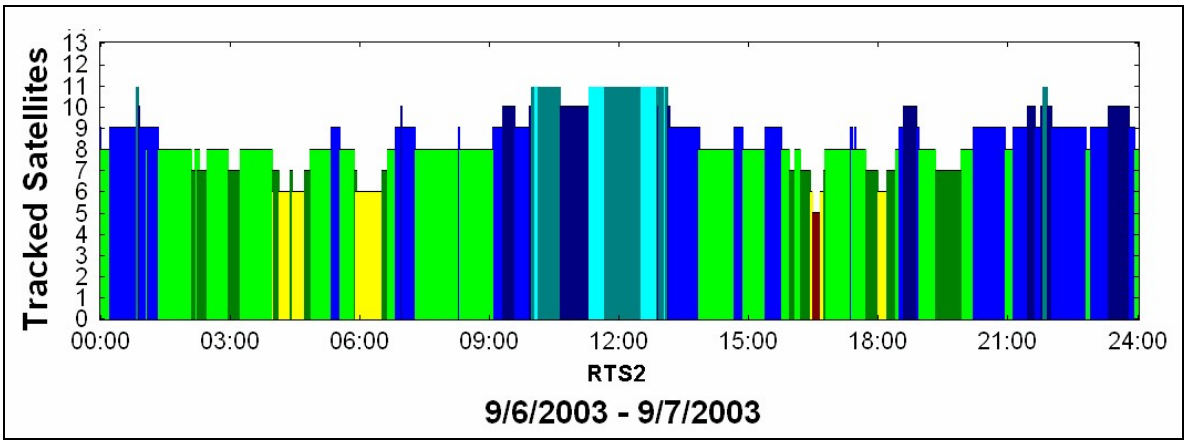

Figure 2.5: Satellite Visibility at RTS2

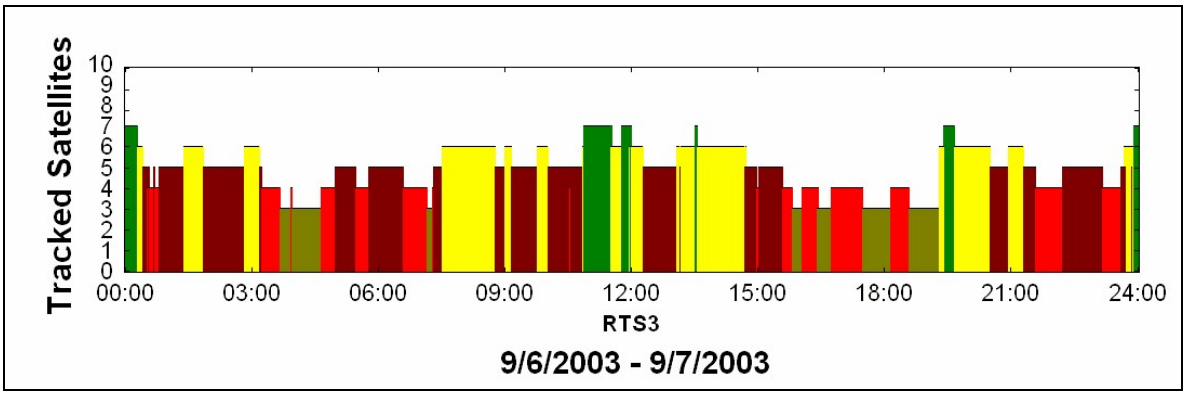

Figure 2.6: Satellite Visibility at RTS3

2.3 Evaluation of Test Results

A 5 day sample of GPS data was processed beginning at 0:00 Sept. 06, 2003 GPST (17:00 Sept. 05, 2003 MT - local time) for this analysis. Trimble Total Control (TTC) software, using a 10s sample rate, 10 degree elevation cut-off angle and Saastamoinen tropospheric model were selected for data processing based on findings by Bond [2004] in an evaluation of commercially available software. The discussion on the obtained

results is focused primarily on differences in ellipsoidal height components of the GPS solutions of three baselines: 424 to RTS3 and 987 to RTS3, which represent the worst case scenarios from each reference station, and the baseline from 987 to RTS2, which is the best case scenario of all the baselines observed.

Baselines were processed using 1, 3, 6, 12 and 24 hour session lengths. Figure 2.7, Figure 2.8 and Figure 2.9 illustrate the effect of session length on the quality of the obtained solution. Table 2.2 and Table 2.3 summarize the results for all baselines that were processed. A 'rejected session' represents a session in which a fixed solution could not be attained.

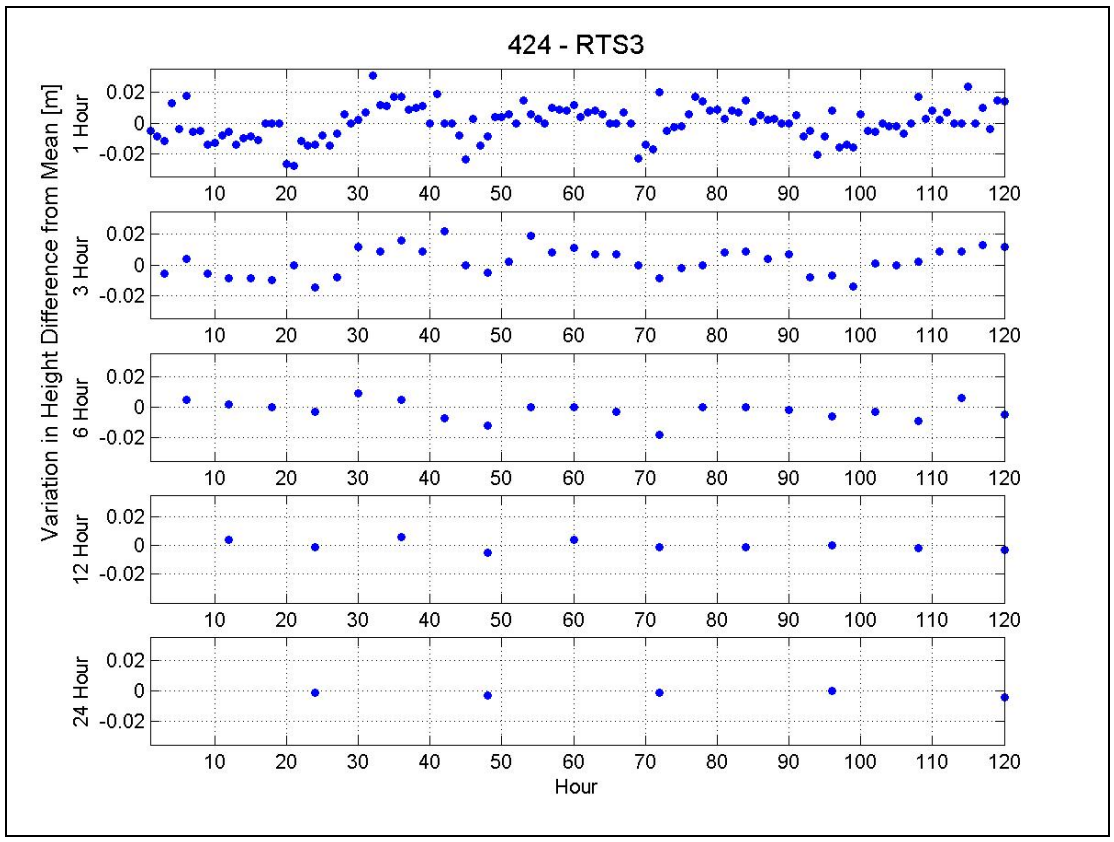

Figure 2.7: 424 – RTS3 Solutions

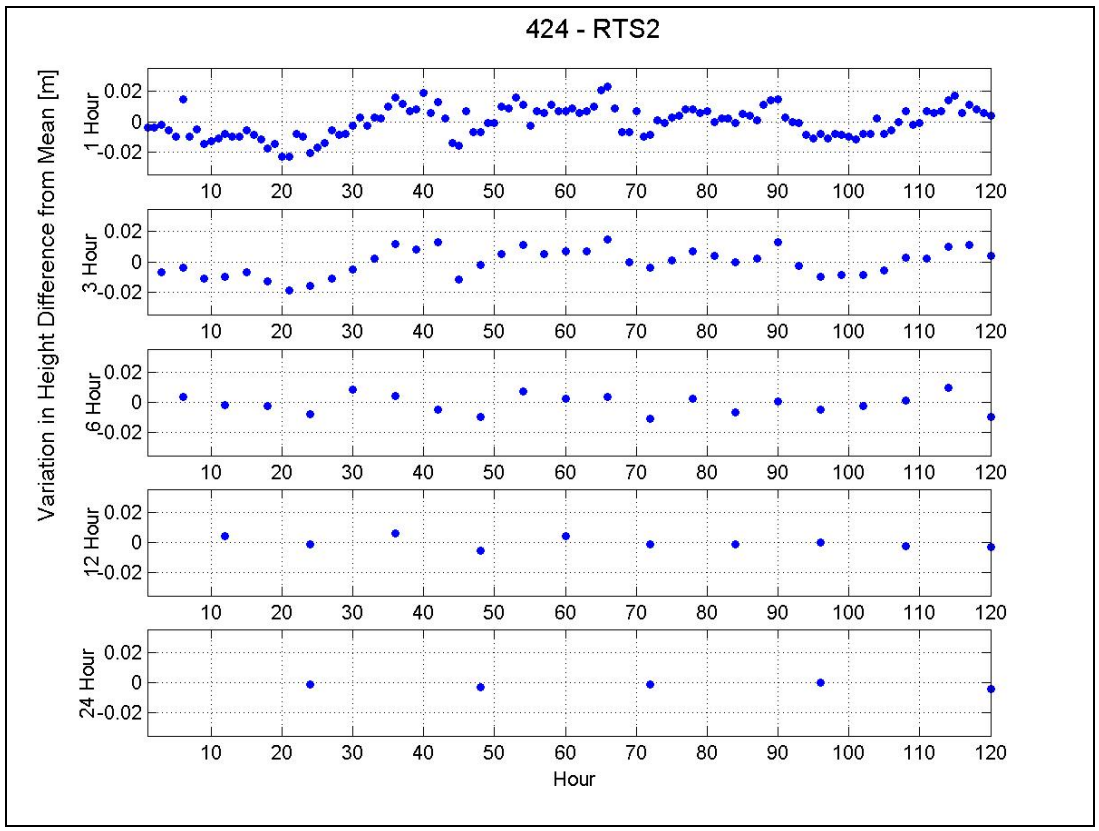

Figure 2.8: 424 – RTS2 Solutions

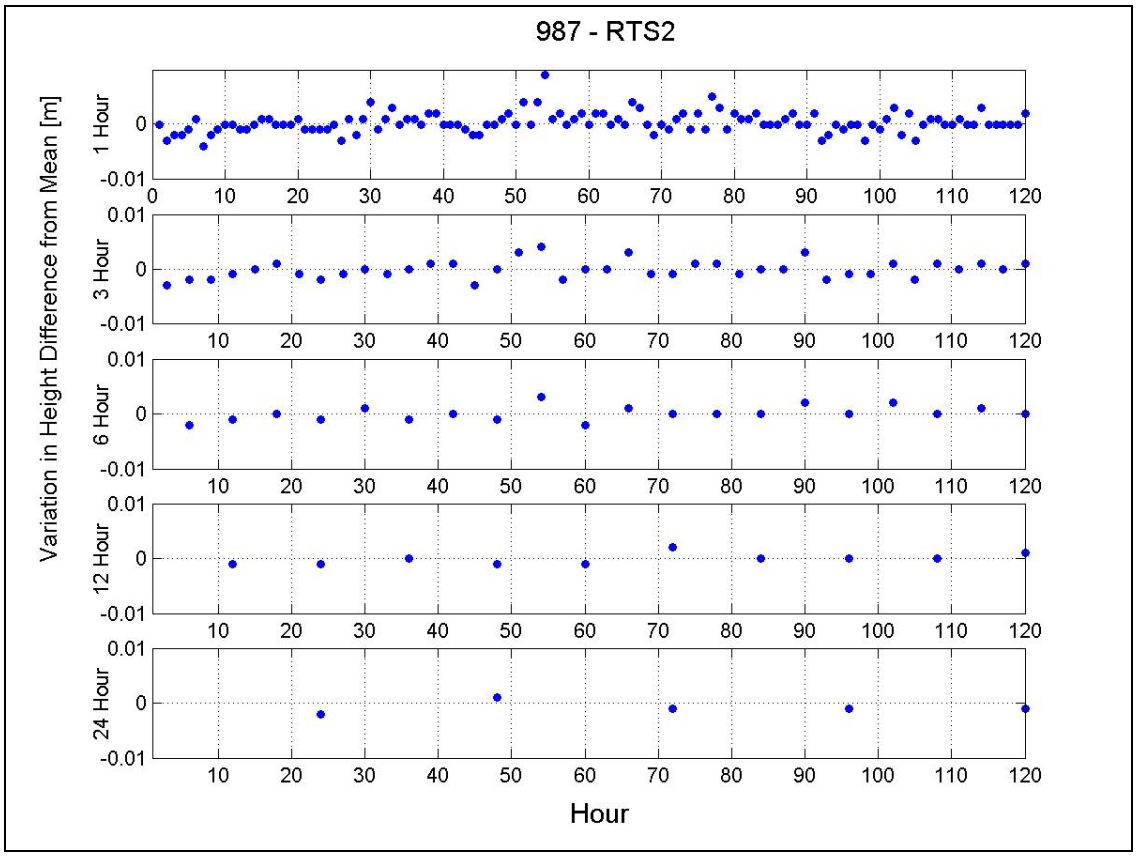

Figure 2.9: 987 – RTS2 Solutions

Table 2.2: Sample Standard Deviations of Baseline Components from 987

Sample Size	To Station	σ N [m]	σ E [m]	σ H [m]	Rejected Sessions
120, 1 Hour Sessions	RTS1	0.0029	0.0061	0.0069	0
	RTS2	0.0010	0.0012	0.0019	0
	RTS3	0.0029	0.0078	0.0077	14
40, 3 Hour Sessions	RTS1	0.0024	0.0023	0.0036	0
	RTS2	0.0007	0.0011	0.0016	0
	RTS3	0.0020	0.0032	0.0059	2
20, 6 Hour Sessions	RTS1	0.0022	0.0020	0.0028	0
	RTS2	0.0007	0.0011	0.0013	0
	RTS3	0.0019	0.0030	0.0078	0
10, 12 Hour Sessions	RTS1	0.0028	0.0022	0.0030	0
	RTS2	0.0007	0.0008	0.0010	0
	RTS3	0.0023	0.0025	0.0059	0
5, 24 Hour Sessions	RTS1	0.0020	0.0008	0.0020	0
	RTS2	0.0007	0.0011	0.0011	0
	RTS3	0.0015	0.0025	0.0042	0

Table 2.3: Sample Standard Deviations of Baseline Components from 424

Sample Size	To Station	σ N [m]	σ E [m]	σ H [m]	Rejected Sessions
120, 1 Hour Sessions	987	0.0041	0.0040	0.0085	0
	RTS1	0.0033	0.0037	0.0108	0
	RTS2	0.0042	0.0047	0.0099	0
	RTS3	0.0048	0.0082	0.0117	15
40, 3 Hour Sessions	987	0.0033	0.0034	0.0075	0
	RTS1	0.0026	0.0029	0.0114	0
	RTS2	0.0033	0.0043	0.0089	0
	RTS3	0.0032	0.0052	0.0094	2
20, 6 Hour Sessions	987	0.0030	0.0029	0.0059	0
	RTS1	0.0026	0.0020	0.0067	0
	RTS2	0.0029	0.0030	0.0062	0
	RTS3	0.0027	0.0033	0.0084	0
10, 12 Hour Sessions	987	0.0022	0.0027	0.0037	0
	RTS1	0.0018	0.0016	0.0049	0
	RTS2	0.0028	0.0035	0.0035	0
	RTS3	0.0018	0.0018	0.0076	0
5, 24 Hour Sessions	987	0.0018	0.0019	0.0023	0
	RTS1	0.0016	0.0016	0.0044	0
	RTS2	0.0024	0.0028	0.0024	0
	RTS3	0.0018	0.0015	0.0029	0

As expected, from Table 2.2 and Table 2.3 one can see that, in most cases, a longer session length improves the quality of result. This is particularly true for baselines having height differences larger than a hundred metres. For baselines with stations having roughly the same height (i.e. 987 to RTS2), there is no appreciable improvement in the quality of the solutions when the session length is increased above 3 hours. However, a difficulty associated with increasing session length is that it reduces the ability of the monitoring system to provide 'real-time' results. In the extreme cases, having to wait 24 hours for an update may not be suitable for the monitoring application. Therefore, more frequent sessions are preferable.

To summarize the results given in Table 2.2 and Table 2.3, the following points are noted:

1. None of the solutions for the baselines 424-RTS3 and 987-RTS3 could satisfy the requirement of achieving the standard deviation ≤ 2.5 mm for each of the three baseline components when using the standard processing techniques with commercial software. The northing and easting components could be determined with the required accuracy when using at least the 12 hour session length.
2. For baseline 987-RTS2, which has a height difference of less than 100 m and good satellite visibility, standard deviations of 2 mm or better are achievable in all three solution components when using 1 hour solutions.
3. The baseline components of 987 to RTS1 (Δh = 197 m) can be determined with standard deviations ≤ 3 mm in all three components when using 6 hour session lengths.
4. For all the baselines, the sample standard deviation of the baseline components can be determined to ≤ 5 mm in all three components using 24 hour session lengths. For the baselines involving RTS3 and the reference stations, the 24 hour session length is the only session that gives a sample standard deviation of ≤ 5 mm for the height component.

The above results indicate that the quality of the solutions deteriorate with the increase in height difference between the baseline stations. This strongly points to the possibility of the tropospheric delay not being adequately modeled when large height

differences exist. Therefore, residual tropospheric delay becomes one of the dominant error sources contaminating the final baseline results.

2.4 Residual Tropospheric Delay

In the Saastamoinen tropospheric model (used in the processing of the test data) as well as in other commonly used models (such as Hopfield, Lanyi, Chao), measured values of meteorological conditions (temperature, T, pressure, P and water vapour pressure, e) are assumed to be available at the GPS receiver site. If this is not the case, profile functions are frequently used to determine these variables as a function of the height above mean sea level [Rizos, 1999b]. Thus for two static stations, the differences in atmospheric conditions and, consequently, the refractivity difference between stations are assumed to be constant.

The meteorological data collected at stations 424 and RTS2 is illustrated in Figure 2.10. Although the figure shows good agreement in the pattern of changes in temperature, barometric pressure, and partial water vapour pressure at both stations, it is apparent that the differences are not constant (Figure 2.11).

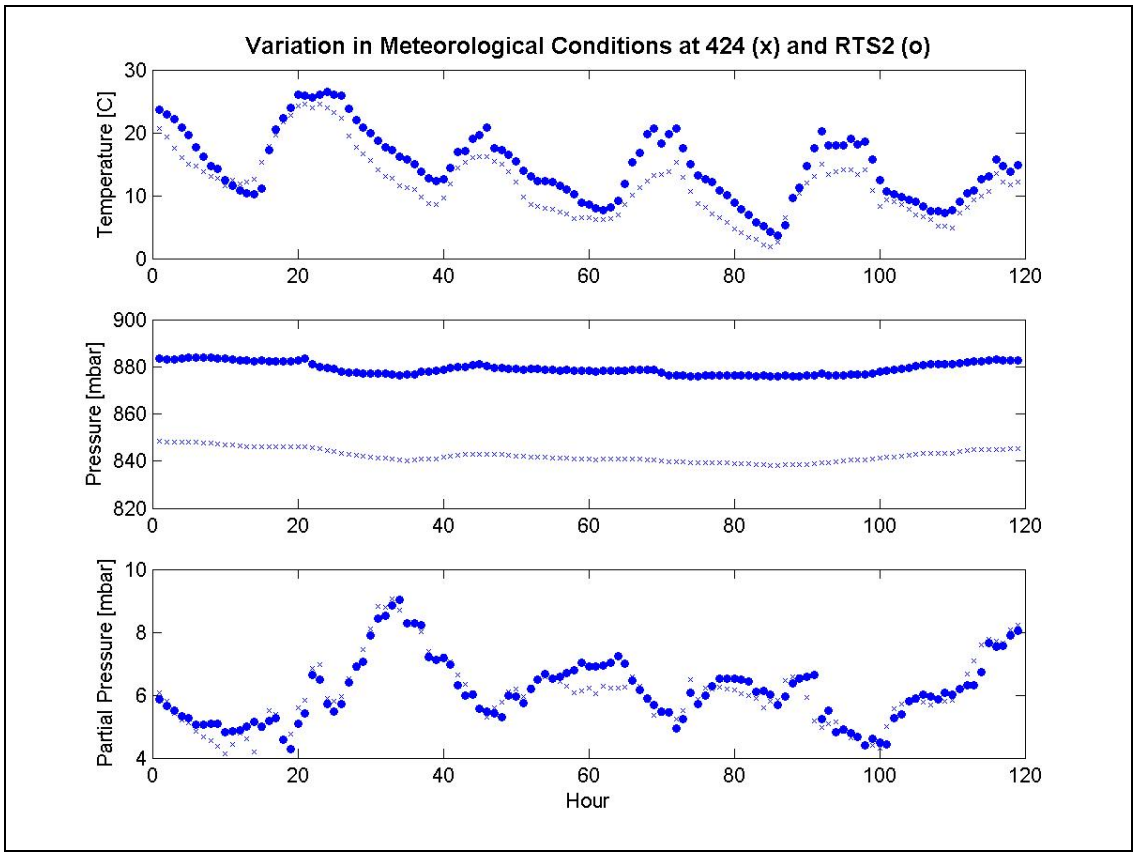

Figure 2.10: Meteorological Observations at 424 and RTS2

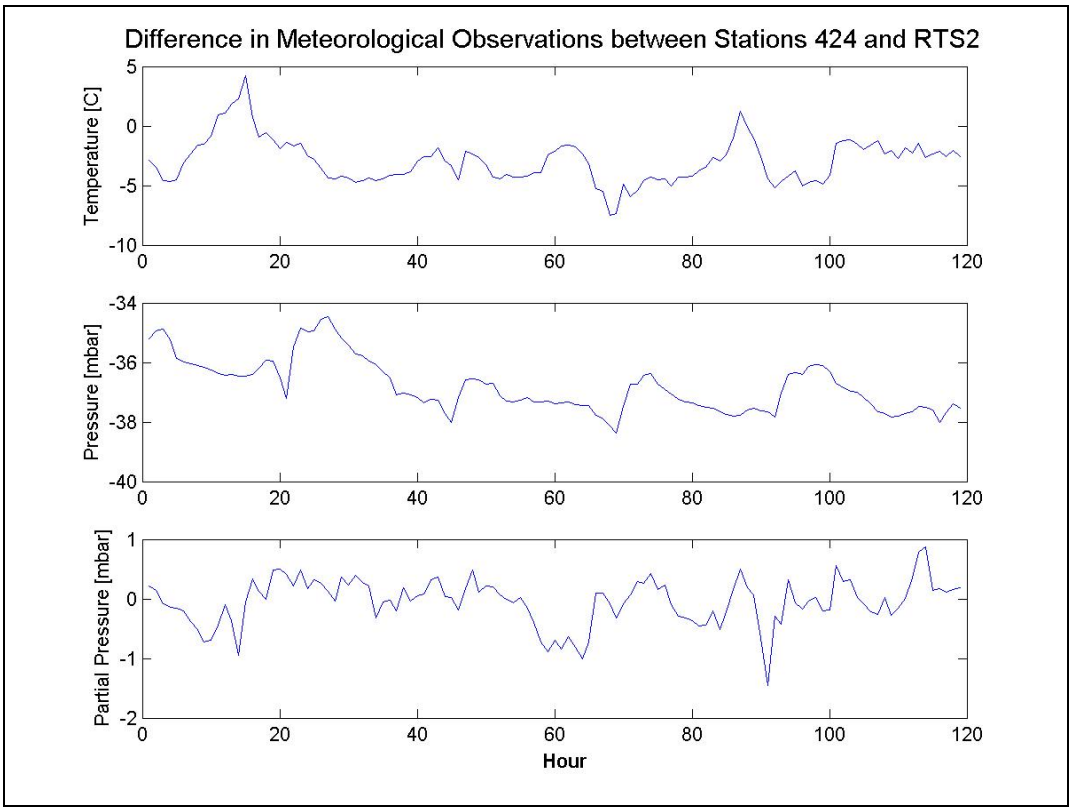

Figure 2.11: Difference in Meteorological Observations between 424 and RTS2

The tropospheric refractivity, *N*, which is used in the determination of the delay of microwave signals, can be calculated from the modified Essen and Froome formula [Rüeger, 1990]:

$$N = (n-1)10^6 = 77.624\frac{P-e}{T} + \frac{64.70}{T}\left(1+\frac{5748}{T}\right)e \qquad (2.1)$$

where :

n	refractive index
T	absolute temperature of air in [K]
P	barometric pressure in [mb]
e	partial water vapour pressure in [mb]

By differentiating Equation (2.1) with respect to T, P and e, one can calculate the change in refractivity, dN, as a function of changes in T, P, and e (dT, dP and de) for given meteorological conditions. Taking average values of T = 288 K, P = 850 mb, and e = 7 mb over this 5 day period, one obtains:

$$dN = -1.0dT + 0.27dP + 4.5de \tag{2.2}$$

Figure 2.11 shows that during the test period, temperature differences between the two stations reached deviations from the mean difference of up to 7 ^{o}C in temperature, 2 mb in barometric pressure, and 1.5 mb in partial water vapour pressure. Since a change in N corresponds to a change in the zenith distance (in ppm), the shown variations in differences of dT , dP, and de could result in the zenith delay changes of 7 ppm, 0.5 ppm, and 6.8 ppm respectively. For the height difference of 360 m between 424 and RTS2, the above values translate into 2.5 mm, 0.1 mm, and 2.4 mm of zenith delay.

Using Equation (2.2) and the collected meteorological data, the total differences dN between stations 424 and RTS2 were calculated. Figure 2.12 portrays the differences in

refractivities between the two stations and the variation of the height solution over the same time period.

Considering the data in Figure 2.12, it can be seen that there are differences in refractivity of about 14 ppm over this 360 m column of air. This causes a difference in zenith delay of about 5 mm for the height component of this baseline.

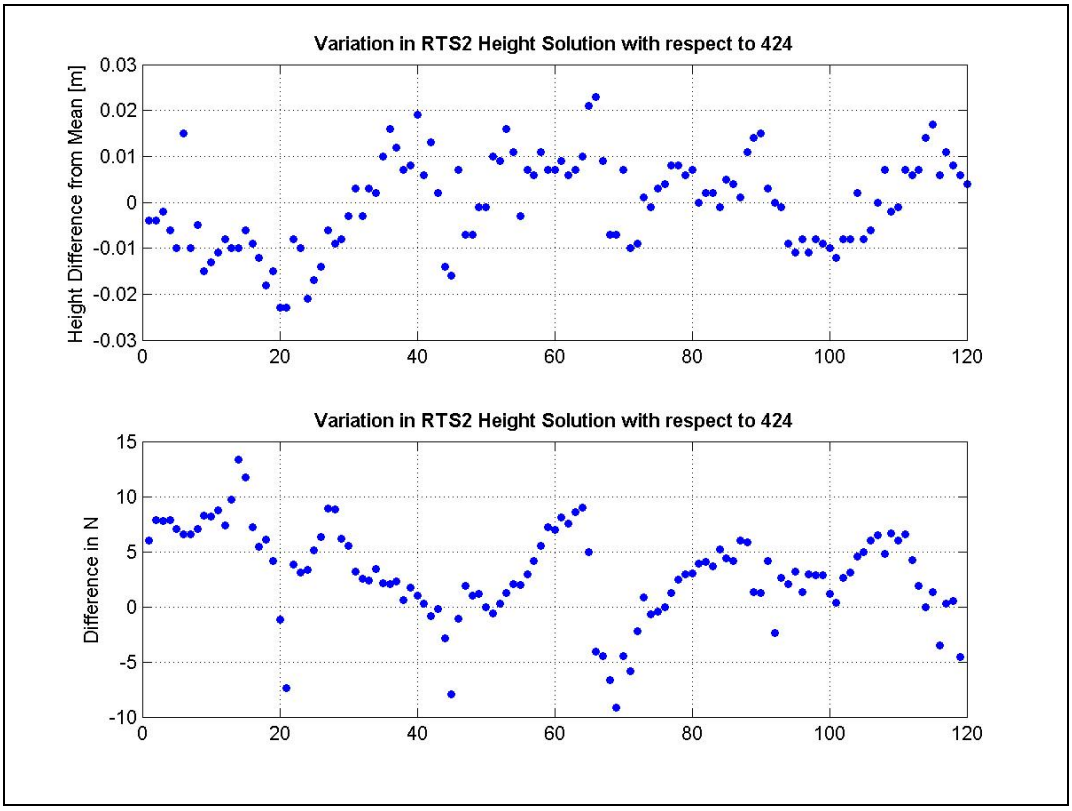

Figure 2.12: Variation in Height Solution and Refractivity, 424 – RTS2

Beutler et al. [1988], have shown that the effect of the differential troposphere can cause a relative height error, Δh_e, calculated to a first approximation for local networks as:

$$\Delta h_e = \Delta d^2 \sec(\Phi_{\max}) \qquad (2.3)$$

where:

Δd the difference in zenith delay between co-observing stations and
$\Phi_{\max}$ the maximum zenith angle observed.

This equation implies that neglecting the differential troposphere causes a 3 to 5 mm relative height error for every millimetre difference in zenith delay between stations. In other words, a 1 mm differential tropospheric bias causes a height error of 3 to 5 mm. Thus, the calculated variation of 14 ppm in refractivity differences between stations 424 and RTS2 could cause variations in the height solution of between 15 to 25 mm. This compares very well with the variations shown in Figure 2.12.

2.5 Improving GPS Results

It can be clearly seen from Figure 2.12 that there is a correlation between some of the crests and troughs between the plots of variations of RTS2 height solution and the variation in the refractivity differences. The variation in the height solution of RTS2 shows a cyclic pattern over this 5 day period. It should be noted that the satellite constellation also contributes to this cyclicity as the satellites repeat their orbits every sidereal day. It was attempted to fit a cyclic function with a 24 hour period to the height

solutions through least squares, from which standard deviations were calculated. There was not a significant improvement in the results using this approach.

Several strategies have been devised for improving the results attained through standard GPS processing techniques (correlating the day-to-day repeatability of multipath, estimating residual tropospheric delay parameters, and recording and using meteorological data). The potential of improving the results through using these techniques was investigated. Similarly, with respect to hardware, new technologies (e.g., pseudolites, GPS+GLONASS enabled receivers) have been introduced to improve GPS results. These technologies were also investigated and assessed for their potential benefits in this situation [Bond, 2004]. The CCGE is currently further investigating the use of pseudolites for deformation monitoring purposes in an open pit mine environment.

Additionally, the CCGE has recently implemented a 'smarter' filtering approach for obtaining GPS solutions. The current strategy uses an optimized filter to estimate the change in baseline components of each RTS relative to a base station. Depending on the conditions and the situation, either triple or double differencing of observations can be utilized in the solution. Preliminary results indicate that trends in the RTS position can easily be identified at the millimetre level. Research at the CCGE is ongoing in the testing and implementation of this technique for use in the ALERT software suite for the automated displacement monitoring. The initial results are encouraging.

2.6 Conclusions

From the presented results it is apparent that it is very difficult to obtain standard deviations ≤ 2.5 mm in the GPS solution components in the open pit mine environment. In order to achieve the accuracy requirements for this project without using special processing techniques, differences in height between baseline stations must be restricted to 100 m or less.

If the ultimate goal of +/- 5 mm displacement detection at 95% confidence is to be achieved, the limitations in such a GPS environment (namely poor satellite visibility and residual tropospheric delay biases) must be addressed. The CCGE is in pursuit of a more sensitive GPS displacement detection mechanism through an optimal filtering approach as well as investigating the use of pseudolites as an augmentation system.

Acknowledgements

This research was funded by the Natural Sciences and Engineering Research Council of Canada.

References

Beutler, G., I. Bauersima, W. Gurtner, M. Rothacher, T. Schildknecht and A. Gieger (1988). "Atmospheric refraction and other important biased in GPS carrier phase observations." *Atmospheric Effects on Geodetic Space Measurements*, Monograph 12, School of Surveying, University of New South Wales, pp.15-43.

Bond, J. (2004). *An Investigation on the Use of GPS for Deformation Monitoring in Open Pit Mines*. MScE thesis, Department of Geodesy and Geomatics Engineering, University of New Brunswick, Fredericton, New Brunswick, Canada, 140 pp.

Chen, Y.Q., A. Chrzanowksi, and J.M. Secord (1990). "A Strategy for the Analysis of the Stability of Reference Points in Deformation Surveys." *CISM Journal*, Vol. 44, No.2, Summer, pp. 39-46.
Available at: http://ccge.unb.ca/publications/all_publications.php, accessed on: 3 October 2007.

Duffy, M., C. Hill and C. Whitaker, A. Chrzanowksi, J. Lutes and G. Bastin (2001). "An Automated and Integrated Monitoring Program for Diamond Valley Lake in California." Proceedings of the *10th FIG International Symposium on Deformation Measurements*, Orange, CA, March 19-22, 2001, CDROM, 21 pp. Available at: http://ccge.unb.ca, accessed on: 3 October 2007.

Langley, R.B. (1995). "Propagation of the GPS Signals." Chapter 3 of *GPS for Geodesy*, Proceedings of the *International School of GPS for Geodesy*, Delft, the Netherlands, March 26 - April 1, pp. 111-185.

Mining Technology (2003). "Highland Valley Copper Mine, Canada." *The Website for the Mining Industry.* Available at:
http://www.mining-technology.com/projects/highland/index.html, accessed on: 12 December 2003.

Rizos, C. (1999b). "Measurement Biases and Errors: Tropospheric Delay." *Principles and Practice of GPS Surveying*. Available at:
http://www.gmat.unsw.edu.au/snap/gps/gps_survey/principles_gps.htm, accessed on: 3 October 2007.

Rüeger, (1990). *Electronic Distance Measurement*. 3rd ed., Springer-Verlag, Berlin Heidelberg, 266 pp.

Wilkins, R., G. Bastin, A. Chrzanowski, W. Newcomen and L. Shwydiuk (2003a). *A Fully Automated System for Monitoring Pit Wall Displacements*. Paper presented at SME 2003, Cincinnati, OH, February 24-26, 2003. Available at: http://ccge.unb.ca, accessed on: 3 October 2007.

Wilkins, R., G. Bastin and A. Chrzanowski (2003b). *ALERT—A fully automated real-time monitoring system*. Proceedings of the *11th FIG Symposium on Deformation Measurements*, May 25-28, Santorini, Greece. Available at: http://ccge.unb.ca, accessed on: 3 October 2007.

CHAPTER 3
BRINGING GPS INTO HARSH ENVIRONMENTS FOR FULLY AUTOMATED DEFORMATION MONITORING

Jason Bond, Adam Chrzanowski and Don Kim
University of New Brunswick, Fredericton New Brunswick Canada

The following was originally published as:

Bond, J., A. Chrzanowski, and D. Kim (2007). "Bringing GPS into Harsh Environments for Deformation Monitoring." *GPS Solutions* (online first status), 11 pp. Available at: http://www.springerlink.com/content/21v2625p46108266/fulltext.pdf, accessed on: 4 October 2007. DOI 10.1007/s10291-007-0059-7

The first author has developed the algorithms to process the data collected, designed the experiments, processed the data, compiled the results and prepared the manuscript. The second author has provided advice on paper content and insight into the theoretical background of deformation monitoring. The third author has provided advice on paper content and insight into the theoretical background of GPS and Kalman filtering.

Abstract

Engineering projects that require deformation monitoring frequently utilize geodetic sensors to measure displacements of target points located in the deformation zone. In situations where control stations and targets are separated by a kilometer or more, GPS can offer higher precision position updates at more frequent intervals than can normally be achieved using total station technology. For large scale deformation projects requiring the highest precision, it is therefore advisable to use a combination of the two sensors.

In response to the need for high precision, continuous, GPS position updates in harsh deformation monitoring environments, software has been developed that employs triple-differenced carrier-phase measurements in a Delayed-State Kalman filter. Two data sets were analyzed to test the capabilities of the software. In the first test, a GPS antenna was displaced using a translation stage to mimic slow deformation. In the second test, data collected at a large open pit mine was processed.

It was shown that the Delayed-State Kalman filter developed could detect millimeter level displacements of a GPS antenna. The actual precision attained depends upon the amount of process noise infused at each epoch to accommodate the antenna displacements. Higher process noise values result in quicker detection times but at the same time increase the noise in the solutions. A slow, 25 mm displacement was detected within 30 minutes of the full displacement with sigma values in E, N and U of ± 10 mm or better. The same displacement could also be detected in less than 5 hours with sigma values in E, N and U of ± 5 mm or better. The software works best for detecting long period deformations (e.g., 20 mm per day or less) for which sigma values of 1 - 2 mm are attained in all three solution components. It was also shown that the triple-differenced carrier-phase observation can be used to significantly reduce the effects of residual tropospheric delay that would normally plague double-differenced observations in harsh GPS environments.

3.1 Introduction

Disasters resulting from the collapse of steep embankments or structures (e.g., avalanches, mudslides, dam failure, collapsing of roofs) do not occur without warning. Strategic monitoring in a hazardous area can create an awareness of any impending danger, resulting in quicker emergency response times and disaster prevention. The Canadian Centre for Geodetic Engineering's fully automated deformation monitoring system, ALERT, has been implemented worldwide for such purposes [Wilkins et al. 2003].

The ALERT system uses robotic total station (RTS) instruments with automatic target recognition as its primary sensors. RTS instruments are presently the most economical method of monitoring displacements when hundreds of target points must be observed in the deformation zone. This approach, however, has its limitations.

When distances between total stations and targets increase, the effects of atmospheric refraction biases and pointing errors become dominant [Chrzanowski and Wilkins, 2006]. If sight lengths are too long, these error sources will result in accuracy requirements not being met. In order to optimize the accuracy, it is not uncommon to place the RTSs within the deformation zone so that they are as close as possible to the targets [Bond et al., 2005]. In such cases, the use of GPS to monitor the stability of the RTSs is recommended. GPS allows the RTSs to be connected to stable reference points while

avoiding these concerns. Implementing GPS for this purpose, however, poses its own challenges.

Discussed is a response to the need for the development of robust, GPS software to provide high precision, fully automated position updates for the purpose of deformation monitoring. Requirements for the system are listed and challenges associated with meeting them are given. Test results are presented demonstrating the advantages of this approach over traditional batch processing methods.

3.2 System Requirements

To meet the needs of deformation monitoring applications, the developed system should have the following characteristics:

a) Fully automated: Position updates must be provided without human intervention. Intelligence must be instilled in the system so that it can handle contingencies (e.g., power outages, poor data and sudden displacements).

b) On-time updates: The user must be made aware of unexpected structural behavior as quickly as possible so that notice can be given of impending danger. The

system must be capable of providing deformation information at regular intervals as dictated by project specifications.

c) Robust: False alarms cannot be tolerated. Quality assurance/quality control measures must be reliable so that there is confidence in the system.

d) High precision: Displacements encountered in deformation monitoring are frequently at the sub-centimeter level. Since the practical resolution of an undifferenced GPS carrier-phase measurement is approximately 2 mm (1% of the L1 carrier wavelength of 0.190 m), monitoring millimeter level displacements in near real time pushes the limits of the system. If millimeter level precision is to be achieved, meticulous effort and care must be devoted to handling all error sources.

3.3 Challenges in Meeting Requirements

Achieving reliable, millimeter level precision in 'real time' using GPS is challenging in favorable monitoring conditions. Attempting to do the same in harsh environments is even more difficult. Presented are some of the challenges faced in designing a system that meets deformation monitoring needs, as were discussed in Kim et al. [2003].

3.3.1 Satellite Visibility

In deformation monitoring environments where there are obstructions hindering satellite visibility (e.g., dams, open pit mines, buildings), dilution of precision values rise due to the degradation in satellite geometry. The system must be able to cope with periods of the day during which there are too few satellites visible to provide a high enough quality solution to meet project requirements.

3.3.2 Residual Tropospheric Delay

In deformation monitoring environments where there are significant changes in elevation (e.g., open pit mines, volcanoes), residual tropospheric delay can cause significant positioning biases, especially in height. The differential troposphere causes a 3 to 5 mm relative height error for every millimeter difference in zenith delay between stations [Beutler et al., 1988]. Residual tropospheric delay must be accounted for if the desired precision is to be achieved.

3.3.3 Multipath

In deformation monitoring environments where multipath sources are abundant (e.g., building structures, vehicles) multipath can contaminate the position solutions. Practically every observation site is affected to some degree by multipath. Multipath biases can reach up to $\lambda/4 \approx 4.8$ cm for the original L1 carrier-phase measurement [Leick, 1994].

3.3.4 Providing On-time Information

Deformation monitoring poses a unique GPS scenario; the points of interest are neither quite static nor kinematic because there is motion but it is usually very small. In providing GPS position updates, it cannot be assumed that the antenna's position at an epoch agrees with that of a prior epoch. One way to handle this is to model the motion as static and to add process noise.

3.4 PPMS Software Description

With regard for the above mentioned requirements and concerns, software is being developed to provide high precision position updates in the harshest deformation

monitoring environments. Some of the details of PPMS (Precise Position Monitoring System) are presented. Future work will be devoted to making the software fully automated.

3.4.1 Choice of Observable

The double-differenced (DD: differencing between receivers followed by differencing between satellites or vice versa), ambiguity-fixed, carrier-phase observation is the most commonly used GPS measurement for high precision applications. This observation type allows for quick convergence on a solution once the ambiguity term has been resolved. The ambiguity term is always present, however, which leaves the possibility of false alarms caused by poorly handled cycle slips.

Remondi [1984] demonstrated the potential for using the triple-differenced (TD: differencing consecutive DD observations) observable as an alternative method of obtaining high precision. Despite introducing another level of differencing which increases the observation noise, the TD approach offers several advantages over the DD, ambiguity-fixed observable which make it an attractive alternative. After removing the error terms for receiver clocks and satellite clocks (which should be eliminated through DD processing when observation simultaneity criteria are met), the TD, carrier-phase observable between times t_1 and t_2 can be written as:

$$\delta \underset{AB}{\Delta} \overset{ij}{\nabla} \varphi(t_{12}) = [\underset{AB}{\Delta} \overset{ij}{\nabla} (\varphi + N + M - \frac{f}{c} I + \frac{f}{c} T + e_{\varphi}) + \varepsilon_{trop}]_{t_2} - [\underset{AB}{\Delta} \overset{ij}{\nabla} (\varphi + N + M - \frac{f}{c} I + \frac{f}{c} T + e_{\varphi}) + \varepsilon_{trop}]_{t_1} \quad (3.1)$$

where:

$\overset{ij}{\nabla}$	single-difference (SD) operator between satellites *i* and *j*
$\underset{AB}{\Delta}$	SD operator between receivers *A* and *B*
δ	SD operator between times t_1 and t_2
φ	carrier-phase observable (cycles)
N	ambiguity (cycles)
M	multipath (cycles)
I	ionospheric delay of the L1 carrier phase (m)
T	tropospheric delay (m)
f	carrier wave frequency (Hz)
c	speed of light in a vacuum (m/s)
ε_{trop}	residual tropospheric delay bias (present over large height differences) (cycles)
e_{φ}	random carrier-phase measurement noise

The TD approach can be considered an extension of the observation difference, least squares approach used for processing deformation monitoring data [Wilkins et al., 2003c]. The attractiveness of the TD observation is that it is a time difference of DD observations and consequently any biases common to both observations will be highly correlated and therefore significantly reduced. This strategy has some important benefits:

a) The user no longer needs to solve for the ambiguity term, which allows the system to be more robust;

b) For observation intervals less than a few seconds, the correlation between atmospheric parameters between times t_1 and t_2 will be large and therefore biases

originating from them will be significantly reduced. This is useful for dealing with residual tropospheric delay biases over large height differences;

c) For observation intervals less than a few seconds, the correlation in the low frequency component of multipath terms at times t_1 and t_2 will be large and therefore biases originating from them will be significantly reduced. The high frequency component still remains.

Equation (3.1) can now be rewritten as:

$$\delta \underset{AB}{\Delta} \overset{ij}{\nabla} \varphi(t_{12}) = [\underset{AB}{\Delta} \overset{ij}{\nabla}(\varphi + M)]_{t_2} - [\underset{AB}{\Delta} \overset{ij}{\nabla}(\varphi + M)]_{t_1} + e_{\delta\Delta\nabla\varphi} \qquad (3.2)$$

Where:

$e_{\delta\Delta\nabla\varphi}$ random noise error of a TD carrier-phase observation

From Equation (3.2) it can be seen that through the differencing process, most major error sources can be significantly reduced so that main remaining sources of error are the random noise error inherent in the TD observable and the high frequency component of multipath. The major disadvantage of the TD approach is that it requires a longer convergence time than for DD processing.

3.4.2 Processing Engine

Batch processing involves the estimation of a static set of unknown parameters. Each set of observations is used to provide a better estimate of the same quantities. Deformation monitoring requires an awareness of the current state of the deformable body rather than an overall average of all previous states. Kalman filtering or modified sequential least squares data processing techniques are preferable since they are able to provide a snapshot image of the current state of the unknown parameters (In this case the same results can be achieved using Kalman filtering and sequential least squares by introducing process noise into the sequential least squares solution, since there are no dynamics in the transition matrix).

The TD observation is an integrated velocity over some time interval, Δt. Model and measurement situations of this type fit the Delayed-State form [Brown and Hwang, 1997]:

$$z_k = H_k x_k + J_k x_{k-1} + v_k ; E[v_k v_k^T] = R_k \tag{3.3}$$

$$x_{k+1} = \phi_k x_k + w_k ; E[w_k w_k^T] = Q_k \tag{3.4}$$

where:

x_k	process state vector at time t_k (x, y, z coordinates of the station)
ϕ_k	transition matrix at time t_k(identity matrix- no dynamics)
w_k	model error at time t_k (white sequence)
z_k	TD observations at time t_k
H_k	DD design matrix at time t_k
J_k	negated DD design matrix at time t_{k-1} *
v_k	observation error at time t_k (white sequence)

* The TD design matrix is the difference of the current and previous DD design matrices. The x, y, z coordinates of the station are treated as constant when populating these matrices. The computed TD observations depend upon the changes in satellite geometry from t_{k-1} to t_k. Over high sample rates these values will be small so care must be taken to carry sufficient precision.

The Delayed-State recursive equations are presented in Table 3.1.

Table 3.1: Delayed-State Equations
[Brown and Hwang, 1997]

Estimate update: Where:	$x_k = x_k^- + K_k(z_k - \hat{z}_k^-)$ $\hat{z}_k^- = H_k \hat{x}_k^- + J_k \hat{x}_{k-1}$
Gain: Where:	$K_k = [P_k^- H_k^T + \phi_{k-1} P_{k-1} J_k^T] L_k^{-1}$ $L_k = H_k P_k^- H_k^T + R_k + J_k P_{k-1} \phi_{k-1}^T H_k^T + H_k \phi_{k-1} P_{k-1} J_k^T + J_k P_{k-1} J_k^T$
Error Covariance Update:	$P_k = P_k^- - K_k L_k K_k^T$
Predictions:	$\hat{x}_{k+1}^- = \phi_k \hat{x}_k$ $P_{k+1}^- = \phi_k P_k \phi_k^T + Q_k$

The Delayed-State Kalman filter implemented is built upon that introduced by Remondi and Brown [2000]. The major difference in the two filters lies in their approaches to handling observation and process noise. Remondi and Brown [2000] estimate the noise as Gauss-Markov parameters. The approach used in PPMS is to estimate each satellite's carrier-phase observation noise to populate the R_k matrix. This is

accomplished by using the time-differenced, geometry-free (GF: differencing between L1 and L2 in the distance unit) SD (between receivers) of each satellite as a measure of the satellite's current noise state. Because the GF combination is used, antenna dynamics are eliminated from the noise estimation process.

The approach employed corresponds to high-pass filtering, as most low-frequency errors in the carrier-phase measurements are significantly reduced. Satellite clock errors are eliminated through the between receivers SD. Tropospheric delay biases are eliminated through the GF combination. Ionospheric delay biases are significantly reduced through the SD process. Between epochs time-differencing further reduces the effects of ionospheric delay and significantly reduces any low frequency component multipath biases. The remaining measurement noise, thermal noise of the receiver and high frequency component multipath biases are used as a measure of the satellite's current noise state. A moving average window is then used to improve the estimate based upon the past n measures of noise, where n is the window size.

The Q_k matrix is a diagonal matrix of Q values. The Q value is a noise parameter that is used to accommodate the expected velocity of the antenna. It dictates how quickly the filter responds to displacements by changing the weight placed on previous solutions and current observations. There is no single correct Q value. Rather, the Q value chosen is dependent upon the magnitude of the expected displacements, the length of time over

which the displacement occurs, the sample rate of the observations and the delay in detection time that can be tolerated.

For example, if one anticipates a 0.005 m displacement in 10 seconds, the sample rate is 10 seconds and the displacement must be detected immediately, then a Q value of $(0.005\ \text{m})^2$ may be appropriate. If a 30 minute delay in detection time can be tolerated then, a Q value of $(0.005\ \text{m})^2 / 1800\ \text{s} / 10\ \text{s} = (0.37\ \text{mm})^2$ may be used. Using a larger Q value increases the size of the minimum detectable bias (MDB). Consequently, there is a tradeoff between detection time and MDB. Alternatively, if the Q value is too small, the filter will not be able to track the displacements and will diverge.

From a theoretical standpoint, the performance of the filter may not be optimal. This is due to the fact that there are potentially non-white components in the observation noise matrices caused by small residual biases that may have not been eliminated through differencing. In practicality, the filter has demonstrated good results.

3.4.3 Cycle Slip Detection

Even though the TD observable eliminates common integer ambiguities, cycle slips still need to be identified and removed to prevent outliers from existing in the observations. The approach used here is based upon that of Kim and Langley [2002]

which allows for instantaneous, real-time cycle-slip detection. The GF, TD observations are compared against a cycle slip threshold. Observations exceeding this threshold are discarded.

3.4.4 Outlier Detection

PPMS currently utilizes an often used "rule of thumb" in detecting outliers that rejects any observation with a residual exceeding 3 times the standard deviation of the observations [Rizos, 1999c]. The software is currently being modified to allow for a more sophisticated outlier detection mechanism that compares the predicted and computed residuals of the Kalman filter [Teunissen, 1998].

3.5 Tests

Two data sets are presented to illustrate the performance of the software. The first data set was observed on the roof of Head Hall at the University of New Brunswick. A translation stage was used to introduce displacements to the rover antenna to determine the sensitivity of the filter. The second data set comes from a large open pit mine, representing a harsh GPS environment. NovAtel DL4 receivers with GPS-600 Pinwheel antennas were used in all tests.

Data were processed using PPMS implementing a 10º elevation cut-off angle and the UNB3 tropospheric model (Saastamoinen zenith delay with lookup tables) with Niell mapping functions [Collins and Langley, 1999]. Results were compared with DD, ambiguity-fixed solutions from commercial software using the same elevation cut-off angle and Saastamoinen tropospheric model with unknown mapping functions. The sample rate for both data sets was 10 seconds.

3.5.1 Translation Stage Test

Using a translation stage to mimic slow displacements caused by deformation, a short baseline (~20 m) was observed to gain an appreciation for the sensitivity of the filter (see Figure 3.1). Approximately 20 hours of data were collected before moving the antenna. Table 3.2 illustrates the sequence of displacements introduced using the translation stage. Data were processed using different Q values to illustrate the impact of this matrix on the solutions.

Figure 3.1: Translation Stage Test

Table 3.2: Displacements Introduced with Translation Stage

Elapsed Time [Hours]	Displacement Introduced [mm] (Total)	Displacement Time [s]
20:00:00	2 (2)	10
20:31:50	2 (4)	10
21:00:00	2 (6)	10
21:25:00	2 (8)	10
22:30:00	2 (10)	10
23:00:00	5 (15)	25
23:32:00	5 (20)	25
24:00:00	5 (25)	25

3.5.1.1 Translation stage results

In this test, displacements of magnitude 2 mm and 5 mm were introduced. The 2 mm displacements occur over a 10 second period and the 5 mm displacements occur over a 25 s period. The duration between displacements is approximately 30 minutes. In the first case, a Q value was chosen to accommodate 5 mm displacements every 30 minutes (Q = $(5\text{ mm})^2$ / 1800 s / 10 s = $(0.4\text{ mm})^2$). The E, N, U displacements detected by PPMS are shown in Figure 3.2. The solid lines crossing the x-axis indicate the beginning (green) of the movements of the translation stage and the end (red). Averaging the solutions over the last hour of the experiment results in detected displacements of 15 mm and 14 mm in the east and north components respectively, for a total detected displacement of 21 mm. The full displacements are detected within 30 minutes of being introduced. After convergence, the average standard deviations in E, N, U components are ± 10, 7 and 9 mm respectively. Interestingly, the more dramatic changes in satellite geometry in the north and up components allow for better displacement detection in these components than in the east component.

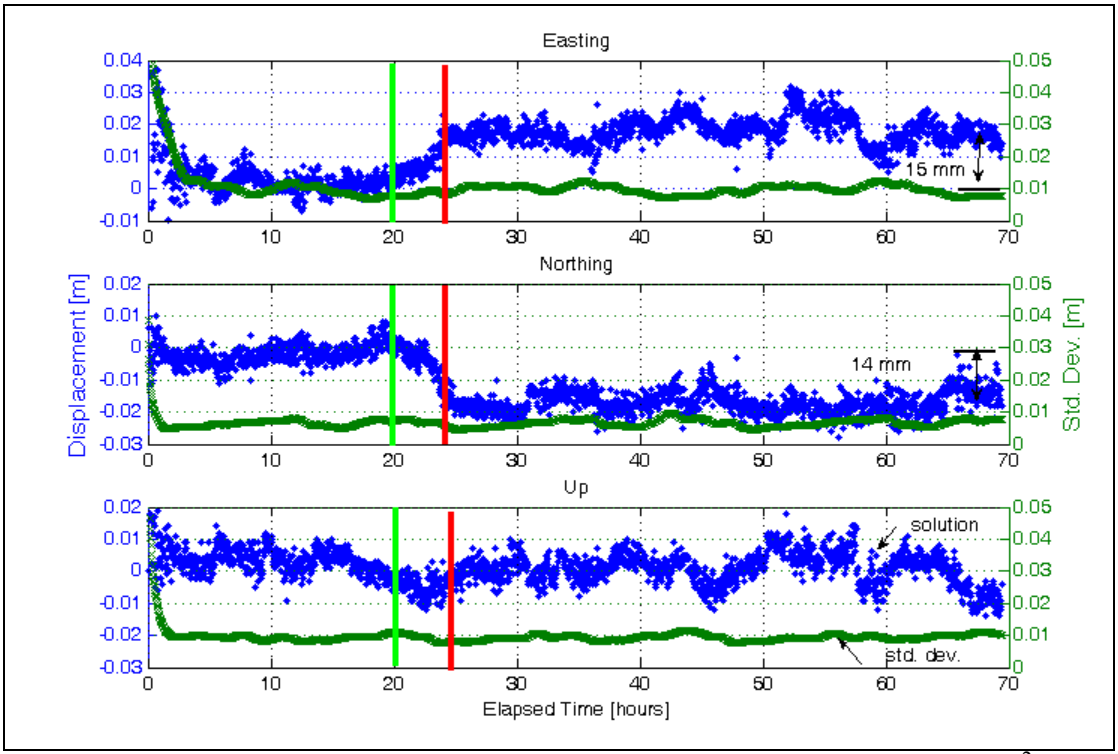

Figure 3.2: Detected Translation Stage Displacements for Q = $(0.4\ \text{mm})^2$

In the second case, a Q value was chosen to accommodate 3 mm displacements every 30 minutes ($Q = (0.2\ \text{mm})^2$). The E, N, U displacements detected by PPMS are shown in Figure 3.3. Averaging the solutions over the last hour of the experiment results in detected displacements of 17 mm and 15 mm in the east and north components respectively, for a total detected displacement of 23 mm. There is about a one hour delay in delay in detecting the full displacement due to the actual velocity of the antenna exceeding the predicted velocity as represented by the Q value. After convergence, the average standard deviations in E, N, U components are ± 7, 5 and 6 mm respectively.

In the third case, a Q value was chosen to accommodate 1.5 mm displacements every 30 minutes ($Q = (0.1 \text{ mm})^2$. The E, N, U displacements detected by PPMS are shown in Figure 3.4. Averaging the solutions over the last hour of the experiment results in detected displacements of 17 mm and 17 mm in the east and north components respectively, for a total detected displacement of 24 mm. There is about a 4.5 hour delay in detecting the full displacement due to the actual velocity of the antenna exceeding the predicted velocity as represented by the Q value. After convergence, the average standard deviations in E, N, U components are ± 5, 3 and 4 mm respectively.

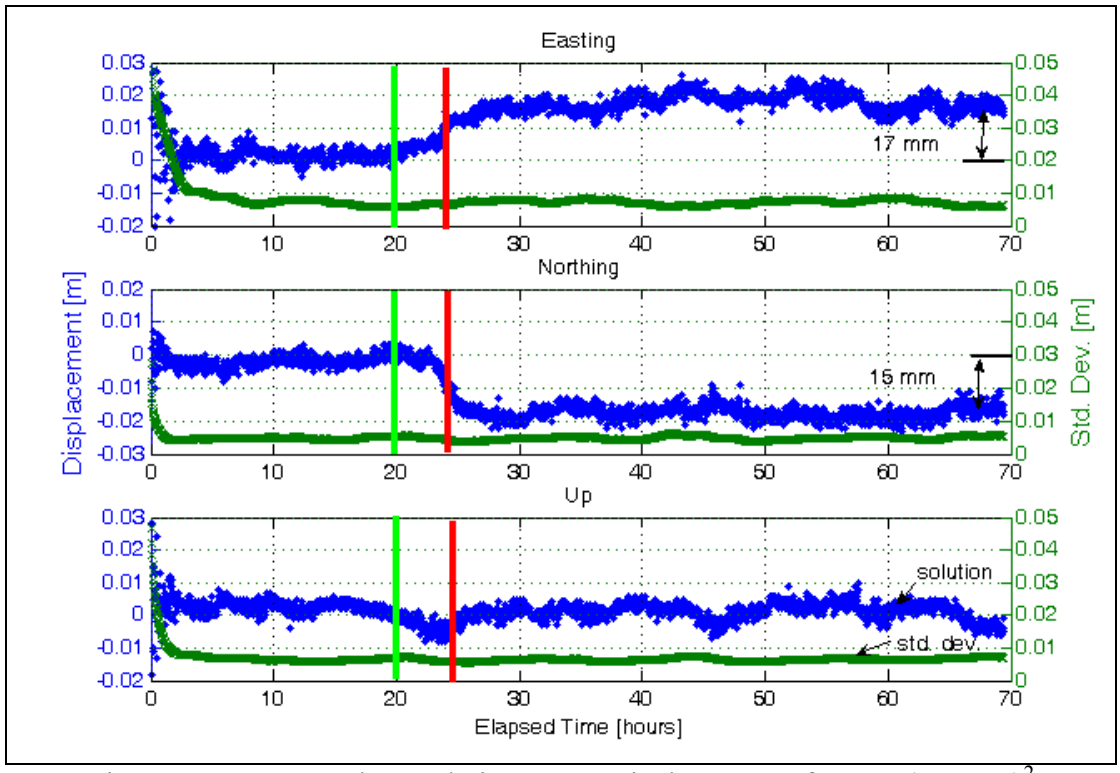

Figure 3.3: Detected Translation Stage Displacements for $Q = (0.2 \text{ mm})^2$

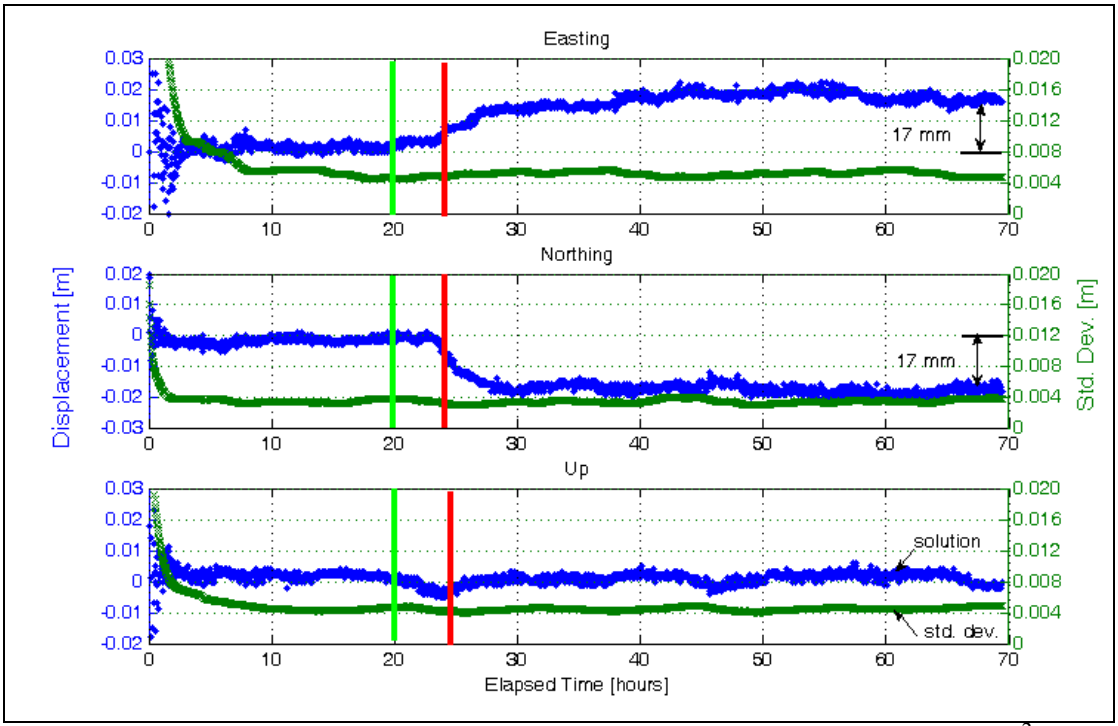

Figure 3.4: Detected Translation Stage Displacements for $Q = (0.1 \text{ mm})^2$

Finally, a fourth case was investigated to gain an appreciation for the achievable precision of the filter when slower displacements are expected. In this scenario, a Q value was chosen to accommodate 0.75 mm displacements every 30 minutes ($Q = (0.05 \text{ mm})^2$. Averaging the solutions over the last hour of the experiment results in detected displacements of 18 mm and 17 mm in the east and north components respectively, for a total detected displacement of 25 mm. There is about a 15 hour delay in delay in detecting the full displacement due to the actual velocity of the antenna exceeding the predicted velocity as represented by the Q value. After convergence, the average standard deviations in E, N, U components are ± 3, 3 and 3 mm respectively.

Larger Q values allow the filter to put more emphasis on the measurements and therefore respond more quickly to the displacements. At the same time, the noise level increases in the solutions. Table 3 summarizes the results of the four scenarios investigated. Column 3- "Delay in Detecting Full Displacement"- represents the length of time after the series of small displacements were introduced that was required to detect the full 25 mm displacement. In all cases investigated, the delay in detecting the full displacement would be approximately 30 minutes if the actual displacements introduced occurred at the rate prescribed by the Q value.

Table 3.3: Displacement Detection Summary

***Q* value**	**Approximate Displacement Rate Accommodated [mm / 30 minutes]**	**Delay in Detecting Full Displacement [Hours]**	**σ_E [±mm]**	**σ_N [±mm]**	**σ_U [±mm]**
$(0.4\ mm)^2$	5	0.5	10	7	9
$(0.2\ mm)^2$	3	1	7	5	6
$(0.1\ mm)^2$	1.5	4.5	5	3	4
$(0.05\ mm)^2$	0.75	15	3	3	3

The filter's delay in detecting displacements is dependent upon the process noise value, Q, the change in satellite geometry and the accuracy of the noise model of the observations (used to populate R). If slow deformations are anticipated (e.g., up to 20 mm per day) then a very small Q value can be used (e.g., 0.001) and sigma values of 2 mm or better can be attained in all three solution components. Further research is required to determine a method of implementing an adaptive Q value that would allow for quicker displacement detection.

3.5.2 Large Open Pit Mine Test

GPS data were collected at 5 stations in a large open pit mine as illustrated in Figure 3.5. Stations 424 and 987 were control stations, while stations RTS1, RTS2 and RTS3 were monitored stations within the pit. Continuous data for 5 days or more were collected. RTS3, located 677 m below station 424, and having periods of the day during which only 3 satellites were visible, represented the most challenging deformation monitoring scenario.

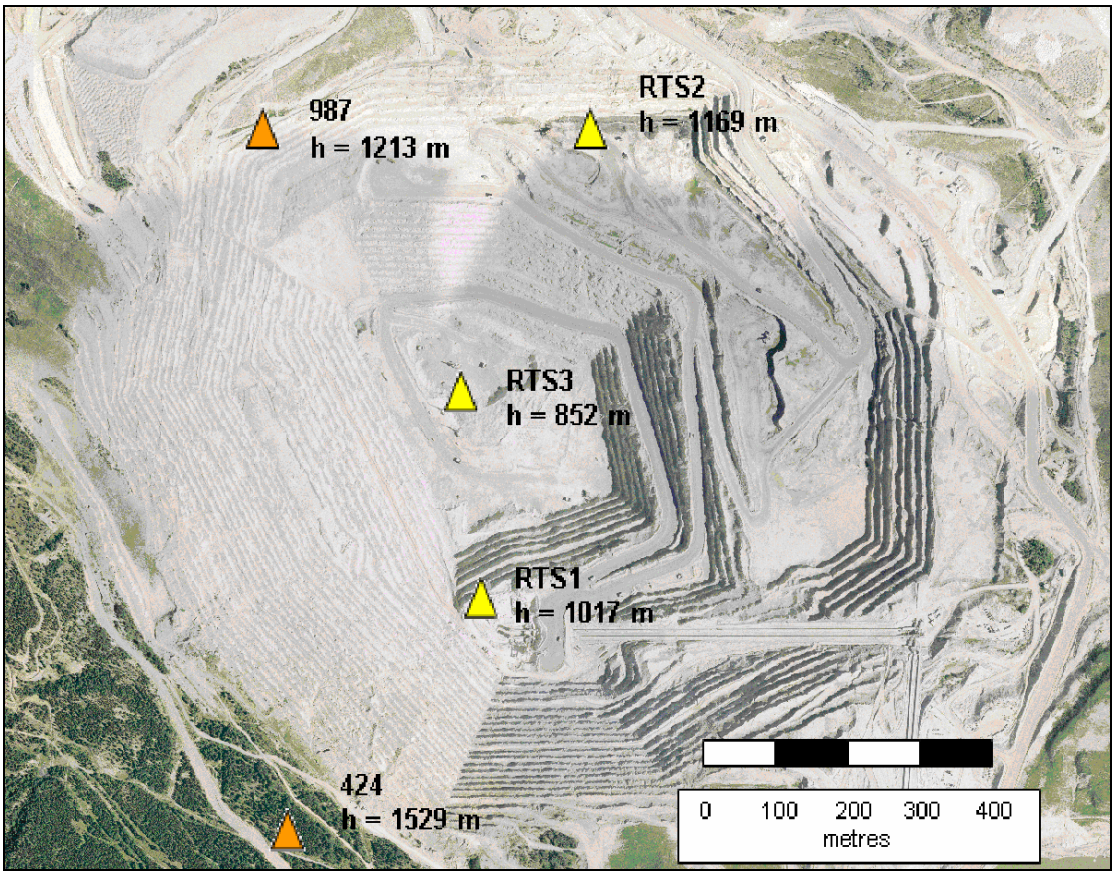

Figure 3.5: Large Open Pit Mine Test (with station heights shown)

3.5.2.1 Large Open Pit Mine Results

The advantages of this filter over batch processing are best revealed by its performance in the environment for which it was designed. Previous analyses of GPS capabilities in this environment were conducted using traditional batch processing methods [Bond, 2004]. This approach did not allow for an examination of the continuous behavior of the monitored points. Furthermore, cyclic patterns in the up component caused by daily meteorological changes biased the results. There were also periods for which no solution could be achieved. To illustrate the results using batch processing, one hour, DD, ambiguity-fixed, up component solutions for baseline 424 to RTS3 are presented in Figure 3.6.

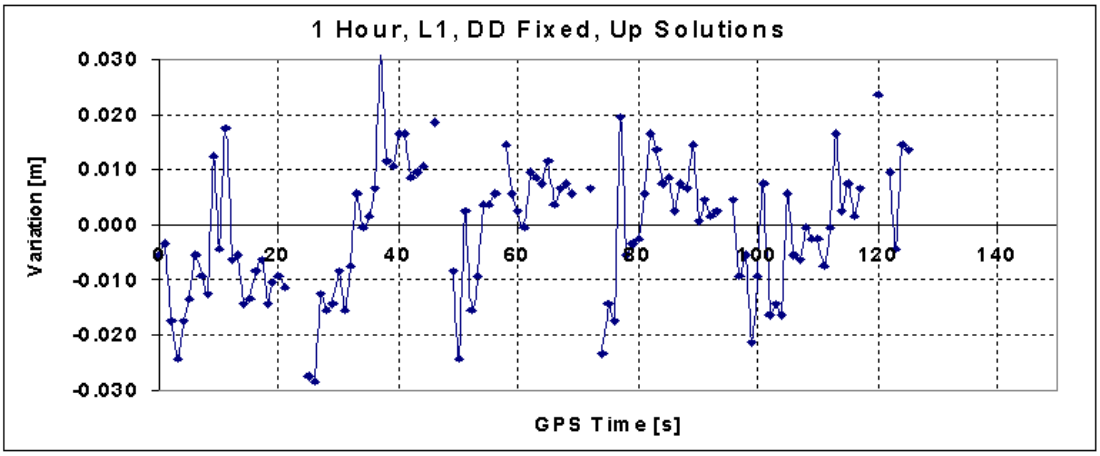

Figure 3.6: 424 to RTS3 Commercial, Up Component Solutions

To determine if the new processing strategy improved the results, all baselines from stations 424 and 987 were processed using PPMS. Selected baselines are presented here to illustrate the software's capabilities.

Baseline 424 to RTS1 represented the second largest height difference observed. Satellite visibility at RTS1 is not limited as severely as at RTS3. The results of this baseline are illustrated in Figure 3.7, from which the following points are noted:

a) A change in height of approximately 5 millimeters occurs shortly after 50 hours have elapsed. This was also seen in all other baselines observed from 424 and from 987, except 987 to RTS2 (the shortest baseline located on the same wall of the pit). DD, ambiguity-fixed results before and after this period confirmed this height change. It is thought that geomechanical activity (such as uplift or subsidence) may be responsible.

b) The cyclic pattern caused by residual tropospheric biases (illustrated in Figure 3.6) has been removed from the up component. Previous analyses revealed that in order to provide high precision solutions over large height differences, one would have to use 24 hour data for the effects of residual tropospheric delay to average out. Since low elevation satellites are not visible in this environment, estimating a residual tropospheric delay parameter at each station does not significantly improve the results [Bond, 2004]. This finding indicates that not only does this processing strategy allow for higher precision solutions, it also allows for more frequent, high precision updates than could normally be achieved using traditional batch processing methods.

c) The filter has successfully recovered from a data gap at near the 20^{th} hour.

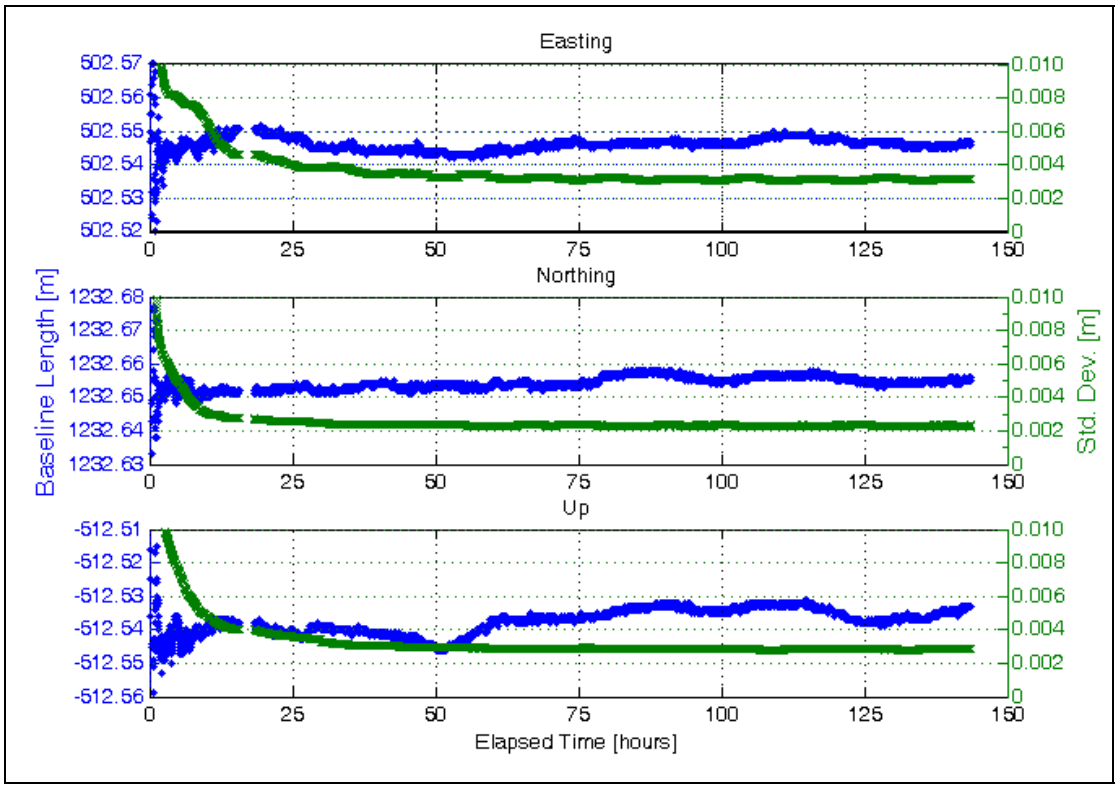

Figure 3.7: 424 to RTS1 Position Solutions

Table 3.4 compares PPMS results with a 24 hour, DD, ambiguity-fixed solution from commercial software after the height change. Standard deviations of the commercial solution are as output by the software.

Table 3.4: 424 t o RTS1 Solution Comparison

Solution Type	**ΔE [m±mm]**	**ΔN [m±mm]**	**ΔU [m±mm]**
Commercial DD Fixed	502.547 ± 0.5	1232.654 ± 0.5	-512.528 ± 0.5
PPMS TD Filter	502.545 ± 3	1232.654 ± 2	-512.534 ± 3

Initial results of the 424 to RTS3 baseline suffered from the limitations of poor satellite visibility. During periods when only 3 satellites were visible, the filter solutions would diverge. It is believed that higher order effects of the receiver clock biased the

range measurements since it was no longer able to steer itself. Further work is required to modify the software so that the best known coordinates of the receiver can be used to estimate the receiver clock bias. This value can subsequently be used to correct the range measurements. Quality control had to be added to the software to prevent providing updates during periods in which the range measurements were potentially biased. The results are shown in Figure 3.8, from which the following points are noted:

a) There is a height change detected shortly after the 50^{th} hour has elapsed (as was seen in Figure 3.7)

b) The effects of poor satellite visibility have less of an impact on update frequency than with batch processing since the filter can provide solution updates as soon as sufficient satellites are available. Despite restricting solution updates to periods with greater than 3 satellites, the longest duration without an update was 74 minutes. In contrast with the batch processing, there were 3 periods each day that one would have to wait 2 hours for a position update, the precision of which could be poor. After convergence and the height change, a peak-to-peak spread of 12 mm in the up component solutions exists (versus 60 mm in Figure 3.6).

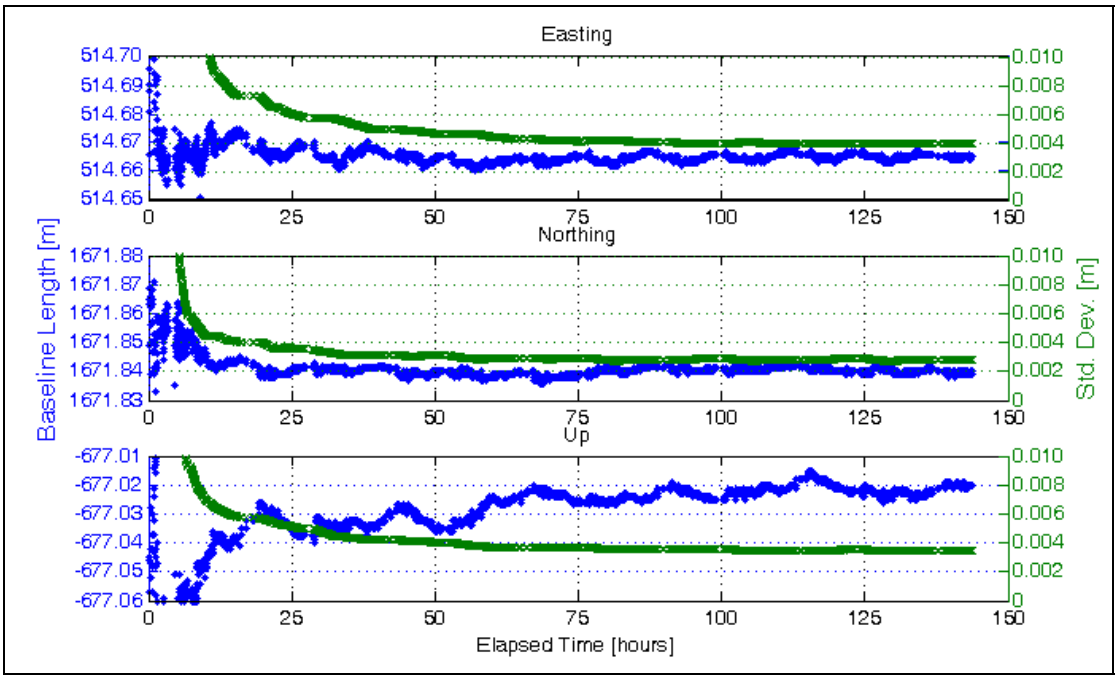

Figure 3.8: 424 to RTS3 Position Solutions

Table 3.5 compares average PPMS results with a 24 hour, DD, ambiguity-fixed solution from commercial software. There are centimeter level discrepancies between the two solutions, possibly caused by the different approaches to tropospheric modelling. These differences become magnified over large height differences and affect the absolute position values. The error in the height component could be improved by providing solutions only when 5 or more satellites are available. This comes at the expense of losing position updates for about a third of the day. The use of pseudolites could aid in providing continuous updates with higher precision.

Table 3.5: 424 to RTS3 Solution Comparison

Solution Type	**ΔE [m±mm]**	**ΔN [m±mm]**	**ΔU [m±mm]**
Commercial DD Fixed	514.685 ± 0.7	1671.852 ± 0.8	-677.044 ± 2
PPMS TD Filter	514.675 ± 4	1671.841 ± 3	-677.025 ± 4

Baseline 987 to RTS2 represents the shortest baseline and a best case scenario in this particular open pit mine. Table 6 compares average PPMS results with a 24 hour, DD, ambiguity-fixed solution from commercial software. The filter solutions are shown in Figure 3.9.

Table 3.6: 987 to RTS2 Solution Comparison

Solution Type	ΔE [m±mm]	ΔN [m±mm]	ΔU [m±mm]
Commercial DD Fixed	434.480 ± 0.4	-97.040 ± 0.4	-44.694 ± 0.9
PPMS TD Filter	434.479 ± 3	-97.040 ± 2	-44.692 ± 3

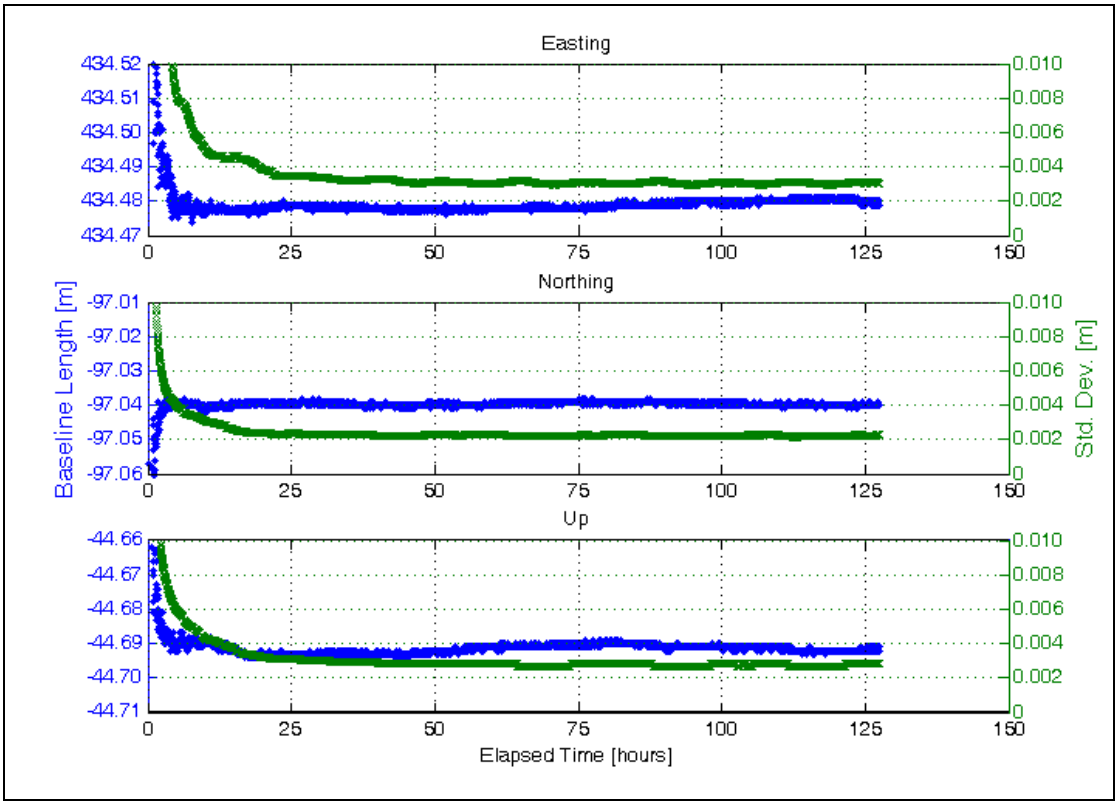

Figure 3.9: 987 to RTS2 Position Solutions

3.6 Conclusions

In response to the need for continuous GPS position updates in harsh deformation monitoring environments, software is being developed that employs TD carrier-phase measurements in a Delayed-State Kalman filter. Besides the obvious benefit of not having to deal with nuances of cycle slip repair, it was shown that the TD observation can be used to significantly reduce the effects of residual tropospheric delay biases. The cost of using the TD observable is slower convergence time than with the DD observable. This is generally not a concern for long term deformation monitoring projects.

Depending upon client requirements and environmental conditions, the filter can be adjusted to be more or less sensitive to the observations. Quicker detection time currently comes at the expense of more noise in the solutions. A slow, 25 mm displacement was detected within 30 minutes of the full displacement with sigma values in E, N and U of ± 10 mm or better. The same displacement could also be detected in less than 5 hours with sigma values in E, N and U of ± 5 mm or better. The software works best for detecting long period deformations (e.g., 20 mm per day or less) for which sigma values of 1 - 2 mm are attained in all three solution components. The filter would benefit from allowing the process noise to be adaptive.

The extreme conditions of harsh environments limit the frequency at which high precision updates could be provided. Using PPMS, updates could be provided at least

every 75 minutes, as opposed to every 24 hours using traditional processing methods. More frequent updates could be provided by utilizing pseudolite technology. PPMS is currently being enhanced to offer this capability.

Acknowledgements

This research was funded by the Natural Sciences and Engineering Research Council of Canada (NSERC) and by the Canadian Wireless Telecommunications Association (CTWA). Special thanks are given to Tomas Beran of Focus Surveys Ltd. for his comments and suggestions.

References

Beutler, G., I. Bauersima, W. Gurtner, M. Rothacher, T. Schildknecht and A. Gieger (1988). *Atmospheric refraction and other important biases in GPS carrier phase observations. Atmospheric Effects on Geodetic Space Measurements*, Monograph 12, School of Surveying, University of New South Wales, pp. 15-43.

Bond, J. (2004). *An Investigation on the Use of GPS for Deformation Monitoring in Open Pit Mines*. M.Sc.E. thesis, Technical Report No. 222, Department of Geodesy and Geomatics Engineering, University of New Brunswick, Fredericton, New Brunswick, Canada, 140 pp.

Bond, J., A. Chrzanowski and F. Wilkins (2005). "Using GPS for Augmenting Deformation Monitoring Systems in Open Pit Mines - Problems and Solutions." *Geomatica* 59(1):73-82

Brown, R.G. and P.Y.C. Hwang (1997). *Introduction to Random Signals and Applied Kalman Filtering*, 3rd ed. John Wiley & Sons, Inc., New York, USA, 484 pp.

Chrzanowski A., F. Wilkins (2006). "Accuracy Evaluation of Geodetic Monitoring of Deformations in Large Open Pit Mines." Proceedings of the *12-th FIG Symposium on Deformation Measurements*, Baden, Austria, 22-24 May, CD ROM. Available at: http://www.fig.net/commission6/baden_2006/PDF/PGO1/Chrzanowski.pdf, accessed on: 4 October 2007.

Collins, J.P. and R.B. Langley (1999). *Nominal and Extreme Error Performance of the UNB3 Tropospheric Delay Model*. Department of Geodesy and Geomatics Engineering Technical Report No. 204, University of New Brunswick, Fredericton, New Brunswick, Canada, 173 pp.

Kim, D., and R.B. Langley (2002). "Instantaneous Real-time Cycle-slip Correction for Quality Control of GPS Carrier-Phase Measurements." *Journal of the Institute of Navigation*, 49(4):205-232

Kim D., R.B. Langley, J. Bond and A. Chrzanowski (2003). "Local deformation monitoring using GPS in an open pit mine: Initial study." *GPS Solutions* 7(3): pp. 176-185. Available at: http://www.springerlink.com/content/0dvd4ddmx9w5k8xx/, accessed on: 4 October 2007. DOI 10.1007/s10291-003-0075-1

Leick, A. (1994). *GPS Satellite Surveying*, 2nd ed. John Wiley & Sons, Inc., New York, USA, 560 pp.

Remondi, B.W. (1984). *Using the Global Positioning System (GPS) Phase Observable for Relative Geodesy: Modeling, Processing, and Results*. Doctoral thesis, Center for Space Research, University of Texas at Austin, 324 pp.

Remondi, B.W. and G. Brown (2000). "Triple Differencing with Kalman Filtering: Making It Work." *GPS Solutions* 3(3):58-64. Available at: http://www.springerlink.com/content/am6adj8qg5q6u94h/, accessed on: 4 October 2007. 10.1007/PL00012805

Rizos, C. (1999c). "Principles and Practice of GPS Surveying, Section 9.1.5: Outlier Testing and Residuals." Available at: http://www.gmat.unsw.edu.au/snap/gps/gps_survey/principles_gps.htm, accessed on: 4 October 2007.

Teunissen, P.J.G. (1998). "Quality Control and GPS." Chapter 7 in *GPS for Geodesy*, 2nd ed., Springer-Verlag, Berlin Heidelberg New York, pp. 271-318.

Wilkins, R., G. Bastin and A. Chrzanowski (2003c). “Monitoring of Structures and Steep Embankments: A Fully Automated Approach.” Paper presented at CSCE Annual Conference, Moncton, NB, Canada, June 4-7, 2003. Available at: http://ccge.unb.ca, accessed on: 4 October 2007.

CHAPTER 4
AUGMENTING GPS WITH PSEUDOLITES FOR DEFORMATION MONITORING IN HARSH ENVIRONMENTS

Jason Bond, Adam Chrzanowski, Don Kim
University of New Brunswick, Fredericton, New Brunswick, Canada

The following has been originally published as:

Bond, J., A. Chrzanowski, and D. Kim (2007). "Augmenting GPS with Pseudolites for Deformation Monitoring in Harsh Environments." Proceedings of the *Institute of Navigation National Technical Meeting* (ION NTM), 22-24 January, San Diego, CA, USA. Available at http://www.ion.org/ and on CDROM.

The first author has developed the algorithms to process the pseudolite data collected, designed the experiments, processed the data, compiled the results and prepared the manuscript. The second author has provided advice on paper content and insight into the theoretical background of deformation monitoring. The third author has provided advice on paper content and insight into the theoretical background of the observation modelling of the pseudolite signals.

Abstract

Deformation monitoring projects that utilize GPS cannot always provide position updates due to harsh environmental conditions. For example, open-pit mines, large dams and urban settings all have obstructions that limit satellite visibility, which in turn limits achievable accuracy and frequency of position updates. For the past decade or so, the use of pseudolites (PLs) has been advocated to overcome this problem. Much has been done in the way of theoretical analysis and simulations to demonstrate the potential benefits of PLs, but few real-world examples of deformation monitoring using PLs exist.

In an effort to demonstrate the practical use of PLs for high-precision deformation monitoring, data were collected in a large open-pit mine in western Canada. Additionally, a displacement test was performed to determine if PLs aid in quicker displacement detection. Both data sets were processed using a unique approach that employs triple-differenced carrier phase measurements in a Delayed-State Kalman filter.

Despite encountering several practical issues that need to be addressed with the implementation of a PL system, sufficient data were collected to demonstrate that PLs can be used in harsh environments to provide a) more frequent solution updates, b) quicker filter convergence and c) quicker displacement detection than could normally be achieved using stand-alone GPS. PLs can be a valuable augmentation device for GPS-based deformation systems where expedient information is critical for human safety.

4.1 Introduction

Recent efforts at the Canadian Centre for Geodetic Engineering (CCGE) at the University of New Brunswick (UNB) to develop GPS software for deformation monitoring in harsh environment conditions have resulted in the emergence of the Precise Position Monitoring System (PPMS) [Bond et al., 2007a]. PPMS utilizes a Delayed-State Kalman filter to process GPS triple-differenced (TD: differencing consecutive double-differenced observations) carrier phases. Test results have indicated that the software is

capable of detecting millimeter level displacements without having to solve for ambiguity terms. The ability to provide high precision solutions that are independent of ambiguities makes PPMS desirable for deformation monitoring since it is less susceptible to false alarms caused by cycle slips than traditional double-differenced (DD: differencing between receivers followed by differencing between satellites or vice versa) processing methods.

GPS data obtained from a large open pit mine indicated that there were several periods during the day for which fewer than 4 satellites were visible. It was decided to investigate the potential of augmenting GPS with pseudolites (PLs) to improve the frequency and precision of solutions.

Several practical issues were encountered while trying to implement a pseudolite system, which are discussed. Additionally, modifications required to allow PPMS to handle PL observations are presented. Two data sets were collected to evaluate the capabilities of PLs. The first data set is a displacement detection test which involved introducing known displacements by means of a translation stage. The second data set comes from a large open-pit mine in western Canada. Results of both tests are presented.

4.2 Practical Considerations for Implementation

The PLs used in the tests were IN200 single frequency (L1) transmitters purchased from IntegriNautics (now Novariant). Since it is illegal to broadcast on the L1 frequency in Canada, a research license had to be attained from Industry Canada before conducting any experiments. More recent products developed by Novariant (called "terralites") avoid this problem by broadcasting their own proprietary signal to their own receivers [Novariant, 2007].

4.2.1 Near/Far Problem

Due to the close proximity of the PL transmitter to the GPS receiver in comparison with the relatively large distance to the GPS satellites, it is necessary to ensure that the PL signal does not saturate the receiver and jam the satellite signals. The IN200 configuration software allows the user to choose between several pulsed signal modes to overcome the near/far problem. Tests have shown that using the RTCM pulsed mode (a pulse is emitted at a variable time offset from the PL's internal clock trigger), the signal can be tracked by the GPS receiver from 10 m to several km away without having to change the PL settings. The signal appears continuous to the receiver since the pulse rate is much higher than the receiver's internal sampling rate.

4.2.2 Working Range

For the open pit mine of interest, the GPS receivers would be located up to 2 km away from the PL and a wide field of view would be necessary. Tests of the range of the IN200 indicated that the signal could be easily tracked at a distance of 3.5 km. Tests of the beam pattern of the PLs showed a nearly uniform pattern to ± 85° of boresight.

4.3 Pseudolite Data Processing Considerations

Being a ground-based transmitter, PL error sources must be handled differently than GPS signal error sources. The IN200 is a single frequency instrument, and therefore one does not have the luxury of using L2 for cycle slip detection. The inexpensive clocks used further complicate processing since the anticipated constant carrier phase observations actually drift with the clock. The PL observations require special attention as subsequently discussed.

4.3.1 Cycle Slip Detection

Although ambiguity terms do not need to be solved for using the TD observable utilized by PPMS, observations containing cycle slips still need to be detected and

removed. The cycle slip detection approach used for GPS signals is based upon that of Kim and Langley [2002] which compares geometry-free (GF: differencing between L1 and L2 in the distance unit), TD observations against a cycle slip threshold. Since the L2 signal is not available for the PL observations, an alternative approach was required. As an example, Figure 4.1 illustrates the variation in PL observations with time at one of the stations involved in the open pit test, RTS1. Despite the PL and GPS receiver being stationary, the carrier phase observations are not constant. To detect cycle slips in PL observations, quadruple differences (QD: differencing consecutive TD observations) are formed and these values are compared against a cycle slip threshold (Figure 4.2).

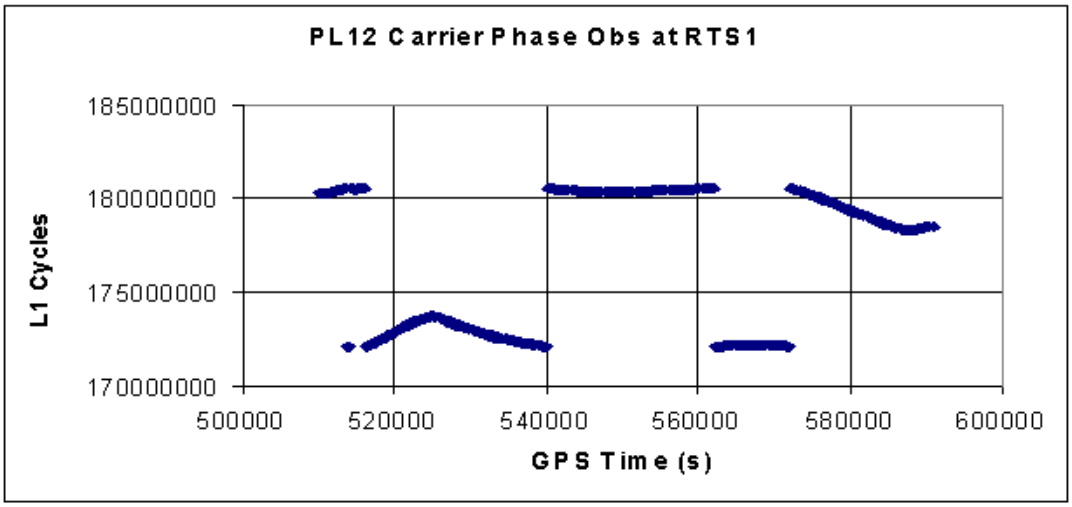

Figure 4.1: PL12 Carrier Phase Observations

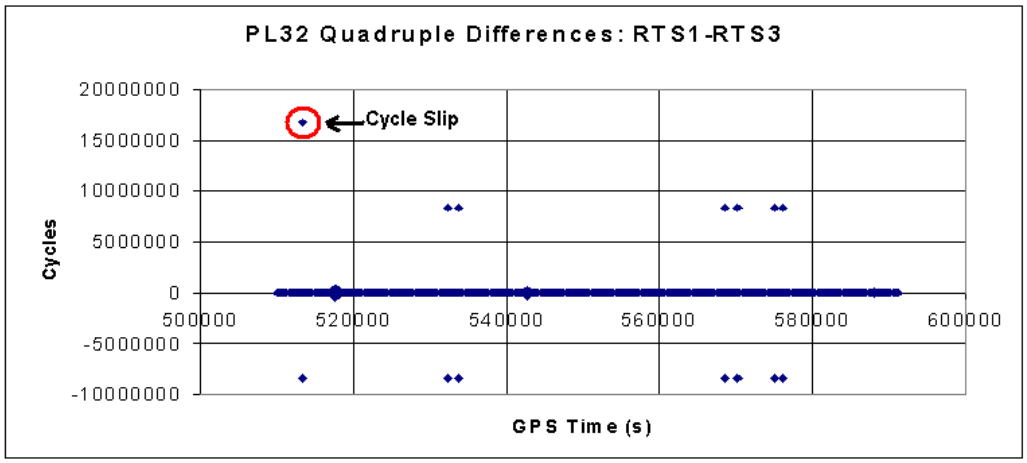

Figure 4.2: PL32 Quadruple Differences

4.3.2 Pseudolite Location

Since the PL location is user dependent, its location must be determined for processing. This is presently achieved through GPS. The IN200 does not broadcast ephemeris information, so the PL location must be fed into the software. Due to the nature of the TD observable, the accuracy tolerance to which the PL coordinates must be known is forgiving. Equation (4.1) presents the computed, geometric, TD observation:

$$\delta \underset{AB}{\Delta} \overset{iPL}{\nabla} \varphi(t_{12}) = [(D_A^i - D_A^{PL}) - (D_B^i - D_B^{PL})]_{t_2} - [(D_A^i - D_A^{PL}) - (D_B^i - D_B^{PL})]_{t_1} \quad (4.1)$$

where:

$\overset{iPL}{\nabla}$ single-difference (SD) operator between satellite, *i*, and pseudolite, *PL*

$\underset{AB}{\Delta}$ SD operator between receivers *A* and *B*

δ SD operator between times t_1 to t_2

D geometric distance (m)

Since the PL is stationary between times t_1 to t_2, and it is assumed that the receivers are stationary, the geometric distance terms involving the PL cancel so that the computed, geometric, TD observation can now be written in the form of Equation (4.2):

$$\delta \underset{AB}{\Delta} \overset{iPL}{\nabla} \varphi(t_{12}) = [(D_A^i - D_B^i)]_{t_2} - [(D_A^i - D_B^i)]_{t_1} \tag{4.2}$$

Equation (4.2) illustrates that only the change in geometry of the reference satellite impacts the computed, geometric, TD observation and therefore the PL coordinates are not critical. Indeed, results obtained using PL coordinates in error of 1000s of km showed biases of 1-2 mm of those produced with true PL coordinates. These biases were likely caused by round-off errors. In practice, it is recommended to perform a point position solution for the PL location to avoid round-off errors caused by manipulating large distances caused by incorrect coordinate values.

Equation (4.2) also shows that for a static application using the TD observable, the PL observations only help to define the change in geometry in the direction of the reference satellite. It is therefore advised that if multiple PLs are used, between satellite differences should be formed using a different reference satellite for each PL. In the case of static applications, this approach is therefore more applicable as an augmentation system than a

stand-alone PL system. In kinematic applications, the change in coordinates between times t_1 to t_2 would prevent the PL geometry from cancelling in Equation (4.1). This would make the accuracy of the PL coordinates more critical.

4.3.3 PL Observation Modelling

Inspired by Remondi and Brown [2000], the TD carrier phase observable is used in PPMS as an alternative method of obtaining high precision GPS solutions. Despite introducing another level of differencing which increases the observation noise, the TD observable offers several advantages over the DD, ambiguity-fixed observable [Bond et al., 2007a]. After removing the error terms for receiver clocks and satellite clocks (which are eliminated through double-differencing over short baselines), the TD carrier phase observable for PLs can be written in the form of Equation (4.3):

$$\delta \underset{AB}{\Delta} \overset{iPL}{\nabla} \varphi(t_{12}) = [\underset{AB}{\Delta} \overset{iPL}{\nabla} (\varphi + N + M - \frac{f}{c} I + \frac{f}{c} T + e_{\varphi}) + \varepsilon_{trop}]_{t_2} - [\underset{AB}{\Delta} \overset{iPL}{\nabla} (\varphi + N + M - \frac{f}{c} I + \frac{f}{c} T + e_{\varphi}) + \varepsilon_{trop}]_{t_1} \quad (4.3)$$

where:

φ	carrier phase observable (cycles)
N	ambiguity (cycles)
M	multipath (cycles)
I	ionospheric delay (m) *
T	tropospheric delay (m)
f	carrier wave frequency (Hz)
c	speed of light in a vacuum (m/s)

ε_{trop} residual tropospheric delay bias (present over large height differences) (cycles)

e_{φ} random carrier phase measurement noise

* There is not an ionospheric delay term for the PL observation since its signal does not travel through the ionosphere, but the reference satellite observation will include this term.

The attractiveness of the TD observable is that it is a time difference of DD observations and consequently biases common to both observations will cancel. This strategy has several important benefits for PL data processing:

a) the user no longer needs to solve for the ambiguity term, which allows the system to be less susceptible to cycle slips;

b) for observation intervals less than a few seconds, the correlation between PL tropospheric delay parameters at times t_1 and t_2 will be large and biases originating from them will be significantly reduced;

c) for observation intervals less than a few seconds, the correlation between low frequency multipath terms at times t_1 and t_2 will be large and biases originating from them will be significantly reduced. The high frequency component still remains.

Equation (4.3) can now be rewritten as:

$$\delta \underset{AB}{\Delta} \overset{iPL}{\nabla} \varphi(t_{12}) = [\underset{AB}{\Delta} \overset{iPL}{\nabla} (\varphi + M)]_{t_2} - [\underset{AB}{\Delta} \overset{iPL}{\nabla} (\varphi + M)]_{t_1} + e_{\delta\Delta\nabla\varphi} \qquad (4.4)$$

where:

$e_{\delta\Delta\nabla\varphi}$ random noise error of a TD carrier phase observation

From Equation (4.4) it can be seen that through triple-differencing, most major error sources can be significantly reduced from the PL observations. This allows for smooth integration of PL data into the existing software infrastructure. The expense of using the TD observation approach is that it requires a longer convergence time than for DD, ambiguity-fixed processing. For deformation monitoring purposes, however, this is generally not a concern.

4.3.4 Receiver Clock Synchronization

Initial results using PPMS showed biases when there were fewer than 4 satellites, despite having the additional PL signal. It was discovered that the NovAtel DL4's clock was accurate to only ± 10 ms during these periods and this was causing range biases (the PL does not provide ephemeris data from which the receiver can calculate its coordinates). This was an important finding because it means that if fewer than 4 satellites are visible, some means of synchronizing the receiver clock to GPS time is required. Otherwise, position solutions should not be provided by using PLs (and solutions should also not be provided by the software using stand-alone GPS). To prevent

divergence, the number of satellites is checked prior to updating the filter. PPMS is being modified so that best known receiver coordinates are used in estimating the receiver clock error when fewer than 4 satellites are visible.

4.4 Tests

Two data sets were collected to determine the benefits of using PLs for deformation monitoring. The first data set was collected on the roof of Head Hall at the UNB campus. Controlled displacements were introduced using a translation stage. The second data set was collected at a large open pit mine in western Canada. This test represented a harsh environment in that is suffered from poor satellite visibility and residual tropospheric delay biases caused by large height differences. An initial investigation into using GPS in this environment was conducted in Bond et al., [2005]. In both tests, NovAtel DL4 receivers and GPS-600 Pinwheel antennas were used to track the PLs.

Using the modified, PL-enabled PPMS, the data sets were processed. Unless otherwise specified, a 10º elevation cut off angle was implemented. The UNB3 tropospheric model (Saastamoinen zenith delay with lookup tables) with Niell mapping functions was used. The sample rate for both data sets was 10 seconds.

4.4.1 Displacement Detection Test at UNB

GPS+PL data were collected to determine the potential benefits of PLs in displacement detection. A rover receiver was located on a translation stage so that horizontal displacements could be introduced. Figure 4.3 illustrates the layout of the master and rover receivers as well as the PL.

Data were collected for just over 14 hours to give the filter time to converge. Then, a series of five 3 mm displacements were introduced using a translation stage, with one hour separating each displacement (for a total displacement of 15 mm). The results of this test are shown in Figure 4.4, where the vertical lines represent the start (green) and end (red) times of the introduced displacements. Since satellite visibility was good, it was not expected that there would be a significant benefit in using the PL in this scenario. It can be seen, however, that the GPS+PL solution (♦s, blue) begins detecting the displacement 20 minutes earlier than stand-alone GPS (x s, red). Both solutions detect the 15 mm displacement, mostly evidenced in the east component of the solution.

Figure 4.3: Displacement Test

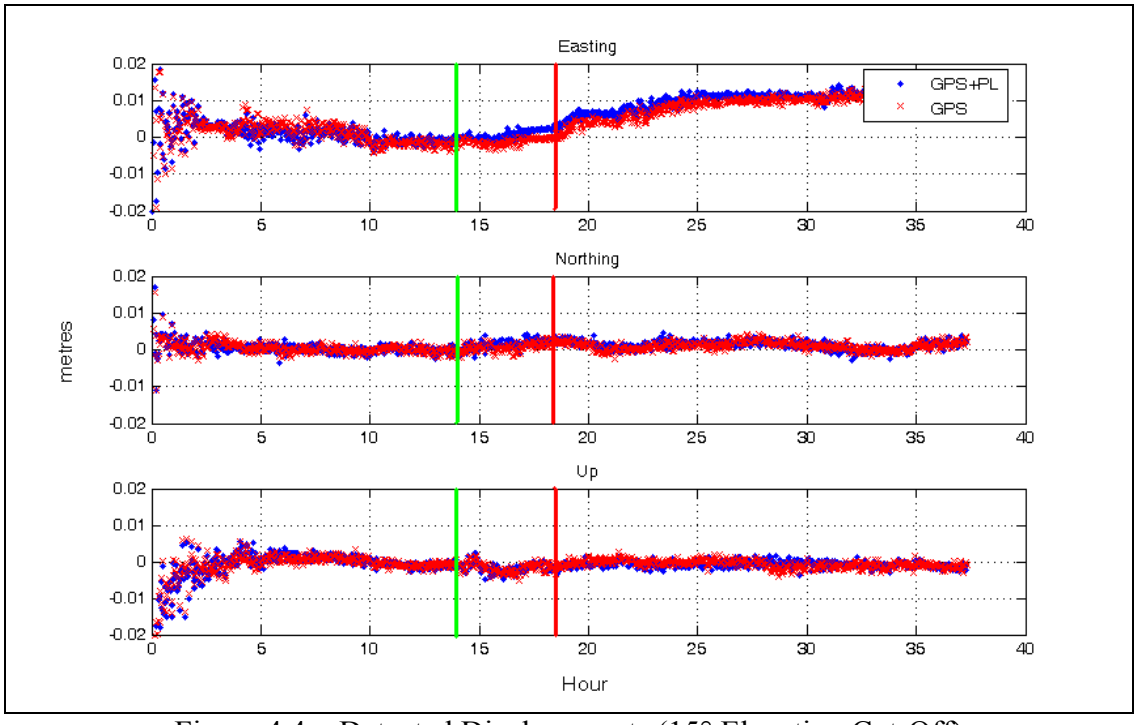

Figure 4.4: Detected Displacements (15° Elevation Cut-Off)

Analyses were also conducted by simulating a harsh environment through implementing a 35° elevation cut-off angle. From Figure 4.5 the benefits of PLs become more apparent. It can be seen that the convergence time for the Kalman filter is reduced from about 10 hours using stand-alone GPS to about 5 hours using GPS+PL. Without low elevation satellites, only 10 mm of the total 15 mm of displacements are detected. The PL allows the displacement to be detected 10 hours quicker than using stand-alone GPS. The use of additional PLs could perhaps aid in detecting the remaining 5 mm.

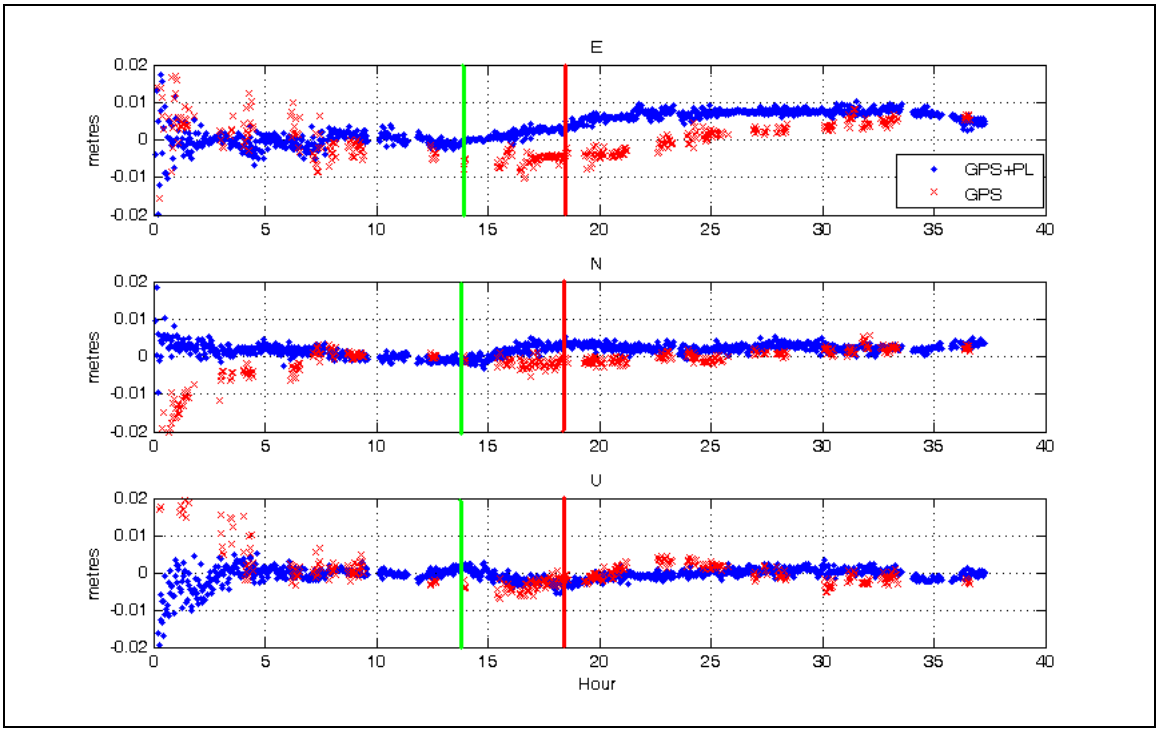

Figure 4.5: Detected Displacements (35° Elevation Cut-Off)

4.4.2 Large Open Pit Mine Test

GPS+PL data were collected at 5 stations in a large open pit mine as illustrated in Figure 4.6. Stations 424 and 987 were control stations, while stations RTS1, RTS2 and RTS3 were monitored stations within the pit. RTS3, which was located 677 m below station 424, and which had periods of the day during which fewer than 4 satellites were visible, represented the most challenging station to be monitored. Three IntegriNautics IN200 PLs were used to augment the GPS constellation, shown as PL12, PL19 and PL 32.

Deploying the PLs in suitable locations proved to be a complicated task. In order to form between receivers differences, it was necessary that the PL was located above both the master and rover stations (since antennas do not track below the horizon) and required line-of-sight to both antennas. Immediately, these requirements eliminated the possibility of locating a PL in the eastern section of the mine. It was also next to impossible to locate a PL above 424 that had line-of-sight to RTS3, without using some sort of tower. Figure 4.7 illustrates the difficulty in seeing into the pit from PL 19.

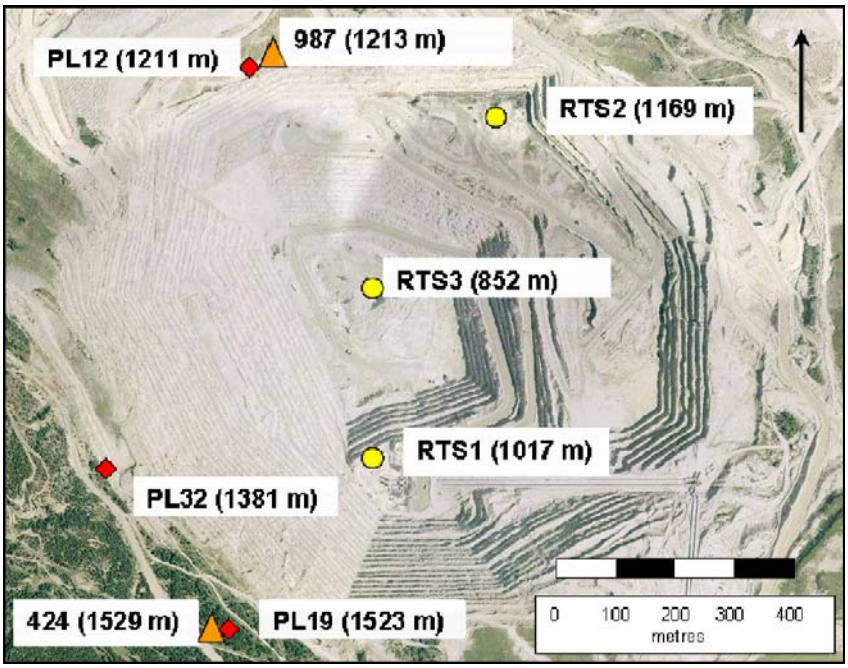

Figure 4.6: GPS Receiver and Pseudolite Locations


Figure 4.7: PL19, looking North

Several days worth of data were attempted to be collected using the illustrated configuration. Two problems were encountered which limited the total amount of data actually obtained. The first problem was caused by the time initialization method used in the NovAtel DL4 receiver. Upon power up, the receiver uses the navigation message of the first satellite it locks onto to adjust its clock. If this satellite happens to be a PL that is not synchronized to GPS time, the data file will have incorrect time tags which render the data unusable. This situation occurred at RTS2. Neither the PLs nor the receivers could be easily modified to address this problem. If a check was implemented by the receiver to see if the first satellite tracked was a PL, this situation could be avoided. Alternatively, the PL could perhaps be modified to allow for synchronization to GPS time (synchrolite). At present, experiments are conducted by turning the PL on after the receiver has initialized to avoid this problem.

Another problem was caused by a power outage which caused one of the receivers to lose its configuration settings. The NovAtel DL4 tracks a PL by assigning the receiver to track it on a certain channel. Unfortunately, the configuration was not saved on the receiver at 987, and after the power outage the receiver no longer tracked any of the PLs.

From the experiment, baseline RTS1 to RTS3 was salvaged. RTS1 tracked PL12 and PL32, while RTS3 tracked only PL32. Since only PL32 was tracked by both receivers, analyses were limited to this PL. Using PPMs software, the baseline was processed.

Figure 4.8 illustrates the results of the RTS1 to RTS3 baseline processing. It takes approximately 12 hours for the filter to converge, after which one would expect mostly stable positions. It can be seen that the GPS and GPS+PL solutions are in close agreement. Using the PL, more continuous updates can be provided (Over this 22.5 hour period, 67% of possible updates are provided using stand-alone GPS, while 89% of possible updates are provided using GPS+PL. The PL assists in providing solutions between the 8th and 9th hours as well as between the 18th and 21st hours when satellite visibility is poor (see Figure 4.9). A slight change in position is shown at hour 21 which was also shown in commercial, DD fixed solutions.

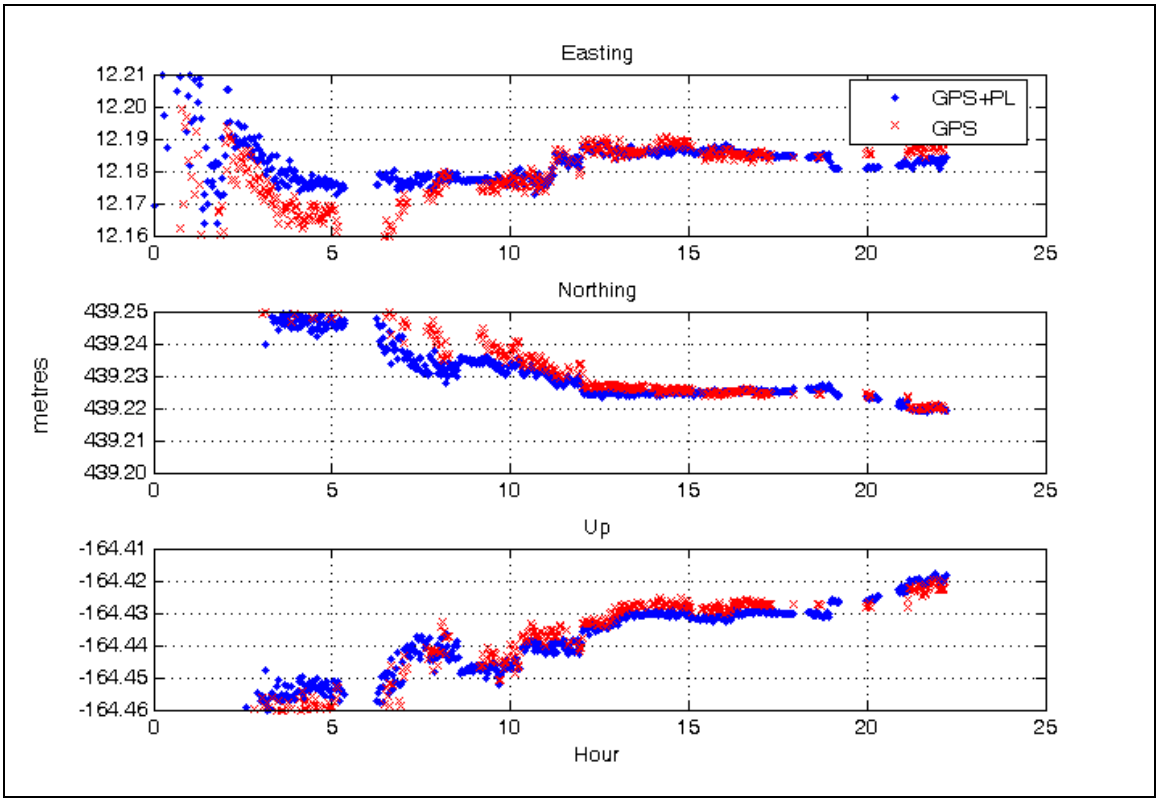

Figure 4.8: RTS1 to RTS3 PL Results (filter converges at ~12 hours)

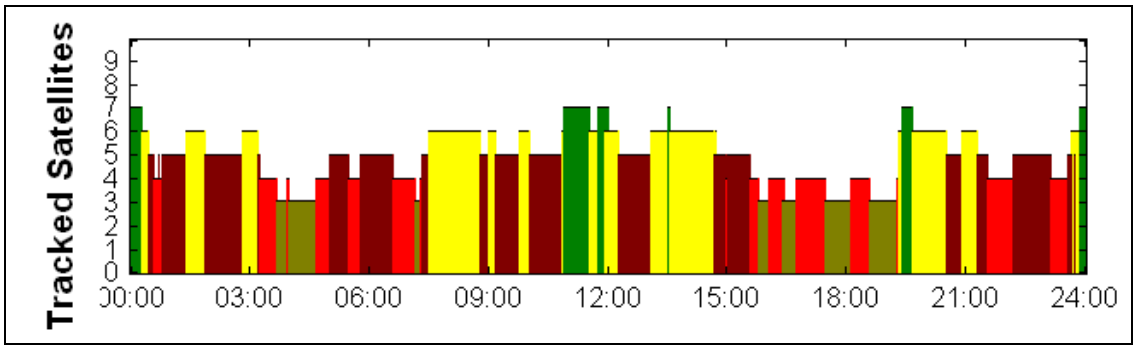

Figure 4.9: Satellite Visibility at RTS3

Satellites were also disabled during processing to simulate periods during which the receiver clock at RTS3 is synchronized to GPS time, despite having only 3 satellites in view. Figure 4.10 presents PPMS' PL solutions obtained when SV11 is disabled. The PL is able to bridge the gap in solutions between the 17th to 21st hours where stand-alone GPS could not. Over this 22.5 hour period with SV11 disabled, 64% of the time updates are provided using stand-alone GPS, whereas 83% of the time updates are provided when using GPS+PL.

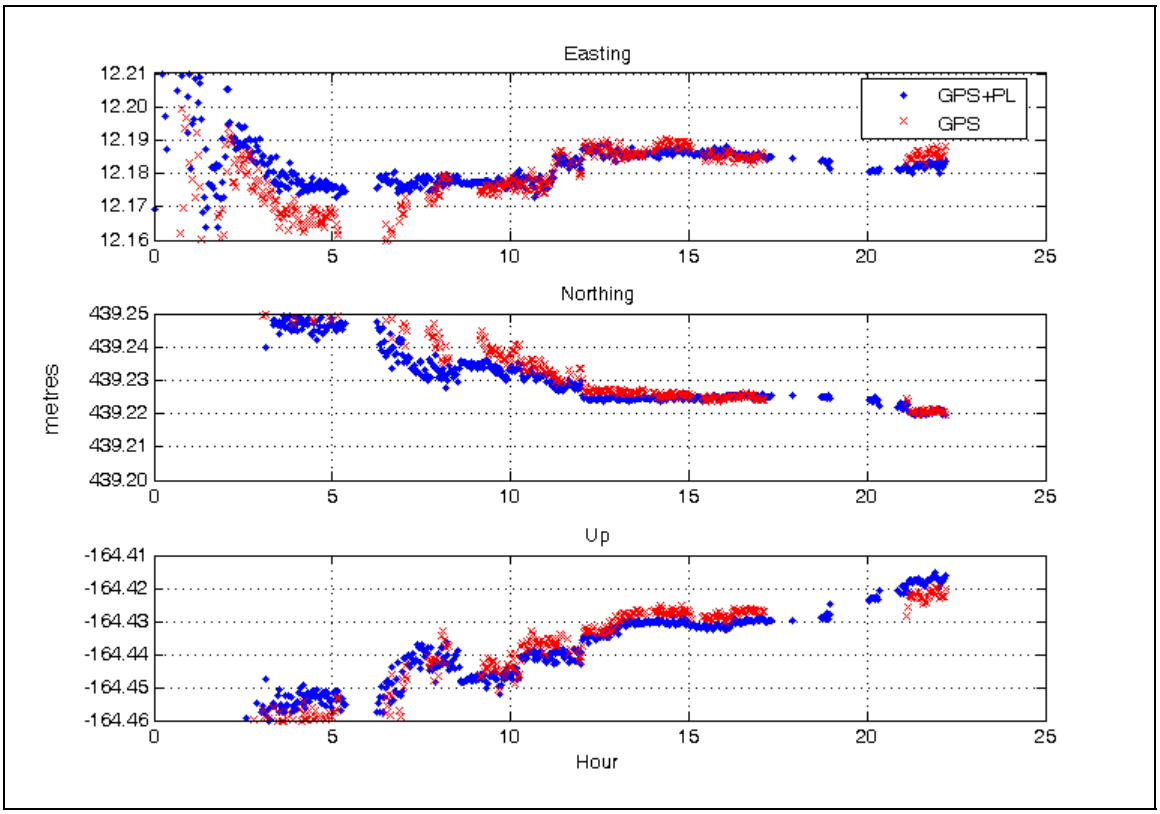

Figure 4.10: RTS1 to RTS3 PL Results with SV11 Disabled
(filter converges at ~12 hours)

In future tests, it may be possible to locate the PLs within the pit. Their stability can be controlled using GPS. Once the position of any of the monitored GPS stations is determined, it can be used as a reference station for the other stations located deep within the pit. As long as the PL is located above the rover stations, between receiver differences can be formed.

4.5 Conclusion

PLs can be used in harsh environments to provide a) more frequent solution updates, b) quicker filter convergence and c) quicker displacement detection than could normally be achieved using stand-alone GPS. PLs can therefore be a valuable augmentation device for GPS-based deformation systems where expedient information is critical for human safety.

There are still some practical issues that need to be addressed before PLs similar to the one tested could be integrated into a deformation monitoring system. The illegality of broadcasting on L1 is perhaps the biggest setback at this time. Unless a modified signal is transmitted to receivers capable of tracking it, or legislation is modified for these devices, this generation of PLs cannot be utilized.

The major advantage of using PLs is having supplementary observations when too few satellites are visible to provide a solution. It was discovered that unless some means of synchronizing the receiver's clock to GPS time is introduced when fewer than 4 satellites are visible, PLs will not be of any use in providing additional solution updates.

The clock initialization method used by NovAtel DL4 receivers allows for the potential of incorrect time synchronization with GPS time. If the receiver locks onto the PL signal first, it will use the time broadcast by the PL to initialize the receiver. Without

any means of synchronizing the IN200 to GPS time, the default time value set in the firmware of the PL is used. Care must be taken to initialize the receiver without having the PL turned on. This becomes cumbersome in the event of power outages. Ideally, the receiver used would be programmed not to initialize with the time obtained from a channel dedicated to tracking a PL.

The TD observation approach used for PL data processing allows for smooth integration of PL observations for high precision applications, since it significantly reduces most major error sources. The expense of using this approach is longer convergence times than would be normally expected using traditional DD methods. This is generally not a concern for long-term deformation monitoring applications.

Acknowledgements

This research could not have been conducted without the financial support of the Natural Sciences and Engineering Research Council of Canada (NSERC), the Atlantic Canada Opportunities Agency (ACOA) and the Canadian Wireless Communications Association (CWTA).

References

Bond, J., A. Chrzanowski, and D. Kim (2007a). "Bringing GPS into Harsh Environments for Deformation Monitoring." *GPS Solutions* (online first status), 11 pp. Available at: http://www.springerlink.com/content/21v2625p46108266/fulltext.pdf, accessed on: 4 October 2007. DOI 10.1007/s10291-007-0059-7

Bond, J., A. Chrzanowski, and F. Wilkins (2005). "Using GPS for Augmenting Deformation Monitoring Systems in Open Pit Mines- Problems and Solutions." *Geomatica*, Vol. 59, No. 1, pp. 73-82.

Kim, D. and R.B. Langley (2002). "Instantaneous Real-Time Cycle-Slip Correction for Quality Control of GPS Carrier-Phase Measurements." *Navigation*, Journal of *The Institute of Navigation*, Alexandria, Virginia, Winter, No. 4, Vol. 49, pp. 205-222.

Novariant, (2007). "News Releases". Available at: www.novariant.com, accessed on: 10 August 2006.

Remondi, B.W. and G. Brown (2000). "Triple Differencing with Kalman Filtering: Making It Work." *GPS Solutions* 3(3):58-64. Available at: http://www.springerlink.com/content/am6adj8qg5q6u94h/, accessed on: 4 October 2007. 10.1007/PL00012805

CHAPTER 5
DESIGN OF GEODETIC DEFORMATION MONITORING SCHEMES USING DETERMINISTIC MODELLING: AN OPEN PIT MINE EXAMPLE

Jason Bond, Anna Szostak-Chrzanowski, and Adam Chrzanowski
Canadian Centre for Geodetic Engineering, University of New Brunswick

The following was originally published as:

Bond, J. A. Szostak-Chrzanowski and A. Chrzanowski (2007). "Design of Geodetic Deformation Monitoring Schemes Using Deterministic Modelling: An Open Pit Mine Example." Proceedings of the *3rd International Symposium on Geo-information for Disaster Management*, Toronto, Ontario, Canada, 22-24 May, CDROM.

The first author has performed the finite element analysis, compiled the results and prepared the manuscript. The second author has provided advice on paper content and insight into the theoretical background of the finite element method and the use of deterministic modelling in the design of geodetic deformation monitoring schemes. The third author has provided advice on paper content and insight into mechanisms of deformation behaviour in open pit mining and the use of deterministic modelling in the design of geodetic deformation monitoring schemes.

Abstract

Deformation monitoring projects require decisions to be made regarding the location, density, and accuracy of geodetic sensors and targets. All too often, however, the location of the instruments is decided upon without regard for the characteristics of the deformable object. This can lead to incorrect values of the observed displacements and misinterpretations of the behaviour of the deformable object. A more rigorous approach is to use deterministic modelling in the design of a geodetic deformation monitoring

scheme. An interdisciplinary approach is presented using an open pit mine scenario as an example. Finite element method was applied to the analysis of the open pit mine to predict displacement fields at various stages of mining sequence. As illustrated in the example, the predicted displacement field serves several functions including: allowing the deformation zone to be delineated so that suitable locations for stable reference points can be chosen; promoting informed decisions about sensor placement to capture displacements of interest; and providing information for predicting global deformation.

5.1 Introduction

Proper design and interpretation of deformation monitoring measurements requires *a priori* knowledge of the expected behaviour of the deformable object. This knowledge aids in making decisions regarding the location, density and accuracy of the geodetic technology employed. Without regard for this information, misinterpretation of the actual displacement field can arise which can have serious consequences when safety issues and remedial measures are involved.

The *a priori* knowledge of the expected displacement field may be obtained through deterministic modelling of the deformation, which utilizes the knowledge of the geometry of the object and its environment, causative factors (loads), properties of the material, and physical laws governing the stress-strain relationship. Since complex differential

equations must be solved in the process of deterministic modelling, numerical methods, for example the finite element method (FEM) are generally employed.

Recent interdisciplinary research at the Canadian Centre for Geodetic Engineering (CCGE) has demonstrated how to successfully incorporate deterministic modelling in the studies of the behaviour of engineered and natural structures [Chrzanowski et al., 2007]. The research has been successfully implemented in ground subsidence studies caused by mining activity [Chrzanowski and Szostak-Chrzanowski, 2004] and by oil withdrawal [Szostak-Chrzanowski et al., 2006], in modelling deformations of large earth and rockfill dams [Szostak-Chrzanowski et al., 2005], and in modelling deformations of concrete structures [Chrzanowski, 1993].

Based upon this research, an interdisciplinary approach to designing geodetic deformation monitoring schemes has been developed using deterministic modelling of the expected displacement field. This approach is illustrated by an example of designing a monitoring scheme for an open pit mine.

5.2 Basic Conditions and Relations in Deterministic Modelling

In order to determine the displacement field using deterministic modelling, the following three basic conditions and relations must be defined:

1. **Conditions of equilibrium of forces**: (used for the static case in the example while Newton's laws of motion are used for dynamic analysis). The equation for equilibrium of forces may be presented in the form:

$$\sigma_{ji} dA_j = dP_i \tag{5.1}$$

where σ_{ji} denotes the stress tensor (symmetric) in the ij plane, dA_j is the incremental area in direction j, and dP_i is the incremental acting force P per unit area, A, in direction i.

If a volume is considered, the condition of equilibrium of forces can be written as:

$$\sigma_{j,ij} = -dP_i \tag{5.2}$$

2. **Kinematic strain-displacement relations**: The kinematic strain-displacement relations are independent of acting forces and the type of material behaviour (elastic or inelastic). The strain tensor is denoted by ε_{ij} and has nine components in the three dimensional space. In the case of a body in motion, the motion is described by dynamic equations. When the displacements, u, are small, the strain tensor components are:

$$\varepsilon_{ij} = \frac{1}{2}(u_{i,j} + u_{j,i}) \tag{5.3}$$

where:

$$u_{i,j} = \frac{\partial u_i}{\partial x_j} \tag{5.4}$$

3. **Stress-strain relations (constitutive laws)**: Linear-elastic constitutive laws can be used to model almost all materials if they are subjected to sufficiently small loads. For linear-elastic materials, Hooke's law for general anisotropic solids is given as:

$$\sigma_{ij} = D_{ijlm}\varepsilon_{lm} \tag{5.5}$$

where D_{ijlm} represents components of the elasticity tensor and i, j, l, m have values of 1, 2, or 3. As an example, in the case of two dimensional plane strain analysis, D_{ijlm} for isotropic solids can be written in matrix notation as:

$$D = \frac{E}{(1+v)(1-2v)}\begin{bmatrix} 1-v & v & 0 \\ v & 1-v & 0 \\ 0 & 0 & \frac{1+2v}{2} \end{bmatrix} \tag{5.6}$$

where E is Young modulus and v is Poisson ratio.

The above conditions and relations can be manipulated to obtain the following equation (Navier's equation):

$$\frac{E}{2(1+v)(1-2v)}[(1-2v)u_{i,ji} + u_{j,ji}] = -P_i \tag{5.7}$$

Equation ((5.7) may be solved using numerical methods (e.g., Finite Element Method (FEM)).

5.3 Modelling of Deformation in an Open Pit Mine

The stability of steep walls in open pit mines is a major safety issue. In general, there is a slow movement of the rock formation followed by acceleration before a failure occurs. With continuous monitoring of creep and acceleration of the rock movement, warning can be given to evacuate equipment and personnel in advance of a failure. One of the crucial conditions of the monitoring scheme is that it is connected to reference control points, which can be considered as stable. Therefore, one of the main tasks of deterministic modelling is to predict the extent of the deformation zone produced by the planned mining activity. Once the deformation zone is delineated, suitable locations for stable reference points can be chosen. Additionally, deterministic modelling provides general information on the expected magnitude of the deformation and on the location of the expected maximum displacements.

The magnitude of the displacement field is a function of the so called deformation characteristics of an open pit. The characteristics include: geometry of the pit and its environment, geology, geomechanical parameters including rock quality parameter, and mining sequence. Additionally, in areas having drastic seasonal climate changes, factors such as the amount of precipitation will have a significant impact on rock face instability.

The mine shown in Figure 5.3 has been used to illustrate the process of deterministic modelling. Though the geometry of the mine has been taken from real life, the geology,

and other characteristics of the mine have been assumed to be significantly simplified for the purpose of this example. Modelling of behaviour of the rock mass was conducted by using a 'large-scale' approach [Szostak-Chrzanowski, 2006b]. The rock formation, consisting of only two types (two layers) of rock was assumed to be of a good quality, isotropic rock mass.

The deterministic modelling of the expected response of the open pit slope and /or stress relaxation was performed to analyze the effects of enlarging the mine from the existing depth of 600 m to the designed final depth of 750 m. An analysis of the expected deformations was performed for five stages of mining sequence as marked in Figure 5.2. Only the effects of extracting the left wall and the bottom of the mine to a depth of 650 m are presented for demonstration purposes. Similar analysis could be conducted for the remaining excavation to the final depth of 750 m.

The geomechanical parameters of the rock strata were selected by using values published by Bieniawski [1984] for similar rock types. The in-situ Young modulus values differ significantly from laboratory values [Szostak-Chrzanowski et al., 2005] and the accepted in-situ values used in the analysis are given in Table 5.1. The behaviour of the rock mass was assumed to be linear-elastic. Two models of the open pit mine were investigated. In the first model it was assumed that the rock strata were homogenous. In the second model, a geological discontinuity (a fault zone) was introduced.

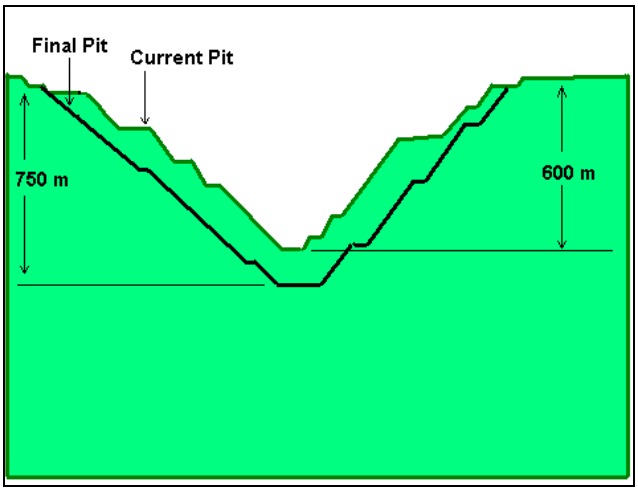

Figure 5.1: Open Pit Mine Scenario

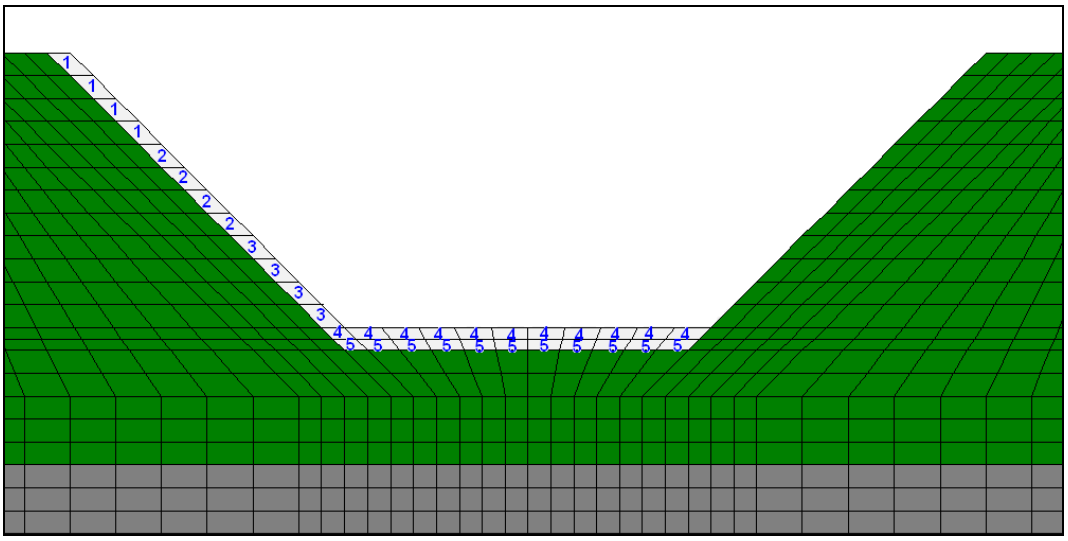

Figure 5.2: Mining Sequence

Table 5.1: Material Properties for Rock Masses in the Open Pit

Material	Young Modulus [kPa]	Poisson Ratio	Unit weight [N]
Ore carrying strata	2000000	0.25	26
Lower Strata	5000000	0.25	26
Fault Zone	20000	0.25	26

Deterministic modelling was performed using FEM supported by GeoStudio SIGMA/W software [GEO-SLOPE, 2007]. The open pit mine displacements were calculated using two-dimensional plane strain analysis. The analysis was preceded by preliminary testing of the mesh size and boundary conditions. Elements comprising the main area of the open pit were designed to have dimensions 50 m x 50 m. Elements on the pit floor were designed as 25 m x 50 m to accommodate excavation in this area. The horizontal extent of the model was determined using a trial and error approach. For the scenario investigated, it was determined that the mesh should extend 9 km from the rim of the pit on both sides to avoid instabilities on the surface greater than 2 mm. A trial and error approach was also used to determine the depth of the model required so that the accuracy of the displacements would not be significantly influenced. It was found that a depth of 1000 m below the final pit bottom was required.

A check was also performed to ensure that the number of elements used was not affecting the accuracy of the displacement results obtained. The mesh was reconstructed using element sizes half of the initial values. When displacement results were compared from the two meshes, 1-2 mm discrepancies existed, which were acceptable for the purposes of this example. With regard for the boundary conditions, horizontal displacements were not permitted along the left and right boundaries and neither horizontal nor vertical displacements were permitted along the bottom boundary.

Figure 5.3 illustrates the finite element model used in this analysis including the fault zone (light blue) to the left of the pit. Table 5.2 summarizes the total expected displacements at selected points (as marked in Figure 5.3) as a result of the mining activity.

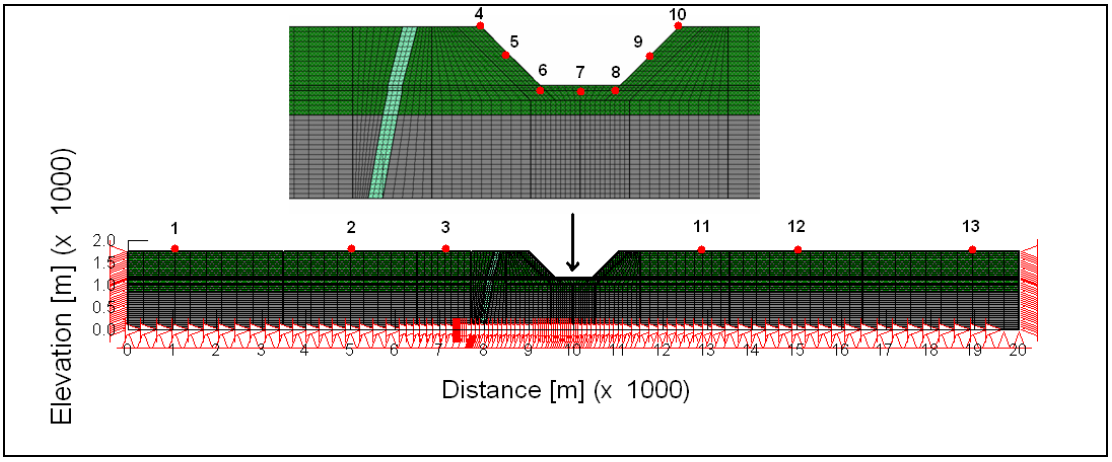

Figure 5.3: Finite Element Mesh of the Open Pit Mine

Table 5.2: Displacement Summary for Selected Points

	Without Fault							With Fault					
	Excavation Stage							Excavation Stage					
Pt #	**1**	**2**	**3**	**4**	**5**	**Total**		**1**	**2**	**3**	**4**	**5**	**Total**
1	0.000	0.000	0.000	0.000	0.000	0.000		0.000	0.000	0.000	0.000	0.000	0.000
2	0.000	0.001	0.003	0.000	0.001	0.005		0.000	0.000	0.000	0.000	0.000	0.001
3	0.001	0.006	0.013	0.001	0.002	0.024		0.000	0.001	0.001	0.002	0.001	0.005
4	0.175	0.065	0.061	0.019	0.006	0.326		0.133	0.050	0.016	0.049	0.031	0.279
5	0.110	0.029	0.107	0.028	0.014	0.289		0.092	0.025	0.031	0.050	0.031	0.229
6	0.019	0.055	0.120	0.119	0.047	0.360		0.016	0.040	0.084	0.139	0.087	0.366
7	0.004	0.008	0.024	0.224	0.141	0.401		0.003	0.006	0.011	0.223	0.144	0.387
8	0.001	0.003	0.009	0.107	0.040	0.161		0.001	0.002	0.004	0.119	0.045	0.169
9	0.001	0.001	0.002	0.024	0.014	0.042		0.000	0.000	0.001	0.029	0.013	0.043
10	0.000	0.001	0.001	0.014	0.006	0.022		0.000	0.000	0.000	0.022	0.009	0.032
11	0.000	0.000	0.001	0.002	0.003	0.007		0.000	0.000	0.000	0.002	0.000	0.003
12	0.000	0.000	0.000	0.001	0.001	0.002		0.000	0.000	0.000	0.000	0.000	0.000
13	0.000	0.000	0.000	0.000	0.000	0.000		0.000	0.000	0.000	0.000	0.000	0.000

It can be seen that maximum displacements (uplifts) of up to 40 cm are expected to occur at the bottom of the pit. At point 2, which is located 4 km to the left of the rim of the pit, the total displacements may still reach 1 mm and 5 mm with and without the fault respectively. As expected, the presence of the fault reduces transfer of tensional stresses beyond the fault. At point 11, which is 2 km to the right of the rim of the pit, the displacements may still reach 3 mm and 7 mm with and without the fault respectively, even though the right slope is not excavated.

To illustrate how misinterpretations of the deformation behaviour can occur, consider the effect of locating a "stable" reference station at Point 10 at the rim of the right wall (which has not been excavated). If it is assumed that Point 10 is stable, the total displacements measured during excavation stage 4 will be in error by 14 mm.

Figure 5.4 shows the displacement fields arising from excavation stages 1, 3 and 5 for the model without the geological fault.

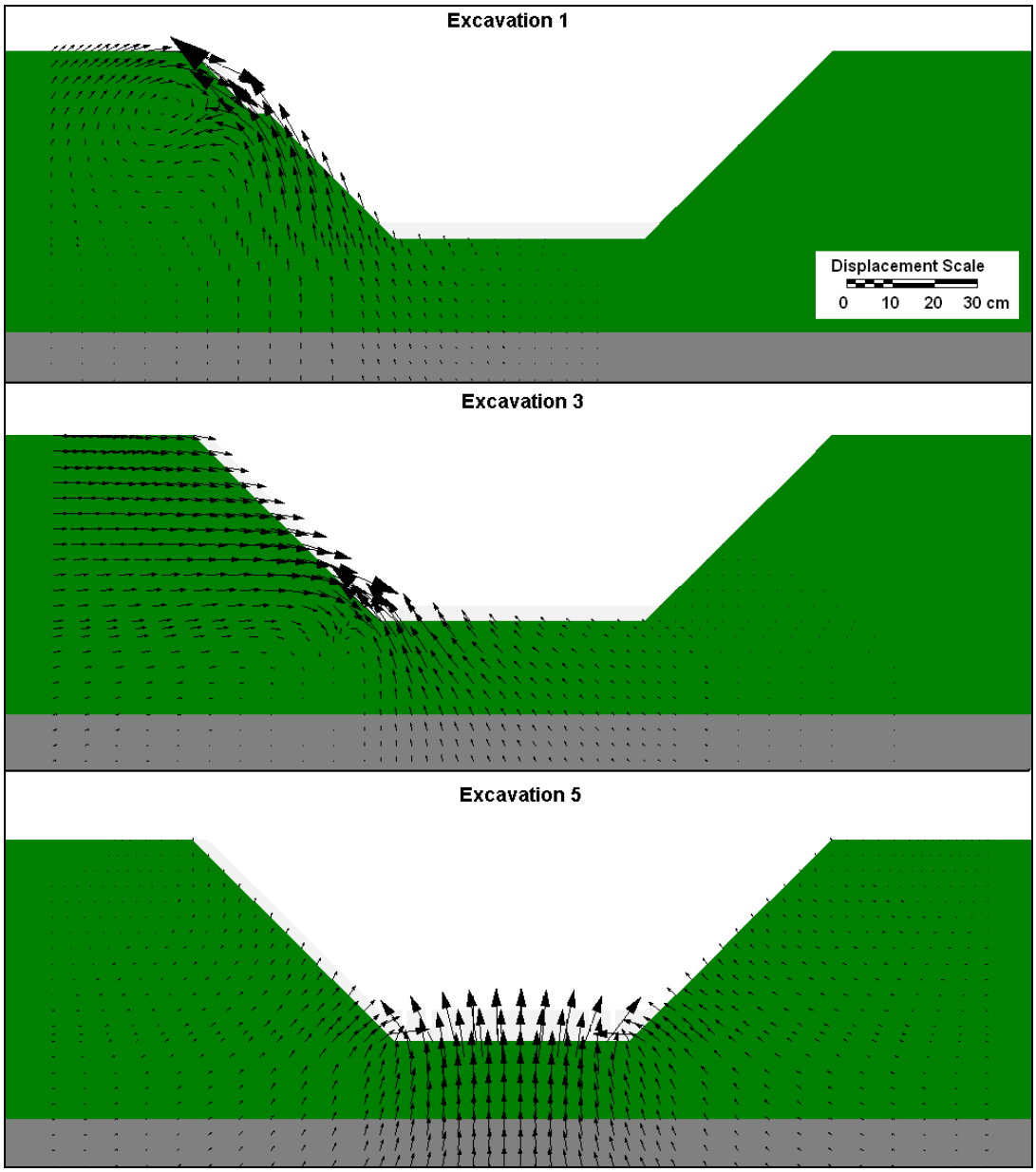

Figure 5.4: Displacement Fields caused by Selected Excavation Stages

It can be seen that:

1. Excavation of the slopes causes the surrounding rock mass to move in the direction of the previously occupied material.
2. The pit floor experiences uplift as a result of excavation of the slope.

3. Excavation of the pit floor is mainly responsible for the displacements occurring along the right (non-excavated) slope.

Graphical presentation of the total accumulated (without the fault) displacements is given in Figure 5.5 (displacement scale is twice that in Figure 5.4). The most significant displacements manifested are uplift vectors occurring along the pit floor. These displacements occur as a result of a relaxation of stresses as the pit floor is excavated. Even though excavation occurs only along the left slope and pit floor, the stability of the right slope is also affected. The rim on both sides of the pit experience displacements. This has important implications for choosing suitable locations for geodetic instrumentation.

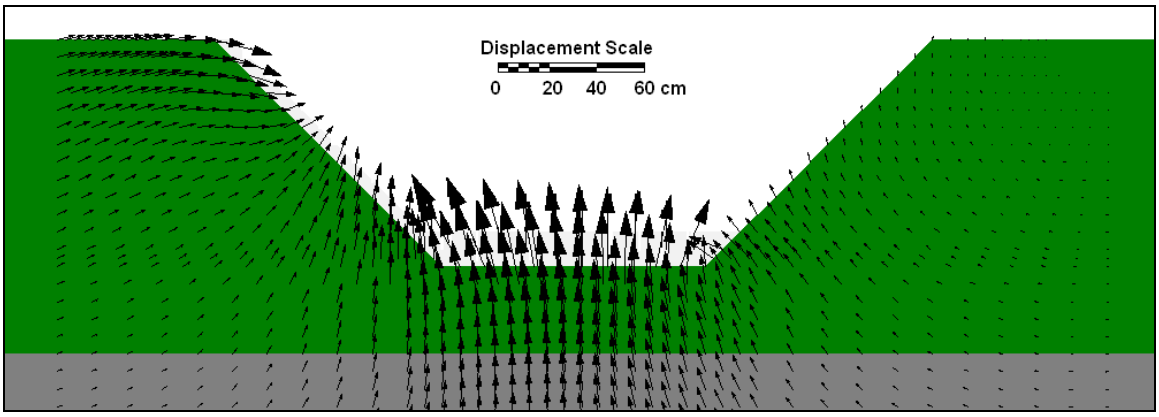

Figure 5.5: Cumulative Displacement Field after all Excavations

As indicated, the fault limits the extent of the region of deformation. Figure 5.6 shows contours of horizontal displacements with and without the fault.

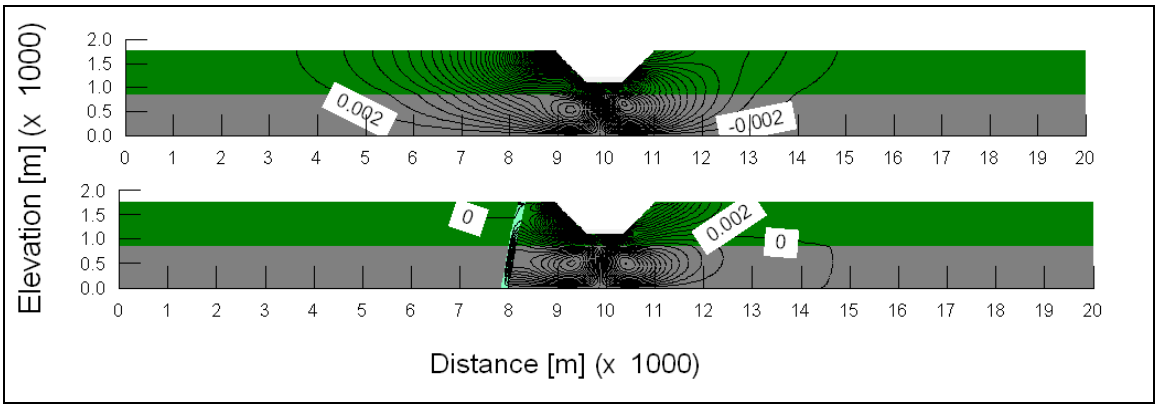

Figure 5.6: Comparison of Horizontal Stability
(top without fault, bottom with fault)

As was shown in Table 5.2 the fault zone allows stable reference points to be located closer to the open pit. This information has further important implications: knowing that a fault limits the extent of the region of instability, geodetic instruments can be used to locate fault zones. For example, if a target point shows stable behaviour in a region thought to be active, this may suggest that a fault exists somewhere between the target and the area of mining activity. Both the finite element model results and actual measurement values should therefore be used to complement each other in the overall physical interpretation process.

5.4 Design of the Monitoring Scheme

Deformation monitoring schemes serve dual purposes: (1) they verify the designed or expected behaviour of the investigated object and (2) they provide a warning system by signalling when observed deformations show irregularities. The latter purpose is the predominant one in the case of deformation monitoring in large open pit mines because the first purpose is a very challenging task. This is due to varying local conditions, discontinuities or fractures, and changeable mechanical properties of the rock mass.

As a result of this complexity, the monitoring system in most large open pit mines requires hundreds of targets to be continuously monitored with sub-centimetre accuracy at the 95% confidence level. The deterministic model provides useful information in the global expected response of the rock strata to the mining activity. This is sufficient for a general design of the monitoring technology and methodology. Detailed information, however, such as where to locate each monitoring target, is based mainly on the experience of the staff responsible for the safety of the mine. Therefore, very detailed monitoring is required, preferably continuous in both space and time domains.

The instability of bench walls is defined empirically by the velocities of observed points located in the deformation area. Newcomen et al. [2003] define the status of point instability using four categories. The “Background” category represents velocities showing the expected response to mining and/or stress relaxation. The “Watch” category

represents increased velocities mostly caused by mining sequence or weather conditions (e.g., rain season). The “Caution” category is used for points having increased velocities associated with accelerations. The “Alert” category describes points having velocities which exceed the previously measured values in the same area.

The actual values of the displacements for each category may significantly vary from one mine to another. For example, two open pit mines of Highland Valley Copper in Western Canada, though only 2 km apart, represent very different conditions for possible wall failure [Newcomen et al., 2003]. Where 50 mm/day displacements may be categorized only as a “watch” category in one mine, a displacement rate of 10 mm/day may already been considered as the “ALERT” category in the second one. Thus, the required accuracy of monitoring may differ significantly from one mine to another.

Based upon the expected displacement rates, the global predicted displacement field generated through deterministic modelling, critical deformation zones identified by the mining engineer, and previous experience, the geodetic engineer can make informed decisions regarding the technology to be used and approximate locations of the instrumentation. Some of the most commonly used geodetic sensors in deformation monitoring are robotic total stations (RTSs), Global Positioning System (GPS) receivers, interferometric synthetic aperture radar (InSAR) and laser scanners, each of which is briefly described.

a. **RTSs**: At the present time, robotic total stations equipped with automatic target recognition (ATR) are one of the most practical methods of monitoring the displacements of target points located throughout a deformation zone [Chrzanowski and Wilkins, 2006]. This sensor can be cost effective when hundreds of targets must be monitored. An RTS measures polar coordinates of target points at a given epoch, so that displacements can be determined between epochs. The range of ATR under average conditions is about 1.5 km. An RTS can only measure to one target at a time, so the time lapse between consecutive epochs is limited by the total number of targets that must be measured. As sight lengths increase, limitations of the technology become more dominant due to the effects of atmospheric refraction and pointing errors. Based on field tests in two large open pit mines, Chrzanowski and Wilkins [2006] concluded that at present, sub-centimetre accuracy of displacement detection at 95% confidence level is achievable on a daily basis (one averaged result every 24 hours) using RTSs. This result is achievable from single RTS observations to target points that have lines of sight of 600 m or less. At distances up to 1200 m, displacements of 20 mm (at 95% confidence level) can be detected with observations from a single RTS. Since the accuracy of distance measurements with RTS is considerable higher than of the direction measurements, the accuracy and frequency of results of horizontal displacements can be dramatically increased when distances to the targets are measured from two or more RTSs simultaneously. Here, one has to weigh accuracy versus economy.

b. **GPS**: a stand-alone GPS deformation monitoring system is only economically feasible when there are a small number of target points to be monitored. The major advantage of GPS is that it does not require line of sight between receivers. This allows stable control points to be established outside of the deformation zone without concern for connectivity. GPS can be used to control the stability of RTSs in large scale projects when the RTS must be located within the deformation monitoring zone. In static applications, millimetre level precisions can be achieved in east, north and up components. Actual values will depend upon baseline length, the observation environment, session length and equipment quality [Bond, 2004].

c. **InSAR**: The major error sources which limit the accuracy of InSAR include atmospheric propagation effects (ionospheric and tropospheric delays), satellite orbit errors, changes in ground surface conditions and temporal decorrelation and poor image corregistration due to limited ground truth points [Chen et al., 2000]. Additionally, the repeat cycle of SAR satellites (RADARSAT, 24 days, ERS 1&2, 35 days and JERS 1, 44 days) may not be sufficient to provide the temporal resolution required for a given application. It is particularly challenging to use InSAR technology to measure steep ground surfaces and areas covered with heavy vegetation. Additionally, InSAR only measures displacement along the radar line of sight [Liu et al., 2004].

d. **Laser Scanners**: Like InSAR, the main advantage of laser scanners over total station and GPS measurements is their ability to provide high spatial resolution. The latest generation of laser scanners offer data acquisition rates of up to 500 000 points per second [Leica Geosystems, 2007b]. This results in "point clouds" of millions of data points for a single setup. Sophisticated processing algorithms are required to transform different scans into one coordinate system. Target points are measured to allow subsequent scans to be linked together through an image registration process. Deformation analysis can be achieved by comparing the results between different epochs of modeled surfaces fit to the scanned object. Alternatively, target points can be used to calculate displacements between epochs. Ranges of up to 300 m can be achieved using a laser scanner such as the Leica ScanStation. However, the working range of this instrument and the Leica HDS6000 is about 50 m when sub-centimetre precision is required [Leica Geosystems, 2007b]. Rain and poor surface reflectivity can further degrade achievable accuracy. [Roberts and Hirst, 2005].

Table 5.3 summarizes the advantages and disadvantages of the 4 technologies discussed:

Table 5.3: Advantages and Disadvantages of Selected Geodetic Technology

Technology	Advantages	Disadvantages
RTS	- cost effective - sub-cm accuracy (average of 24 hours) for distances < 600 m - presently available in fully automated mode	- spatial resolution limited to number of targets used - strongly affected by refraction - accuracy degrades rapidly with increased distances
GPS	- line of sight not required between stations - mm precision for short baselines (< 10 km) - presently available in fully automated mode	- expensive when a large number of target points must be monitored - spatial resolution limited to number of targets used - environment dictates achievable accuracy
InSAR	- continuous spatial resolution - sub-centimeter accuracy	- not presently available in fully automated mode - highest temporal resolution is 24 days - displacement detection limited to line-of-sight direction - strongly affected by environmental conditions
Laser Scanner	- continuous spatial resolution - sub-centimeter accuracy	- limited range - not presently available in fully automated mode - achievable accuracy dependent upon surface reflectivity - rain degrades accuracy

The scale of the presented example eliminates the possibility of using a laser scanner for deformation monitoring. The temporal resolution requirements eliminate InSAR as an option. Consequently, robotic total stations and/or GPS are left as the most viable options for geodetic sensors. One possible arrangement of a combined RTS+GPS deformation monitoring system is illustrated in Figure 5.7. In this arrangement, two GPS control stations are located in such positions as to have instabilities less than 2 mm, while still maintaining short baseline status (< 10 km). These control stations are used to redundantly monitor the stability of two RTS stations located within the pit. The RTS

stations are then used to monitor target points strategically placed on the pit walls based upon the advice of a geotechnical engineer. A traditional geodetic pre-analysis exercise should be conducted to ensure accuracy requirements are met. In practice, the project budget will dictate what combination of technology will actually be used.

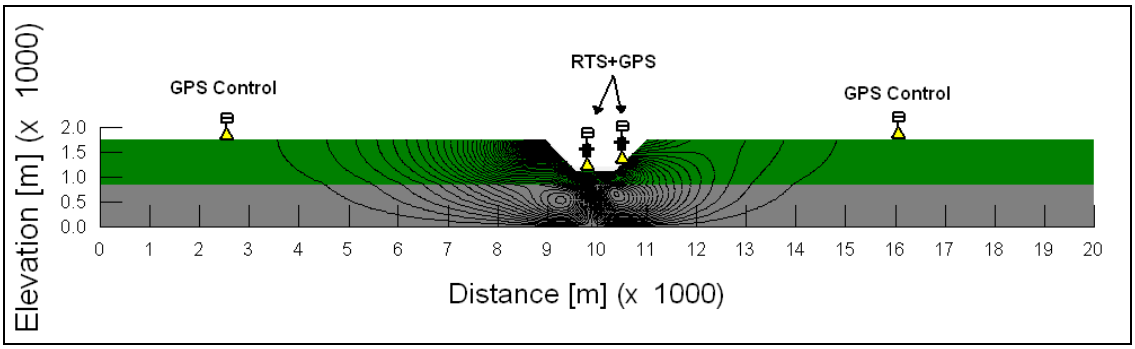

Figure 5.7: A Geodetic Deformation Monitoring Scheme based upon Deterministic Modelling

5.5 Conclusion and Recommendations

In order for the monitoring scheme to be effective, it must be connected to stable reference points. Deterministic modelling aids in fulfilling this requirement by allowing the extent of the deformation zone to be assessed based upon the designed mining activity. Once the deformation zone has been delineated, suitable locations for stable reference points can be chosen. Additionally, deterministic modelling provides a method for predicting global displacement behaviour and determination of the areas of maximum expected deformation.

An interdisciplinary approach to designing a geodetic deformation monitoring scheme has been illustrated in an open pit mine example. It was shown how an injudicious decision regarding the location of instruments can lead to incorrect displacement measurements. This can have serious consequences when safety is a concern and remedial measures are involved. The terms 'deformation monitoring' and 'safety' typically go hand in hand. It is the engineer's responsibility to ensure that all measures are taken to properly design the deformation monitoring system. Consequently, it is advised to use an interdisciplinary approach in designing a geodetic deformation monitoring scheme to take advantage of additional sources of information that can help prevent such calamities.

Acknowledgements

This research could not have been completed without the support of the Public Safety and Emergency Preparedness Canada Research Fellowship in honour of Stuart Nesbitt White, the Natural Sciences and Engineering Research Council of Canada (NSERC) and Atlantic Canada Opportunities Agency (ACOA).

References

Bond, J. (2004). *An Investigation on the Use of GPS for Deformation Monitoring in Open Pit Mines*. M.Sc.E. thesis, Department of Geodesy and Geomatics Engineering, University of New Brunswick, Fredericton, New Brunswick, Canada, 143 pp.

Bieniawski, Z.T. (1984). *Rock Mechanics Design in Mining and Tunnelling*, Rotterdam, Netherlands, A.A. Balkema, 272 pp.

Chen, Y.Q., G. Zhang, X. Ding and Z. Li (2000). "Monitoring Earth Surface Deformations with InSAR Technology: Principle and Some critical Issues." *Journal of Geospatial Engineering,* Vol. 2, No. 1, pp. 3-21.

Chrzanowski A. (1993). "Modern Surveying Techniques for Mining and Civil Engineering." Chapter 33 in Vol. III of *Comprehensive Rock Engineering,* Ed. J. Hudson, Pergamon Press, New York, pp. 773-809.

Chrzanowski, A., and A. Szostak-Chrzanowski (2004). "Physical Interpretation of Ground Subsidence Surveys – A Case Study." *Journal of Geospatial Engineering*, Hong Kong Institute of Engineering Surveyors, pp. 21-29.

Chrzanowski, A., A. Szostak-Chrzanowski, J. Bond and R. Wilkins (2007). "Increasing Public and Environmental Safety through Integrated Monitoring and Analysis of Structural and Ground Deformations." Proceedings of the *3rd International Symposium on Geo-information for Disaster Management,* Toronto, Ontario, Canada, 22-24 May, 12 pp., CDROM.

Chrzanowski, A. and R. Wilkins (2006). Accuracy Evaluation of Geodetic Monitoring of Deformations in Large Open Pit Mines. Proceedings of the *3rd IAG Symposium on Geodesy for Geotechnical and Structural Engineering and 12-th FIG Symposium on Deformation Measurements*, Eds. H. Kahmen and A. Chrzanowski, Baden, Austria, 22-24 May, CD ROM

GEO-SLOPE (2007). "Products." *GEO-SLOPE International Ltd*., http://www.geo-slope.com, accessed on: 14 March 2007.

Leica Geosystems (2007b). "HDS Systems, The HDS Product Family." *Leica Geosystems,* http://www.leica-geosystems.com/corporate/en/ndef/lgs_5570.htm, accessed on: 6 February.

Liu, G.X., Y.Q. Chen, X.L. Ding, Z.L. Li and Li ZW (2004). "Monitoring Ground Settlement in Hong Kong with Satellite SAR Interferometry." *Photogrammetric Engineering and Remote Sensing*, 70(10):1151-1156.

Newcomen, W.H., C. Murray and L. Shwydiuk (2003). "Monitoring pit wall deformations in real time at Highland Valley Copper." Proceedings of the *Fourth International Conference on Computer Applications in the Minerals Industry*, Calgary, Alberta, Canada, 8-10 September, CD-ROM.

Roberts, G., and L. Hirst (2005). "Deformation Monitoring and Analysis of Structures Using Laser Scanners." *Proceedings of FIG Working Week 2005*, Cairo, Egypt, 16-21 April, TS32.8.

Szostak-Chrzanowski A., A. Chrzanowski and M. Massiéra (2005). "Use of Geodetic Monitoring Measurements in Solving Geomechanical Problems in Engineering and Geosciences." *Engineering Geology Vol. 79, Issues.1-2: Application of Geodetic Techniques in Engineering Geology*, Eds. S. Stiros and A. Chrzanowski, 3 June, pp. 3-12.

Szostak-Chrzanowski, A. (2006). "Interdisciplinary Approach to Deformation Analysis in Engineering, Mining, and Geosciences Projects by Combining Monitoring Surveys with Deterministic Modelling – Part I." *Technical Sciences Journal*, UWM, Olsztyn, pp. 147-172.

Szostak-Chrzanowski, A, A. Chrzanowski, and E. Ortiz (2006b). "Modelling of Ground Subsidence in Oil Fields." *Technical Sciences Journal*, UWM, Olsztyn, pp. 133-146.

CHAPTER 6

DEVELOPMENT OF A FULLY AUTOMATED, GPS BASED MONITORING SYSTEM FOR DISASTER PREVENTION AND EMERGENCY PREPAREDNESS: PPMS^{+RT}

Jason Bond, Don Kim, Adam Chrzanowski and Anna Szostak-Chrzanowski
University of New Brunswick, Fredericton New Brunswick Canada

The following was originally published as:

Bond, J., D. Kim, A. Chrzanowski, A. Szostak-Chrzanowski (2007). "Development of A Fully Automated, GPS Based Monitoring System for Disaster Prevention and Emergency Preparedness: PPMS^{+RT}" *Sensors* 2007, (7) Special Issue: *Sensors for Disaster and Emergency Management Decision Making*, Eds. J. Levy and Y.Gao, pp. 1028-1046. Available at: http://www.mdpi.org/sensors/list07.htm#new, accessed on: 4 October 2007.

The first author has designed the real-time processing algorithms to create the real-time version of the software, designed the experiment, compiled the results and prepared the manuscript. The second author has provided advice on paper content and insight into the theoretical background of real-time data handling strategies and improving the Kalman filter response time required to detect displacements. The third author has provided advice on paper content and insight into the real-time data handling requirements for deformation monitoring applications. The fourth author has provided advice on paper content and insight into the role of deterministic modelling in the design of geodetic deformation monitoring schemes.

Abstract

The increasing number of structural collapses, slope failures and other natural disasters has lead to a demand for new sensors, sensor integration techniques and data processing strategies for deformation monitoring systems. In order to meet extraordinary

accuracy requirements for displacement detection in recent deformation monitoring projects, research has been devoted to integrating Global Positioning System (GPS) as a monitoring sensor. Although GPS has been used for monitoring purposes worldwide, certain environments pose challenges where conventional processing techniques cannot provide the required accuracy with sufficient update frequency. Described is the development of a fully automated, continuous, real-time monitoring system that employs GPS sensors and pseudolite technology to meet these requirements in such environments. Ethernet and/or serial port communication techniques are used to transfer data between GPS receivers at target points and a central processing computer. The data can be processed locally or remotely based upon client needs. A test was conducted that illustrated a 10 mm displacement was remotely detected at a target point using the designed system. This information could then be used to signal an alarm if conditions are deemed to be unsafe.

6.1 Introduction

Disasters such as landslides, avalanches and structural failures do not occur without warning. Through strategic monitoring of the deformable object, abnormal behaviour can be detected and used to warn of imminent failure. The increasing number of structural collapses, slope failures and other natural disasters has lead to a demand for new sensors,

sensor integration techniques and data processing strategies for deformation monitoring systems.

The Canadian Centre for Geodetic Engineering (CCGE) at the University of New Brunswick (UNB) is involved in the development of new methods and techniques for integrated monitoring, integrated analysis, and prediction (deterministic modelling) of structural and ground deformations. Recent, large scale, deformation monitoring projects in open pit mines have placed extraordinary demands for displacement detection accuracy.

In large open pit mines and in other steep embankment areas, the stability of steep walls is a major safety issue. In general, there is slow movement of the rock formation followed by acceleration before a failure occurs. With continuous monitoring of creep and acceleration of the rock movement, warning can be given to evacuate equipment and personnel in advance of a failure. In order to perform such tasks, monitoring accuracies of up to ± 5 mm with 95% confidence have been requested.

These requirements can be extremely difficult to meet since the achievable precision of geodetic technologies can be severely limited by the characteristics of an open pit. It is not uncommon for the degradation in precision of geodetic technologies to be so large that the minimum detectable displacement exceeds the mine's requirements. For this

reason, large open pit mines may be considered one of the most challenging deformation monitoring scenarios.

For example, in large scale projects where the pit diameter exceeds 1 km, refraction and pointing errors limit the effectiveness of direction measurements made by total station instruments and laser scanners [Bond et al., 2005]. The steep pit walls limit the effectiveness of space borne interferometric, synthetic aperture radar [Chen et al., 2000]. The steep pit walls also limit the effectiveness of satellite positioning technologies by diluting the geometric strength of solutions and reducing the frequency at which updates can be provided. Additionally, large height differences between master and rover stations can lead to significant height biases in baseline solutions [Bond et al. , 2005].

This research focuses on providing fully automated, continuous, high precision position updates using one of the above mentioned geodetic technologies: the Global Positioning System (GPS). Although GPS has been used for monitoring purposes worldwide, certain environments pose challenges where conventional processing techniques cannot provide the required accuracy with sufficient update frequency. Discussed are the challenges encountered in using GPS in harsh environments and the innovations that have been introduced in order to successfully integrate this technology for deformation monitoring in such scenarios.

6.2 Using GPS for Deformation Monitoring in Harsh Environments

GPS (and in general, Global Navigation Satellite Systems (GNSS)) offers potential advantages over other geodetic technologies that allows for continuous and high accuracy displacement detection. These include:

a) Line of sight is not required between stations;
b) Updates can be provided at frequencies of 1 Hz and higher;
c) 3 dimensional position information is provided; and
d) Millimetre level position information is possible for baselines potentially up to 10 km in length.

The major disadvantage of using GPS is the cost of a geodetic grade receiver and antenna. This will ultimately limit the number of units that can be afforded and dictate the spatial resolution of targets that can be monitored using this technology. In most cases it will be more economical to integrate GPS to monitor the stability of other sensors that can provide higher spatial resolution at a cheaper cost in localized areas (e.g., total stations, laser scanners).

To determine if the above advantages of GPS could be realized in a harsh environment, GPS data were collected at 5 stations in a large open pit mine as illustrated in Figure 6.1. Stations 424 and 987 were reference stations, while stations RTS1, RTS2

and RTS3 were monitored stations within the pit. Continuous data for 5 days or more were collected.

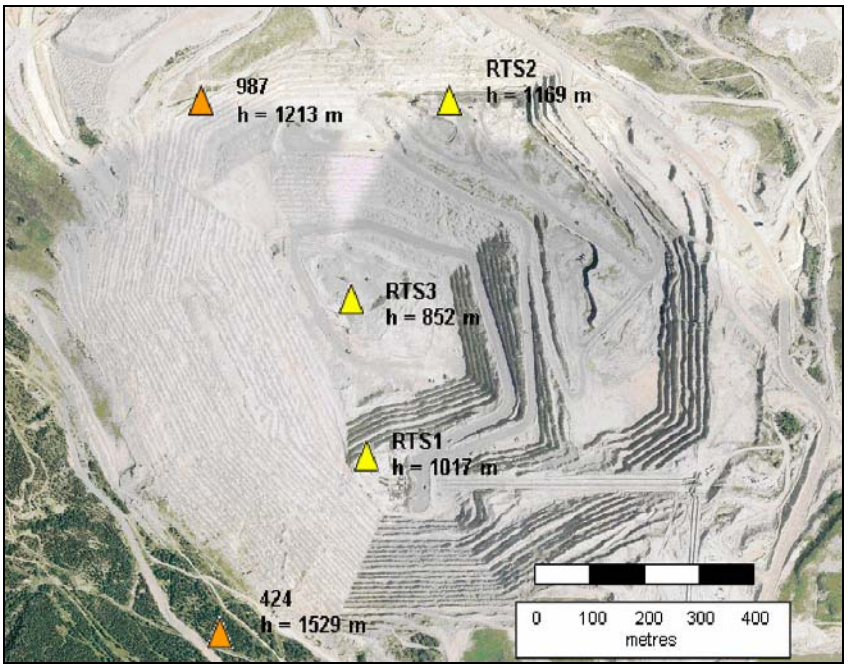

Figure 6.1: Large Open Pit Mine Test (with station heights shown).

Initial analyses of the GPS data were conducted using traditional batch processing methods in commercial and scientific software [Kim et al., 2003; Bond et al., 2005]. To illustrate, 3 hour, commercial software results are presented in Figure 6.2 showing the 'up' (height) component solutions (generally the poorest precision) for baseline 424 to RTS2. RTS2 represents the best case scenario of the monitored stations in terms of satellite visibility and height differences with reference stations. The results have been obtained using conventional double-differenced, L1 carrier phase processing methods. The height difference between master and rover stations is 361 meters. It can be seen that a peak-to-peak spread of over 4 cm exists. Since there is a large height difference, the

unmodelled portion of the atmosphere between the stations causes biases in the height component as meteorological conditions vary from day to day. The RMS error for this sample is ± 9 mm. There are also 4 sessions for which a fixed position solution could not be obtained due to poor data quality. Results for stations RTS1 and RTS3 show larger biases in the height component and more solution outages.

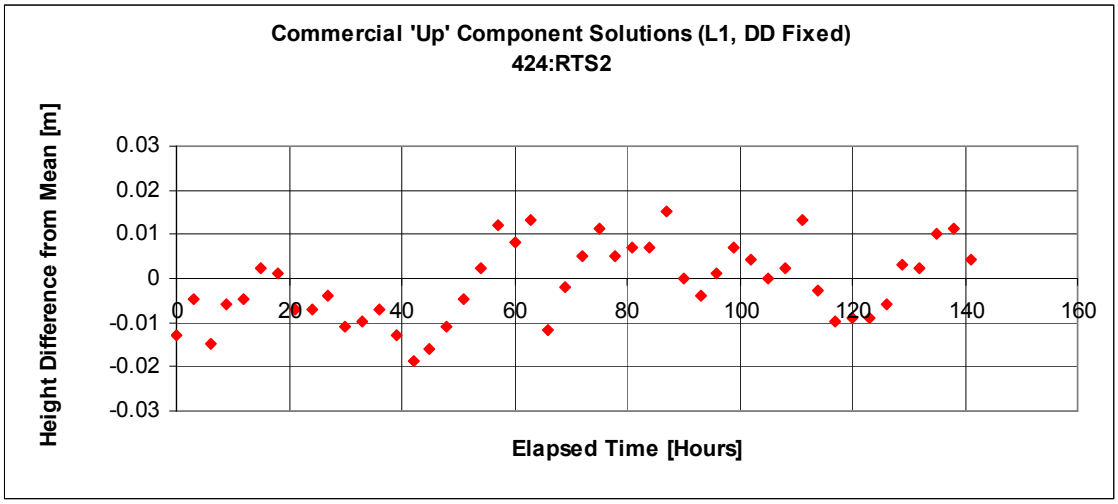

Figure 6.2: Commercial, 3 Hour, DD Fixed, 'Up' Component Solutions.

Further investigation was conducted to determine if longer session lengths would improve the quality of the position of estimates [Bond et al., 2005]. Other commercial and scientific (UNB's Differential Positioning Package- DIPOP, University of Bern's Bernese) software were also tested. Although the precision of the results improved with longer session lengths, the delay between position updates (sometimes up to 24 hours) would not satisfy project requirements.

From the above results, it is apparent that in order to use GPS to provide sub-centimetre displacement detection with 95% confidence, there are some major challenges that need to be addressed. Additional obstacles arise when attempting to provide fully automated updates for continuous monitoring of target points. The major challenges involved in using GPS for deformation monitoring in harsh deformation monitoring environments are:

a) Mitigating residual troposheric delay biases: Residual tropospheric delay is the portion of tropospheric delay that remains after modelling. Due to large height differences between master and rover stations, residual tropospheric delay biases can contaminate the vertical component of GPS baseline solutions. Beutler et al. [1988] have illustrated that neglecting the differential troposphere causes a 3-5 mm relative height error for every millimetre of difference in zenith delay between stations. Estimating residual tropospheric delay bias terms is the usual approach to improving accuracy in such situations. The strength of the bias estimates, however, depends upon low elevation satellites which are generally not visible [Langley, 1995]. In order to meet sub-centimetre accuracy requirements in large open pit mines using GPS, a new methodology is required to mitigate this bias.

b) Providing continuous updates with limited satellite visibility: The steep pit walls of open pit mines obstruct satellite visibility. This limits the reliability of the

solutions as well as the frequency at which updates can be provided. In order to meet sub-centimetre accuracy requirements with sufficient update frequency, new technologies must be integrated with GPS.

c) Connecting to stable reference points: As precise as the GPS software may be, the overall accuracy of the solution depends upon the validity of the assumption that each reference point is stable. Tremendous care must be taken in choosing suitable reference station locations. Additional sources of information regarding the properties of the rock mass must be utilized to make informed decisions.

d) Developing a fully automated GPS processor: A fully automated GPS processor is required to provide continuous updates in real time. Ideally, the results from the processor can be used to provide 'on-time' warnings of impending danger. The processor must be designed to be robust so that false alarms do not occur. Additionally, the precision of the solutions must satisfy sub-centimetre displacement detection requirements with 95% confidence. Communication links must also be built into the software to allow for data transfer between GPS receivers located on site at target points and a central processing computer.

6.3 Overcoming GPS Deformation Monitoring Challenges

In order to capitalize on the benefits of GPS, the aforementioned challenges need to be addressed. Research has been devoted to answering each of these needs [Bond et al., 2007a; Bond et al., 2007b; Bond et al., 2007c]. Discussed are the innovations introduced to overcome these obstacles.

6.3.1 Mitigating Residual Tropospheric Delay

A common technique of eliminating biases is through differencing of observations. For example, between-receivers differencing (SD: single difference) of GPS observations to the same satellite eliminates satellite clock biases and between-satellite differencing of GPS observations to the same receiver eliminates receiver clock biases. Further differencing between-receivers SDs and between-satellite SDs results in a double-differenced (DD) observable free of both receiver clock and satellite clock biases.

The devised methodology is based upon time differencing of successive DD observations and gives the triple-differenced (TD) observable [Remondi, 1984]. The appeal of the TD observable to most users is its absence of the integer ambiguity term which cancels out through the time difference if a cycle slip has not occurred. Although the TD observable is not new, obtaining high precision results in environments where the

DD observable suffers from residual tropospheric delay biases presents another beneficial use.

After removing the error terms for receiver clocks and satellite clocks (which should be eliminated through DD processing when observation simultaneity criteria are met), the TD, carrier-phase observable between times t_1 and t_2 can be written as:

$$\delta \underset{AB}{\Delta} \overset{ij}{\nabla} \varphi(t_{12}) = [\underset{AB}{\Delta} \overset{ij}{\nabla} (\varphi + N + M - \frac{f}{c} I + \frac{f}{c} T + e_{\varphi}) + \varepsilon_{trop}]_{t_2} - [\underset{AB}{\Delta} \overset{ij}{\nabla} (\varphi + N + M - \frac{f}{c} I + \frac{f}{c} T + e_{\varphi}) + \varepsilon_{trop}]_{t_1} \quad (6.1)$$

where:

$\overset{ij}{\nabla}$	SD operator between satellites i and j
$\underset{AB}{\Delta}$	SD operator between receivers A and B
δ	differentiator between times t_1 and t_2
φ	carrier-phase observable (cycles)
N	ambiguity (cycles)
M	multipath (cycles)
I	ionospheric delay of the L1 carrier phase (m)
T	tropospheric delay (m)
f	carrier wave frequency (Hz)
c	speed of light in a vacuum (m/s)
ε_{trop}	residual tropospheric delay bias (present over large height differences) (cycles)
e_{φ}	random carrier-phase measurement noise

For observation intervals less than a few seconds, the correlation in atmospheric parameters between times t_1 and t_2 is large and therefore biases originating from them are

significantly reduced. Since the ambiguity term N cancels, Equation (6.1) can be rewritten as:

$$\delta \underset{AB}{\Delta} \overset{ij}{\nabla} \varphi(t_{12}) = [\underset{AB}{\Delta} \overset{ij}{\nabla}(\varphi + M)]_{t_2} - [\underset{AB}{\Delta} \overset{ij}{\nabla}(\varphi + M)]_{t_1} + e_{\delta\Delta\nabla\varphi} \tag{6.2}$$

where:

$e_{\delta\Delta\nabla\varphi}$ random noise error of a TD carrier-phase observation

The TD observable may be considered as an integrated (radial) velocity measurement which is used to determine position. The measurement form is [Brown and Hwang, 1997]:

$$\begin{aligned} (measurement)_k &= \int_{t_{k-1}}^{t_k} (velocity)dt + noise \\ &= (position)_k - (position)_{k-1} + noise \end{aligned} \tag{6.3}$$

In mathematical form, the measurement equation can be written as:

$$z_k = H_k x_k + J_k x_{k-1} + v_k \tag{6.4}$$

where H_k (= -J_k) is a directional cosine matrix.

This form does not fit the general format for the usual Kalman filter equations due to the x_{k-1} term. The general Kalman filter equations must be modified to accommodate this

term as well as any correlation in process and measurement noise. The modified version is known as the Delayed-State Kalman filter. The interested reader can find the Delayed-State equations in [Brown and Hwang, 1997], [Bond et al., 2007a].

Recently, the Precise Position Monitoring System (PPMS) software has been developed that employs a Delayed-State Kalman filter to process triple-differenced carrier phase observations [Bond et al., 2007a]. Initial test results have been promising, showing that mm level precisions are attainable in horizontal and vertical position components without having to solve for the ambiguity term. The expense of using this technique is slow filter convergence time due to the nature of the TD observable (it reflects the change in satellite geometry from one epoch to the next). This is generally not a concern for long term deformation monitoring applications.

Figure 6.3 presents the east, north and up components of the 424:RTS2 baseline processed using PPMS. There is a height change of a few mm that is detected after hour 50, which is not so easily identified in Figure 6.2**.** The peak-to-peak spread of the up component in Figure 6.3 is in the order of 1 cm after the change in height, as opposed to 4 cm in Figure 6.2. This can be attributed to the effects of residual tropospheric delay being reduced by the TD approach. The improved precision combined with more continuous updates allows for a clearer picture of the deformation behavior of the target point. A comparison of DD batch processing with the TD Delayed-State Kalman filter approach is presented in Table 6.1.

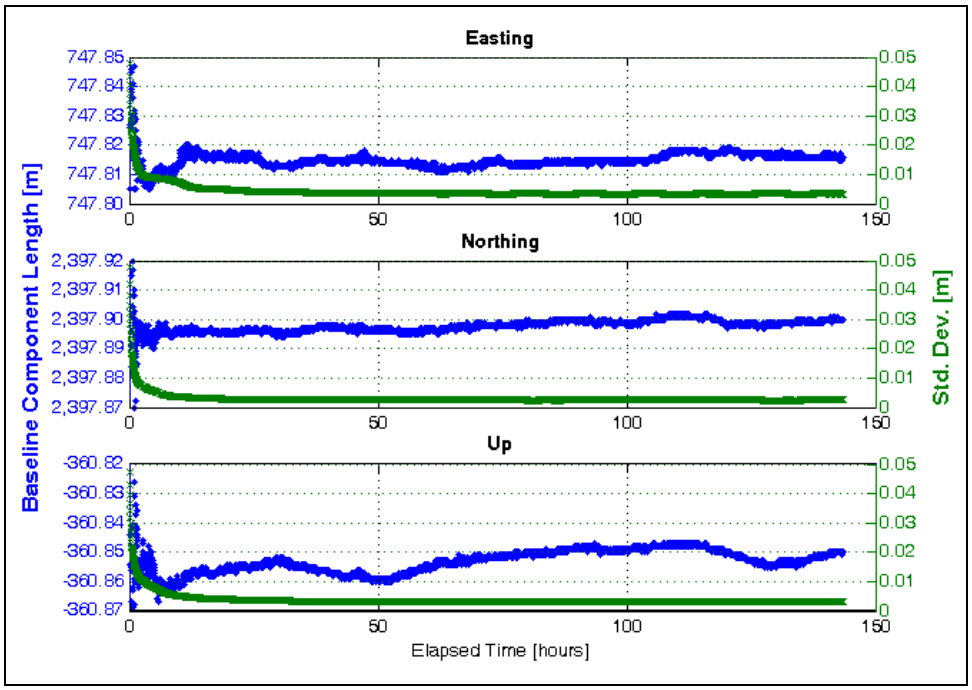

Figure 6.3: Continuous, TD, Easting, Northing and Up Solutions using PPMS

Table 6.1: Comparison of DD Batch Processing with TD Kalman Filter Processing Methods.

Processing Strategy	Advantages	Disadvantages
DD Batch Processing	- High precision results - Lower level of differencing results in less observation noise	- Results are not continuous - Height biases caused by residual tropospheric delay over large height differences when low elevation satellites are not visible
TD Kalman Filter	- High precision results - Results provided at sample rate - Significantly reduces atmospheric biases (residual tropospheric delay) over high sample rates - Less chance of false alarms caused by cycle slips	- Slow convergence time - Increased observation noise caused by additional level of differencing

6.3.2 Improving Continuity in Solution Updates

Analysis of the GPS data obtained from the previously described large open pit mine indicated that there were several periods during the day for which fewer than 4 satellites were visible. This leads to degradation in the precision of the solutions as well as a reduction in the frequency of updates. Consequently, the potential of augmenting GPS with pseudolites (PLs) has been investigated to improve the frequency and precision of solutions [Bond et al., 2007b]. The devised approach incorporates the PL observations into the TD Delayed-State Kalman Filter.

Being a ground-based signal transmitter, PL error sources must be handled differently than GPS signal error sources. PPMS was modified to address nuances in PL data processing which include cycle slip detection, PL location determination and PL observation modelling. As before, after removing the error terms for receiver clocks and satellite clocks (which are eliminated through double-differencing over short baselines), the TD carrier phase observable for PLs can be written in the form of Equation (6.5):

$$\delta \underset{AB}{\Delta} \overset{iPL}{\nabla} \varphi(t_{12}) = [\underset{AB}{\Delta} \overset{iPL}{\nabla} (\varphi + N + M - \frac{f}{c} I + \frac{f}{c} T + e_{\varphi}) + \varepsilon_{trop}]_{t_2} - [\underset{AB}{\Delta} \overset{iPL}{\nabla} (\varphi + N + M - \frac{f}{c} I + \frac{f}{c} T + e_{\varphi}) + \varepsilon_{trop}]_{t_1}^{*} \quad (6.5)$$

* There is not an ionospheric delay term for the PL observation since its signal does not travel through the ionosphere, but the reference satellite observation will include this term.

The attractiveness of the TD PL observable is that it is a time difference of DD observations and consequently biases common to both observations will cancel. This strategy allows for smooth integration of PL data into the existing software infrastructure due to the following benefits:

a) the user no longer needs to solve for the ambiguity term, which allows the system to be less susceptible to biases caused by cycle slips;

b) for observation intervals less than a few seconds, the correlation between PL tropospheric delay parameters at times t_1 and t_2 will be large and biases originating from them will be significantly reduced;

c) for observation intervals less than a few seconds, the correlation between low frequency multipath terms at times t_1 and t_2 will be large and biases originating from them will be significantly reduced. The high frequency component still remains;

d) since the PL is stationary between times t_1 to t_2 and it is assumed that the receivers are stationary, the geometric distance terms involving the PL cancel so that the computed, geometric, TD is solely dependent upon the change in the geometry of the reference satellite. Consequently, the accuracy to which the PL coordinates must be known is very forgiving. Approximate coordinates are necessary simply for computing elevation angles to PLs if an elevation cut off constraint is imposed.

Figure 6.4 illustrates the results of a baseline that was observed in a harsh environment (having a 35 degree elevation cut-off) while using a PL. A slow, 10 mm displacement occurs in the horizontal plane beginning at hour 14 and ending at hour 18 as indicated by the green and red vertical lines respectively. It takes approximately 10 hours for the solution to converge. It can be seen that the combined GPS+PL system allows for more continuous solution updates and quicker displacement detection than stand-alone GPS.

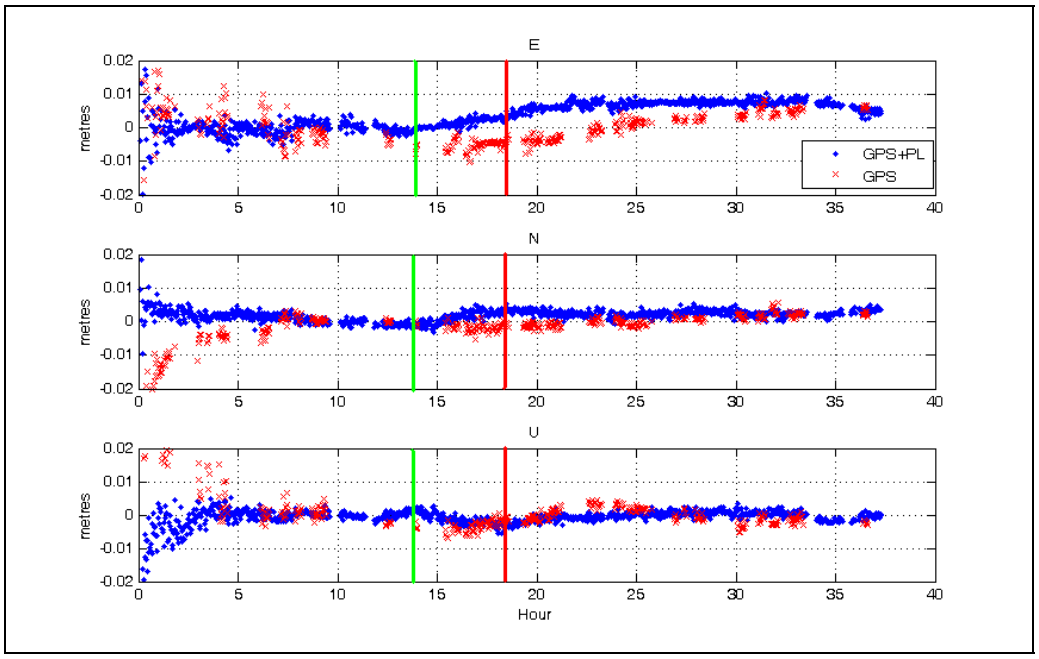

Figure 6.4: Detected Displacements with and without PL observations.

6.3.3 Predicting Station Behaviour using Deterministic Modelling

Analysis of PPMS results of the GPS baselines observed in the open pit raised two important questions regarding station stability: a) is it reasonable to expect upward movements of the monitored stations located at discrete points along the pit walls as was detected by the software and b) are the reference stations stable? To answer these questions, research has been devoted to predicting deformation behaviour of the open pit and its surroundings using deterministic modelling [Bond et al., 2007c]. Deterministic modelling takes into account the material properties and geometry of the deformable object, loading conditions and the physical laws governing the behaviour of the deformable object, to predict displacement patterns. In most cases, the closed form solution is difficult to obtain and therefore numerical methods are used.

Figure 6.5 illustrates the predicted displacement field in an open pit mine that occurs as a result of excavating a layer of rock along the left pit wall and pit floor. The results were obtained using the finite element method. This displacement pattern is very useful for addressing the two questions raised. First, it can be used in delineating the zone of significant deformation so that locations for stable reference points can be recommended. Additionally, this information provides an indication of the expected magnitude and direction of the displacement vectors. These results validate that it is possible that a target point located along the pit walls can experience upward movement as was captured in Figure 6.3.

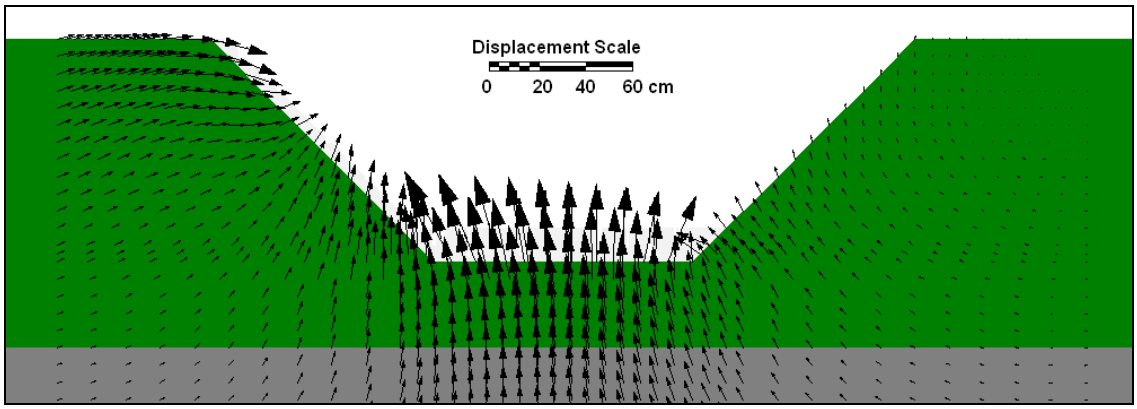

Figure 6.5: Predicted Displacement Pattern as a Result of Excavating the Left Pit Wall and Pit Floor

6.3.4 Developing a Fully Automated, GPS Monitoring System

To take full advantage of the capabilities of PPMS for deformation monitoring, a fully automated version has been created: the Precise Position Monitoring System plus Real Time (PPMS^{+RT}). Discussed are some of the practical issues involved in the development of the real-time version of the software. A displacement detection test is presented illustrating the potential of PPMS^{+RT} in a deformation monitoring scenario.

6.3.4.1 Monitoring system infrastructure

PPMS^{+RT} currently accepts two methods of data communication between GPS sensors and the central processing computer: (1) via Ethernet connection (either a Local Area Network (LAN) or Wireless LAN (WLAN)) and (2) via serial port (either directly

or through radio modem). A monitoring system may be designed to include all Ethernet connections, all serial port connections or a combination of both. The network infrastructure to support each method of communication is illustrated in Figure 6.6 and Figure 6.7 respectively.

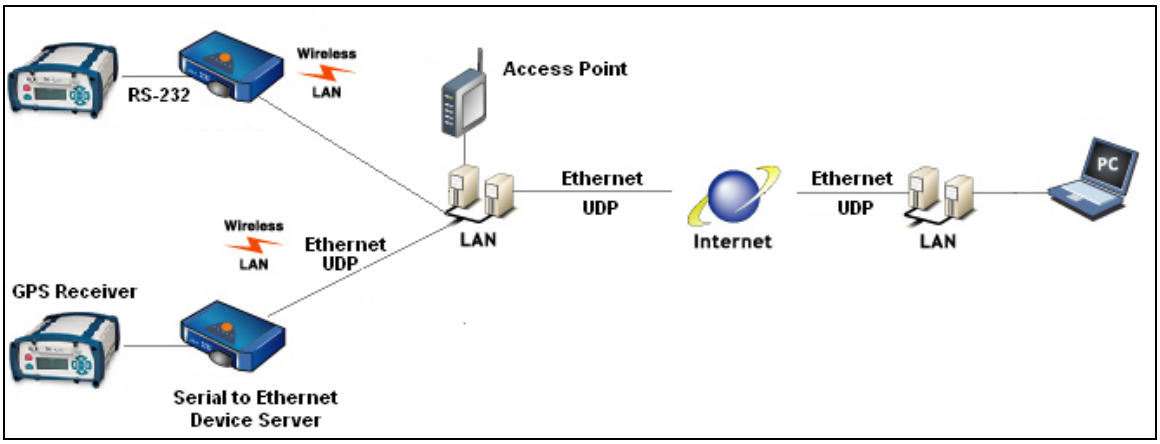

Figure 6.6: Ethernet based design
(based on [Sollae Systems Ltd. Co., 2007a])

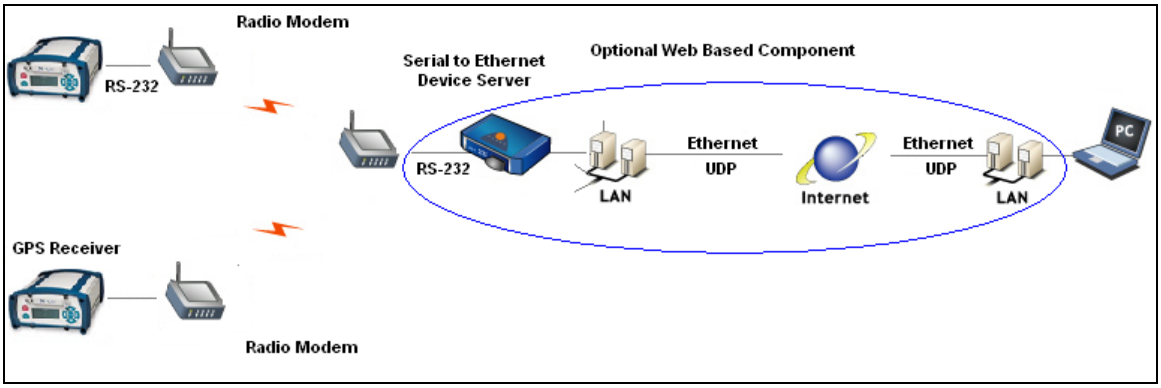

Figure 6.7: Serial Port based Design.

In the first method, a serial-to-Ethernet device server (e.g., Sollae Systems EZL-400S) is used. Although the maximum data rate is limited here by the serial communication between the receiver and serial-to-Ethernet device server, new model

GPS receivers (e.g., NovAtel DL-V3, Trimble NetR7) offer direct Ethernet connection. Thus, this first method offers potentially higher data rates than the next to be discussed. Either LAN or WLAN can be used to communicate between the serial-to-Ethernet device server and the destination PC which will process the data. Local conditions and available broadband infrastructure will dictate which method is the most suitable to connect the GPS receiver to a wired network.

The second method's design is similar to the first. An optional web based component is illustrated in Figure 6.7, which would allow for remote access of the data. A serial-to-Ethernet device server would be required to take advantage of this option so that the 'receive' radio modem could send its data online. Otherwise the data is directly streamed into the destination PC via serial port.

6.3.4.2 PPMS modifications

In order to receive data packets in real time from the GPS receiver, 'listening' threads are employed in the software to decode each receiver's binary data packets. In the case of an Ethernet based system, advantage is taken of the 'socket' class offered in the .NET development environment [MSDN, 2007b]. Various options for sockets exist as illustrated in Figure 6.8. "Asynchronous" sockets listen for incoming data on a separate thread without blocking operations on the main thread. "Synchronous" sockets are used

for applications that only require one thread during execution since they block operations on other threads until their operations have completed. For this application, an asynchronous socket is preferred so that all incoming data is received.

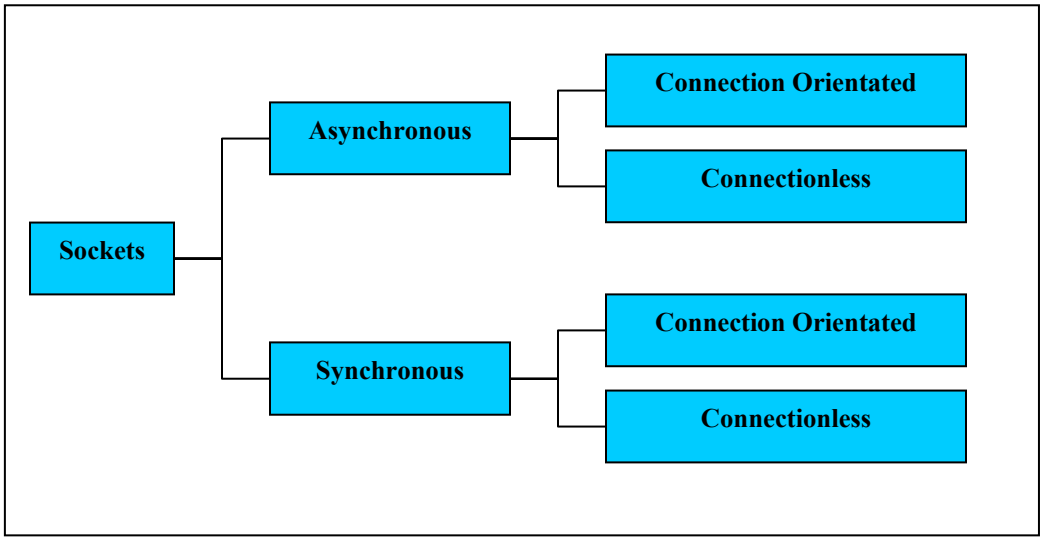

Figure 6.8: Types of Sockets

Sockets can be further classified as "connection orientated" or "connectionless" depending upon the data transfer protocol. Connection orientated sockets can use Transmission Control Protocol (TCP) for transferring data. TCP requires a connection to be established with a remote endpoint and then uses that connection to send and receive data packets. An advantage of using TCP is that it ensures that data packets are sent to an endpoint and that they assembled in the correct order when they arrive [MSDN, 2007c]. A disadvantage of this approach is that there may be delays in ensuring that the correct data packets are being sent. These delays may not be tolerated when high data rates are used and latency must be minimized.

Connectionless sockets can use User Datagram Protocol (UDP) for transferring data. UDP offers the advantages of simplicity, quick data transfer and the ability to broadcast messages to multiple addresses at the same time. The disadvantage of this approach is that UDP datagrams are not guaranteed to arrive, nor are they guaranteed to arrive in the same sequence in which they were sent. Consequently, applications which use this protocol must be prepared to handle missing and out of sequence datagrams [MSDN, 2007d].

The concepts of TCP and UDP are illustrated in Figure 6.9 and Figure 6.10 respectively. It can be seen that prior to establishing a connection, all data sent by the GPS receiver are ignored in TCP mode. Once the connection is established, there is constant communication between the host GPS receiver and client PC.

In UDP mode, two parameters are used by the serial-to-Ethernet device server to determine when to send the GPS receiver's data: (1) a watermark value representing the maximum number of bytes that will be stored in its buffer before sending the data and (2) a timeout value that represents the length of time to wait after the first packet is received before sending the data. It does not matter whether or not there is a client listening. Once either one of these conditions is satisfied, the data stored in the serial-to-Ethernet device server's buffer are sent.

For purposes of this application, UDP is the preferred method of communication due to: a) its ability to transfer data quickly and b) its simplicity, which makes it less susceptible to breakdowns in communication between client and host devices. The user must specify the IP address of the destination PC that will receive the data in the serial-to-Ethernet device server. The IP address of the serial-to-Ethernet device server must be specified in PPMS^{+RT} as illustrated in Figure 6.11.

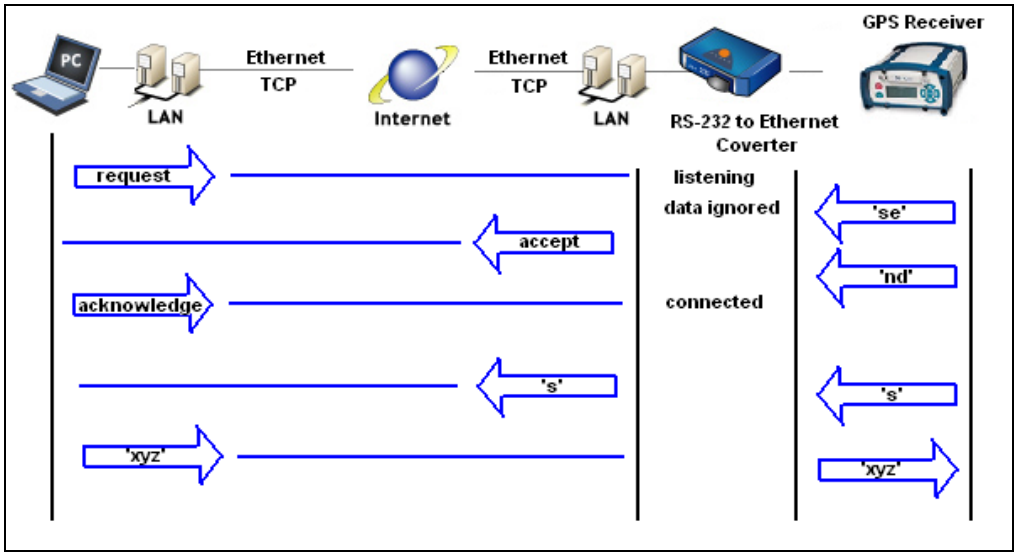

Figure 6.9: TCP Data Transfer Sequence
(based upon [Sollae Systems Ltd. Co., 2007b]).

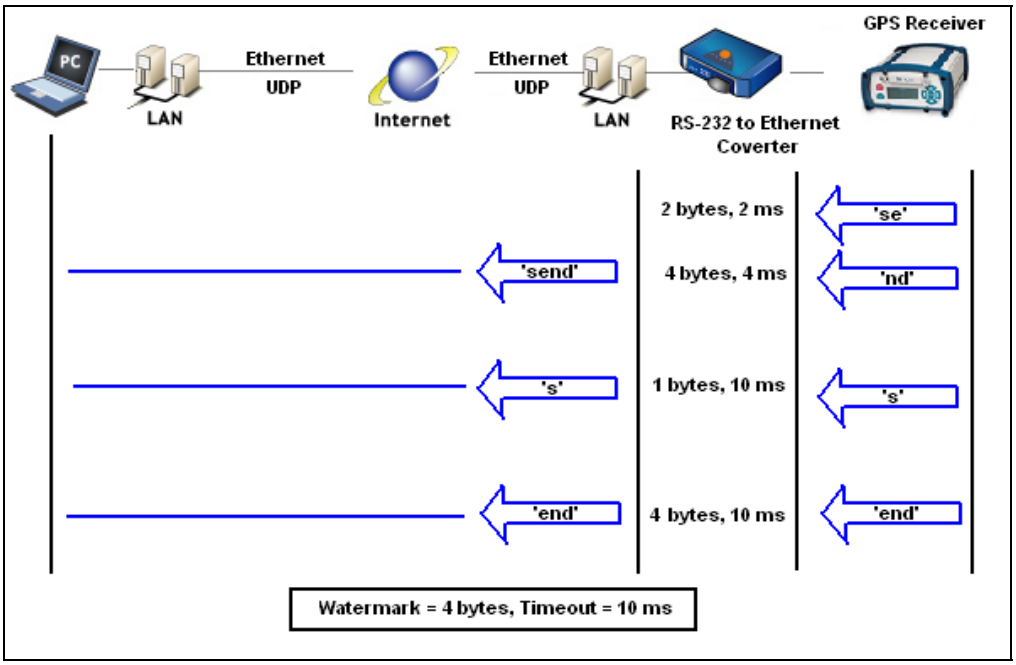

Figure 6.10: UDP Data Transfer Sequence
(based upon [Sollae Systems Ltd. Co., 2007b])

An asynchronous approach is also used for receiving data via serial port. A separate listening thread is invoked so that other operations are not blocked on the processing PC. Serial port settings are specified in PPMS^{+RT} software as illustrated in Figure 6.11.

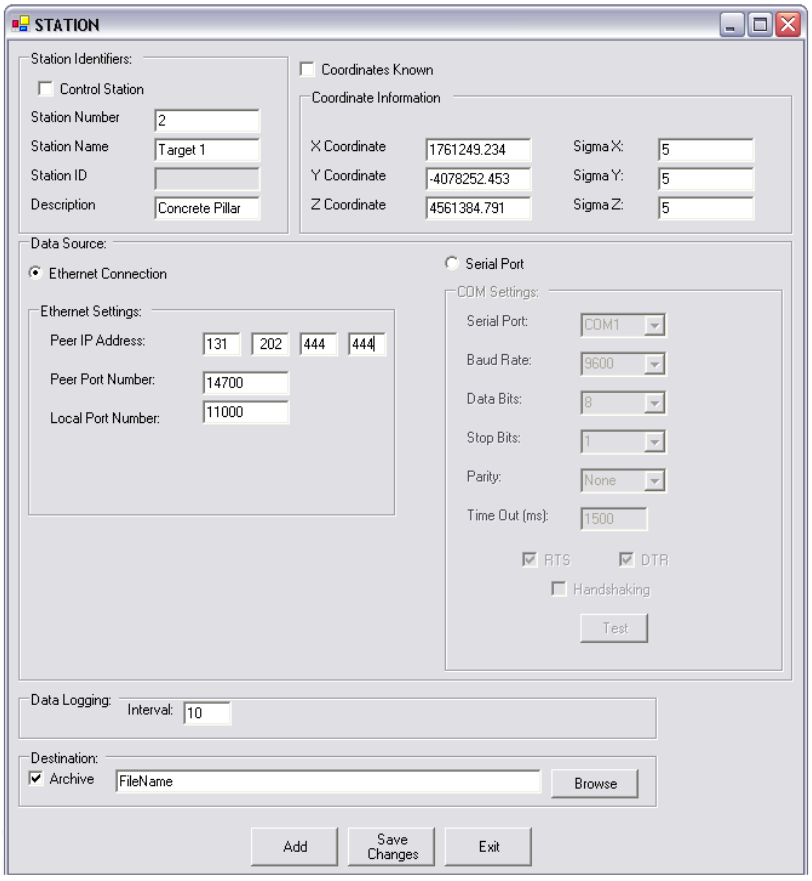

Figure 6.11: Adding a New GPS Station with Ethernet or Serial Port Connection.

6.3.4.3 Real-time implementation

To demonstrate the capabilities of the system, a real-time displacement detection test was performed. Two NovAtel DL-4 GPS receivers with GPS-600 Pinwheel antennas were used to monitor the stability of a target point located on a translation stage. The target point was moved horizontally 10 mm. An IntegriNautics (now Novariant) IN200 pseudolite [Novariant, 2007] was also used in this test to aid in quicker displacement detection [Bond et al., 2007b]. The experiment configuration is illustrated in Figure 6.12.

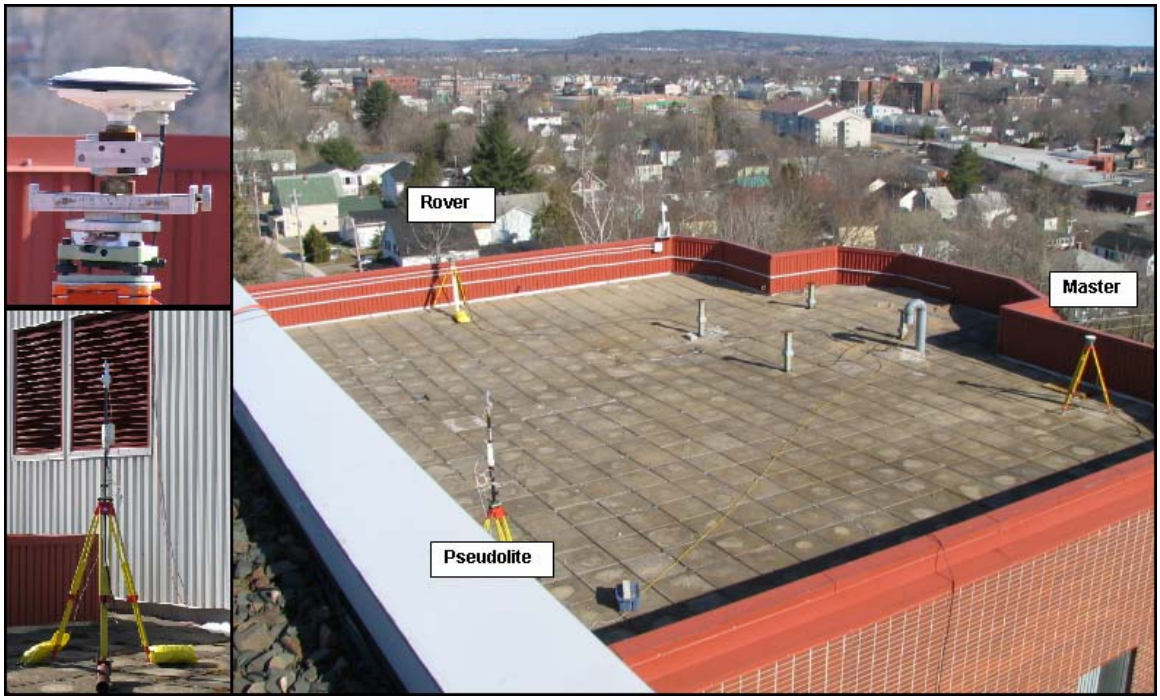

Figure 6.12: Displacement Detection Experiment Configuration
(Top Left: Rover Antenna on Translation Stage, Bottom Left: IN200 Pseudolite, Right: Observed Baseline).

Two Sollae Systems serial-to-Ethernet device servers (model EZL-400S) were used to provide Ethernet connections to the receivers. A notebook PC with Intel Celeron 2.20 GHz processor was used to run the software. The network infrastructure and system configuration are illustrated in Figure 6.13.

Initial tests of the monitoring system showed frequent gaps in the GPS data from each receiver and incomplete data packets being received. These problems were attributed to the watermark and timeout settings in the EZL-400S. If the watermark or timeout values were too small, the data would be sent to the remote PC as an incomplete data packet.

The solution to this problem was to determine the maximum packet size that would be sent by the DL-4 receiver. The watermark value was then set to a value larger than the maximum packet size so that it would never trigger the data being sent.

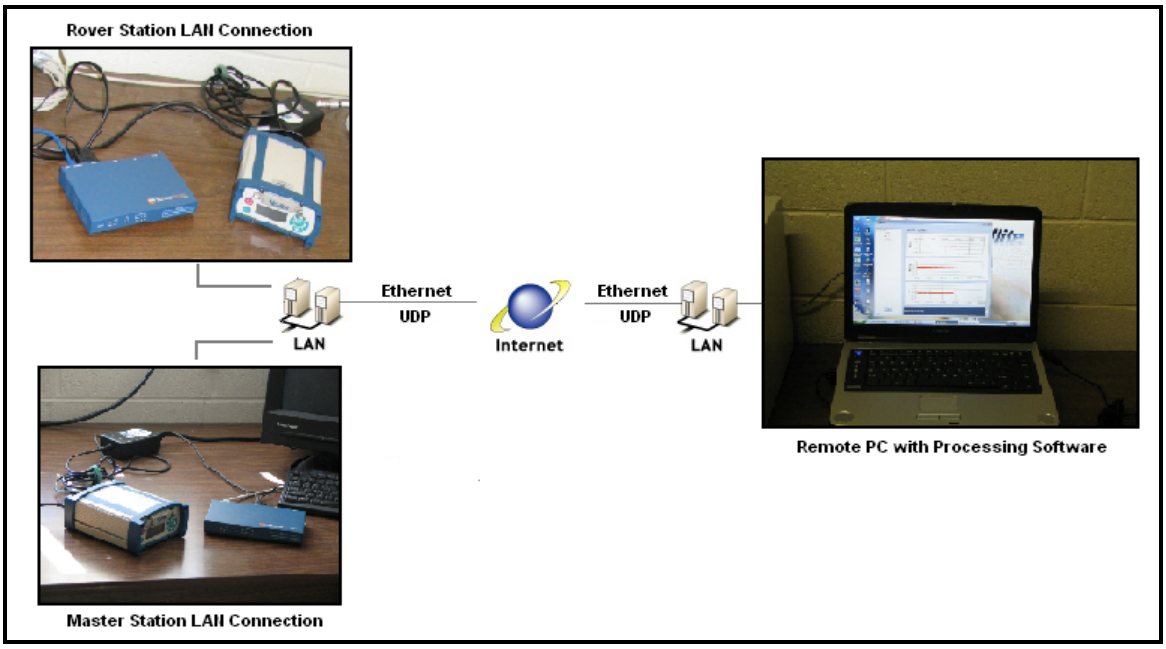

Figure 6.13: Network Infrastructure and System Configuration for Data Transfer and Remote Processing.

Based upon the baud rate of the DL-4 serial connection (57600 bps), the number of bits per packet (10: 1 start bit, 8 data bits and 1 stop bit) and the maximum data packet size (624 bytes) it was determined that approximately 5760 bytes / second could be sent or 5.76 bytes / millisecond. Accordingly, a timeout value of at least 110 ms was required. Since the timeout value of the EZL-400S has a precision of ± 10 ms [Lee, 2007], a timeout value of 120 ms was used.

Because data is transmitted in UDP mode, the EZL-400S sends data regardless of whether or not the remote PC is listening. It is necessary to allow sufficient time for the PC to receive messages from each receiver. This is especially important in this case since the DL-4 receiver clocks are synchronized at microsecond level with GPS time (and therefore with each other). If the same timeout value is used for each receiver, it is possible that while the PC is busy receiving packets from one receiver it may miss packets sent by another receiver in UDP mode. It is therefore recommended to stagger the timeout values for each receiver.

Figure 6.14 illustrates the output of PPMS software on the remote PC. The horizontal scale on the position plots represents GPS second of week. Prior to moving the translation stage, the coordinates of the target point are Easting: -14.075 m, Northing: 0.403 m and Up: 0.015 m. At ~303325 s the 10 mm displacement is introduced. Approximately 1 hour later (~307000 s) the displacement is reflected in the Easting and Northing solution plots. After 4 hours (~318000 s) the coordinates of the target point are Easting: -14.068 m, Northing: 0.393 m and Up: 0.018 m indicating a total horizontal displacement of ~ 12 mm. This information can be used to signal an alarm if conditions are deemed to be unsafe.

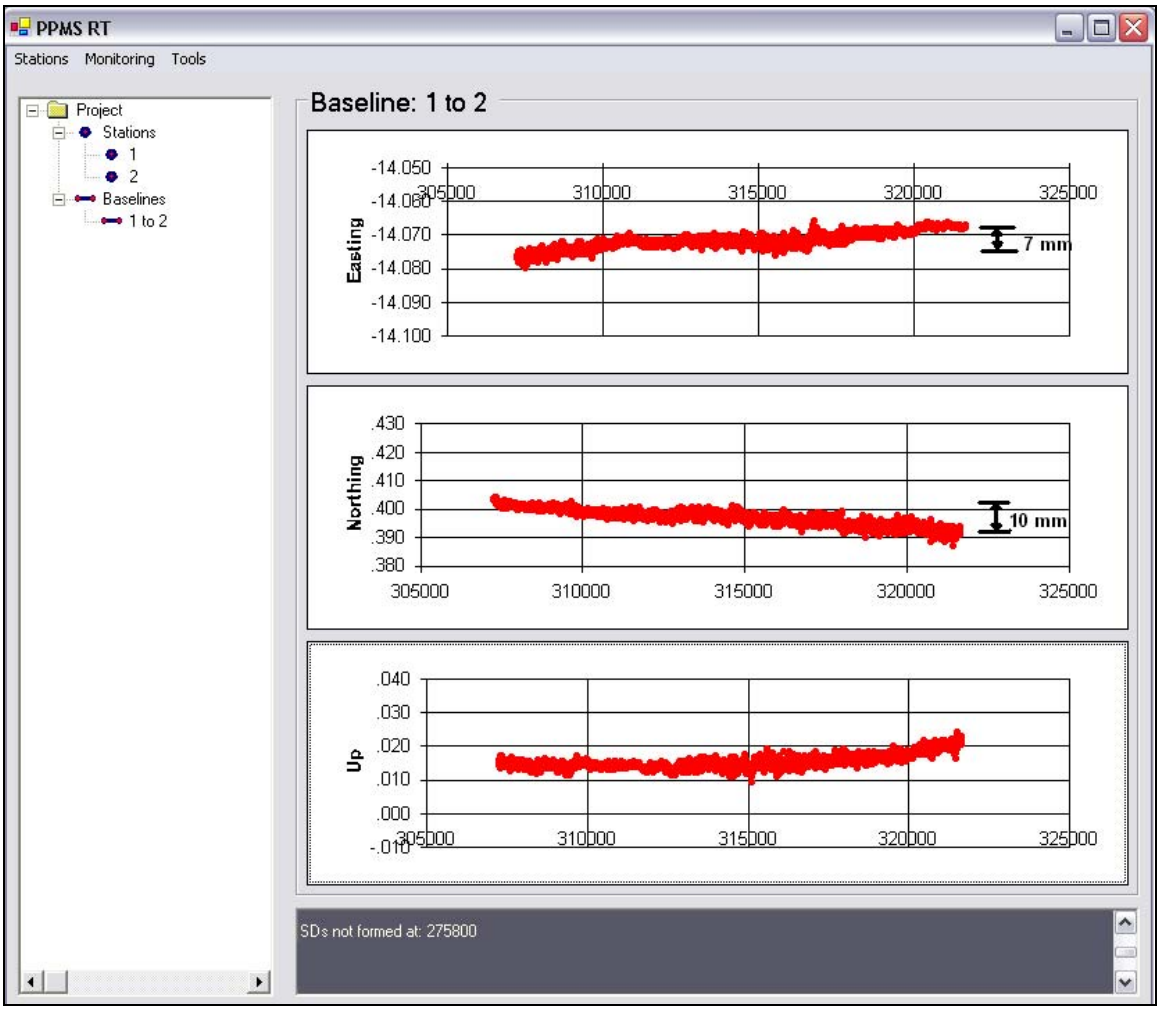

Figure 6.14: PPMS Graphical Display of Target Position

6.4 Conclusions

A fully automated, continuous, real-time monitoring system has been developed that employs GPS sensors. The system is capable of providing sub-centimeter precisions without having to solve for the integer ambiguity, making it suitable for many deformation monitoring applications. Four major obstacles have had to be addressed to

develop such a system. First, the effects of residual tropospheric delay biases have had to be mitigated from the height component of the solutions. This was addressed through the use of the TD observable over a high sample rate. Second, it was necessary to improve the continuity of the updates. Pseudolite technology was incorporated into the software to provide more frequent solutions. Third, a method of predicting the stability of reference points was required. It was shown how the results of deterministic modelling (and, in particular, the finite element method) could be used to achieve this end. Last, a fully-automated system was needed for providing continuous GPS position updates and this has been developed. Two communication options are currently available between GPS receivers at target points and a central processing computer: Ethernet or serial port. Both approaches allow the data to be processed locally or remotely based upon project needs.

The increasing number of catastrophes in recent years has lead to a demand for new sensors, sensor integration techniques and data processing strategies for improved deformation monitoring systems. Further research is required to integrate this technology with other sensors to create more reliable and more adaptable monitoring systems.

Acknowledgements

This research could not have been completed without the support of the Public Safety and Emergency Preparedness Canada Research Fellowship in honour of Stuart Nesbitt White, the Natural Sciences and Engineering Research Council of Canada (NSERC) and Atlantic Canada Opportunities Agency (ACOA). Special thanks to Sollae Systems Co., Ltd. for providing equipment necessary to conduct this research.

References

Beutler, G., I. Bauersima, W. Gurtner, M. Rothacher, T. Schildknecht and A. Gieger, (1988).Atmospheric refraction and other important biased in GPS carrier phase observations. *Atmospheric Effects on Geodetic Space Measurements*, Monograph 12, School of Surveying, University of New South Wales, pp.15-43.

Bond, J., A. Chrzanowski, and D. Kim (2007a). "Bringing GPS into Harsh Environments for Deformation Monitoring." *GPS Solutions* (online first status), 11 pp. Available at: http://www.springerlink.com/content/21v2625p46108266/fulltext.pdf, accessed on: 4 October 2007. DOI 10.1007/s10291-007-0059-7

Bond, J., A. Chrzanowski, D. Kim D (2007b). "Augmenting GPS with Pseudolites for Deformation Monitoring in Harsh Environments." Proceedings of the *Institute of Navigation National Technical Meeting* (ION NTM), 22-24 January, San Diego, CA, USA, pp. 486-492, CDROM. Available at http://www.ion.org/, accessed on 4 October, 2007.

Bond, J., A. Chrzanowski, and F. Wilkins (2005). "Using GPS for Augmenting Deformation Monitoring Systems in Open Pit Mines - Problems and Solutions." *Geomatica*, 59(1):73-82.

Bond, J., A. Szostak-Chrzanowski A and A. Chrzanowski (2007c). "Design of Geodetic Monitoring Schemes Using Deterministic Modelling: An Open Pit Mine Example." Proceedings of the *3rd International Symposium on Geo-information for Disaster Management*, Toronto, Ontario, Canada, 22-24 May, Canadian Inst. of Geomatics, 11 pp., CDROM.

Brown, R.G. and P.Y.C. Hwang (1997). *Introduction to Random Signals and Applied Kalman Filtering*, 3rd ed. John Wiley & Sons, Inc., New York, USA, pp. 1-484.

Chen, Y.Q., G. Zhang, X. Ding and Z. Li (2000). "Monitoring Earth Surface Deformations with InSAR Technology: Principle and Some critical Issues." *Journal of Geospatial Engineering* 2(1):3-21.

Kim D., R.B. Langley, J. Bond and A. Chrzanowski (2003). "Local deformation monitoring using GPS in an open pit mine: Initial study." *GPS Solutions* 7(3): pp. 176-185. Available at: http://www.springerlink.com/content/0dvd4ddmx9w5k8xx/, accessed on: 4 October 2007. DOI 10.1007/s10291-003-0075-1

Langley, R.B. (1995). "Propagation of the GPS Signals." Chapter 3 of *GPS for Geodesy*, Proceedings of the *International School of GPS for Geodesy*, Delft, the Netherlands, March 26 - April 1, pp. 111-185.

Lee, M., (2007). Email communication. Technical Support Representative, Sollae Systems Co., Ltd., 30 March.

Microsoft Developer Network (MSDN) (2007b). "System.net.sockets namespace," *Microsoft*, http://msdn2.microsoft.com/en-us/library/system.net.sockets(vs.71).aspx , accessed on: 18 April 2007.

Microsoft Developer Network (MSDN) (2007c). "Using TCP Services," *Microsoft* website: http://msdn2.microsoft.com/en-us/library/k8azesy5.aspx , accessed on: 19 April 2007.

Microsoft Developer Network (MSDN) (2007d). "Using UDP Services," *Microsoft*, http://msdn2.microsoft.com/en-us/library/tst0kwb1.aspx , accessed on: 19 April 2007.

Novariant (2007). "Mining Products. Terralite XPS." *Novariant,* http://www.novariant.com/mining/products/index.cfm, accessed on: 21 April 2007.

Remondi, B.W. (1984). *Using the Global Positioning System (GPS) Phase Observable for Relative Geodesy: Modeling, Processing, and Results*. Doctoral thesis, Center for Space Research, University of Texas at Austin, pp. 1-324.

Sollae Systems Co., Ltd. (2007a). “Products. EZL-400S.” *Sollae Systems Co., Ltd.,* http://www.eztcp.com/en/Products/ezl-400s.php, accessed on: 18 April 2007.

Sollae Systems Co., Ltd. (2007b). “Products EZL-400S: User’s Manual.” *Sollae Systems Co., Ltd.,* http://www.eztcp.com/Support/ezl400sen.pdf, accessed on: 18 April 2007.

CHAPTER 7
CONCLUSION AND RECOMMENDATIONS

The main objective of this research was to devise a methodology to improve the continuity in GPS position updates in harsh environments that is presently achievable using existing systems. In order to accomplish this, traditional discipline boundaries between geodetic engineering, geomechanical engineering and GNSS studies have had to be transcended. Through innovative processing techniques, integration of new technology and an interdisciplinary approach to designing the deformation monitoring scheme, this goal has been achieved. The conclusions and findings emanating from this research are now summarized. Recommendations for further research are also presented.

7.1 Development of a Residual Tropospheric Delay Mitigation Technique

It was demonstrated that the TD observation can be used to significantly reduce the effects of residual tropospheric delay biases. This is a major contribution to GPS applications involving large height differences where centimetre level biases in the height component are not uncommon. Instead of having to wait up to 24 hours for the effects of residual tropospheric delay to average out, its effects can be significantly reduced in real time. This technique is extremely advantageous for deformation monitoring applications where continuous displacement updates are often required. Further research is required to

quantify the degradation in correlation between residual tropospheric delay biases over consecutive epochs as the sample rate decreases. This would aid in determining the minimum sample rate required to ensure that most of the residual tropospheric delay is cancelled out through triple-differencing.

7.2 Development of High Precision, Post-Processing GPS Software

In order to test the triple-differenced observation approach described above, post-processing GPS software was required to process the data collected at the HVC mine. A fully interfaced Microsoft Windows based application has been developed in the Microsoft Visual Studio.NET development environment: the Precise Position Monitoring System (PPMS). The software was designed with the ultimate goal of being adapted to provide high precision, fully automated, on-time and robust solution updates to meet industrial needs.

PPMS employs TD carrier-phase measurements in a Delayed-State Kalman filter. Although the TD approach employed requires longer convergence time than DD methods, this is generally not a concern for long term deformation monitoring applications.

Depending upon client requirements and environmental conditions, the filter can be adjusted to be more or less sensitive to the observations. Quicker detection time currently comes at the expense of more noise in the solutions. A slow, 25 mm displacement was detected within 30 minutes of the full displacement with standard deviations in E, N and U of ± 10 mm or better. The same displacement could also be detected in less than 5 hours with standard deviations in E, N and U of ± 5 mm or better. The software works best for detecting long period deformations (e.g., 20 mm per day or less) for which sigma values of 1 - 2 mm are attained in all three solution components. The filter may benefit from allowing the process noise to be adaptive. It is therefore recommended that further research be conducted in this area.

The extreme conditions of the large open pit mine investigated limited the frequency at which high precision updates could be provided. Using PPMS, millimetre level updates could be provided at least every 75 minutes, as opposed to every 24 hours using traditional processing methods. Updates may be provided 100% of the time if the quasi-static nature of the rover point is used to estimate the receiver clock error when fewer than 4 satellites are visible. The receiver clock bias can then be used to correct the raw observations. Further enhancement of PPMS is recommended to incorporate this strategy.

7.3 Integration of Pseudolites for Improved Continuity in GPS Updates

PLs can be used in harsh environments to provide a) more frequent solution updates, b) quicker filter convergence and c) quicker displacement detection than could normally be achieved using stand-alone GPS. PLs can therefore be a valuable augmentation device for GPS-based deformation systems where expedient information is critical for human safety.

There are still some practical issues that need to be addressed before PLs similar to the one tested (IN200) could be integrated into a deformation monitoring system. It is currently illegal to broadcast on the L1 and L2 frequencies used by GPS satellites. Testing could not be conducting without obtaining permission from the Canadian government. Unless the signal is modified to use a frequency outside of the restricted band (and receivers are designed to track the modified signal) or legislation is modified for these devices, this generation of PLs cannot be utilized commercially. Based upon the results illustrated, further investigation into the latest generation of pseudolites ("terralites") produced by Novariant (which transmit their own proprietary signal) would be a worthy endeavour.

The major advantage of using PLs is having supplementary observations when too few satellites are visible to provide a solution. As previously discussed, unless some

means of synchronizing the receiver's clock to GPS time is introduced when fewer than 4 satellites are visible, PLs will not be of any use in providing additional solution updates. This serves as further incentive to take advantage of the quasi-static rover coordinate values to estimate the receiver clock error. Alternatively, an external oscillator could be connected to the GPS receiver.

The clock initialization method used by NovAtel DL4 receivers allows for the potential of incorrect time synchronization with GPS time. If the receiver locks onto the PL signal first, it will use the time broadcast by the PL to initialize the receiver. Without any means of synchronizing the IN200 to GPS time, the default time value set in the firmware of the PL is used. Care must be taken to initialize the receiver without having the PL turned on. This becomes cumbersome in the event of power outages. Ideally, the receiver used would be programmed not to initialize with the time obtained from a channel dedicated to tracking a PL. Firmware modifications are needed to address this issue.

The TD observation approach used for PL data processing allows for smooth integration of PL observations for high precision applications, since it significantly reduces tropospheric delay biases and the impact of PL location error. A quadruple-differenced observation technique was introduced to identify PL L1 cycle slips. Additionally, a technique to model the PL noise was devised based upon the L1

quadruple-differenced observations (details of this implementation are presented in Appendix II).

7.4 Demonstration of an Interdisciplinary Approach to Designing Geodetic Deformation Monitoring Schemes

In order for the monitoring scheme to be effective, it must be connected to stable reference points. An interdisciplinary approach that combines the principles of rock mechanics and engineering surveys to designing a geodetic deformation monitoring scheme has been illustrated in an open pit mine example. This approach does not pre-empt traditional methods of designing geodetic networks through geometrical simulation, rather it should be used as a complement to it. Deterministic modelling was used to assess the extent of the deformation zone based upon the designed mining activity. Once the deformation zone was delineated, suitable locations for stable reference points could be chosen.

Deterministic modelling also provides predictions of the global displacement field from which areas of maximum expected deformation can be identified. This information is useful for choosing suitable locations for targets and sensors. Once the geodetic monitoring network is in place, the measured displacements are useful for verifying the correctness of the deformation model. The two sources of information are therefore

complementary in nature and are continually used to update the monitoring scheme and model as more information is learned about the deformation behaviour.

It was also shown how a poor decision regarding the location of instruments can lead to an incorrect determination of displacement values. This can have serious consequences when safety is a concern and remedial measures are involved. It is the engineer's responsibility to ensure that all measures are taken to properly design the deformation monitoring system. It is therefore advised to use an interdisciplinary approach in designing a geodetic deformation monitoring scheme to take advantage of additional sources of information that can help prevent calamities.

7.5 Development of a Fully Automated, GPS based Monitoring System

A fully automated, real-time, GPS based, monitoring system has been developed in an effort to provide 'on-time' warnings of impending danger. PPMS^{+RT} offers sub-centimetre precisions without having to solve for the integer ambiguity, making it less susceptible to false alarms caused by poorly handled cycle slips. It also integrates PL data processing capabilities, marking it as one of the few high precision GPS software to offer this option. Two communication options are currently available between GPS receivers at target points and a central processing computer: Ethernet or serial port. Both approaches

allow the data to be processed locally or remotely based upon client needs. Solution updates are depicted graphically in real time for the user.

7.6 Implementation of an Interdisciplinary Research Approach

In a world of increasing complexity the importance of interdisciplinary research cannot be emphasized enough. The goals of this research could not have been achieved without the tremendous insight and expertise that world experts had to offer in their respective fields. This research has demonstrated how an assimilation of methodologies and technology from different disciplines can lead to innovation and progress.

APPENDIX I
ADDITIONAL PROCESSING INFORMATION

Provided are additional results and analysis to Chapter 3 from Paper 2: "Bringing GPS into Harsh Environments for Fully Automated Deformation Monitoring."

I.1 Delayed-State Kalman Filter Derivation for Processing Correlated Process and Measurement Noise (based upon Brown and Hwang [1997])

The general Delayed-State Kalman filter recursive are subsequently derived. The equations required to process integrated velocity measurements over some interval (i.e., GPS triple-differenced carrier phase observations) are then presented. A summary of the symbology used in the derivation is provided in Table I.1. 'm' represents the number of observations and 'n' represents the number of unknowns.

Table I.1: Summary of Symbol Meanings for Delayed-State Kalman Filter Derivation

Symbol	Meaning
$_k$	epoch of variable
$\bar{}$	predicted value
$\hat{}$	estimated value
^{T}	matrix transpose
$^{-1}$	matrix inverse
I	identity matrix
x_k	(n x 1) state vector (x, y, z position)
ϕ_k	(n x n) transition matrix (identity matrix) that relates x_k to x_{k-1}
w_k	(n x 1) vector whose elements are white sequence
z_k	(m x 1) vector of measurements
e_k	(nx1) state error vector
v_k	(m x 1) vector of measurement errors whose elements are white sequence
Q_k	(nxn) Process noise matrix
R_k	(mxm) Observation noise matrix
K_k	(mxm) Gain matrix
C_k	(nxm) matrix of correlated measurement and process noise values
P_k	(nxn) error covariance matrix
H_k	(m x n) design matrix relating observations z_k and states x_k.
J_k	(m x n) negated design matrix of previous epoch ($J_k = -H_{k-1}$)

I.1.1 General Derivation of Correlated Process and Measurement Noise Discrete Filter

To derive a model that accounts for correlated measurement and process noise, the general form of the Kalman filter equations is first taken:

$$x_{k+1} = \phi_k x_k + w_k \tag{I.1}$$

$$z_k = H_k x_k + v_k \tag{I.2}$$

where:

x_k (n x 1) state vector (x, y, z position) of the process at time t_k

ϕ_k (n x n) transition matrix (identity matrix) that relates x_k to x_{k-1}
w_k (n x 1) vector whose elements are white sequence
z_k (m x 1) vector of measurements at time t_k
H_k (m x n) design matrix relating observations z_k and states x_k.
v_k (m x 1) vector of measurement errors whose elements are white sequence

$$E[w_k w_i^T] = \begin{cases} Q_k, i = k \\ 0, i \neq k \end{cases}$$

$$E[v_k v_i^T] = \begin{cases} R_k, i = k \\ 0, i \neq k \end{cases}$$

$$E[w_k v_i^T] = 0$$

After rewriting Equation (I.1) as:

$$x_k = \phi_{k-1} x_{k-1} + w_{k-1} \tag{I.3}$$

it becomes apparent that it is the cross correlation between w_{k-1} and v_k that needs to be accounted for in the discrete model over the interval (t_{k-1}, t_k). A new term is introduced to account for the anticipated correlated measurement and process noise, C_k.

$$E[w_{k-1} v_k^T] = C_k \tag{I.4}$$

The general Kalman filter update equation used to update state $\hat{x}_k$ with an error covariance matrix P_k is:

$$\hat{x}_k = \hat{x}_k^- + K_k (z_k - H_k \hat{x}_k^-) \tag{I.5}$$

where:

K_k blending factor or 'gain matrix' ($= P_k^- H_K^T (H_k P_k^- H_k^T + R_k)^{-1}$)

$\hat{x}_k^-$ predicted state estimates (superscript '-' denotes predicted)

The estimation error can be denoted as:

$$\begin{aligned} e_k &= x_k - \hat{x}_k \\ &= x_k - [\hat{x}_k^- + K_k (z_k - H_k \hat{x}_k^-)] \\ &= (I - K_k H_k) e_k^- - K_k v_k \end{aligned} \tag{I.6}$$

The correlation between e_k^- and v_k can be denoted as:

$$\begin{aligned} E[e_k^- v_k^T] &= E[(x_k - \hat{x}_k^-) v_k^T] \\ &= E[(\phi_{k-1} x_{k-1} + w_{k-1} - \phi_{k-1} \hat{x}_{k-1}) v_k^T] \end{aligned} \tag{I.7}$$

Since v_k is not correlated with either x_{k-1} or $\hat{x}_{k-1}$ because of its whiteness property, Equation (I.7) reduces to:

$$E[e_k^- v_k^T] = E[w_{k-1} v_k^T] = C_k \tag{I.8}$$

Usiing Equation (I.6), the expression for the error covariance matrix P_k is obtained:

$$\begin{aligned} P_k &= E[e_k e_k^T] \\ &= E\{[(I - K_k H_k) e_k^- - K_k v_k][(I - K_k H_k) e_k^- - K_k v_k]^T\} \end{aligned} \tag{I.9}$$

Expanding Equation (I.9) and using Equation (I.8) yields the following general equation for the error covariance:

$$P_k = (I - K_k H_k) P_k^- (I - K_k H_k)^T + K_k R_k K_k^T$$
$$-(I - K_k H_k) C_k K_k^T - K_k C_k^T (I - K_k H_k)^T \quad \text{(I.10)}$$

To find the optimal gain, it is necessary to differentiate the trace of P_k with respect to K_k and set the result equal to 0, where:

$$\frac{d(trace(P_k))}{dK_k} = -2(H_k P_k^-)^T + 2K_k (H_k P_k^- H_k^T + R_k) \quad \text{(I.11)}$$

The resulting optimal gain is:

$$K_k = (P_k^- H_k^T + C_k)[H_k P_k^- H_k^T + R_k + H_k C_k + C_k^T H_k^T]^{-1} \quad \text{(I.12)}$$

The optimal gain Equation (I.12) can be substituted into the general P_k equation (Equation (I.10)) to get the *a posteriori* P_k equation. Through algebraic manipulation the result is:

$$P_k = (I - K_k H_k) P_k^- - K_k C_k^T \quad \text{(I.13)}$$

The projection equations are not affected by the cross correlation between w_{k-1} and v_k because of the whiteness property of each. The projection equations remain the same as in the general form:

$$\hat{x}_{k+1}^- = \phi_k \hat{x}_k \quad \text{(I.14)}$$

$$P_{k+1}^- = \phi_k P_k \phi_k^T + Q_k \quad \text{(I.15)}$$

Equations (I.5), (I.12), (I.13), (I.14) and (I.15) comprise the complete set of recursive equations for the correlated process and measurement noise case.

I.1.2 Delayed-State Filter for Processing of Integrated Velocity Measurements

For applications where integration may be performed on the (radial) velocity measurement to determine position (triple-differenced carrier phase observations), the measurement form is:

$$\begin{aligned}(measurement)_k &= \int_{t_{k-1}}^{t_k} (velocity)dt + noise \\ &= (position)_k - (position)_{k-1} + noise\end{aligned}$$

In mathematical form, the measurement equation can be written as:

$$z_k = H_k x_k + J_k x_{k-1} + v_k \tag{I.16}$$

where $J_k = -H_{k-1}$

This form does not fit the general format for the usual Kalman filter equations due to the x_{k-1} term. The general Kalman filter equations must be modified to accommodate this term as well as any correlation in process and measurement noise.

Rearranging Equation (I.3) gives:

$$x_{k-1} = \phi_{k-1}^{-1} x_k - \phi_{k-1}^{-1} w_{k-1} \tag{I.17}$$

This can be substituted into Equation (I.16) to give:

$$z_k = (\underbrace{H_k + J_k\phi_{k-1}^{-1}}_{\text{New } H_k})x_k + (\underbrace{-J_k\phi_{k-1}^{-1}w_{k-1} + v_k}_{\text{New } v_k}) \tag{I.18}$$

Equation (I.18) now fits the Kalman filter general form. However, it is apparent that the new v_k term is correlated with w_{k-1}. It is therefore necessary to utilize the equations derived in the previous section to account for this correlation. First, it is necessary to calculate the covariance expression for the new v_k term (R_k^{New}) and to obtain an expression for C_k:

$$R_k^{New} = E[(-J_k\phi_{k-1}^{-1}w_{k-1} + v_k)(-J_k\phi_{k-1}^{-1}w_{k-1} + v_k)^T] \tag{I.19}$$

Since v_k and w_{k-1} are uncorrelated,

$$R_k^{New} = J_k\phi_{k-1}^{-1}Q_{k-1}\phi_{k-1}^{-1T}J_k^T + R_k \tag{I.20}$$

Using Equation (I.4) we can write C_k as:

$$C_k = E[(w_{k-1}(-J\phi_{k-1}^{-1}w_{k-1} + v_k)^T] = -Q_{k-1}\phi_{k-1}^{-1T}J_k^T \tag{I.21}$$

For this application, the following replacements can be made into Equations (I.5), (I.12) and (I.13), where "$\rightarrow$" denotes "is replaced by".

$$H_k \rightarrow H_k + J_k\phi_{k-1}^{-1} \tag{I.22}$$

$$R_k \rightarrow R_k + J_k\phi_{k-1}^{-1}Q_{k-1}\phi_{k-1}^{-1T}J_k^T \tag{I.23}$$

$$C_k \rightarrow -Q_{k-1}\phi_{k-1}^{-1T}J_k^T \tag{I.24}$$

The ϕ_{k-1}^{-1} term can be eliminated through appropriate algebraic substitutions including the following:

$$Q_{k-1} = P_k^- - \phi_{k-1}P_{k-1}\phi_{k-1}^T \tag{I.25}$$

It is also necessary to take advantage of the fact that the inverse of the transpose is the transpose of the inverse.

The final resulting recursive equations for the Delayed-State measurement scenario are as follows:

Estimate update:

$$\hat{x}_k = \hat{x}_k^- + K_k(z_k - \hat{z}_k^-) \tag{I.26}$$

Where:

$$\hat{z}_k^- = H_k\hat{x}_k^- + J_k\hat{x}_{k-1} \tag{I.27}$$

Gain:

$$K_k = [P_k^- H_k^T + \phi_{k-1}P_{k-1}J_k^T]L_k^{-1} \tag{I.28}$$

Where:

$$L_k = H_k P_k^- H_k^T + R_k + J_k P_{k-1}\phi_{k-1}^T H_k^T + H_k\phi_{k-1}P_{k-1}J_k^T + J_k P_{k-1}J_k^T \tag{I.29}$$

Error covariance update:

$$P_k = P_k^- - K_k L_k K_k^T \tag{I.30}$$

Projection:

$$\hat{x}_{k+1}^{-} = \phi_k \hat{x}_k \tag{I.31}$$

$$P_{k+1}^{-} = \phi_k P_k \phi_k^T + Q_k \tag{I.32}$$

Equations (I.26) through (I.32) represent the complete set of recursive equations that must be implemented for the optimal solution for the Delayed-State measurement problem.

I.2 Sensitivity Analysis

For the Delayed-State Kalman Filter algorithm used to generate position updates, the estimated precision of the solutions (i.e., covariance matrix) is a function of:

a) the change in satellite geometry between epochs t_{k-1} and t_k,

b) the number of visible satellites,

c) the observation processing interval,

d) the process noise parameter, Q_k, and

e) the variances of the observables as represented by the R_k matrix.

The size of the biases which can be statistically detected as well the influence of undetected errors on the estimation results are frequently of interest. These are measures of internal and external reliability respectively. A summary of the symbology used in this

analysis is provided in Table I.2. 'm' represents the number of observations and 'n' represents the number of unknowns.

Table I.2: Summary of Symbol Meanings used in Sensitivity Analysis

Symbol	**Meaning**
$_k$	epoch of variable
t^k	test statistic
c_k	model error candidate operator (vector or matrix – depending on the dimension of test - with 1 in the place of residual test candidates and 0s elsewhere.)
v_k	(mx1) residual vector
Q_{v_k}	(mxm) residual covariance matrix
H_k	(m x n) design matrix relating observations z_k and states x_k.
J_k	(m x n) negated design matrix of previous epoch ($J_k = -H_{k-1}$)
α_0	level of significance of the test
γ_0	power of the test
∇	unknown vector of model errors- minimum detectable bias (MDB)
λ_0	non-centrality parameter
K_k	(mxm)gain matrix
∇x_k	bias in the state vector
λ_x	bias to noise ratio (BNR)
P_k	(nxn) error covariance matrix

I.2.1 Internal Reliability

Internal reliability is a measure of the magnitude of the model error that can be detected by the test statistic, t^k, with a certain probability [Teunissen, 1998]:

$$t^k = \frac{c_k^T Q_{v_k}^{-1} v_k}{\sqrt{c_k^T Q_{v_k}^{-1} c_k}} \tag{I.33}$$

where:

k	epoch
c_k	model error candidate operator (vector or matrix – depending on the dimension of test - with 1 in the place of residual test candidates and 0s elsewhere.)
v_k	residual vector
Q_{v_k}	residual covariance matrix, as calculated from Equation (I.34):

$$Q_{v_k} = R_k + (H_k + J_k) P_k^- (H_k + J_k)^T \tag{I.34}$$

The size of an unspecified model error that can be detected by the one-dimensional test statistic t^k for a certain level of significance α_0 and with power γ_0 is known as the minimum detectable bias (MDB) and is equal to [Teunissen 1998]:

$$\nabla = \sqrt{\frac{\lambda_0}{c_k^T Q_{v_k}^{-1} c_k}} \tag{I.35}$$

where:

λ_0	is a function of the significance level and power of the test for the one dimensional case: $\lambda(\alpha_0, 1, \gamma_0)$

λ_0 is known as the *noncentrality parameter* and can be calculated as:

$$\lambda_0 = (c_k \nabla)^T Q_{v_k}^{-1} c_k \nabla \tag{I.36}$$

I.2.2 External Reliability

External reliability is the influence of an undetected model error on state estimates [Teunissen, 1998]. Since there is a probability that an unspecified model error will not be detected by the test statistic, t^k, it is important to know how large an effect a particular model error will have on the state vector. The biases in the state estimates caused by a model error the size of the MDB is:

$$\nabla x_k = K_k c_k \nabla \tag{I.37}$$

where:

K_k gain matrix at time k

A measure of the significance of the bias in the state vector is the bias to noise ratio (BNR):

$$\lambda_x = \nabla x_k^T P_k^{-1} \nabla x_k \tag{I.38}$$

Typically the square root of BNR is examined to allow for a direct comparison with the ratio between the biases and the standard deviations of the states [Salzmann, 1993].

I.2.3 Relationship between MDB, BNR, α_0, γ_0 and λ_0

The MDB and BNR values are a function of the aforementioned factors affecting precision as well as the selected significance level, α_0 and power of the test, γ_0. α symbolizes a *Type I Error*: rejecting the null hypothesis, H_0, when it is in fact true and accepting an alternative hypothesis, H_1, instead. It represents the probability of a false alarm. γ symbolizes a *Type II Error*: not rejecting the null hypothesis when it is in fact false. The offset between central values for the H_0 and H_1 distributions is known as the non-centrality parameter, λ. The relationship between between α_0, γ_0 and λ_0 is illustrated in Figure I.1. As an example, if values are selected such that $\alpha_1 = 0.001$ and $\gamma_0 = 0.80$, it follows that $\lambda_0 = 17.075$ [Teunissen, 1998].

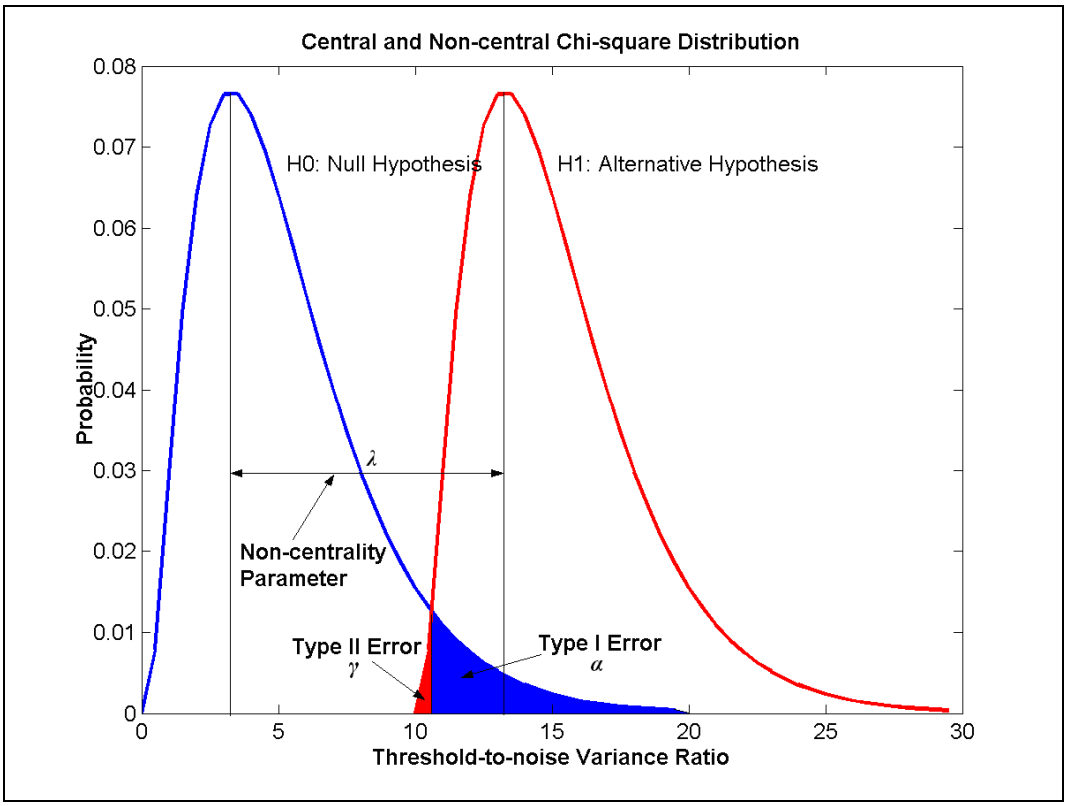

Figure I.1: Relationship between α, γ and λ [Kim, 2007]

From Equation (I.35) it can be seen that the MDB is directly proportional to λ_0 and inversely proportional to Q_{v_k}; when the MDB gets larger so does the non-centrality parameter, λ. Additionally, the power γ gets larger as λ increases. According to Equation (I.36) the non-centrality parameter depends upon [Teunissen, 1998]:

a) the model error c_k,

b) the covariance matrix of the estimates P_x, and

c) the design matrices H_k and J_k .

Since the model error cannot be changed, only changes in the variance matrix and design matrix will allow one to increase λ and therefore to also increase the power of the test, γ. This can be accomplished by using more precise equipment or by changing the structure of the design matrix (e.g., adding observations).

As can be seen from Equation (I.38), the BNR is the ratio between the external reliability ∇x_k and the state precision P_k. An increase in BNR values requires an improvement in state precision P_k (smaller denominator) or an increase in the bias vector ∇x_k (larger numerator) or both. This latter option requires either an increase in the gain matrix K_k (see Equation (I.37)) or an increase in MDB∇ (which is generally not desirable).

I.2.4 System Analysis

For this open pit mine deformation application, statistical values of $\alpha_1 = 0.05$, $\gamma_0 = 0.99$ have been selected from which it follows that $\lambda_0 = 18.37$. This implies that there is a 5% chance of committing a *Type I* error and 1% chance of committing a *Type II* error. *Type II* errors (not rejecting the null hypothesis when it is false) can have serious consequences in deformation monitoring applications, and therefore a stringent value has been chosen. Based upon these parameters, the change in MDB and BNR values as a result of changes in the process noise values (constant diagonal terms of Q matrix) has

been analyzed. The MDB and BNR values are taken from a randomly selected epoch after 40 hours of processing. The results are summarized in Table I.3. The following points are noted:

a) Increasing the Q value decreases the precision of the solutions. This is apparent from Equation (I.32).

b) The best achievable precision is approximately ± 2 mm in all three solution components (regardless of how small the Q value is).

c) Increasing the Q value increases the BNR values. Since an increase in the Q value decreases the precision of the solutions, an increase in the Q value must also lead to an increase in the bias vector ∇x_k. As can be seen from Equation (I.38), the increasing BNR values imply that the bias vector ∇x_k is growing more rapidly than the standard deviations of the states.

d) For the range of Q values investigated, changing the Q matrix constant does not significantly change the MDB values. This can be explained by taking a closer look at Equations (I.35) and (I.35). The residual covariance matrix Q_{v_k} is the only parameter that is changing from one analysis to the next. It is dependent upon the observation noise matrix R_k and the $(H_k + J_k)P_k^-(H_k + J_k)^T)$ term. Typical magnitudes for elements of the R_k matrix are 10^{-5} or larger whereas typical magnitudes for the latter term are 10^{-9} when the sample rate is 10 seconds. The largest $(H_k + J_k)$ term in this scenario is approximately 0.020 m. The smallest R_k term is approximately (0.002 m)^2. A quick calculation shows that in order for the

influence of the latter term to be dominant, the Q value must be greater than or equal to approximately 0.100 m. A target moving at 0.100 m / sample interval is moving much too quickly to be tracked by this filter since it defies the static model. For all intents and purposes, the MDB is dictated by the observation noise matrix R_k.

Table I.3: Changes in Precision, MDB and √BNR Values with Changes in Process Noise (R_k unscaled)

Q_k Diagonal Value [mm /sample rate (10s)]	σ_E [m]	σ_N [m]	σ_U [m]	SV	MDB [m]	√BNR [m]
0.00001	0.0021	0.001	0.0016	G10	0.008	0.021
				G07	0.016	0.017
				G15	0.017	0.013
				G06	0.019	0.010
				G29	0.005	0.022
				G08	0.015	0.018
				G21	0.006	0.039
				G18	0.011	0.014
0.001	0.0021	0.001	0.0016	G10	0.008	0.022
				G07	0.016	0.017
				G15	0.017	0.013
				G06	0.019	0.010
				G29	0.005	0.022
				G08	0.015	0.018
				G21	0.006	0.039
				G18	0.011	0.014
0.03	0.0028	0.002	0.0026	G10	0.008	0.042
				G07	0.016	0.028
				G15	0.017	0.021
				G06	0.019	0.021
				G29	0.005	0.040
				G08	0.015	0.025
				G21	0.006	0.071
				G18	0.011	0.020
0.1	0.0047	0.0037	0.0048	G10	0.008	0.079
				G07	0.016	0.048
				G15	0.017	0.032
				G06	0.019	0.046
				G29	0.005	0.070
				G08	0.015	0.043
				G21	0.006	0.124
				G18	0.011	0.030
0.3	0.0072	0.0067	0.0088	G10	0.008	0.152
				G07	0.016	0.074
				G15	0.017	0.026
				G06	0.019	0.114
				G29	0.005	0.097
				G08	0.015	0.089
				G21	0.006	0.159
				G18	0.011	0.033

Additional analyses were conducted to examine the impact of scaling the observation noise matrix R_k and holding the Q value (process noise) fixed. The MDB and BNR values are taken from the same epoch as the previous analyses after 40 hours of processing. The results are summarized in Table I.4. The following points are noted:

a) Smaller scale parameters k reduce the MDB. This is in accord with the aforementioned item (d). If the scale parameter k is unrealistically small, however, the test on the variance factor will fail resulting in the observations being rejected.

b) Larger scale parameters k decrease the precision of the state estimates. This is intuitive as an increase in the uncertainty in the observables will result in an increase in the uncertainty of the estimates.

c) Larger scale parameters k decrease the BNR values. As can be seen from Equation (I.38), since the precision of the state estimates is decreasing the bias vector ∇x_k must be increasing (analyses have shown it increases) less quickly than the standard deviations of the states.

Table I.4: Changes in Precision, MDB and √BNR Values with Changes in Scaling of Observation Noise Matrix R_k. (Q = 0.03 mm / 10 s)

k (R_k scale)	σ_E [m]	σ_N [m]	σ_U [m]	SV	MDB [m]	√BNR [m]
0.5	0.0023	0.0017	0.0022	G10	0.006	0.050
				G07	0.011	0.033
				G15	0.012	0.024
				G06	0.013	0.026
				G29	0.004	0.048
				G08	0.011	0.029
				G21	0.004	0.085
				G18	0.008	0.023
1	0.0028	0.002	0.0026	G10	0.008	0.042
				G07	0.016	0.028
				G15	0.017	0.021
				G06	0.019	0.021
				G29	0.005	0.040
				G08	0.015	0.025
				G21	0.006	0.071
				G18	0.011	0.020
2	0.0036	0.0024	0.0031	G10	0.011	0.035
				G07	0.023	0.024
				G15	0.024	0.018
				G06	0.026	0.017
				G29	0.007	0.034
				G08	0.021	0.022
				G21	0.009	0.060
				G18	0.016	0.018
10	0.007	0.0038	0.0056	G10	0.025	0.026
				G07	0.051	0.019
				G15	0.053	0.014
				G06	0.059	0.012
				G29	0.016	0.025
				G08	0.047	0.019
				G21	0.020	0.045
				G18	0.036	0.015

1.3 Finite Impulse Response (Non-Recursive) Filter Characteristics for Satellite Noise Modelling

Geometry free, single-differenced (between receivers) observations are used to model each satellite's noise state. A second order, time differentiator is implemented to generate noise observations which can be expressed as:

$$noise^{i}_{AB}(k) = SD^{i}_{AB}(k) - 2SD^{i}_{AB}(k-1) + SD^{i}_{AB}(k-2) \tag{I.39}$$

where:

$SD^{i}_{AB}(k)$ between receivers, single-differenced, geometry free observation from receiver *A* to satellite *i* at epoch *k*.

The transfer function for this filter is:

$$\frac{y(n)}{x(n)} = [1 - 2z^{-1} - z^{-2}]$$

for which the filter coefficients are a = [1 0 0], b = [1 -2 1]. This second order, three terms, difference filter is a high pass filter as illustrated in Figure I.2 (a sample rate of 1 Hz has been assumed). The cut-off frequency is determined as the frequency where the amplitude reaches $1/\sqrt{2}$ of the maximum amplitude. As illustrated by the dashed lines in Figure I.2, it is approximately 0.32 Hz.

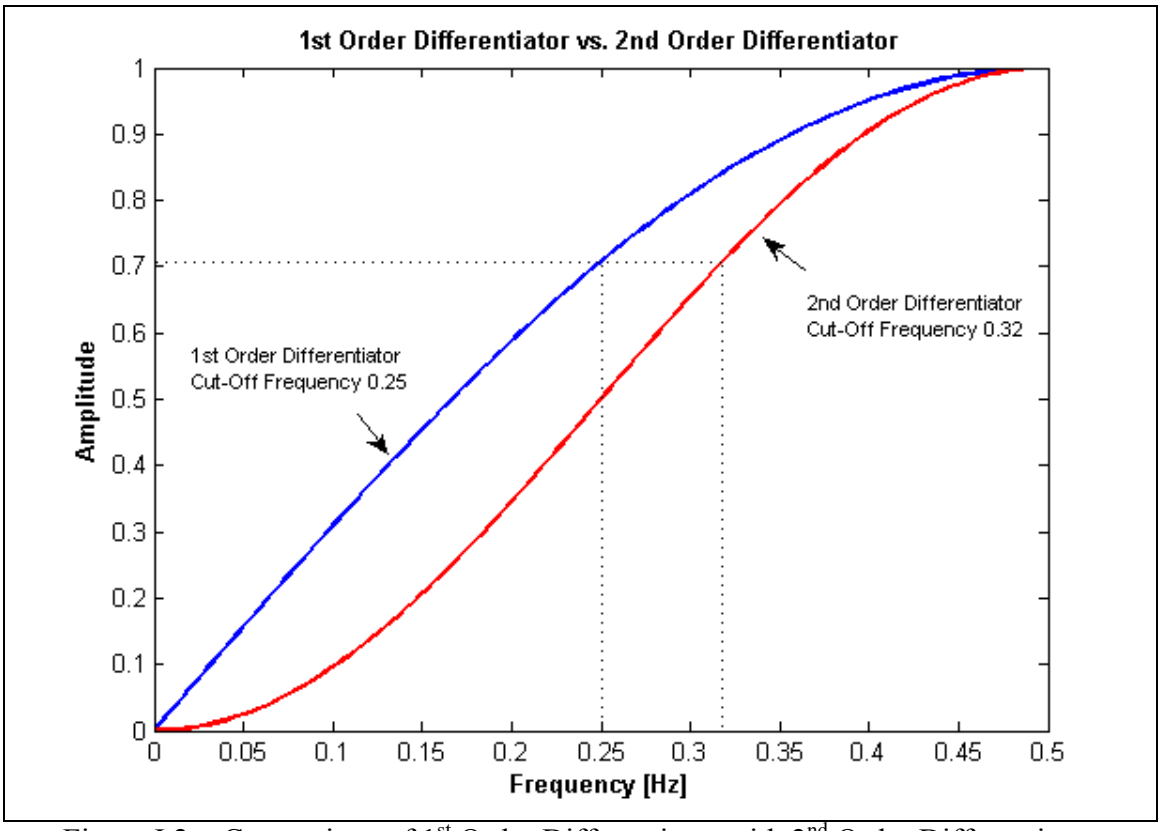

Figure I.2: Comparison of 1st Order Differentiator with 2nd Order Differentiator Frequency Response Curves

For comparison purposes, the frequency response curve for a first order, two terms, difference filter having coefficients a = [1 0], b = [1 -1] is also plotted in Figure I.2. It can be seen that the 2nd order differentiator has definite bandstop and bandpass roll off regions whereas the first order differentiator does not, thus making it more effective at reducing the effects of low frequency biases.

The characteristics of the frequency response curve for the 2nd order differentiator implemented have important implications regarding the limitations of this noise modelling approach. These can be better identified by looking at potential error sources

individually and identifying those which may contribute non-white components to the noise estimates:

a) Satellite clock errors will cancel through between-receivers single-differencing and should not impact the whiteness property of the estimate.
b) Receiver clock errors will cancel due to the nature of the geometry free observable.
c) Tropospheric delay biases will also cancel through the GF combination.
d) Low frequency biases caused by ionospheric delay will be significantly reduced by the 2nd order differentiator. Ionospheric delay frequency components not cancelled through this differentiator will appear mainly as measurement noise.
e) Low frequency multipath biases typically occur as result of slowly changing satellite geometry. These biases will be significantly reduced by the 2nd order differentiator. High frequency multipath biases are typically caused by changing conditions at the antenna site (which generally does not occur in static conditions) and by signal diffraction caused by nearby reflectors. High frequency multipath not stopped by this differentiator will appear mainly as measurement noise.

Although the 2nd order differentiator approach works well in practice, this approach could be improved by implementing a more conventional digital filter such as a 2nd order Butterworth [Brown and Hwang, 1997] . The frequency response curve for this filter is illustrated in Figure I.3. Arbitrarily selected maximum bandpass attenuation and minimum bandstop attenuation values of 40 dB and 0.087 dB (corresponding to output to

input ratios of 99% and 1% respectively) were chosen to generate comparison bandstop and bandpass values. It can be seen that the 2nd order differentiator (bandstop frequency: 0.035 Hz and bandpass frequency: 0.465 Hz) is inferior in performance to the Butterworth filter (bandstop frequency: 0.106 Hz and bandpass frequency: 0.496 Hz).

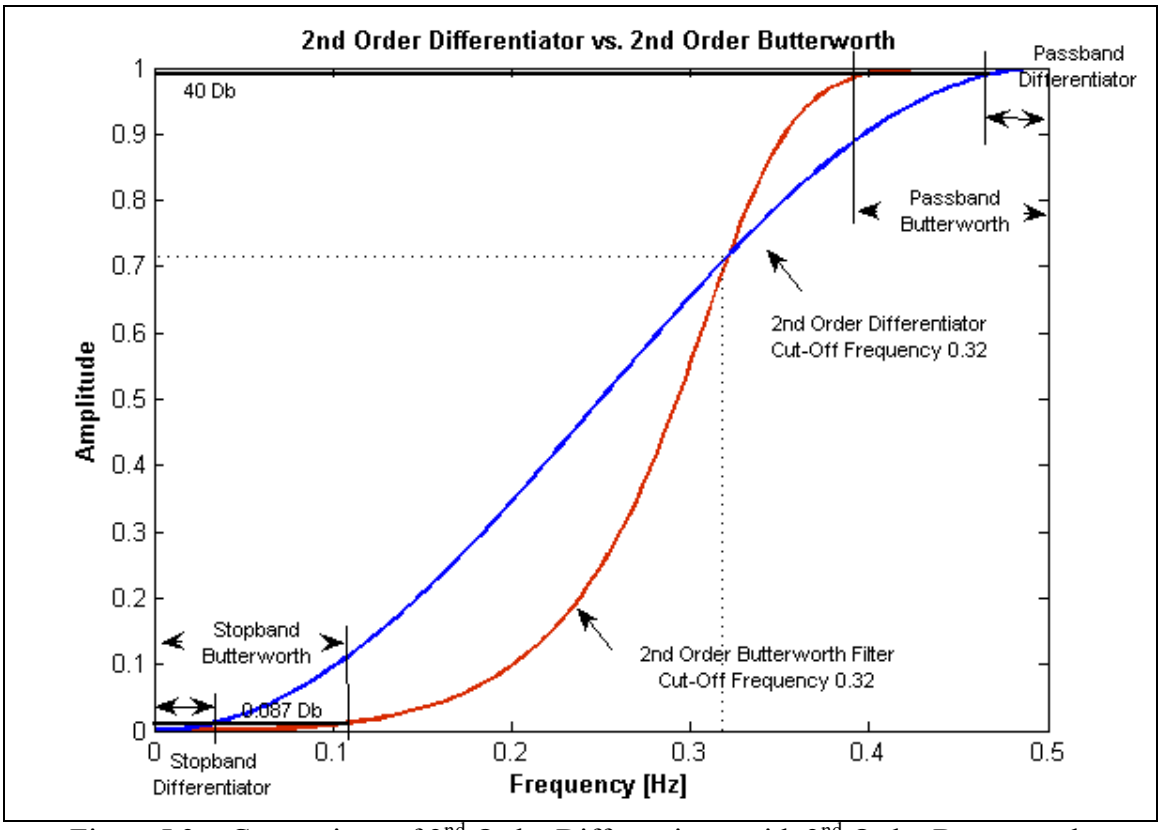

Figure I.3: Comparison of 2nd Order Differentiator with 2nd Order Butterworth Frequency Response Curves

I.4 Highland Valley Copper Processing Results

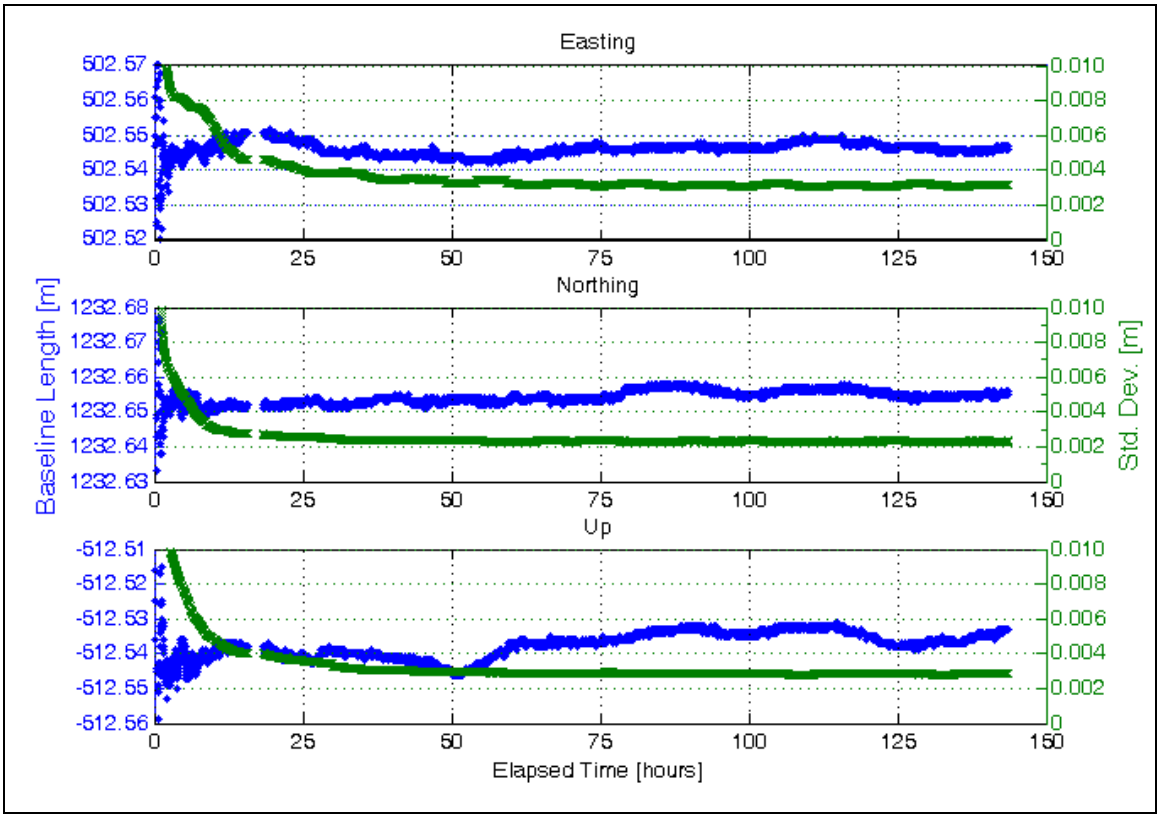

Figure I.4: 424 to RTS1

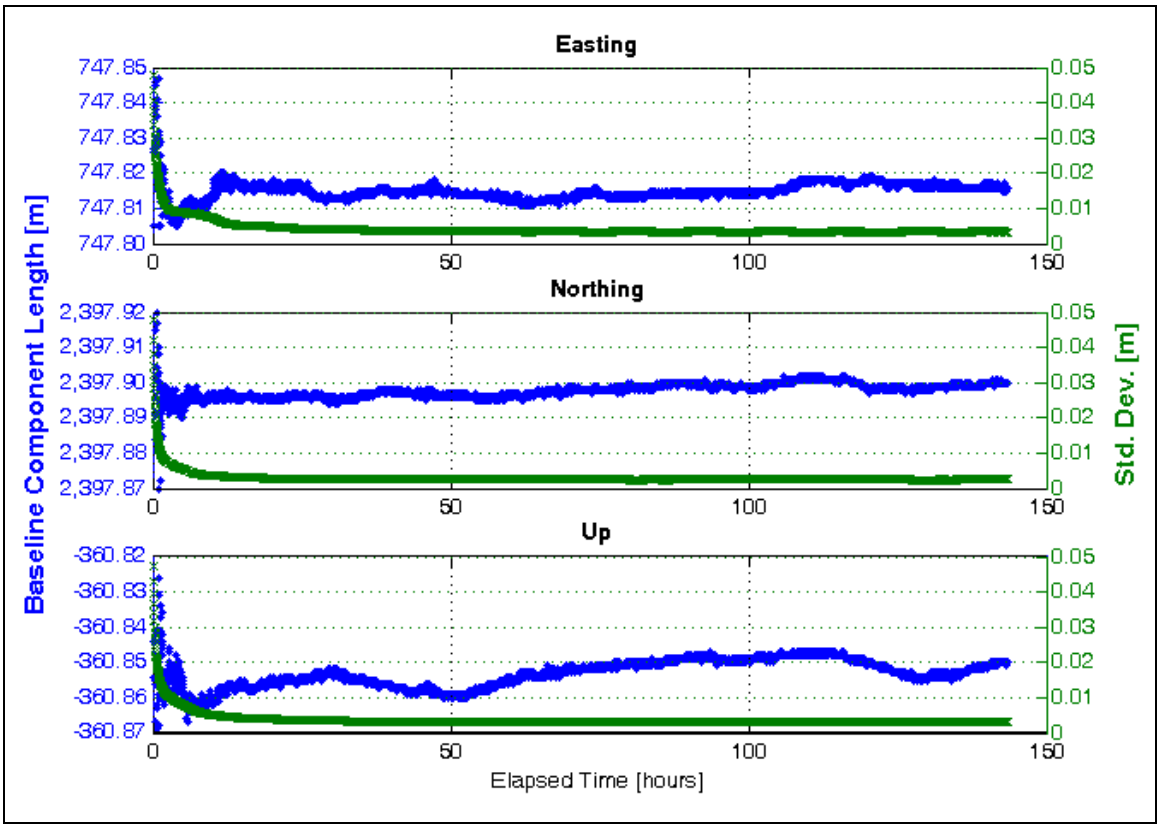

Figure I.5: 424 to RTS2

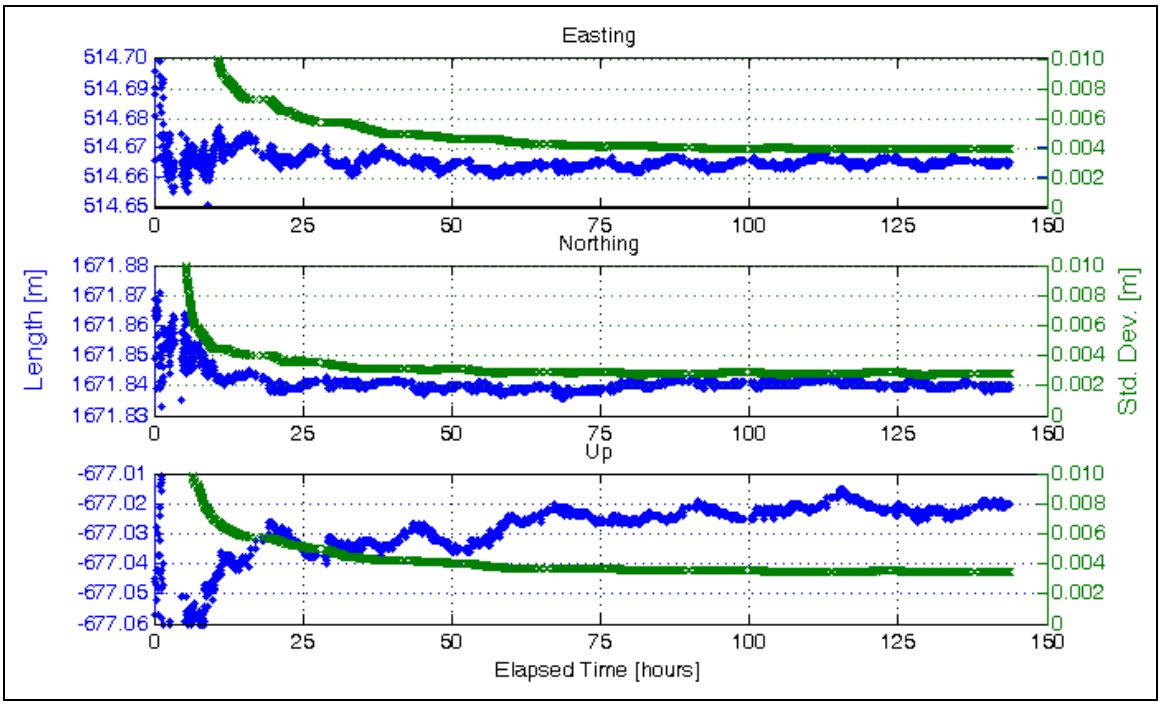

Figure I.6: 424 to RTS3

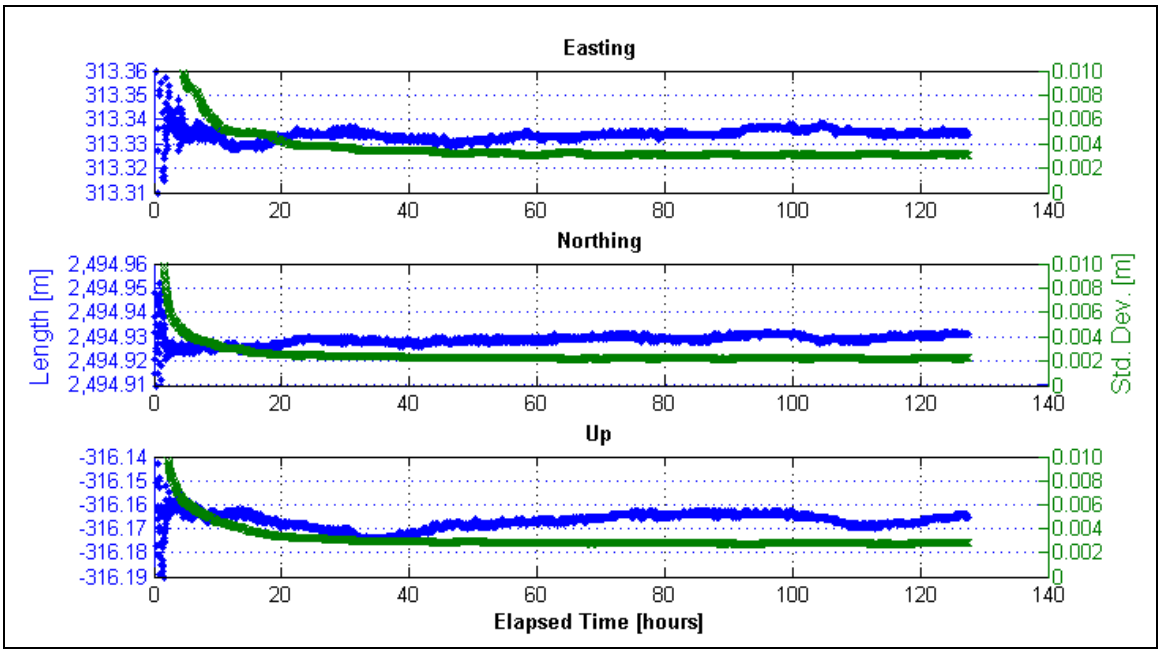

Figure I.7: 424 to 987

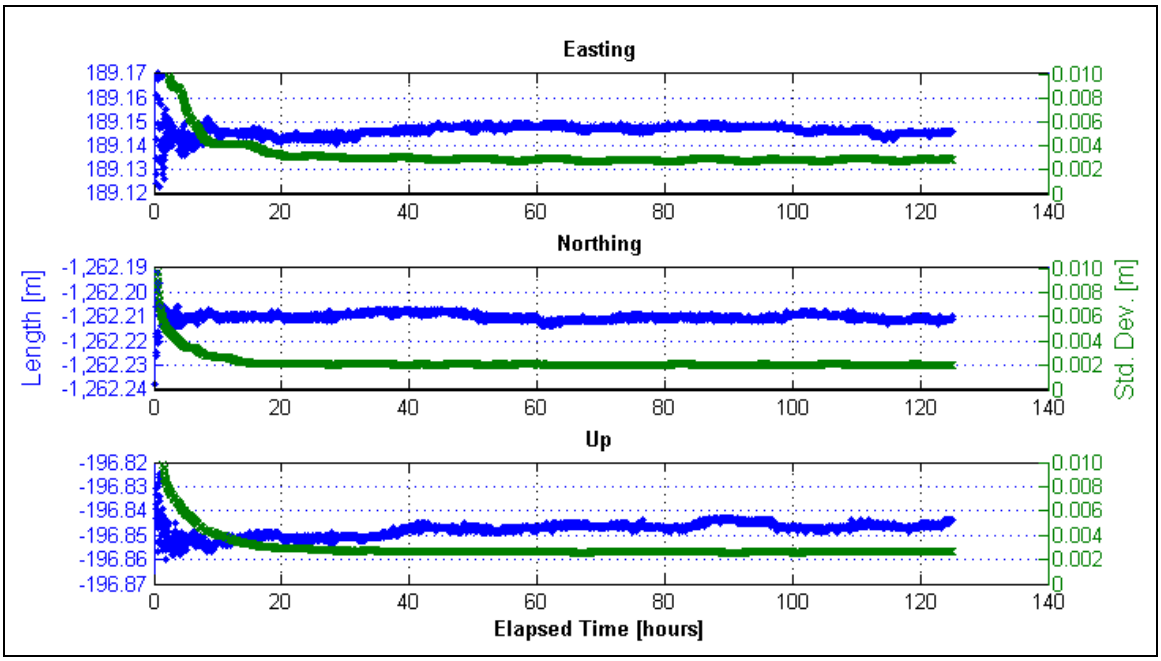

Figure I.8: 987 to RTS1

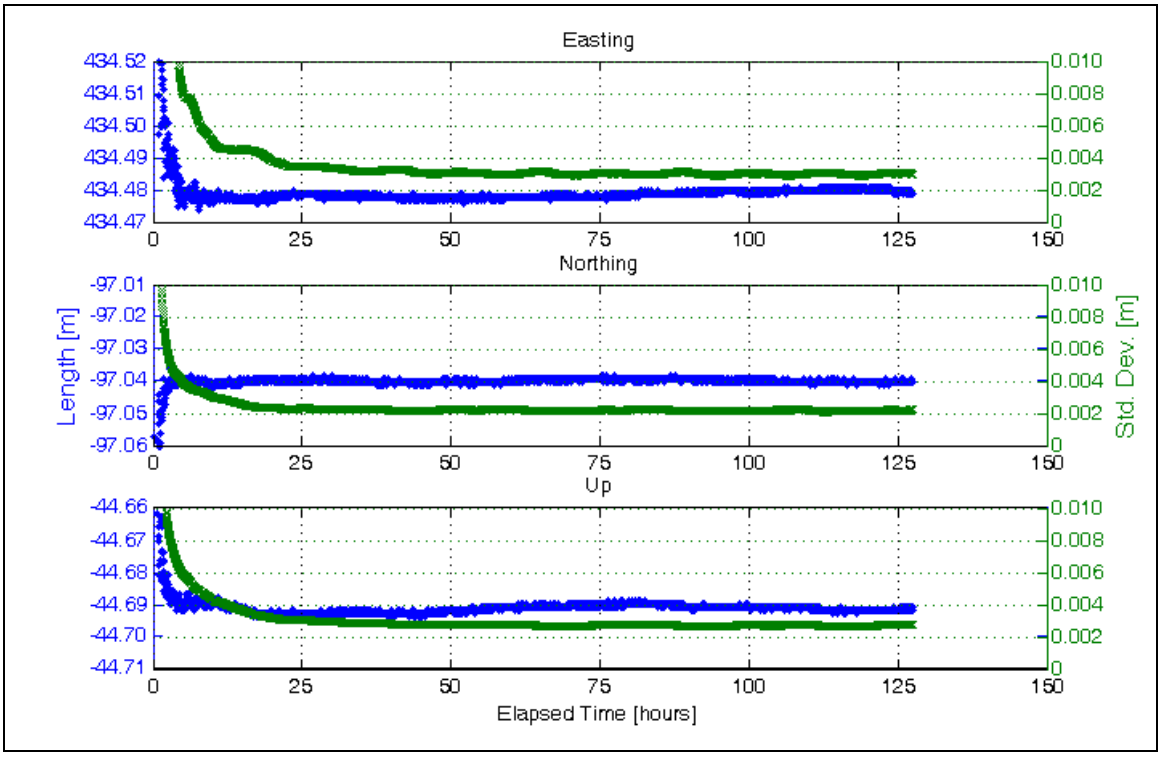

Figure I.9: 987 to RTS2

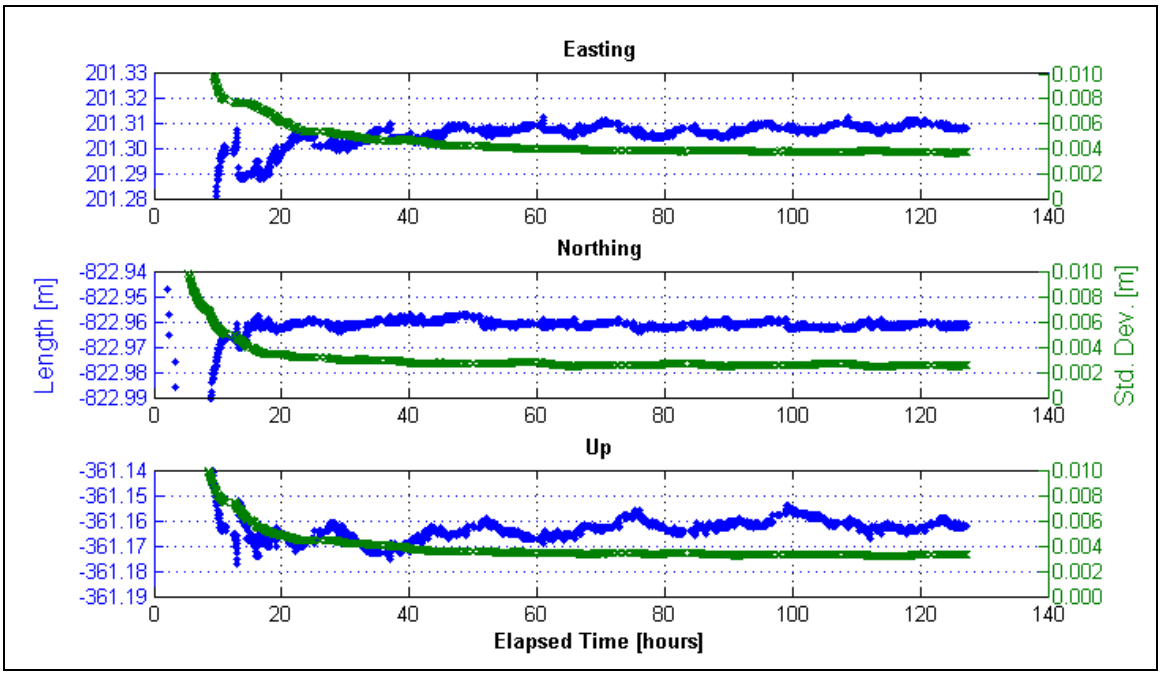

Figure I.10: 987 to RTS3

APPENDIX II
PSEUDOLITE OBSERVATIONS AND NOISE MODELLING

Provided are additional results and analysis to Chapter 4 from Paper 3: "Augmenting GPS with Pseudolites for Deformation Monitoring in Harsh Environments."

II.1 Sample Pseudolite (PL) Observations

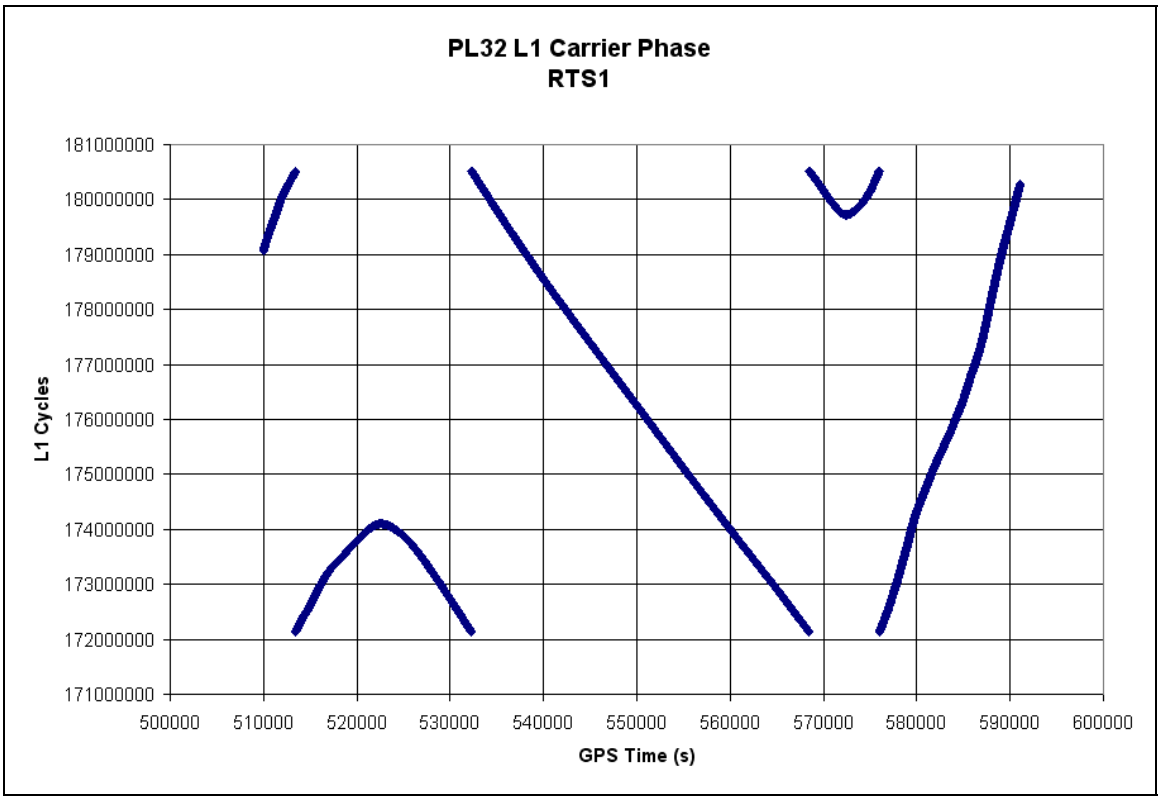

Figure II.1: PL32, L1, Carrier Phase Observations at Station RTS1

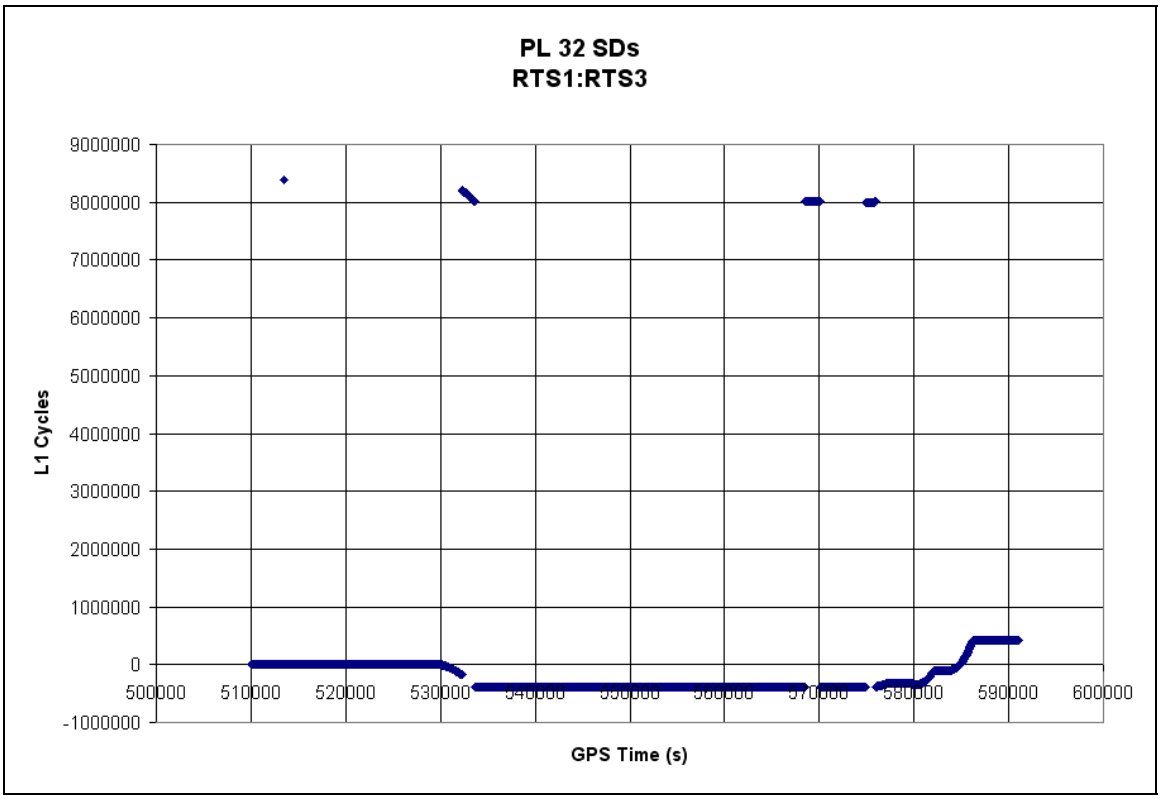

Figure II.2: PL 32, L1 Single-Differenced Observations formed between Stations RTS1 and RTS3 at HVC

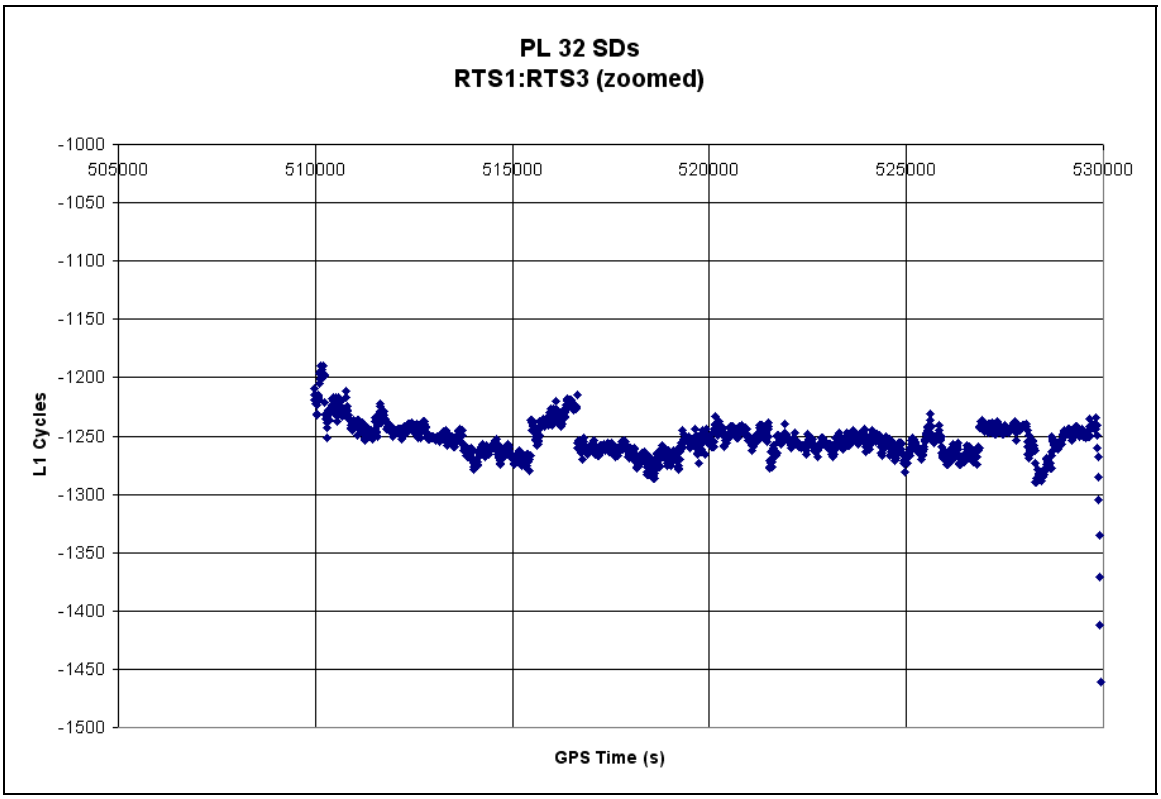

Figure II.3: Zoomed View of Figure II.2

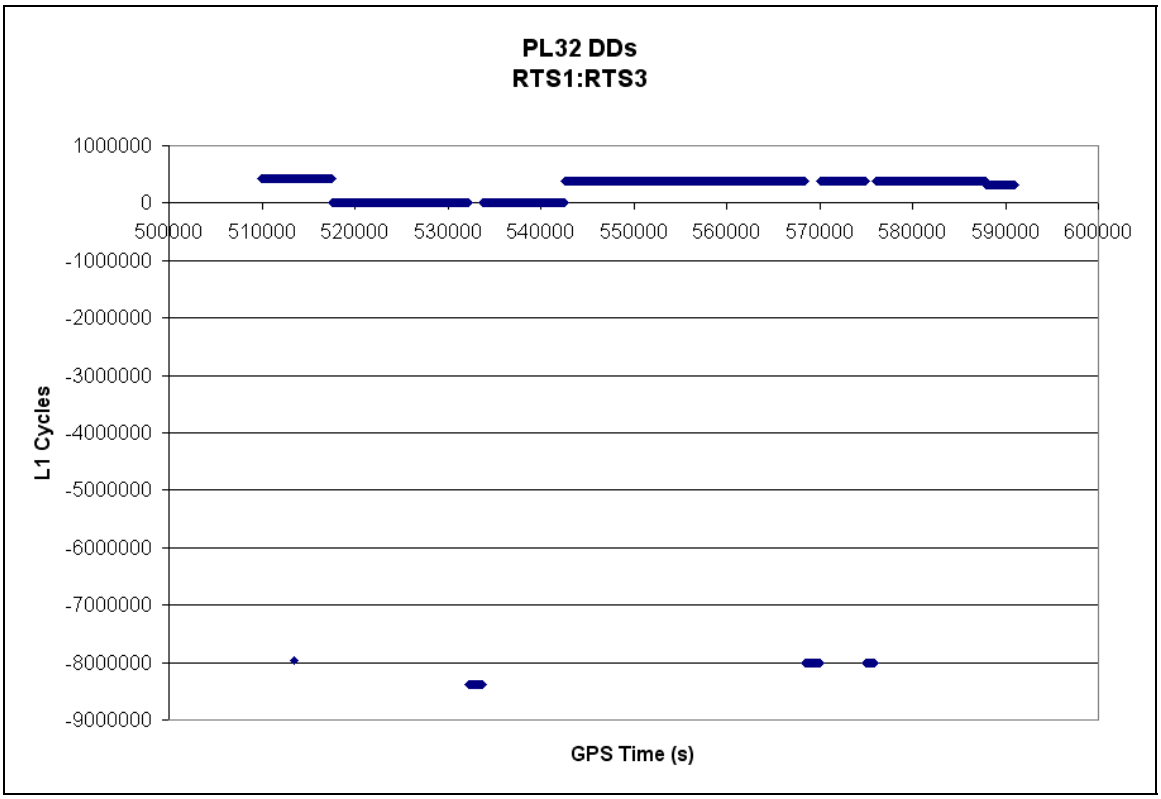

Figure II.4: Double-Differenced, L1 Observations formed between PL32 and Highest Elevation Satellite and between Stations RTS1 and RTS3 at HVC

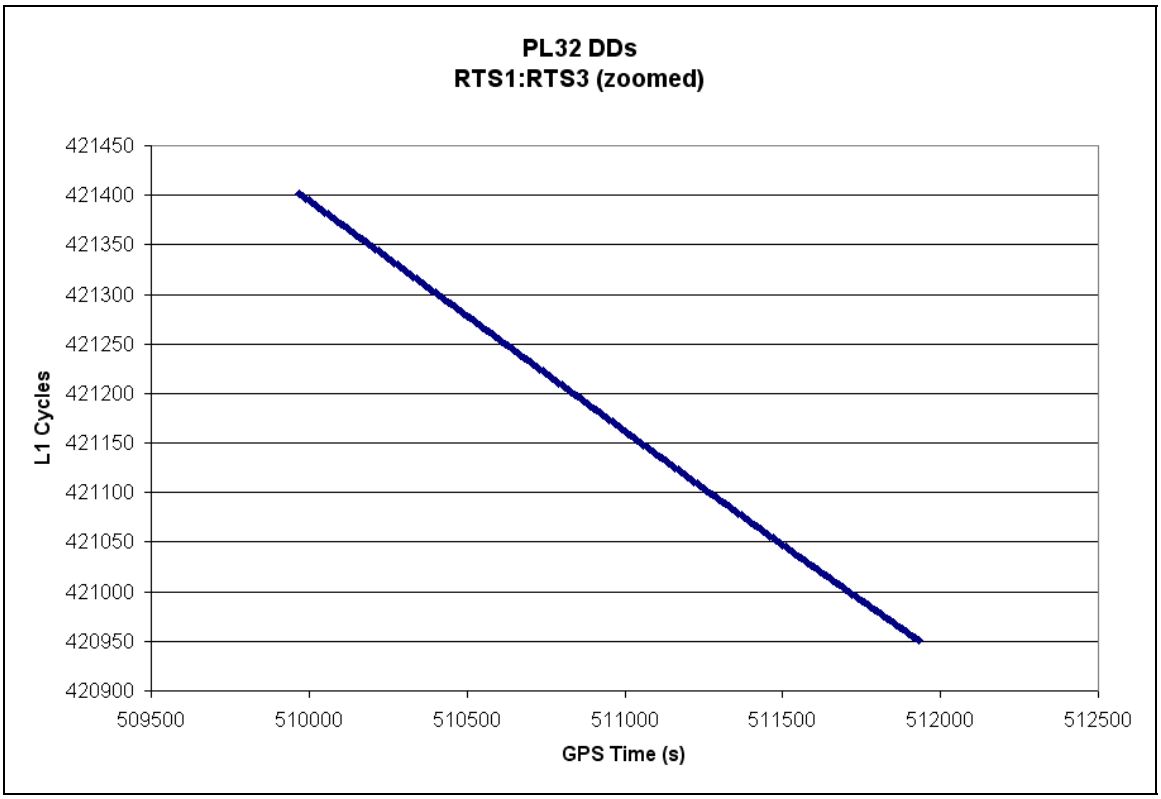

Figure II.5: Zoomed view of Figure II.4

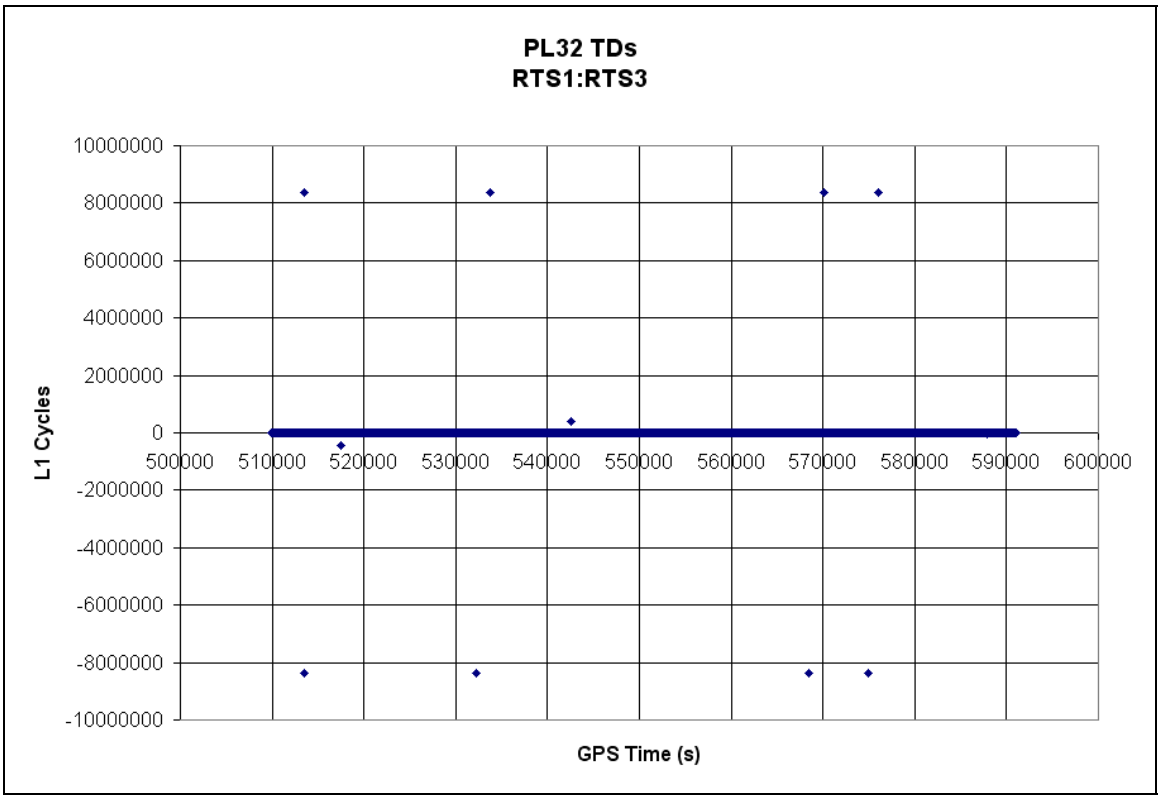

Figure II.6: Triple-Differenced, L1 Observations formed between PL32 and Highest Elevation Satellite and between Stations RTS1 and RTS3 at HVC

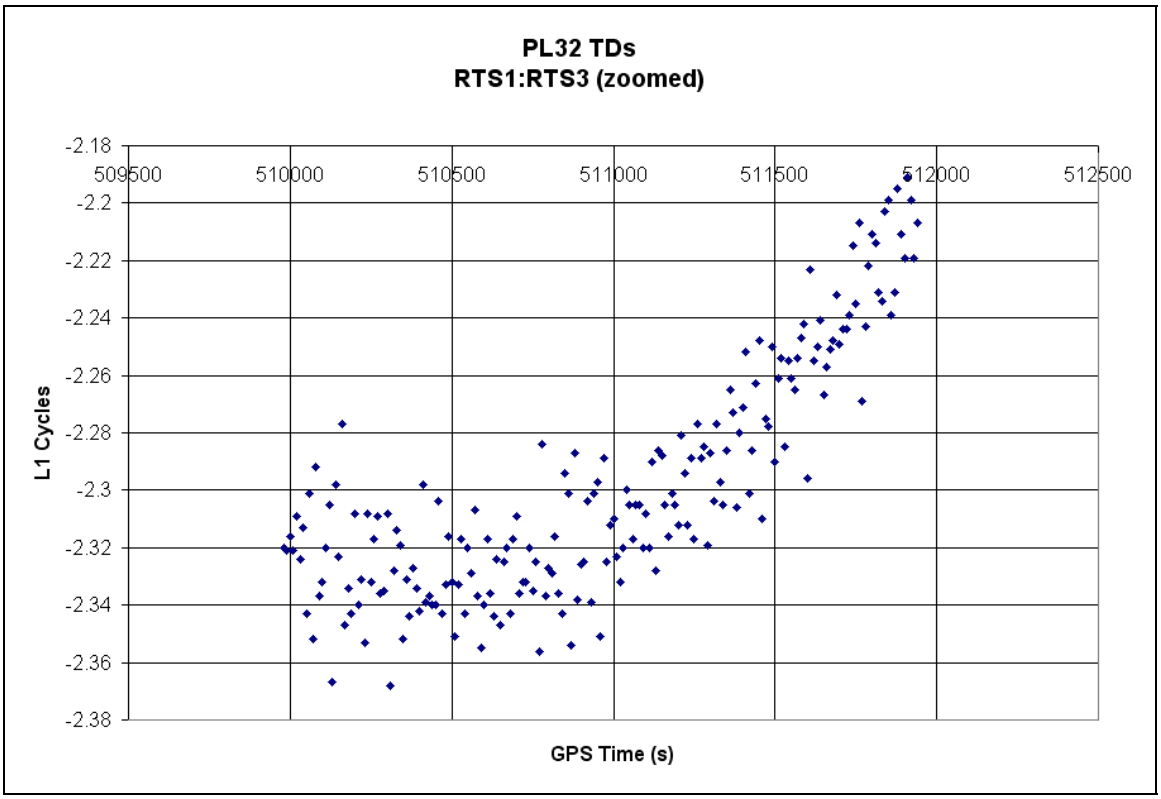

Figure II.7: Zoomed View of Figure II.6

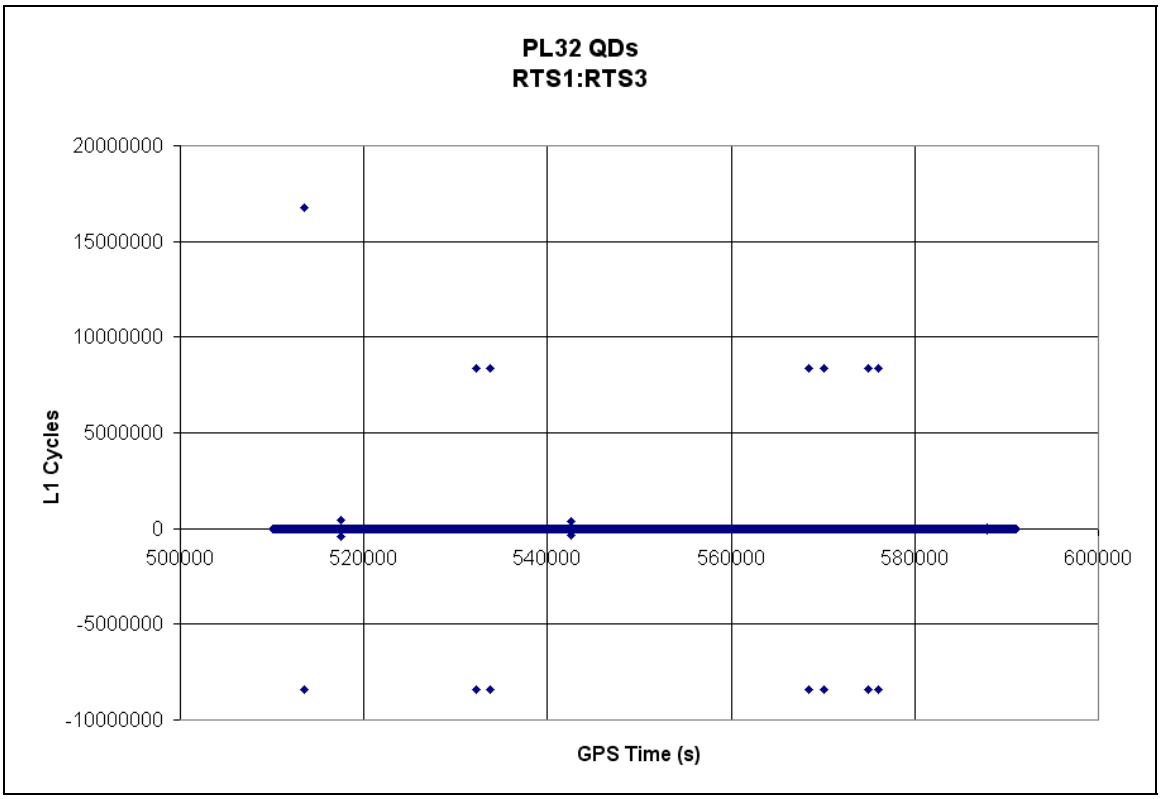

Figure II.8: Quadruple-Differenced, L1 Observations formed between PL32 and Highest Elevation Satellite and between Stations RTS1 and RTS3 at HVC

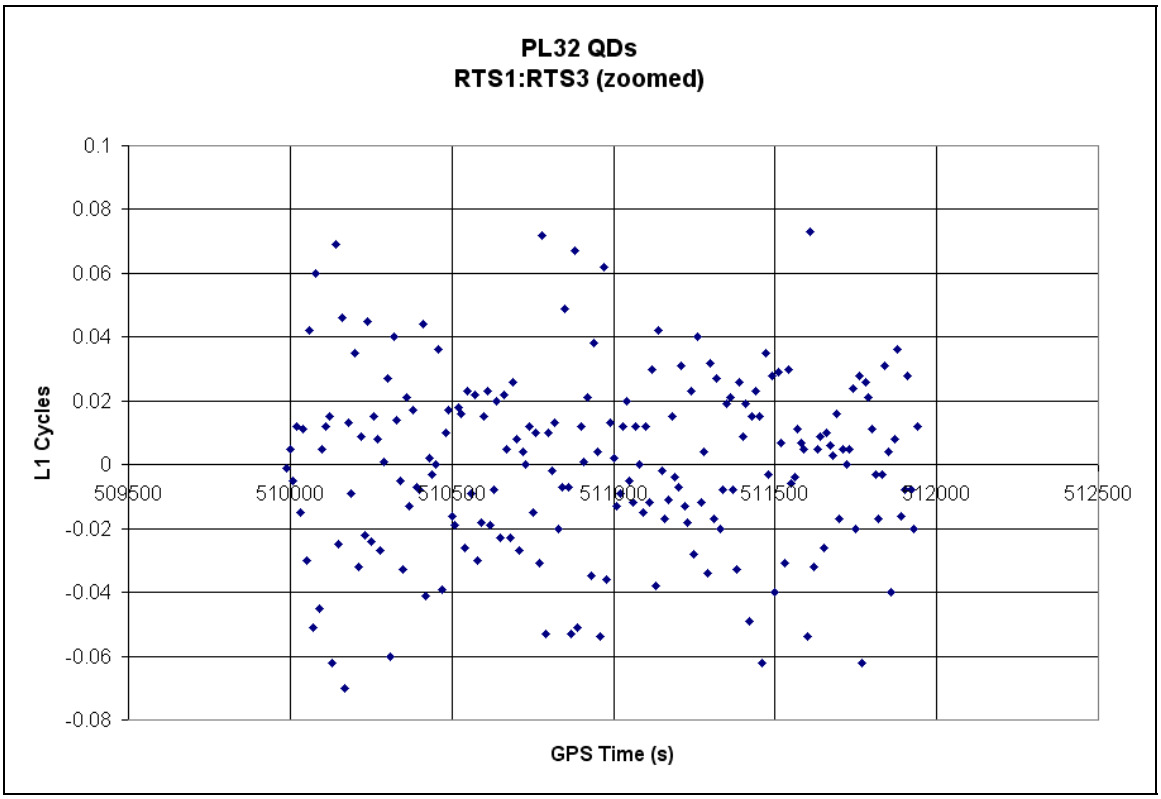

Figure II.9: Zoomed View of Figure II.8

II.2 Observation Noise Modelling Strategy

An estimate of the variance of the between receivers single-differenced carrier phase observation at time k is required for the pseudolite ($\sigma^2_{SD(k)^{PL}_{AB}}$) in the Delayed-State Kalman Filter for processing. Because the PL tested was a single frequency transmitter, the approach presented in Chapter 3 for modelling the SD noise levels of individual GPS satellites (time-differenced, geometry-free, single differenced observations) could not be used. The devised approach uses the quadruple-differenced (QD) observations illustrated

in the previous section, which corresponds to a 2nd order differentiator high pass filter (see Section II.3).

The quadruple difference at time k between receivers A and B and between satellite i and pseudolite PL ($QD(k)_{AB}^{iPL}$) is the time difference of consecutive triple-differenced (TD) observations:

$$QD(k)_{AB}^{iPL} = TD(k)_{AB}^{iPL} - TD(k-1)_{AB}^{iPL} \tag{II.1}$$

Rewriting Equation (II.1) in terms of double-differenced (DD) observations gives:

$$QD(k)_{AB}^{iPL} = (DD(k)_{AB}^{iPL} - DD(k-1)_{AB}^{iPL}) - (DD(k-1)_{AB}^{iPL} - DD(k-2)_{AB}^{iPL}) \tag{II.2}$$

Rewriting Equation (II.2) in terms of single-differenced (SD) observations gives:

$$\begin{aligned} QD(k)_{AB}^{iPL} = {} & ((SD(k)_{AB}^{i} - SD(k)_{AB}^{PL}) - (SD(k-1)_{AB}^{i} - SD(k-1)_{AB}^{PL})) \\ & - ((SD(k-1)_{AB}^{i} - SD(k-1)_{AB}^{PL}) - (SD(k-2)_{AB}^{i} - SD(k-2)_{AB}^{PL})) \end{aligned} \tag{II.3}$$

Simplifying (II.3) yields:

$$\begin{aligned} QD(k)_{AB}^{iPL} = {} & SD(k)_{AB}^{i} - SD(k)_{AB}^{PL} - 2SD(k-1)_{AB}^{i} + 2SD(k-1)_{AB}^{PL} \\ & + SD(k-2)_{AB}^{i} - SD(k-2)_{AB}^{PL})) \end{aligned} \tag{II.6}$$

The variance of $QD(k)_{AB}^{iPL}$ can be calculated as:

$$\sigma^2_{QD(k)_{AB}^{iPL}} = \sigma^2_{SD(k)_{AB}^{i}} + \sigma^2_{SD(k)_{AB}^{PL}} + 4\sigma^2_{SD(k-1)_{AB}^{i}} + 4\sigma^2_{SD(k-1)_{AB}^{PL}} + \sigma^2_{SD(k-2)_{AB}^{i}} + \sigma^2_{SD(k-2)_{AB}^{PL}} \tag{II.4}$$

To estimate $\sigma^2_{SD(k)^{PL}_{AB}}$ it is approximated that $\sigma^2_{SD(k)^{i}_{AB}} = \sigma^2_{SD(k+1)^{i}_{AB}}$ and likewise for $\sigma^2_{SD(k)^{PL}_{AB}}$. Equation (II.4) is now written as:

$$\sigma^2_{QD(k)^{iPL}_{AB}} \approx 6\sigma^2_{SD(k)^{i}_{AB}} + 6\sigma^2_{SD(k)^{PL}_{AB}} \tag{II.5}$$

Rearranging Equation (II.5), $\sigma^2_{SD(k)^{PL}_{AB}}$ can now be solved for using:

$$\sigma^2_{SD(k)^{PL}_{AB}} \approx \frac{\sigma^2_{QD(k)^{iPL}_{AB}} - 6\sigma^2_{SD(k)^{i}_{AB}}}{6} \tag{II.6}$$

where $\sigma^2_{SD(k)^{i}_{AB}}$ is calculated using the geometry-free single-differenced method discussed in Chapter 3 and a moving average window is used to estimate the variance of the noise estimates $\sigma^2_{QD(k)^{iPL}_{AB}}$.

II.3 Finite Impulse Response (Non-Recursive) Filter Characteristics for Pseudolite Noise Modelling

Quadruple-differenced, L1 observations are used to model each satellite's noise state. This differentiator can be expressed as:

$$\begin{aligned} noise^{PL}_{AB}(k) = {} & SD^{i}_{AB}(k) - SD^{PL}_{AB}(k) - 2SD^{i}_{AB}(k-1) + 2SD^{PL}_{AB}(k-1) \\ & + SD^{i}_{AB}(k-2) - SD^{PL}_{AB}(k-2) \end{aligned} \tag{II.7}$$

where:

$SD_A^{PL}(k)$ Single-differenced L1 carrier phase observation from receiver *A* to pseudolite *PL* at epoch *k*.

The transfer function for this filter is:

$$\frac{y(n)}{x(n)} = [1 - 2z^{-1} + z^{-2}]$$

for which the filter coefficients are a = [1 0 0], b = [1 -2 1] . This second order, three terms, difference filter is a high pass filter as illustrated in Figure I.2 (a sample rate of 1 Hz has been assumed). The cut-off frequency is determined as the frequency where the amplitude reaches $1/\sqrt{2}$ of the maximum amplitude. As illustrated by the dashed lines in Figure I.2, it is approximately 0.32 Hz. The characteristics of the frequency response curve for this filter have important implications regarding the limitations of this noise modelling approach. These can be better identified by looking at potential error sources individually and identifying those which may contribute non-white components to the noise estimates:

a) Receiver clock errors and PL clock errors will cancel through double-differencing and should not impact the whiteness property of the estimate
b) The response curve shows that this differentiator significantly reduces low frequency components of the signal. Consequently, slowly changing biases such as those caused by the atmosphere will be significantly reduced. Any remaining contribution of atmospheric biases to the signal will colour the noise estimates.
c) Low frequency multipath biases typically occur as result of slowly changing satellite geometry. These biases will be significantly reduced by the 2nd order differentiator. High frequency multipath biases are typically caused by changing

conditions at the antenna site (which generally does not occur in static conditions) and by signal diffraction caused by nearby reflectors. High frequency multipath biases will appear mainly as measurement noise.

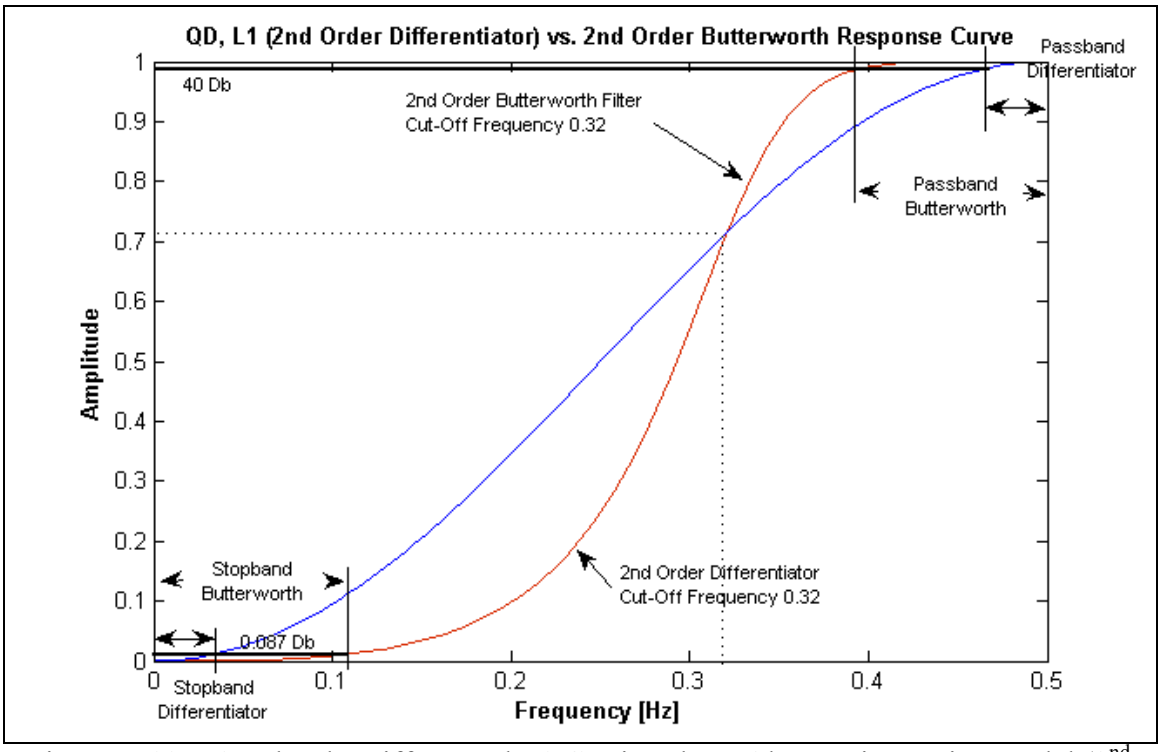

Figure II.10: Quadruple-Differenced L1 Carrier Phase Observation Noise Model (2nd Order Differentiator) Compared with 2nd Order Butterworth Filter

Although the 2nd order differentiator approach works well in practice, this approach could be improved by implementing a more conventional digital filter such as a 2nd order Butterworth [Brown and Hwang, 1997]. Figure I.2 illustrates the difference in bandstop and bandpass frequencies for the two frequency response curves. Arbitrarily selected maximum bandpass attenuation and minimum bandstop attenuation values of 40 dB and 0.087 dB (corresponding to output to input ratios of 99% and 1% respectively)

were chosen to generate comparison bandstop and bandpass values. It can be seen that the 2nd order differentiator (bandstop frequency: 0.035 Hz and bandpass frequency: 0.465 Hz) is inferior in performance to the Butterworth filter (bandstop frequency: 0.106 Hz and bandpass frequency: 0.496 Hz). Although the devised approach works, further research is required for optimal filter performance.

The addition of a second frequency to the pseudolite would allow for the estimation of a PL noise state directly using the method implemented in Appendix I (2nd order differentiator used on GF observations). Since the PL observations could then be analyzed independently from the reference satellite, pseudolite noise can be more effectively estimated without introducing DD operation which amplifies the residual high frequency components of the biases and errors.

APPENDIX III
ADDITIONAL FINITE ELEMENT METHOD RESULTS

Provided are additional results and analysis to Chapter 5 from Paper 4: "Design of Geodetic Deformation Monitoring Schemes using Deterministic Modelling: An Open Pit Mine Example."

III.1 X and Y Components of Displacements from Table 5.2: "Displacement Summary for Selected Points"

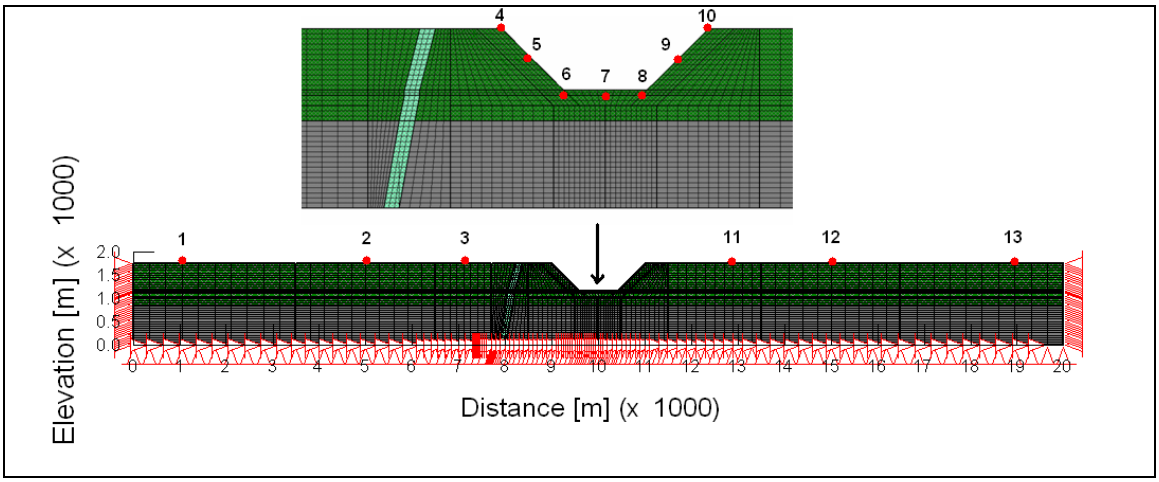

Figure III.1: Finite Element Mesh of the Open Pit Mine
(Figure 5.2 repeated for reference)

Table III.1: X- Displacements of Selected Points without Fault [m]

	Excavation Stage					
Pt #	1	2	3	4	5	Total
1	0.000	0.000	0.000	0.000	0.000	0.000
2	0.000	0.001	0.003	0.000	0.001	0.005
3	0.001	0.006	0.013	0.000	0.002	0.023
4	0.158	0.064	0.060	-0.013	0.000	0.269
5	-0.051	0.012	0.105	-0.010	0.005	0.061
6	-0.007	-0.017	-0.066	-0.035	0.018	-0.106
7	-0.002	-0.003	-0.017	-0.001	0.003	-0.021
8	-0.001	-0.002	-0.007	0.019	-0.019	-0.010
9	0.000	-0.001	-0.002	0.002	-0.008	-0.009
10	0.000	-0.001	-0.001	0.007	-0.003	0.002
11	0.000	0.000	-0.001	-0.002	-0.003	-0.006
12	0.000	0.000	0.000	-0.001	-0.001	-0.002
13	0.000	0.000	0.000	0.000	0.000	0.000

Table III.2: Y- Displacements of Selected Points without Fault [m]

	Excavation Stage					
Pt #	1	2	3	4	5	Total
1	0.000	0.000	0.000	0.000	0.000	0.000
2	0.000	0.000	0.000	0.000	0.000	-0.001
3	0.000	0.000	0.000	-0.001	-0.001	-0.001
4	-0.075	-0.008	-0.011	0.014	0.006	-0.074
5	0.098	-0.027	-0.022	0.026	0.013	0.088
6	0.018	0.052	0.100	0.114	0.043	0.328
7	0.003	0.008	0.016	0.224	0.141	0.392
8	0.001	0.002	0.006	0.106	0.035	0.150
9	0.000	0.000	0.001	0.024	0.012	0.038
10	0.000	0.000	0.000	0.012	0.005	0.017
11	0.000	0.000	0.000	-0.001	-0.001	-0.002
12	0.000	0.000	0.000	0.000	0.000	0.000
13	0.000	0.000	0.000	0.000	0.000	0.000

Table III.3: X- Displacements of Selected Points with Fault [m]

	Excavation Stage					
Pt #	1	2	3	4	5	Total
1	0.000	0.000	0.000	0.000	0.000	0.000
2	0.000	0.000	0.000	0.000	0.000	0.000
3	0.000	0.001	0.001	-0.001	-0.001	0.000
4	0.125	0.049	0.013	-0.046	-0.029	0.113
5	-0.033	0.007	0.027	-0.040	-0.025	-0.064
6	-0.004	-0.008	-0.025	-0.042	-0.046	-0.125
7	-0.001	0.000	-0.003	0.029	0.030	0.056
8	0.000	0.000	-0.002	0.052	0.025	0.075
9	0.000	0.000	0.000	0.016	0.005	0.021
10	0.000	0.000	0.000	0.018	0.006	0.024
11	0.000	0.000	0.000	0.002	0.000	0.001
12	0.000	0.000	0.000	0.000	0.000	0.000
13	0.000	0.000	0.000	0.000	0.000	0.000

Table III.4: Y- Displacements of Selected Points with Fault [m]

	Excavation Stage					
Pt #	1	2	3	4	5	Total
1	0.000	0.000	0.000	0.000	0.000	0.000
2	0.000	0.000	0.000	0.000	0.000	0.000
3	0.000	0.000	0.000	0.000	0.000	0.000
4	-0.047	0.010	0.009	0.017	0.010	-0.001
5	0.086	0.024	0.013	0.031	0.018	0.173
6	0.015	0.040	0.081	0.133	0.073	0.342
7	0.003	0.006	0.011	0.221	0.141	0.381
8	0.001	0.002	0.003	0.106	0.037	0.149
9	0.000	0.000	0.001	0.024	0.012	0.037
10	0.000	0.000	0.000	0.014	0.006	0.021
11	0.000	0.000	0.000	-0.001	0.000	-0.001
12	0.000	0.000	0.000	0.000	0.000	0.000
13	0.000	0.000	0.000	0.000	0.000	0.000

III.2 Comparison of Fault Modelling Approaches

a) Fault zone modeled using transversely isotropic (stratified) behavior of the material

b) Young modulus of fault zone (E_f) modeled by scaling the Young Modulus (E) of the surrounding material (e.g., $E_f = 0.1\ E$)

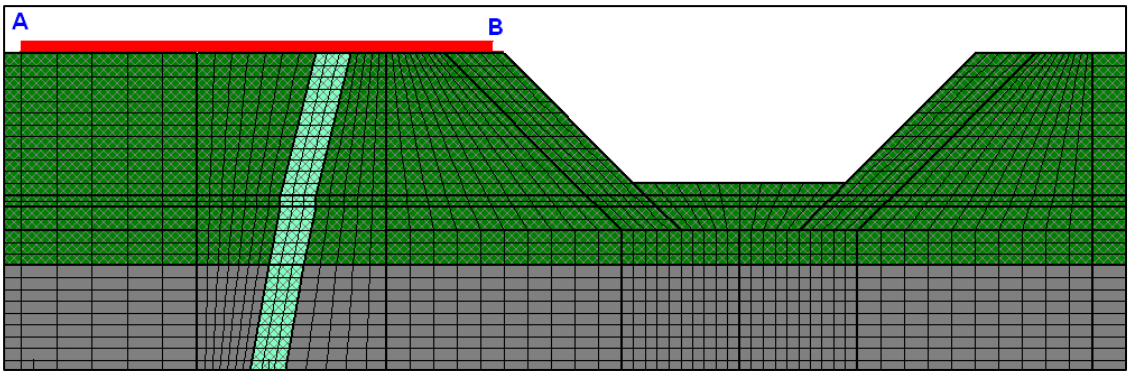

Figure III.2: ‘A’ to ‘B’ Region of Analyzed Displacements

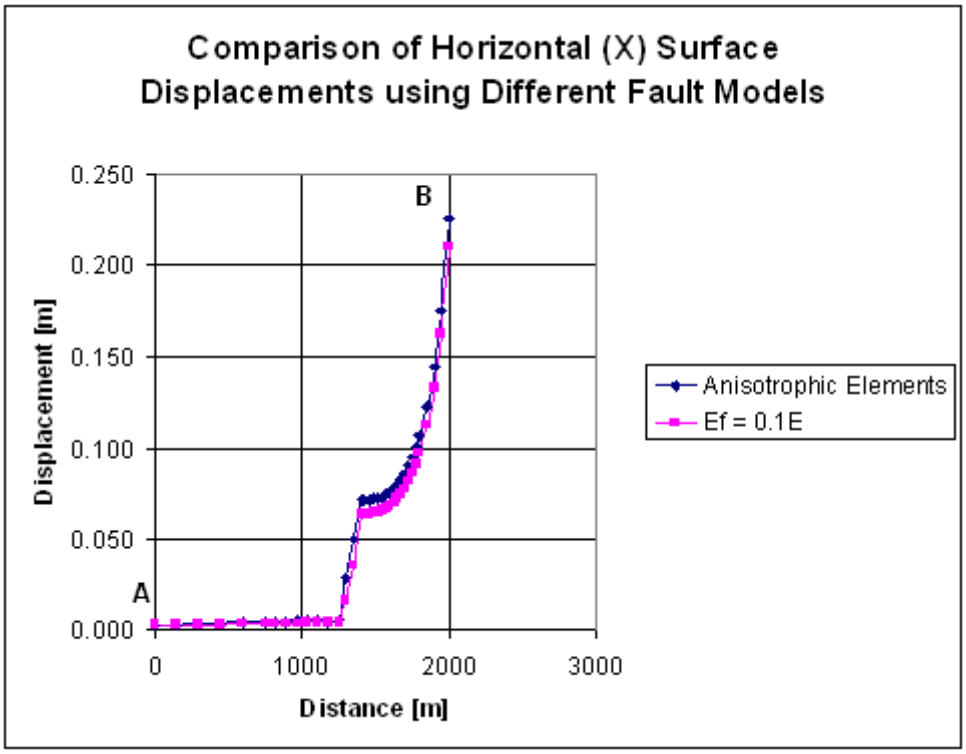

Figure III.3: Comparison of Horizontal Displacements

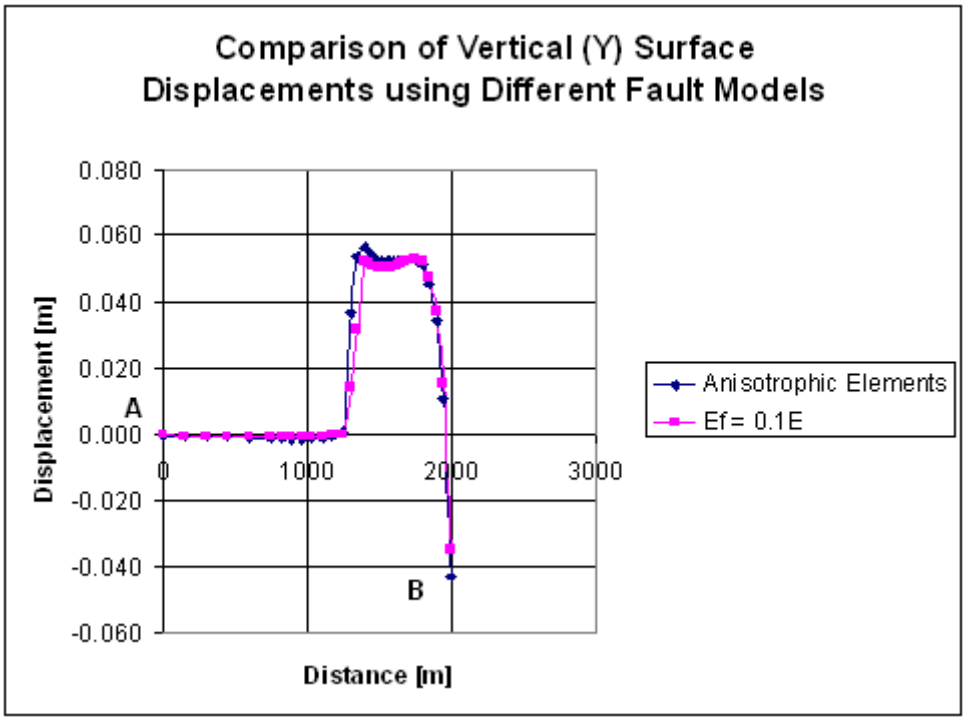

Figure III.4: Comparison of Vertical Displacements

III.3 Stress Plots

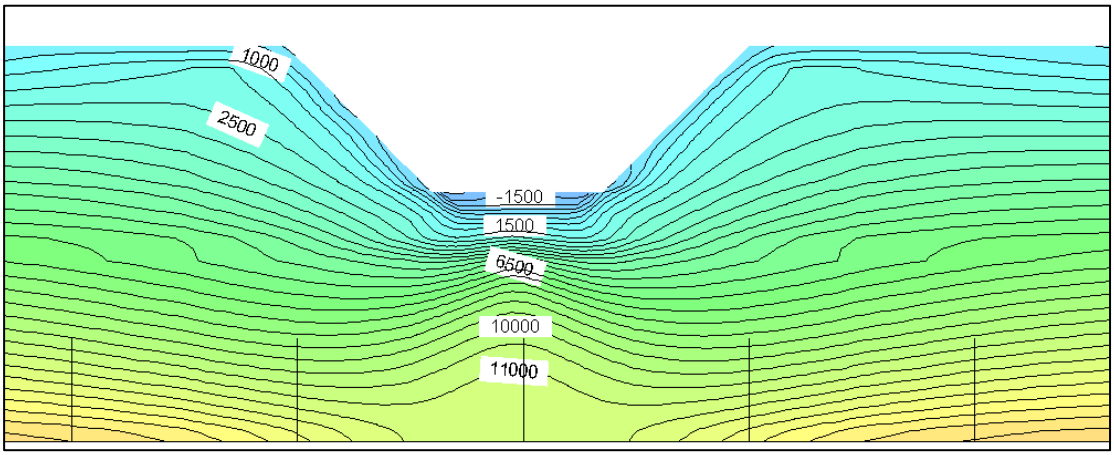

Figure III.5: Minimum Total Stress without Fault [kPa]

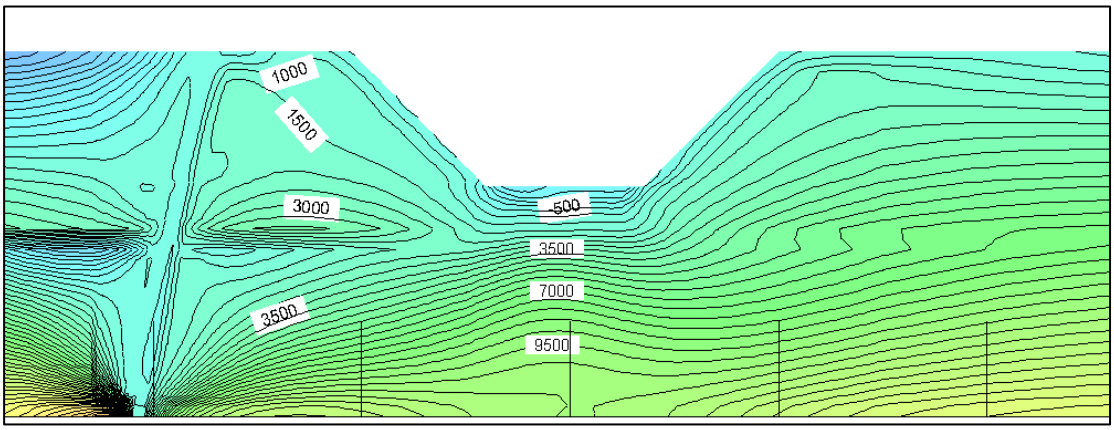

Figure III.6: Minumum Total Stress with Fault [kPa]

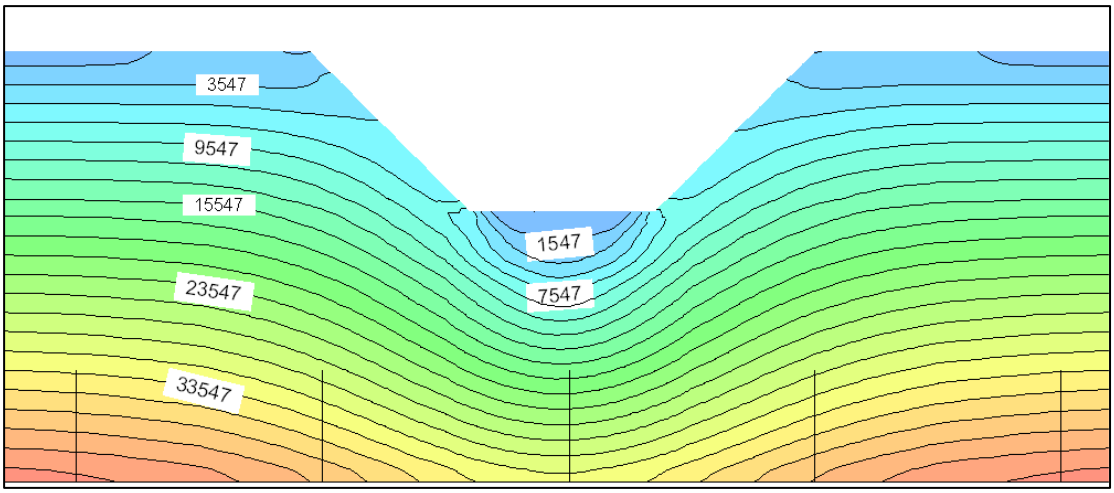

Figure III.7: Maximum Total Stress without Fault [kPa]

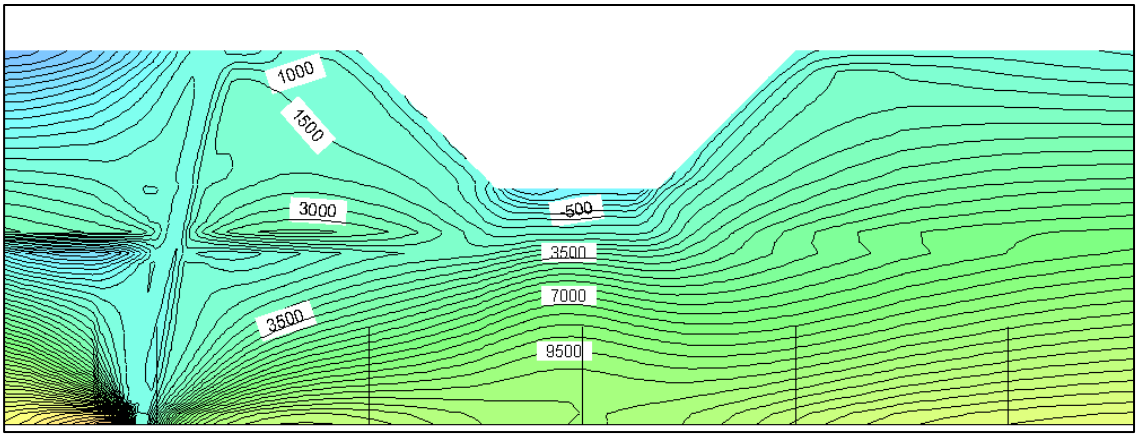

Figure III.8: Maximum Total Stress with Fault [kPa]

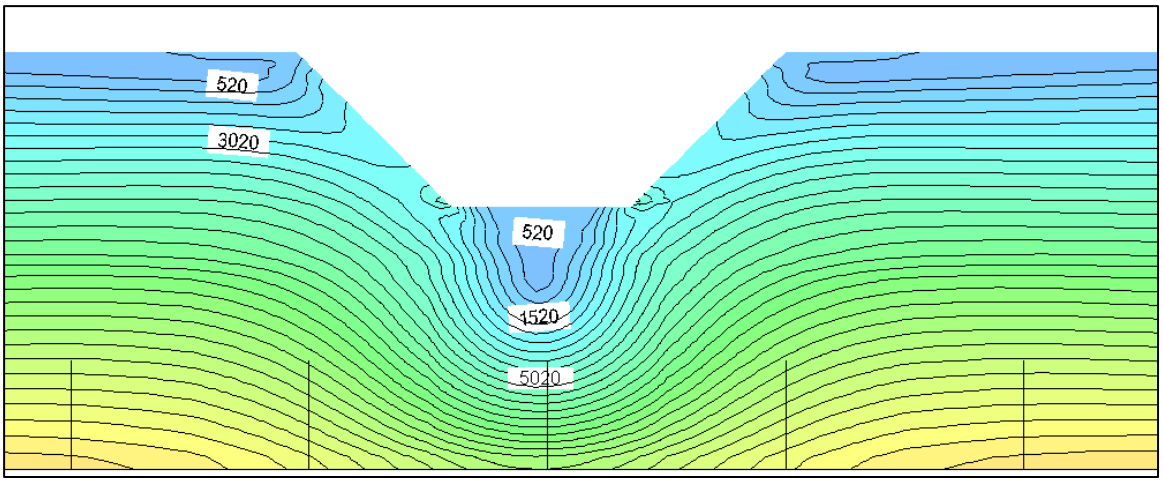

Figure III.9: Maximum Shear Stress without Fault [kPa]

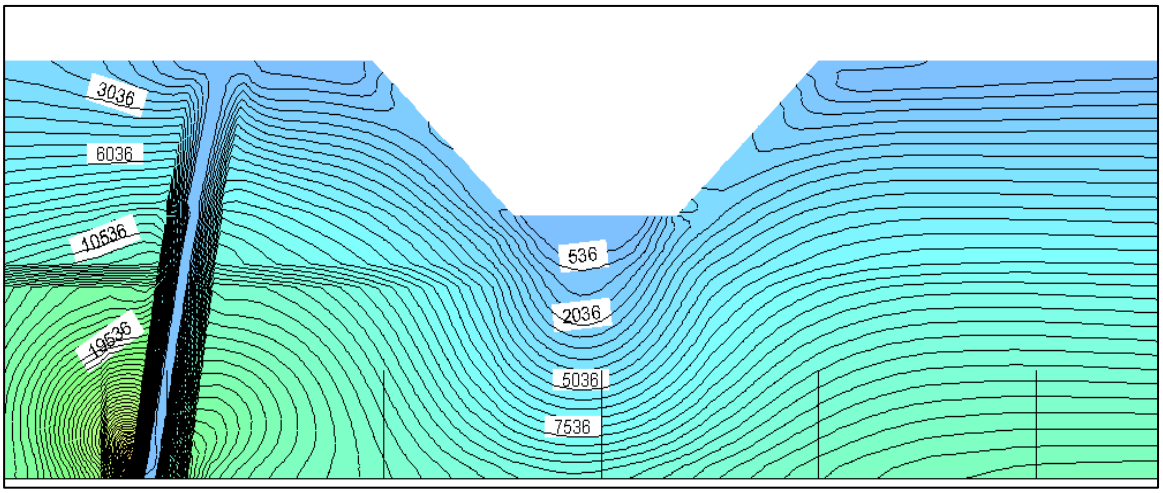

Figure III.10: Maximum Shear Stress with Fault [kPa]

III.4 Strain Plots

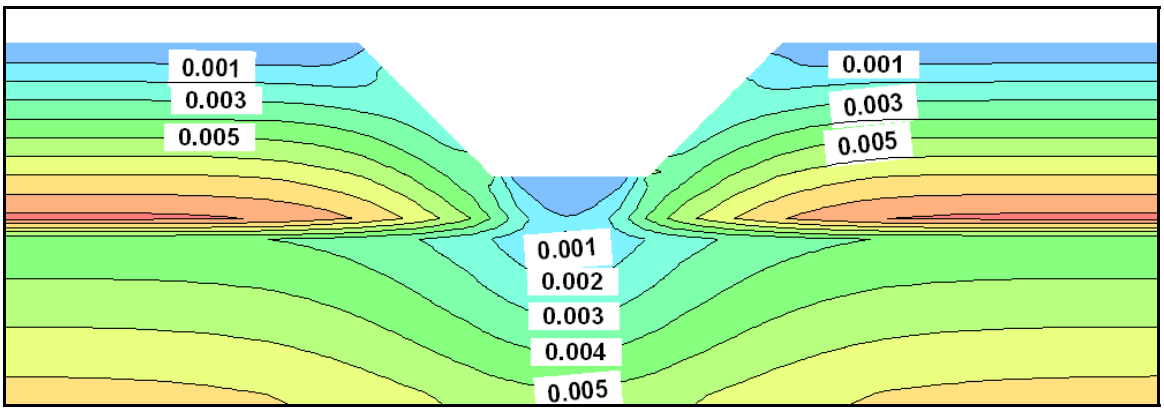

Figure III.11: Maximum Strain without Fault

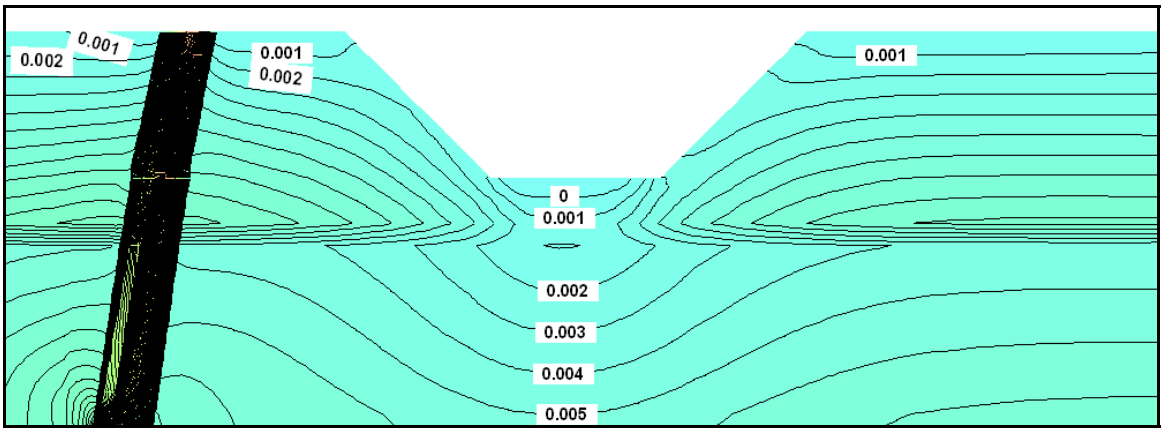

Figure III.12: Maximum Strain with Fault

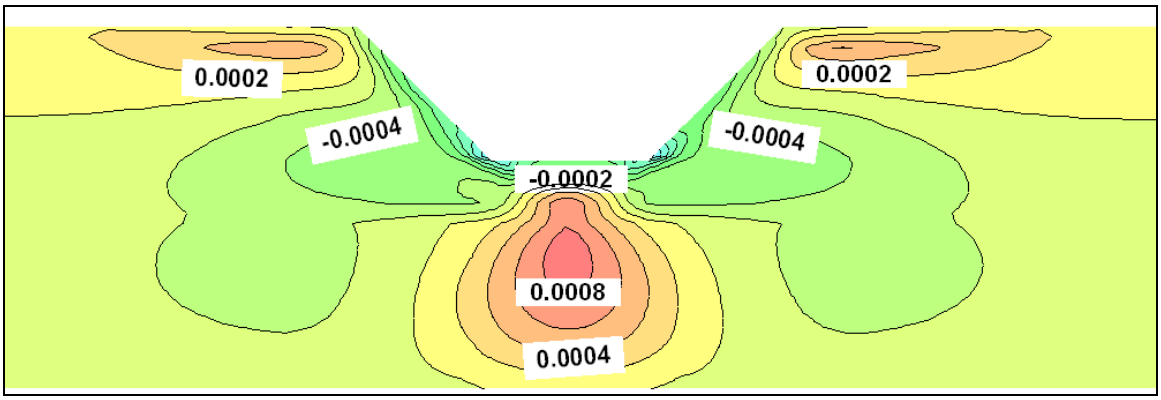

Figure III.13: Minimum Strain without Fault

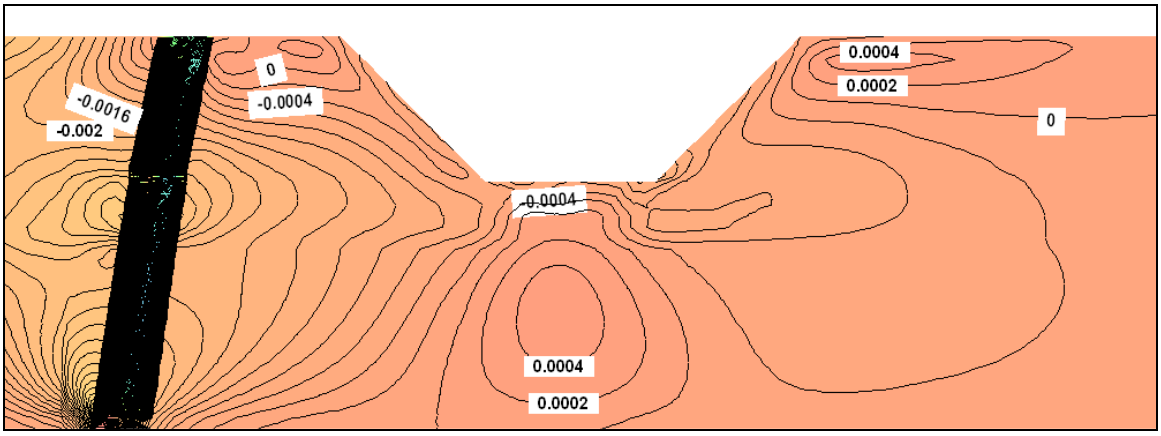

Figure III.14: Minimum Strain with Fault

APPENDIX IV
SOFTWARE DESIGN

IV.1 Scope of Application: the General Deformation Monitoring Process

Deformation monitoring is a continuous process which begins by collecting available information regarding the behaviour of the deformable object of interest. In this case of slope stability, for example, this information may include geotechnical information about fault zones and soil characteristics as well historical records of displacement rates. This information can then be used to model the behaviour of the deformable object and to predict deformation behaviour.

Based upon this expected displacement behaviour, monitoring network simulation and advice of the personnel responsible for the safety of the object, decisions can be made regarding the design of the monitoring scheme (e.g., number and type of sensors and targets, locations and accuracy requirements). Instruments should be calibrated before being installed on site and modifications may have to be made to suit environmental conditions.

Once the monitoring network has been installed, data collection can begin. Data is collected at predefined intervals as dictated by the project requirements. The data is analyzed from a geometrical perspective to determine displacements and displacement

rates which can be used to signal unsafe conditions. The data is also analyzed from a deterministic perspective to compare predicted with actual displacement behaviour. Since the ultimate goal of the deterministic modelling is to be able to predict actual displacements, modifications are made to the model to better reflect actual behaviour. The monitoring network may have to be modified so that more information can be obtained. The general deformation monitoring process is summarized in Figure IV.1.

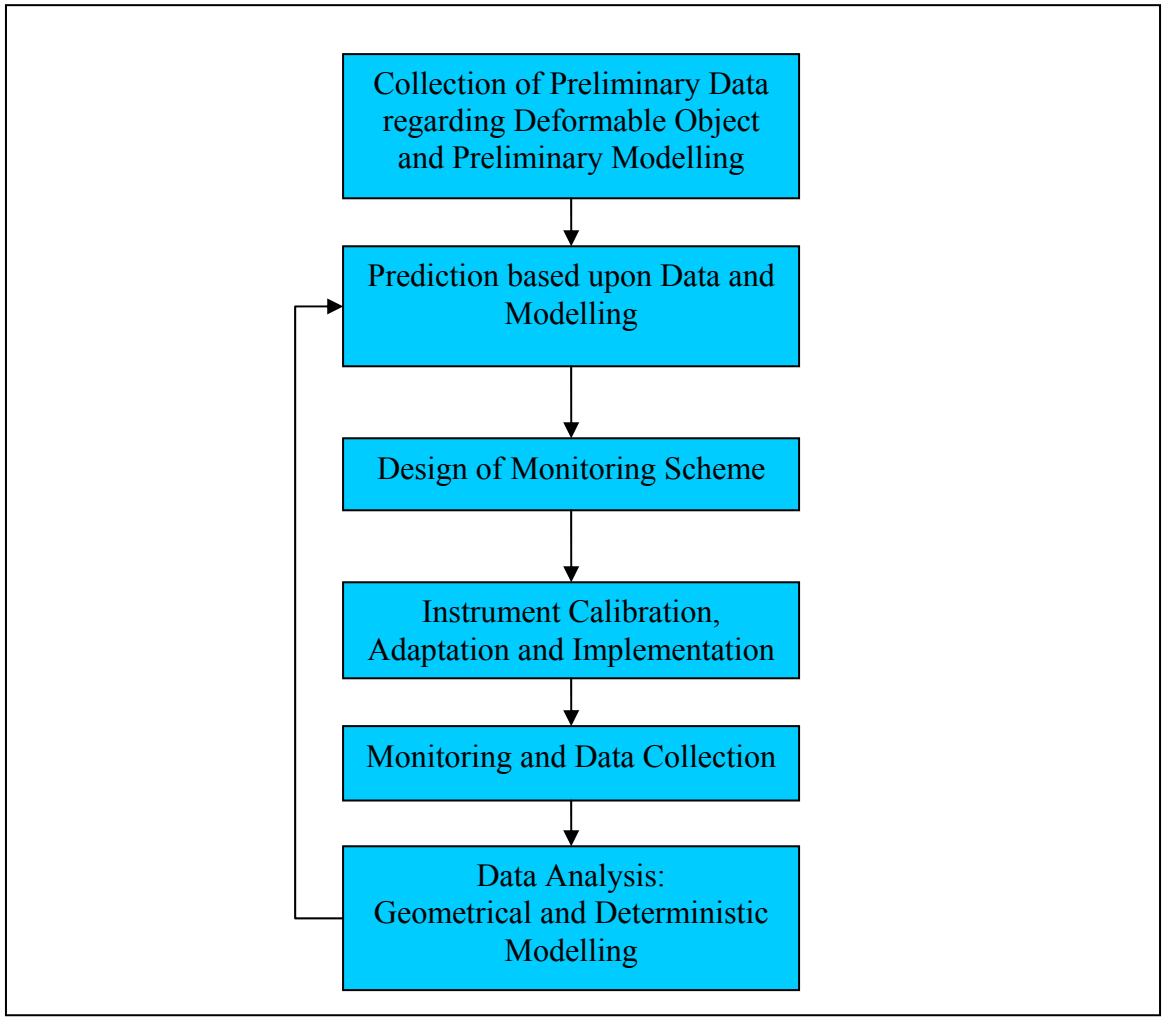

Figure IV.1: General Deformation Monitoring Process

IV.2 PPMS' Role

The Precise Position Monitoring System (PPMS) has been developed to improve monitoring capabilities as indicated by the 'Monitoring' component in Figure IV.1. The software has been designed to provide continuous, three dimensional position updates of target points using Global Positioning System and pseudolite observations. The position and variance-covariance results can be interpreted directly to signal impending danger and be used to provide position updates of other sensors (e.g., total stations, laser scanners, accelerometers) whose stability may be in question. These two scenarios are reflected in Figure IV.2 and Figure IV.3.

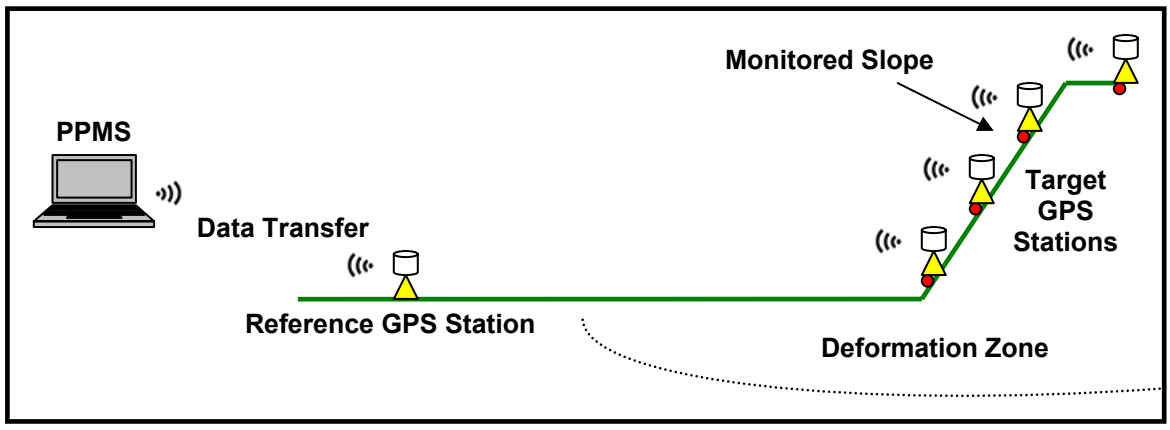

Figure IV.2: Stand-alone GPS Based Monitoring System using PPMS

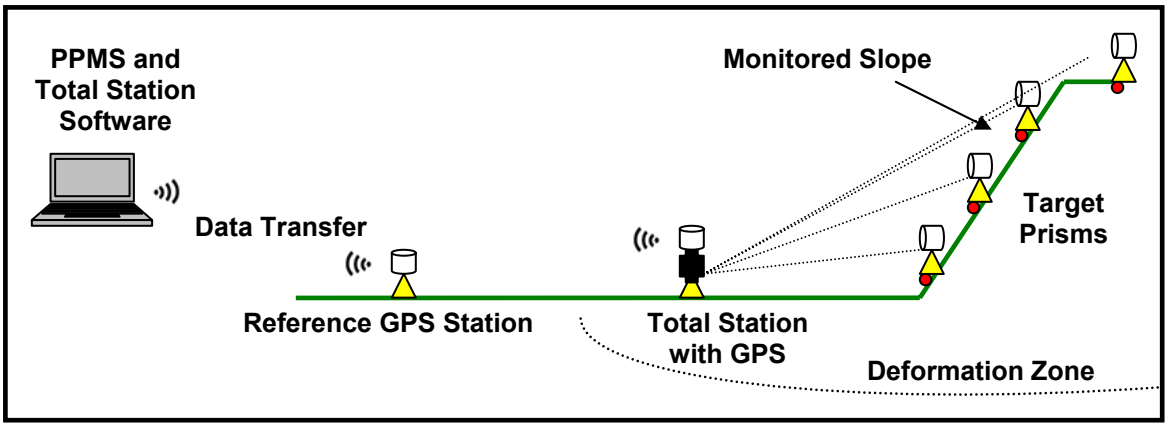

Figure IV.3: GPS and Total Station Based Monitoring System using PPMS and Total Station Software

IV.3 PPMS Software Development

PPMS has been created in Microsoft Visual Studio.NET 2003 development environment [MSDN, 2007a]. The general processing strategy implemented in PPMS is illustrated in Figure IV.4. The same processing strategy has been implemented in the real-time version of the software PPMS^{+RT} and therefore only a feedback loop needs to be added to reflect this version.

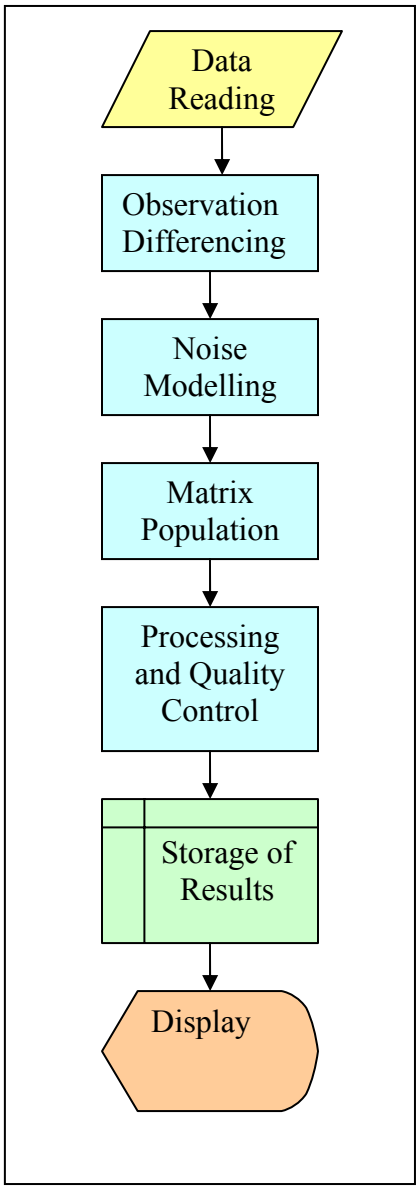

Figure IV.4: General Processing Strategy Implemented in PPMS

The software has been developed using Object Orientated Programming (OOP) and therefore consists of a number of classes that contain their own respective fields, events, properties and methods (functions and subroutines). In developing PPMS^{+RT}, more sophisticated processing methods were required to account for real-time data handling

strategies. Classes designed specifically for real-time data handling have 'RT' annotated to their name. A summary of the classes developed is provided in Table IV.1 through Table IV.8. The tables have been categorized according to class purpose.

Table IV.1: Receiver Independent Exchange (RINEX) Format Classes

Namespace	Class	Description	Language
NAV_RECORD	NAV_RECORD	Storage unit for broadcast ephemeris	VB.NET
NAV_RECORD	NAV_RECORD_MOD	Contains NAV_RECORD related methods	VB.NET
RINEX_HEADER	RINEX_HDR_MOD	Contains methods for manipulating RINEX_HEADERS	VB.NET
RINEX_HEADER	RINEX_HEADER	Storage unit for a RINEX file header	VB.NET
RINEX_NAV_FILE	RINEX_NAV_FILE	Storage unit for NAV_RECORDs	VB.NET
RINEX_NAV_FILE	RINEX_NAV_MOD	Contains methods for manipulating RINEX_NAV_FILEs	VB.NET
RINEX_OBS_FILE	RINEX_OBS_FILE	Storage unit for EPOCHS	VB.NET
RINEX_OBS_FILE	RINEX_OBS_MOD	Contains methods for manipulating RINEX_OBS_FILEs	VB.NET

Table IV.2: General Data Manipulation Classes

Namespace	Class	Description	Language
BUFFER	RES_RB	Used to store residuals from PPMS+RT in temporary memory. A "ring" is used to work around memory constraints	VB.NET
BUFFER	RING_BUFFER	Used to directly store bytes from the GPS receiver. A "ring" is used to work around memory constraints.	VB.NET
BUFFER	SOL_RB	Used to store solutions from PPMS in temporary memory. A "ring" is used to work around memory constraints	VB.NET
COORD_LIB	CONVERT	Contains coordinate conversion methods	VB.NET
LIST_LIB	CALCS	Contains methods for performing calculations on a list of values (e.g., max., min., avg.)	VB.NET
LIST_LIB	LIST	Contains methods for performing non-numerical manipulation of lists (e.g., union, join)	VB.NET
MATH_LIB	ANGLES	Contains methods for converting angle units	VB.NET
MATH_LIB	COORDS	Contains methods pertaining to coordinates (e.g., get distance, direction cosines)	VB.NET
MATRIX_LIB	MATRIX_LIB	Contains methods for matrix algebra	VB.NET

Table IV.3: GPS Observation Handling Classes

Namespace	Class	Description	Language
ATMOS_LIB	DIONO	Contains ionospheric delay methods	VB.NET
ATMOS_LIB	DTROP	Contains tropospheric delay methods	VB.NET
ATMOS_LIB	MAP_FUNC	Contains mapping functions methods	VB.NET
CYCLE_SLIPS	CS_FILE	Storage unit for CS_RECORDS	VB.NET
CYCLE_SLIPS	CS_RECORD	Storage unit for an EPOCH's cycle slips	
DD_FILE	DD_FILE	Storage unit for DD_RECORDS	VB.NET
DD_RECORD	DD_RECORD	Storage unit for double-differenced observations	VB.NET
GPS_SOL_LIB	POINT_POS	Contains point position method	VB.NET
KF_LIB	DELAYED_STATE	Contains Delayed-State Kalman Filter method	VB.NET
NOISE	NOISE_ARRAY	Window of noise observations for a SV	VB.NET
NOISE	NOISE_FILE	Storage unit for NOISE RECORDS	VB.NET
NOISE	NOISE_MODULE	Contains methods related to handling NOISE_ARRAY, NOISE_FILE and NOISE_RECORD	VB.NET
NOISE	NOISE_RECORD	Storage unit for an epoch of noise observations	VB.NET
OUTLIERS	OUTLIER_FILE	Storage unit for OUTLIER_RECORDs	VB.NET
OUTLIERS	OUTLIER_MOD	Contains methods for handling OUTLIER_FILEs and OUTLIER_RECORDs	VB.NET
OUTLIERS	OUTLIER_RECORD	Storage unit for an epoch's outlier information	VB.NET
RESIDUALS	FILE	Storage unit for residual RECORDs	VB.NET
RESIDUALS	RECORD	Storage unit for an epoch's residual information	VB.NET
SD_FILE	SD_FILE	Storage unit for an epoch's SD_RECORDs	VB.NET
SD_FILE	SD_FILE_MOD	Contains methods for manipulating SD_FILEs	VB.NET
SD_RECORD	SD_RECORD	Storage unit for an epoch's SD observations	VB.NET
SV_LIB	SV	Contains methods used to manipulate satellite information	VB.NET
SV_LIB	SV_COORD_RECORD	Storage unit for SV coordinates for an epoch	VB.NET
SV_LIB	SV_NAV	Contains methods pertaining to satellite navigation message data extraction	VB.NET
SV_LIB	SV_OBS	Contains methods used to manipulate satellite observations to achieve linear combinations	VB.NET
TD_FILE	TD_FILE	Storage unit for an epoch's TD_RECORDs	VB.NET
TD_RECORD	TD_RECORD	Storage unit for an epoch's TD observations	VB.NET
TIME_LIB	CONVERT	Contains methods for converting time from one format to another	VB.NET
TIME_LIB	GPSTime	Storage unit for time in GPS Time format	VB.NET
TIME_LIB	YMDHMS	Storage unit for time in year, month, day, hour, minute, second format	VB.NET

Table IV.4: Data Storage Classes

Namespace	Class	Description	Language
BASELINE	BASELINE	Houses two occupations forming a baseline and related baseline info.	VB.NET
BASELINE	RT_BASELINE	Houses two stations forming a baseline. Used for real-time applications.	VB.NET
EPOCH	EPOCH	Storage unit for a GPS epoch of observations	VB.NET
GPS_SOLUTIONS	SOL_RECORD	Storage unit for an epoch's solution	VB.NET
OCCUPATION	OCCUPATION	Storage unit for an observation session	VB.NET
STATION	RT_STATION	Storage unit for station related information (used for real-time applications)	VB.NET
STATION	STATION	Storage unit for station related information	VB.NET

Table IV.5: Communications Classes

Namespace	Class	Description	Language
C_RS232	C_RS232	Contains methods for serial port communication	VB.NET
MyUDPAsyncServer	MyUDPAsyncServer	Inherits from C# Class	VB.NET
UDPAsyncServer	UDPAsyncServer	Object for establishing User Datagram Protocol communication through asynchronous methods	VC#.NET

Table IV.6: Pseudolite Classes

Namespace	Class	Description	Language
PL	PL	Storage unit for PL information	VB.NET
PL	PL_GF_FILE	Storage unit for PL_GF_RECORDS	VB.NET
PL	PL_GF_RECORD	Storage unit for an epoch's geometry-free observations	VB.NET
PL	PL_MODULE	Contains methods for manipulating PLs, PL_GF_FILEs, PL_GF_RECORDs	VB.NET

Table IV.7: NovAtel OEM4 Classes

Namespace	Class	Description	Language
CRC32	CRC32	Calculates 32 bit checksum for binary data decoding	VC#.NET
NOVATEL_OEM4	ALMANAC_LOG	Storage unit for NovAtel's OEM4 almanac log	VB.NET
NOVATEL_OEM4	DATA_FILE	Storage unit for all NovAtel OEM4 data logs	VB.NET
NOVATEL_OEM4	FILDHDR_LOG	Storage unit for NovAtel's OEM4 file header log	VB.NET
NOVATEL_OEM4	GROUPDEF_LOG	Storage unit for NovAtel's OEM4 group definition log	VB.NET
NOVATEL_OEM4	LOG_HEADER	Storage unit for NovAtel's OEM4 log header	VB.NET
NOVATEL_OEM4	NOVOEM4_MODULE	Contains methods for extracting NovAtel OEM4 binary data logs	VB.NET
NOVATEL_OEM4	RANGECMP_LOG	Storage unit for NovAtel's OEM4 range compressed log	VB.NET
NOVATEL_OEM4	RT_DATA_FILE	Storage unit for NovAtel's OEM4 data logs (for real-time applications)	VB.NET
NOVATEL_OEM4	TIME_LOG	Storage unit for NovAtel's OEM4 time log	VB.NET
NOVATEL_OEM4	VERSION_LOG	Storage unit for NovAtel's OEM4 version log	VB.NET

Table IV.8: Graphical User Interface (GUI) Classes

Namespace	Class	Description	Language
PPMS_RT_GUIs	baseline_properties	GUI for displaying BASELINE properties	VB.NET
PPMS_RT_GUIs	ChartPropertiesForm	GUI for displaying MsChart properties	VB.NET
PPMS_RT_GUIs	OPTIONS	GUI for PPMS^{+RT} display options	VB.NET
PPMS_RT_GUIs	PPMS_RT	Main GUI for PPMS^{+RT}	VB.NET
PPMS_RT_GUIs	SETTINGS	GUI for displaying processing settings	VB.NET
PPMS_RT_GUIs	STATION	GUI for displaying STATION properties	VB.NET
software_driver	software_driver	Main GUI for PPMS	VB.NET
software_driver	nav_file_info	GUI for displaying RINEX_NAV_FILE information	VB.NET
software_driver	navigation_record_table	GUI for displaying NAV_RECORDs	VB.NET
software_driver	observation_table	GUI for displaying EPOCHs of observations	VB.NET
software_driver	occupation_info	GUI for displaying OCCUPATION information	VB.NET
software_driver	solution_comp_plot	GUI for displaying time series of solutions	VB.NET
software_driver	sv_plot_info	GUI for displaying observations from a particular satellite	VB.NET
software_driver	XYScatterPlot	GUI for displaying XY scatter plots	VB.NET

Each class has been commented so that Microsoft Developer's Network (MSDN) style documentation can be automatically generated. To illustrate, sample documentation for the NOISE project is provided:

NOISE Namespace

Namespace hierarchy

Class	Description
NOISE_ARRAY	NOISE_ARRAY Virtual window of NOISE observations for a SV
NOISE_FILE	NOISE_FILE Storage unit for NOISE RECORDS
NOISE_MODULE	NOISE_FILE Contains methods for manipulating objects of NOISE namespace
NOISE_RECORD	NOISE_RECORD storage unit for noise observations

NOISE_ARRAY Methods

The methods of the **NOISE_ARRAY** class are listed below. For a complete list of **NOISE_ARRAY** class members, see the NOISE_ARRAY Members topic.

Public Instance Methods

Equals (inherited from **Object**)	Determines whether the specified Object is equal to the current **Object**.
GetGPSTime	
GetHashCode (inherited from **Object**)	Serves as a hash function for a particular type, suitable for use in hashing algorithms and data structures like a hash table.
GetNoiseState	
GetNumNoiseObs	
GetPreviousObsTime	
GetType (inherited from **Object**)	Gets the Type of the current instance.
ToString (inherited from **Object**)	Returns a String that represents the current Object.
UpdateNoiseArray	

Protected Instance Methods

Finalize (inherited from **Object**)	Allows an Object to attempt to free resources and perform other cleanup operations before the **Object** is reclaimed by garbage collection.
MemberwiseClone (inherited from **Object**)	Creates a shallow copy of the current Object.

See Also

NOISE_ARRAY Class | NOISE Namespace

NOISE_ARRAY.GetNoiseState Method

```
[Visual Basic]
Public Function GetNoiseState() As Double
[C#]
public double GetNoiseState();
```

Return Value

Gets current noise state in [mm^2]

NOISE_ARRAY.GetNumNoiseObs Method

```
[Visual Basic]
Public Function GetNumNoiseObs() As Integer
[C#]
public int GetNumNoiseObs();
```

Return Value

Gets noise array length

NOISE_ARRAY.GetPreviousObsTime Method

```
[Visual Basic]
Public Function GetPreviousObsTime() As GPSTime
[C#]
public GPSTime GetPreviousObsTime();
```

Return Value

Gets GPS time that last noise observation was added

NOISE_ARRAY.GetGPSTime Method

```
[Visual Basic]
Public Function GetGPSTime( _
   ByVal int_AN_INDEX As Integer _
) As GPSTime
[C#]
public GPSTime GetGPSTime(
   int int_AN_INDEX
);
```

Parameters

int_AN_INDEX
noise array index

Return Value

Gets GPS Time at specified array index

NOISE_ARRAY.UpdateNoiseArray Method

```
[Visual Basic]
Public Sub UpdateNoiseArray( _
   ByVal PASS_GPSTIME As GPSTime, _
   ByVal dbl_PASS_NOISE_OBS As Double, _
   ByVal int_PASS_OBS_INT As Integer, _
   ByVal int_A_PERCENT_MAX_GAPS As Integer _
)
[C#]
public void UpdateNoiseArray(
   GPSTime PASS_GPSTIME,
   double dbl_PASS_NOISE_OBS,
   int int_PASS_OBS_INT,
   int int_A_PERCENT_MAX_GAPS
);
```

Parameters

PASS_GPSTIME
: Current GPS Time

dbl_PASS_NOISE_OBS
: Current noise observation to add to the list

int_PASS_OBS_INT
: Observation interval

int_A_PERCENT_MAX_GAPS
: Maximum number of empty values in the noise observation list that will be tolerated before setting the not available flag of '-1'

Remarks

Updates the current noise array and noise state based upon the current values in the list.

NOISE_FILE Methods

The methods of the **NOISE_FILE** class are listed below. For a complete list of **NOISE_FILE** class members, see the NOISE_FILE Members topic.

Public Instance Methods

Equals (inherited from **Object**)	Determines whether the specified Object is equal to the current **Object**.
GetHashCode (inherited from **Object**)	Serves as a hash function for a particular type, suitable for use in hashing algorithms and data structures like a hash table.
GetNoiseRecord	
GetNumNoiseRecords	
GetType (inherited from **Object**)	Gets the Type of the current instance.
ToString (inherited from **Object**)	Returns a String that represents the current Object.

Protected Instance Methods

Finalize (inherited from **Object**)	Allows an Object to attempt to free resources and perform other cleanup operations before the **Object** is reclaimed by garbage collection.
MemberwiseClone (inherited from **Object**)	Creates a shallow copy of the current Object.

See Also

NOISE_FILE Class | NOISE Namespace

NOISE_FILE.GetNoiseRecord Method

```
[Visual Basic]
Public Function GetNoiseRecord( _
   ByVal int_INDEX As Integer _
) As NOISE_RECORD
[C#]
public NOISE_RECORD GetNoiseRecord(
   int int_INDEX
);
```

Parameters

int_INDEX
noise record index

Return Value

Gets NOISE RECORDS at specified index

NOISE_FILE.GetNumNoiseRecords Method

```
[Visual Basic]
Public Function GetNumNoiseRecords() As Integer
[C#]
public int GetNumNoiseRecords();
```

Return Value

Gets number of NOISE RECORDS in file

NOISE_MODULE Methods

The methods of the **NOISE_MODULE** class are listed below. For a complete list of **NOISE_MODULE** class members, see the NOISE_MODULE Members topic.

Public Static (Shared) Methods

GetNoiseFile	Creates a file of NOISE RECORDS from a single differenced, geometry-free file
GetNoiseRecord	Creates a NOISE RECORD from consecutive single differenced, geometry-free records
GetSVNum	Removes the letter (G,R) from the 3 space designation for the SV number
GetTimeDiffSVList	Creates a list of common svs between epochs
UpdateNoiseArrayList	Overloaded. Updates the Noise Array List (for all SVs and PLs) for the process with the given NOISE RECORD. Overloaded.

Public Instance Methods

Equals (inherited from **Object**)	Determines whether the specified Object is equal to the current **Object**.
GetHashCode (inherited from **Object**)	Serves as a hash function for a particular type, suitable for use in hashing algorithms and data structures like a hash table.
GetType (inherited from **Object**)	Gets the Type of the current instance.
ToString (inherited from **Object**)	Returns a String that represents the current Object.

Protected Instance Methods

Finalize (inherited from **Object**)	Allows an Object to attempt to free resources and perform other cleanup operations before the **Object** is reclaimed by garbage collection.
MemberwiseClone (inherited from **Object**)	Creates a shallow copy of the current Object.

See Also

NOISE_MODULE Class | NOISE Namespace

NOISE_MODULE.GetNoiseFile Method

Creates a file of NOISE RECORDS from a single differenced, geometry-free file

```
[Visual Basic]
Public Shared Function GetNoiseFile( _
   ByVal A_GF_SD_FILE As SD_FILE, _
   ByVal A_NOISE_THRESHOLD As Double _
) As NOISE_FILE
[C#]
public static NOISE_FILE GetNoiseFile(
   SD_FILE A_GF_SD_FILE,
   double A_NOISE_THRESHOLD
);
```

Parameters

A_GF_SD_FILE
: Geometry free, single-differenced file

A_NOISE_THRESHOLD
: Threshold value within which noise observations should lie

Return Value

A NOISE FILE

NOISE_MODULE.GetNoiseRecord Method

Creates a NOISE RECORD from consecutive single differenced, geometry-free records

```
[Visual Basic]
Public Shared Function GetNoiseRecord( _
   ByVal A_PREV_SD_RECORD As SD_RECORD, _
   ByVal A_CUR_SD_RECORD As SD_RECORD, _
   ByVal A_NOISE_THRESHOLD As Double _
) As NOISE_RECORD
[C#]
public static NOISE_RECORD GetNoiseRecord(
   SD_RECORD A_PREV_SD_RECORD,
   SD_RECORD A_CUR_SD_RECORD,
   double A_NOISE_THRESHOLD
);
```

Parameters

A_PREV_SD_RECORD
Previous Geometry free, single-differenced record

A_CUR_SD_RECORD
Current Geometry free, single-differenced record

A_NOISE_THRESHOLD
Threshold value within which noise observations should lie

Return Value

A NOISE RECORD

NOISE_MODULE.GetSVNum Method

Removes the letter (G,R) from the 3 space designation for the SV number

```
[Visual Basic]
Public Shared Function GetSVNum( _
   ByVal str_SV_NUM As String _
) As Integer
[C#]
public static int GetSVNum(
   string str_SV_NUM
);
```

Parameters

str_SV_NUM
string value of SV number

Return Value

integer value of SV number after removing satellite system designator

NOISE_MODULE.GetTimeDiffSVList Method

Creates a list of common svs between epochs

```
[Visual Basic]
Public Shared Function GetTimeDiffSVList( _
   ByVal str_A_PREV_REF_SV As String, _
   ByVal str_A_PREV_SV_LIST As String(), _
   ByVal str_A_CURRENT_REF_SV As String, _
   ByVal str_A_CURRENT_SV_LIST As String() _
) As String()
[C#]
public static string[] GetTimeDiffSVList(
   string str_A_PREV_REF_SV,
   string[] str_A_PREV_SV_LIST,
   string str_A_CURRENT_REF_SV,
   string[] str_A_CURRENT_SV_LIST
);
```

Parameters

str_A_PREV_REF_SV
: Previous reference satellite

str_A_PREV_SV_LIST
: list of SVS from previous GF SD record

str_A_CURRENT_REF_SV
: Current reference satellite

str_A_CURRENT_SV_LIST
: list of SVS from current GF SD record

Return Value

list of common SVs between epochs

NOISE_MODULE.UpdateNoiseArrayList Method (NOISE_ARRAY[], NOISE_RECORD, Int32, Int32)

Updates the Noise Array List (for all SVs and PLs) for the process with the given NOISE RECORD. Overloaded.

```
[Visual Basic]
Overloads Public Shared Sub UpdateNoiseArrayList( _
   ByRef PASS_NOISE_ARRAY_LIST As NOISE_ARRAY(), _
   ByVal A_NOISE_RECORD As NOISE_RECORD, _
   ByVal int_AN_OBS_INTERVAL As Integer, _
   ByVal int_A_PERCENT_MAX_GAPS As Integer _
)
[C#]
public static void UpdateNoiseArrayList(
   ref NOISE_ARRAY[] PASS_NOISE_ARRAY_LIST,
   NOISE_RECORD A_NOISE_RECORD,
   int int_AN_OBS_INTERVAL,
   int int_A_PERCENT_MAX_GAPS
);
```

Parameters

PASS_NOISE_ARRAY_LIST
List of all SV noise arrays

A_NOISE_RECORD
a new noise record

int_AN_OBS_INTERVAL
Observation interval [s]

int_A_PERCENT_MAX_GAPS
maximum number of missing noise observations tolerated before the not available flag is returned (-1)

NOISE_MODULE.UpdateNoiseArrayList Method (NOISE_ARRAY[], PL_GF_RECORD, Int32, Int32)

Updates the Noise Array List (for all SVs and PLs) for the process with the given NOISE RECORD. Overloaded.

```
[Visual Basic]
Overloads Public Shared Sub UpdateNoiseArrayList( _
   ByRef PASS_NOISE_ARRAY_LIST As NOISE_ARRAY(), _
   ByVal A_GF_PL_RECORD As PL_GF_RECORD, _
   ByVal int_AN_OBS_INTERVAL As Integer, _
   ByVal int_A_PERCENT_MAX_GAPS As Integer _
)
[C#]
public static void UpdateNoiseArrayList(
   ref NOISE_ARRAY[] PASS_NOISE_ARRAY_LIST,
   PL_GF_RECORD A_GF_PL_RECORD,
   int int_AN_OBS_INTERVAL,
   int int_A_PERCENT_MAX_GAPS
);
```

Parameters

PASS_NOISE_ARRAY_LIST
List of all SV noise arrays

A_GF_PL_RECORD
geometry free record for pseudolites

int_AN_OBS_INTERVAL
Observation interval [s]

int_A_PERCENT_MAX_GAPS
maximum number of missing noise observations tolerated before the not available flag is returned (-1)

NOISE_RECORD Methods

The methods of the **NOISE_RECORD** class are listed below. For a complete list of **NOISE_RECORD** class members, see the NOISE_RECORD Members topic.

Public Instance Methods

Equals (inherited from **Object**)	Determines whether the specified Object is equal to the current **Object**.
GetGpsTime	
GetHashCode (inherited from **Object**)	Serves as a hash function for a particular type, suitable for use in hashing algorithms and data structures like a hash table.
GetNoiseObs	Overloaded.
GetNumObs	
GetSV	
GetSVList	
GetType (inherited from **Object**)	Gets the Type of the current instance.
GetYMDHMS	
ToString (inherited from **Object**)	Returns a String that represents the current Object.

Protected Instance Methods

Finalize (inherited from **Object**)	Allows an Object to attempt to free resources and perform other cleanup operations before the **Object** is reclaimed by garbage collection.
MemberwiseClone (inherited from **Object**)	Creates a shallow copy of the current Object.

See Also

NOISE_RECORD Class | NOISE Namespace

NOISE_RECORD.GetGpsTime Method

```
[Visual Basic]
Public Function GetGpsTime() As GPSTime
[C#]
public GPSTime GetGpsTime();
```

Return Value

Gets current GPS time

NOISE_RECORD.GetNoiseObs Method ()

```
[Visual Basic]
Overloads Public Function GetNoiseObs() As Double()
[C#]
public double[] GetNoiseObs();
```

Return Value

Gets list of noise observations

NOISE_RECORD.GetNoiseObs Method (Int32)

```
[Visual Basic]
Overloads Public Function GetNoiseObs( _
   ByVal int_INDEX As Integer _
) As Double
[C#]
public double GetNoiseObs(
   int int_INDEX
);
```

Parameters

int_INDEX
noise observation index

Return Value

Gets noise observation at specifed index

NOISE_RECORD.GetNumObs Method

```
[Visual Basic]
Public Function GetNumObs() As Integer
[C#]
public int GetNumObs();
```

Return Value

Gets Number of noise observations

NOISE_RECORD.GetSV Method

```
[Visual Basic]
Public Function GetSV( _
   ByVal int_INDEX As Integer _
) As String
[C#]
public string GetSV(
   int int_INDEX
);
```

Parameters

int_INDEX
SV index

Return Value

Gets satellite at specified index

NOISE_RECORD.GetSVList Method

```
[Visual Basic]
Public Function GetSVList() As String()
[C#]
public string[] GetSVList();
```

Return Value

Gets list of SVs

NOISE_RECORD.GetYMDHMS Method

```
[Visual Basic]
Public Function GetYMDHMS() As YMDHMS
[C#]
public YMDHMS GetYMDHMS();
```

Return Value

Gets current time in YMDHMS format

REFERENCES

Barnes, J., C. Rizos, M. Kanli, D. Small, G. Voigt, N. Gambale and J. Lamance (2004). "Structural Deformation Monitoring Using Locata." Proceedings of the *1st FIG International Symposium on Engineering Surveys for Construction Works and Structural Engineering*, Nottingham, United Kingdom, 28 June - 1 July.

Beutler, G., I. Bauersima, W. Gurtner, M. Rothacher, T. Schildknecht and A. Gieger (1988). "Atmospheric refraction and other important biases in GPS carrier phase observations." *Atmospheric Effects on Geodetic Space Measurements*, Monograph 12, School of Surveying, University of New South Wales, pp.15-43.

Bieniawski, Z.T. (1984). *Rock Mechanics Design in Mining and Tunnelling*, Rotterdam, Netherlands, A.A. Balkema, 272 pp.

Bock, Y. (2004). "Instantaneous Network RTK Positioning in Regions of Active Deformation." Proceedings of *Instititute of Navigation (ION) GNSS 2004 17th International Technical Meeting of the Satellite Division*, Long Beach, CA, USA, 21-24 September, CDROM. Available at: http://www.ion.org, accessed on: 3 October 2007.

Bond, J. (2004). *An Investigation on the Use of GPS for Deformation Monitoring in Open Pit Mines*. M.Sc.E. thesis, Technical Report No. 222, Department of Geodesy and Geomatics Engineering, University of New Brunswick, Fredericton, New Brunswick, Canada, 143 pp.

Bond, J., A. Chrzanowski, and D. Kim (2007a). "Bringing GPS into Harsh Environments for Deformation Monitoring." *GPS Solutions* (online first status), 11 pp. Available at: http://www.springerlink.com/content/21v2625p46108266/fulltext.pdf, accessed on: 4 October 2007. DOI 10.1007/s10291-007-0059-7

Bond, J., A. Chrzanowski, D. Kim D (2007b). "Augmenting GPS with Pseudolites for Deformation Monitoring in Harsh Environments." Proceedings of the *Institute of Navigation National Technical Meeting* (ION NTM), 22-24 January, San Diego, CA, USA, CDROM, pp. 486-492. Available at http://www.ion.org/, accessed on 4 October, 2007.

Bond, J., A. Szostak-Chrzanowski A and A. Chrzanowski (2007c). "Design of Geodetic Monitoring Schemes Using Deterministic Modelling: An Open Pit Mine Example." Proceedings of the *3rd International Symposium on Geo-information for Disaster Management*, Toronto, Ontario, Canada, 22-24 May, Canadian Inst. of Geomatics, 11 pp., CDROM.

Bond, J., A. Chrzanowski and F. Wilkins (2005). "Using GPS for Augmenting Deformation Monitoring Systems in Open Pit Mines - Problems and Solutions." *Geomatica* 59(1):73-82

Brown, R.G. and P.Y.C. Hwang (1997). *Introduction to Random Signals and Applied Kalman Filtering*, 3rd ed. John Wiley & Sons, Inc., New York, USA, 484 pp.

Chen, Y.Q., A. Chrzanowksi, and J.M. Secord (1990). "A Strategy for the Analysis of the Stability of Reference Points in Deformation Surveys." *CISM Journal*, Vol. 44, No.2, Summer, pp. 39-46.
Available at: http://ccge.unb.ca/publications/all_publications.php, accessed on: 3 October 2007.

Chen, Y.Q and X. He (2006). "Pseudolite-Augmented GPS Survey Technique for Deformation Monitoring: Analysis and Experimental Study." Proceedings of the *3rd IAG Symposium on Geodesy for Geotechnical and Structural Engineering and 12th FIG Symposium on Deformation Measurements*, Eds. H. Kahmen and A. Chrzanowski, Baden, Austria, 22-24 May, CD-ROM. Available at: http://www.fig.net/commission6/baden_2006/proceedings.htm, accessed on: 3 October 2007.

Chen, Y.Q., G. Zhang, X. Ding and Z. Li (2000). "Monitoring Earth Surface Deformations with InSAR Technology: Principle and Some Critical Issues." *Journal of Geospatial Engineering* 2(1):3-21.

Chrzanowski A. (1993). "Modern Surveying Techniques for Mining and Civil Engineering." Chapter 33 in Vol. III of *Comprehensive Rock Engineering,* Ed. J. Hudson, Pergamon Press, New York, pp. 773-809.

Chrzanowski, A. and A. Szostak-Chrzanowski (1993). "Enhancement of Deformation Modelling in Engineering and Geosciences by Combining Deterministic and Generalized Geometrical Analyses." Proceedings of the *Canadian Society for Civil Engineering (CSCE) Annual Conference*, Fredericton, Canada, June, pp. 479-488.

Chrzanowski, A., and A. Szostak-Chrzanowski (2004). "Physical Interpretation of Ground Subsidence Surveys – A Case Study." *Journal of Geospatial Engineering*, Hong Kong Institute of Engineering Surveyors, pp. 21-29.

Chrzanowski, A., A. Szostak-Chrzanowski, D. Forrester (1998). "100 Years of Ground Subsidence Studies." Proceedings of the *100th General Meeting of Canadian Institute of Mining (CIM)*, Montreal, 3-7 May, CD-ROM.

Chrzanowski, A., A. Szostak-Chrzanowski, J. Bond and R. Wilkins (2007). "Increasing Public and Environmental Safety through Integrated Monitoring and Analysis of Structural and Ground Deformations." Proceedings of the *3rd International Symposium on Geo-information for Disaster Management,* Toronto, Ontario, Canada, 22-24 May, 12 pp., CDROM.

Chrzanowski A., F. Wilkins (2006). "Accuracy Evaluation of Geodetic Monitoring of Deformations in Large Open Pit Mines." Proceedings of the *12-th FIG Symposium on Deformation Measurements*, Baden, Austria, 22-24 May, CD ROM. Available at: http://www.fig.net/commission6/baden_2006/PDF/PGO1/Chrzanowski.pdf, accessed on: 4 October 2007.

Collins, J.P. and R.B. Langley (1999). *Nominal and Extreme Error Performance of the UNB3 Tropospheric Delay Model*. Department of Geodesy and Geomatics Engineering Technical Report No. 204, University of New Brunswick, Fredericton, New Brunswick, Canada, 173 pp.

Dai, L., J. Wang, C. Rizos and S. Han (2001). *Applications of Pseudolites in Deformation Monitoring Systems*. Availaable at: www.gmat.unsw.edu.au/snap/publications/dai_etal2001a.pdf, accessed on: 23 October 2002.

Dai, L., J. Zhang, C. Rizos, S. Han, and J. Wang (2000). *GPS and Pseudolite Integration for Deformation Monitoring Applications*. Available at: www.gmat.unsw.edu.au/snap/publications/dai_etal2000a.pdf, accessed on: 30 March 2005.

Dai, L., J. Wang, C. Rizos and S. Han (2002). "Pseudo-Satellite Applications in Deformation Monitoring." *GPS Solutions* 5(3):80-87. DOI: 10.1007/PL00012902 Available at: http://www.springerlink.com/content/6xjd3qbrywp53aa4/fulltext.pdf, accessed on: 3 October 2007.

Ding, X.L., D.F. Huang, J.H. Yin, Y.Q. Chen, C.K. Lau, Y.W. Yang, Y.R. Sun, W. Chen, and X.F. He (2003). "Development and Field Testing of a Multi-Antenna GPS System for Deformation Monitoring." Wuhan Univeristy Journal of Natural Sciences, Vol. 8, No. 2B, pp. 671-676.

Ding, X.L., W.J. Dai, W.T. Yang, X.W. Zhou, J. Lam, Q. Zhang and L. Wang (2007). "Application of multi-antenna GPS technology in monitoring stability of slopes." Proceedings of *Strategic Integration of Surveying Services*, *FIG Working Week 2007*, Hong Kong, 13-17 May, 11 pp. (CDROM).

Ding, X.L. Y.Q. Chen, D.F. Huang, J.J. Zhu, M. Tsakiri and M. Stewart (2000). "Slope Monitoring using GPS: a multi-antenn approach." *GPS World,* No. 3, Vol. 11, pp 52-55.

Duffy, M., C. Hill and C. Whitaker, A. Chrzanowksi, J. Lutes and G. Bastin (2001). "An Automated and Integrated Monitoring Program for Diamond Valley Lake in California." Proceedings of the *10th FIG International Symposium on Deformation Measurements*, Orange, CA, March 19-22, 2001, CDROM, 21 pp. Available at: http://ccge.unb.ca, accessed on: 3 October 2007.

Forward, T.A. (2002). *Quasi-Continuous GPS Steep Slope Monitoring: A Multi-Antenna Array Approach*. Doctoral dissertation, Department of Spatial Sciences, Curtin University of Technology, Perth, Western Australia. Available at: http://adt.curtin.edu.au/theses/available/adt-WCU20021025.152012/, accessed on: 3 October 2007.

Ge, L. S. Han and C. Rizos (2000). "Multipath Mitigation of Continuous GPS Measurements Using an Adaptive Filter." *GPS Solutions*, 4(2):19-33. Available at: http://www.springerlink.com/content/p8qr83gtka04yhbn/ , accessed on: 5 October 2007. DOI 10.1007/PL00012838.

Geoscience Australia (2005). *Continuous GPS Station Network: South Pacific Sea Level Climate Monitoring Program (SPSLCMP)*. Available at: http://www.ga.gov.au/geodesy/slm/spslcmp/network.jsp, accessed on: 3 October 2007.

GEO-SLOPE (2007). *GEO-SLOPE International Ltd: Products: SIGMA/W 2004*, Available at: http://www.geo-slope.com/products/sigmaw2004.aspx, accessed on 27 April.

Gurtner, W., G. Beutler, S. Botton, M. Rothacher, A. Geiger, H.G. Kahle, D. Schneider and A. Wiget (1989). "The Use of the Global Positioning System in Mountainous Areas." *manuscipta geodaetia,* 14:53-60.

GPS World (2005). "NovAtel's New Multipath Mitigation." *GPS World,* October. Available at: http://www.gpsworld.com/gpsworld/article/articleDetail.jsp?id=184133 , accessed on: 5 October 2007.

Hudnut, K.W., Y. Bock, J.E. Galetzka, F.H. Webb and W.H. Young (2001). "The Southern California Integrated GPS Network (SCIGN)". Proceedings of the *10th FIG International Symposium on Deformation Measurements*, Orange CA, USA, 19-22 March, pp.129-148. Available at: http://www.fig.net/com6_orange/pdf/Session%20IV_Paper%201.pdf, accessed on: 3 October 2007.

Jäger, R. S. Kälber, M. Oswald and M. Bertges (2006). "GNSS/GPS/LPS based Online Control and Alarm System (GOCA) - Mathematical Models and Technical Realisation of a System for Natural and Geotechnical Deformation Monitoring and Analysis - ". Proceedings of the *3rd IAG Symposium on Geodesy for Geotechnical and Structural Engineering and 12th FIG Symposium on Deformation Measurements*, Eds. H. Kahmen and A. Chrzanowski, Baden, Austria, 22-24 May, CD-ROM. Available at: http://www.fig.net/commission6/baden_2006/proceedings.htm, accessed on: 3 October 2007.

Jin, X.X. (1996). *Theory of Carrier Adjusted DGPS Positioning Approach and Some Experimental Results*. Delft University Press, Delft, the Netherlands, 162 pp.

Kee, C., D. Yun, T. Lagenstein, B. Parkinson, S. Pullen, H. Jun (2001). "Centimeter-Accuracy Indoor Navigation Using GPS-Like Pseudolites." *GPS World*, November. Available at: http://www.gpsworld.com/gpsworld/article/articleDetail.jsp?id=3086, accessed on: 3 October 2007.

Kim, D. (2007). Personal Communication. Senior Research Associate, University of New Brunswick, Fredericton, New Brunswick Canada.

Kim, D. and R.B. Langley (2002). "Instantaneous Real-Time Cycle-Slip Correction for Quality Control of GPS Carrier-Phase Measurements." *Navigation*, Journal of *The Institute of Navigation*, Alexandria, Virginia, Winter, No. 4, Vol. 49, pp. 205-222.

Kim, D. and R.B. Langley (2001). "Mitigation of GPS Carrier Phase Multipath Effects in Real-Time Kinematic Applications." Proceedings of the *14th International Technical Meeting of the Satellite Division of the Institute of Navigation (ION GPS 2001)*, 11-14 September 2001, Salt Lake City, UT. Available at: http://www.ion.org, accessed on: 3 October 2007.

Kim D., R.B. Langley, J. Bond and A. Chrzanowski (2003). "Local deformation monitoring using GPS in an open pit mine: Initial study." *GPS Solutions* 7(3): pp. 176-185. Available at: http://www.springerlink.com/content/0dvd4ddmx9w5k8xx/, accessed on: 4 October 2007. DOI 10.1007/s10291-003-0075-1

Krantz, E., S. Riley and P. Large (2001). *GPS Antenn Design and Performance Advancements: The Trimble Zephyr.* Available at: http://www.seilerinst.com/images/gps/products/gps5700/5700WPZephyrE.pdf , accessed on: 5 October 2007.

Langley, R.B. (1995). "Propagation of the GPS Signals." Chapter 3 of *GPS for Geodesy*, Proceedings of the *International School of GPS for Geodesy*, Delft, the Netherlands, March 26 - April 1, pp. 111-185.

Lee, M., (2007). Email communication. Technical Support Representative, Sollae Systems Co., Ltd., 30 March.

Leica Geosystems (2007a). "GPS 1200." *Leica Geosystems*, http://leica.loyola.com/products/system1200/gps1200.html, accessed on 5 October 2007.

Leica Geosystems (2007b). "HDS Systems, The HDS Product Family." *Leica Geosystems,* http://www.leica-geosystems.com/corporate/en/ndef/lgs_5570.htm, accessed on: 6 February.

Leick, A. (1994). *GPS Satellite Surveying*, 2nd ed. John Wiley & Sons, Inc., New York, USA, 560 pp.

LeMaster, E.A., and S.M. Rock (2000). "Field Results for a Self-Calibrating Pseudolite Array." Proceedings of *ION GPS 2000*, September 2000, Salt Lake City, UT.

Lienhart, W. (2007). *Analysis of Inhomogeneous Structural Monitoring Data*, Doctoral Dissertation, Dept. of Engineering Geodesy and Measurement Systems, Graz University of Technology, Shaker Verlag, 269 pp.

Liu, G.X., Y.Q. Chen, X.L. Ding, Z.L. Li and Li ZW (2004). "Monitoring Ground Settlement in Hong Kong with Satellite SAR Interferometry." *Photogrammetric Engineering and Remote Sensing*, 70(10):1151-1156.

Martin, W. and J. Ladd (1999). "GPS+GLONASS Surveying: Post-Processed and Real-Time Results." *Magellan: Technical Papers*. Available at: http://pro.magellangps.com/en/support/apptechnotes.asp#7, accessed on: 3 October 2007.

Michalson, W.R., and I.F. Progri (2000). 'Assessing the Accuracy of Underground Positioning Using Pseudolites.' Proceedings of the *13th International Technical Meeting of the Satellite Division of the Institute of Navigation (ION GPS 2000)*, 19-22 September 2000, Salt Lake City, UT.

Mining Technology (2003). "Highland Valley Copper Mine, Canada." *The Website for the Mining Industry,* http://www.mining-technology.com/projects/highland/index.html, accessed on: 12 December 2003.

Microsoft Developer Network (MSDN) (2007a). "Visual Studio Develop Center." *Microsoft*, http://msdn2.microsoft.com/en-us/vstudio/default.aspx, accessed on: 3 October 2007.

Microsoft Developer Network (MSDN) (2007b). "System.net.sockets namespace," *Microsoft*, http://msdn2.microsoft.com/en-us/library/system.net.sockets(vs.71).aspx , accessed on: 18 April 2007.

Microsoft Developer Network (MSDN) (2007c). "Using TCP Services," *Microsoft*, http://msdn2.microsoft.com/en-us/library/k8azesy5.aspx , accessed on: 19 April 2007.

Microsoft Developer Network (MSDN) (2007d). "Using UDP Services," *Microsoft*, http://msdn2.microsoft.com/en-us/library/tst0kwb1.aspx , accessed on: 19 April 2007.

Minami, M., H. Morikawa and T. Aoyama (2000). "An Adaptive Multipath Mitigation Technique for GPS Signal Reception." Proceedings of 52nd Vehicular Technology Conference, Boston, MA, USA, 24-28 September, pp. 1625-1629. Available at: http://ieeexplore.ieee.org/iel5/6849/18408/00851402.pdf , accessed on 5 October 2007.

Novariant (2007). "Mining Products. Terralite XPS." *Novariant,* http://www.novariant.com/mining/products/index.cfm, accessed on: 21 April 2007.

Newcomen, W.H., C. Murray and L. Shwydiuk (2003). "Monitoring pit wall deformations in real time at Highland Valley Copper." Proceedings of the *Fourth International Conference on Computer Applications in the Minerals Industry*, Calgary, Alberta, Canada, 8-10 September, CD-ROM.

NRCan, (2007). "Western Canada Deformation Array." *Natural Resources Canada*, http://gsc.nrcan.gc.ca/geodyn/wcda/index_e.php, accessed on: 7 October 2007.

Radovanovic, R. (2000). "High Accuracy Deformation Monitoring Via Multipath Mitigation by Day-To-Day Correlation Analysis." Proceedings of the 13th International Technical Meeting of the Satellite Division of the Institute of Navigation (ION GPS 2000), 19-22 September 2000, Salt Lake City, UT, pp. 35-44. Available at: http://www.ion.org, accessed on: 3 October 2007.

Remondi, B.W. (1984). Using the Global Positioning System (GPS) Phase Observable for Relative Geodesy: Modeling, Processing, and Results. Doctoral thesis, Center for Space Research, University of Texas at Austin, 324 pp.

Remondi, B.W. and G. Brown (2000). "Triple Differencing with Kalman Filtering: Making It Work." *GPS Solutions* 3(3):58-64. Available at: http://www.springerlink.com/content/am6adj8qg5q6u94h/, accessed on: 4 October 2007. 10.1007/PL00012805

Rizos, C. (1999a). "Measurement Biases and Errors: Tropospheric Delay." *Principles and Practice of GPS Surveying*, http://www.gmat.unsw.edu.au/snap/gps/gps_survey/principles_gps.htm, accessed on: 3 October 2007.

Rizos, C. (1999b). "Measurement Biases and Errors: Multipath Disturbance and Signal Interference." *Principles and Practice of GPS Surveying*, http://www.gmat.unsw.edu.au/snap/gps/gps_survey/principles_gps.htm, accessed on: 5 October 2007.

Rizos, C. (1999c). "Section 9.1.5: Outlier Testing and Residuals." *Principles and Practice of GPS Surveying*, http://www.gmat.unsw.edu.au/snap/gps/gps_survey/principles_gps.htm, accessed on: 4 October 2007.

Roberts, G., and L. Hirst (2005). "Deformation Monitoring and Analysis of Structures Using Laser Scanners." *Proceedings of FIG Working Week 2005*, Cairo, Egypt, 16-21 April, TS32.8.

Rothacher, M., G. Beutler, W. Gurtner, A. Geiger, H.G. Kahle and D.Schneider (1986). "The Swiss 1985 GPS Campaign." Proceedings of the *Fourth International Geodetic Symposium on Satellite Positioning*, Austin, Texas, USA, pp. 979-991.

Rüeger, (1990). *Electronic Distance Measurement*. 3rd ed., Springer-Verlag, Berlin Heidelberg, 266 pp.

Rutledge, D., J. Gnipp and J. Kramer (2001). "Advances in Real-time GPS Deformation Monitoring for Landslides, Volcanoes, and Structures." Proceedings of the *10th International Symposium on Deformation Measurements*, Orange, CA, USA, 19-22 March.

Rutledge, D., S. Meyerholtz, N. Brown and C. Baldwin (2006). "Dam Stability. Assessing the Performance of a GPS Monitoring System." *GPS World*, October, pp. 26-33. Available at: http://www.gpsworld.com/gpsworld/content/printContentPopup.jsp?id=374824, accessed on: 7 October 2007.

Rutledge, D. B. Remondi, R. Koerner and C. Henderson (2002). "Staying Afloat: GPS Monitors Oilfield Subsidence." *GPS World*, Oct. Available at: http://www.gpsworld.com/gpsworld/article/articleDetail.jsp?id=34931, accessed on: 3 October 2007.

Rzepecka, Z., A. Wasilewski, S. Cellmer and J. Rapinski (2006). "Integration of gps (sic) and pseudolites – effect on height determination accuracy." Proceedings of the *3rd IAG Symposium on Geodesy for Geotechnical and Structural Engineering and 12th FIG Symposium on Deformation Measurements*, Eds. H. Kahmen and A. Chrzanowski, Baden, Austria, 22-24 May, CD-ROM. Available at: http://www.fig.net/commission6/baden_2006/proceedings.htm, accessed on: 3 October 2007.

Sagiya, T. (1998). "Continuous GPS Array of Japan and its Application to Crustal Activity Modeling." Proceedings of the *First APEC Cooperation for Earthquake Simulation Workshop,* May 4-8, 1998, Brisbane, Australia, pp.401-404.

Sagiya, T., S. Miyazaki and T. Tada (2000). "Continuous GPS Array and Present-day Crustal Deformation of Japan." *Pure and Applied Geophysics,* 157(2000):2303-2322. Available at: http://www.springerlink.com/content/qllm0dr20hmjf2nc/fulltext.pdf, accessed on: 3 October 2007.

Salzmann, M.A. (1993). *Least Squares Filtering and Testing for Geodetic Navigation Applications*. Ph.D. Dissertation, Faculty of Geodetic Engineering, Delft University of Technology, Netherlands.

Satirapod, C., and C. Rizos (2004). "Multipath Mitigation by Wavelet Analysis for GPS Base Station Applications." *University of New South Wales Publications*, http://www.gmat.unsw.edu.au/snap/publications/satirapod_etal2004a.pdf , accessed on: 5 October 2007.

Sollae Systems Co., Ltd. (2007a). "Products. EZL-400S." *Sollae Systems Co., Ltd.,* http://www.eztcp.com/en/Products/ezl-400s.php, accessed on: 18 April 2007.

Sollae Systems Co., Ltd. (2007b). "Products EZL-400S: User's Manual." *Sollae Systems Co., Ltd.,* http://www.eztcp.com/Support/ezl400sen.pdf, accessed on: 18 April 2007.

Szostak-Chrzanowski, A. (2006). "Interdisciplinary Approach to Deformation Analysis in Engineering, Mining, and Geosciences Projects by Combining Monitoring Surveys with Deterministic Modelling – Part I." *Technical Sciences Journal*, UWM, Olsztyn, pp. 147-172.

Szostak-Chrzanowski, A, A. Chrzanowski, and E. Ortiz (2006b). "Modelling of Ground Subsidence in Oil Fields." *Technical Sciences Journal*, UWM, Olsztyn, pp. 133-146.

Szostak-Chrzanowski A., A. Chrzanowski, and M. Massiéra (2003). "Use of Geodetic Monitoring Measurements in Solving Geomechanical Problems in Engineering and Geosciences." Proceedings of the *11th FIG Symposium on Deformation Measurements*, Santorini Island, Greece, 25-28 May, pp.273-288.

Szostak-Chrzanowski A., A. Chrzanowski and M. Massiéra (2005). "Use of Geodetic Monitoring Measurements in Solving Geomechanical Problems in Engineering and Geosciences." *Engineering Geology Vol. 79, Issues. 1-2: Application of Geodetic Techniques in Engineering Geology*, Eds. S. Stiros and A. Chrzanowski, 3 June, pp. 3-12.

Szostak-Chrzanowski A., and M. Massiéra (2006). "Relation Between Monitoring and Design Aspects of Large Earth Dams." Proceedings of the *3rd IAG Symposium on Geodesy for Geotechnical and Structural Engineering and 12th FIG Symposium on Deformation Measurements*, Eds. H. Kahmen and A. Chrzanowski, Baden, Austria, 22-24 May, CD-ROM. Available at: http://www.fig.net/commission6/baden_2006/proceedings.htm, accessed on: 3 October 2007.

Szostak-Chrzanowski, A., W. Prószynski and W. Gambin (2006a). "Continuum Mechanics as a Support for Deformation Monitoring, Analysis, and Interpretation." Proceedings of the *3rd IAG Symposium on Geodesy for Geotechnical and Structural Engineering and 12th FIG Symposium on Deformation Measurements*, Eds. H. Kahmen and A. Chrzanowski, Baden, Austria, 22-24 May, CD-ROM. Available at: http://www.fig.net/commission6/baden_2006/proceedings.htm, accessed on: 3 October 2007.

Teunissen, P.J.G. (1998). "Quality Control and GPS." Chapter 7 in *GPS for Geodesy*, 2nd ed., Springer-Verlag, Berlin Heidelberg New York, pp. 271-318.

Trimble (2002). "Trimble News Release: Trimble and Condor Earth Technologies to Provide Real-Time GPS Monitoring of Civil Infrastructure." Available at: http://www.trimble.com/news/release.aspx?id=040402a, accessed on: 3 October 2007.

Ueno, M., K. Itani and R.B. Langley (2003). "Real-time GPS Landslide Monitoring Under Poor Satellite Visibility." Proceedings of *2003 International Symposium on GPS/GNSS*, Tokyo, Japan, 15-18 November 2003; pp. 5l15-522. Available at: http://gauss.gge.unb.ca/papers.pdf/gpsgnss2003.ueno.pdf, accessed on: 7 October 2007.

Van Cranenbroeck, J. and L. Troyer (2004). "Leica GPS Spider for Deformation Monitoring." Proceedings of the *1st FIG International Symposium for Construction Works and Structural Engineering*, Nottingham, UK, 28 June-1 July. Available at: http://www.fig.net/nottingham/proc/gs_07_cranenbroeck.pdf, accessed on: 3 October 2007.

Van Diggelen (1997). "GPS and GPS+GLONASS RTK" Proceedings of the *10th International Technical Meeting of the Satellite Division of the Institute of Navigation*, Kansas City, MO, USA, 16-19 Sept.

Wang, J. (2002). Pseudolite Applications in Positioning and Navigation: Progress and Problems. *Journal of Global Positioning Systems*, Vol. 1 No.1, pp. 48-56. Available at: http://www.gmat.unsw.edu.au/wang/jgps/v1n1/v1n1pF.pdf, accessed on: 3 October 2007

Whitaker, C. and Y. Bock (2006). "Design and Implementation of a Real-Time GPS Network for the Metropolitan Water District of Southern California." Proceedings of the *3rd IAG Symposium on Geodesy for Geotechnical and Structural Engineering and 12th FIG Symposium on Deformation Measurements*, Eds. H. Kahmen and A. Chrzanowski, Baden, Austria, 22-24 May, CD-ROM. Available at: http://www.fig.net/commission6/baden_2006/proceedings.htm, accessed on: 3 October 2007.

Wilkins, R., G. Bastin, A. Chrzanowski, W. Newcomen and L. Shwydiuk (2003a). *A Fully Automated System for Monitoring Pit Wall Displacements*. Paper presented at SME 2003, Cincinnati, OH, February 24-26, 2003. Available at: http://ccge.unb.ca, accessed on: 3 October 2007.

Wilkins, R., G. Bastin and A. Chrzanowski (2003b). *ALERT—A fully automated real-time monitoring system*. Proceedings of the *11th FIG Symposium on Deformation Measurements*, May 25-28, Santorini, Greece. Available at: http://ccge.unb.ca, accessed on: 3 October 2007.

Wilkins, R., G. Bastin and A. Chrzanowski (2003c). "Monitoring of Structures and Steep Embankments: A Fully Automated Approach." Paper presented at CSCE Annual Conference, Moncton, NB, Canada, June 4-7, 2003. Available at: http://ccge.unb.ca, accessed on: 4 October 2007.

Wübbena, G., A. Bagge, G. Boettcher, M. Schmitz, P. Andree (2001). "Permanent Object Monitoring with GPS with 1 Millimeter Accuracy." Proceedings of the *14th International Technical Meeting of the Satellite Division of the Institute of Navigation (ION GPS 2001)*, 11-14 Sept., Salt Lake City, UT, USA, pp.1000-1008. Available at: http://www.ion.org, accessed on: 3 October 2007.

Zienkiewicz, O.C. (1977). *The Finite Element Method*. 3rd ed., McGraw-Hill Book Company Limited, London, 787 pp.

VITA

Candidates Full Name: Donald Jason Bond

Education:

Master of Science in Engineering
Dept. Geodesy and Geomatics Engineering
University of New Brunswick, 2004

Bachelor of Science in Engineering
Dept. Geodesy and Geomatics Engineering
University of New Brunswick, 2002

Diploma of Geomatics Engineering Technology
College of Geographic Sciences (COGS), 1999

Publications:

Bond, J., D. Kim, A. Chrzanowski, A. Szostak-Chrzanowski (2007). "Development of A Fully Automated, GPS Based Monitoring System for Disaster Prevention and Emergency Preparedness: PPMS^{+RT}" *Sensors* 2007, (7) Special Issue: *Sensors for Disaster and Emergency Management Decision Making*, Eds. J. Levy and Y.Gao, pp. 1028-1046. Available at: http://www.mdpi.org/sensors/list07.htm#new, accessed on: 4 October 2007.

Bond, J., A. Chrzanowski, and D. Kim (2007). "Bringing GPS into Harsh Environments for Deformation Monitoring." *GPS Solutions* (online first status), 11 pp. Available at: http://www.springerlink.com/content/21v2625p46108266/fulltext.pdf, accessed on: 4 October 2007. DOI 10.1007/s10291-007-0059-7

Chrzanowski, A., A. Szostak-Chrzanowski, J. Bond and R. Wilkins (2007). "Increasing Public and Environmental Safety through Integrated Monitoring and Analysis of Structural and Ground Deformations." Chapter in *Geomatics Solutions for Disaster Management*, Springer, New York, pp. 401-426.

Szostak-Chrzanowski A., A. Chrzanowski, and J. Bond (2007). "Deterministic Modeling of Deformations as a Tool for Designing Geodetic Monitoring Schemes." *Reports on Geodesy*, Polish Academy of Sciences, Warsaw, (in print).

Bond, J., A. Chrzanowski and F. Wilkins (2005). "Using GPS for Augmenting Deformation Monitoring Systems in Open Pit Mines- Problems and Solutions." *Geomatica*, 59 (1):73-82.

Bond, J. (2004). "Demographic Study of Land Surveyors in the Maritime Provinces." *Geomatica,* 58 (1): 23-31.

Kim D., R.B. Langley, J. Bond and A. Chrzanowski (2003). "Local deformation monitoring using GPS in an open pit mine: Initial study." *GPS Solutions,* 7(3):176-185. Available at: http://www.springerlink.com/content/0dvd4ddmx9w5k8xx/, accessed on: 4 October 2007. DOI 10.1007/s10291-003-0075-1

Conference Proceedings:

Bond, J., A. Szostak-Chrzanowski and A. Chrzanowski (2007). "Design of Geodetic Monitoring Schemes Using Deterministic Modelling: An Open Pit Mine Example." Proceedings of the *3rd International Symposium on Geo-information for Disaster Management*, Toronto, Ontario, Canada, 22-24 May, Canadian Inst. of Geomatics, 11 pp., CDROM.

Bond, J., A. Chrzanowski, D. Kim D (2007b). "Augmenting GPS with Pseudolites for Deformation Monitoring in Harsh Environments." Proceedings of the *Institute of Navigation National Technical Meeting* (ION NTM), 22-24 January, San Diego, CA, USA, pp. 486-492, CDROM. Available at http://www.ion.org/, accessed on: 4 October, 2007.